Distinct Functions of ARTD1 and ARTD2 in Cell Cycle Entry and the Genotoxic Stress Response

Dissertation

zur

Erlangung der naturwissenschaftlichen Doktorwürde

(Dr. sc. nat.)

vorgelegt der

Mathematisch-naturwissenschaftlichen Fakultät

der

Universität Zürich

von

Karolin Leger

(geb. Meyer)

aus

Deutschland

Promotionskomitee

Prof. Dr. Dr. Michael O. Hottiger

(Vorsitz und Leitung der Dissertation)

Prof. Dr. Roland Wenger

Prof. Dr. Anja Groth

PD Dr. Stefano Ferrari

Zürich 2013

SUMMARY

ADP-ribosyltransferases (ARTs) are important enzymes involved in diverse biological functions of the cell. ARTD1 and ARTD2 are two chromatin-associated proteins that share a similar catalytic domain, which is responsible for the modification of these proteins and other target proteins. Despite the high degree of amino-acid conservation between ARTD1 and ARTD2 and the limited number of studies of ARTD2, there are initial indications that ARTD2 might regulate distinct cellular processes, although molecular details and mechanistic insights remain elusive. The aim of the thesis was to provide additional insights that ARTD1 and ARTD2 regulate different cellular processes or use different mechanisms to regulate common processes. Therefore, we studied the role of ARTD1 and ARTD2 in response to genotoxic stress as well as in cell cycle regulation, in particular during G_0 to G_1 progression.

H_2O_2 or MNNG both induce genotoxic stress, which is known to activate ARTD1 and to a lesser extent ARTD2. Interestingly, the combined treatment of H_2O_2 or MNNG with low doses of Actinomycin D induced strong ARTD2-dependent poly-ADP-ribose formation. Actinomycin D treatment lead to the accumulation of short rRNA transcripts *in vivo*, which strongly activated ARTD2 *in vitro*, while comparable DNA fragments were not able to do so. Interestingly, ARTD1 was activated more by DNA and to a lesser extent by RNA.

A second project focusing on cell cycle re-entry revealed distinct functions for both proteins, ARTD1 and ARTD2. Knockdown of ARTD1 by siRNA treatment of T24 cells (urinary bladder carcinoma cells) repressed the expression of *Cyclin E* and thereby lead to decelerated cell cycle entry and progression. In contrast, down-regulation of ARTD2 specifically affected *p27* expression as well as its protein level and rendered T24 unable to re-enter the cell cycle. Analysis of the histone modifications and compositions at the two promoters (*Cyclin E* and *p27*) suggested that ARTD1 and ARTD2 repress transcription by different means.

Together, these findings identified RNA as new activator for ARTD2-dependent ADP-ribosylation and provide further strong evidence, that ARTD1 and ARTD2 regulate cell cycle regulation and the cellular genotoxic stress response as well as possibly other biological processes in the nucleus by different mechanisms.

ZUSAMMENFASSUNG

ADP-ribosyl-transferasen (ARTs) sind wichtige Enzyme, die in diversen biologischen Prozessen eine Rolle spielen. ARTD1 und ARTD2 sind chromatin-assozierte Proteine, die eine sehr ähnliche Domänenstruktur aufweisen und deren katalytische Domänen homolog sind. Diese Domänen sind für die Automodifizierung und die Modifizierung anderer Zielproteine verantwortlich. Abgesehen von dem hohen Grad der Homologie beider Enzyme, und abgesehen davon, dass die meisten biochemischen Studien nur mit ARTD1 durchgeführt wurden, gibt es erste Hinweise, dass ARTD2 unterschiedliche zelluläre Prozesse reguliert, auch wenn molekulare Details und mechanistische Erkenntnisse oft noch nicht genau geklärt sind.

Das Ziel dieser Doktorarbeit war es, zusätzliche Erkenntnisse zu gewinnen, wie ARTD1 und ARTD2 verschiedene zelluläre Prozesse beeinflussen oder wie diese Enzyme die gleichen Prozesse mittels verschiedener Mechanismen regulieren. Daher haben wir die Rolle von ARTD1 und ARTD2 in der Antwort auf oxidativen Stress eruiert und den Zellzyklus untersucht, besonders während des Übertritts von der G_0 zur G_1 Phase.

H_2O_2 und MNNG sind Substanzen, die genotoxischen Stress auslösen können. Es ist bekannt, dass dieser Stress ARTD1 und in geringerem Masse auch ARTD2 aktiviert. Interessanterweise führt die kombinierte Behandlung von H_2O_2 oder MNNG mit Actinomycin D in geringer Konzentration zur starken Aktivierung von ARTD2. Behandlung mit Actinomycin D führte durch die Inhibierung von RNA polymerase I *in vivo* zur Anreicherung von kurzen rRNA Transkripten, welche ARTD2 auch *in vitro* stark aktivieren konnte, während DNA Fragmente selber keine Induktion hervorgerufen haben. Interessanterweise, wurde ARTD1 stärker durch DNA aktiviert als durch RNA.

Das zweite Projekt befasste sich mit dem Zellzyklus-Wiedereintritt und hat gezeigt, dass ARTD1 und ARTD2 dabei unterschiedliche Funktionen haben. Die Herunterregulierung von ARTD1 mittels siRNA in T24 Zellen (Blasenkarzinom-Zellen) hemmte die Expression von *Cyclin E* und führte damit zu einem verlangsamten Zellzykluseintritt und –verlauf. Im Gegensatz dazu beeinflusste die Herunterregulierung von ARTD2 die *p27* Expression sowie den p27 Porteingehalt positiv, wodurch T24 Zellen nicht in der Lage waren in den Zellzyklus einzutreten. Analysen der Histonmodifizierung und der Zusammensetzung beider Promotoren (*Cyclin E und p27*) legten nahe, dass ARTD1 und ARTD2 die Transkription auf verschiedene Weise reprimierten.

Zusammenfassend zeigen diese Ergebnisse, dass RNA ein neuer Aktivator von ARTD2-abhängiger ADP-Ribosylierung ist und beweisen, dass ARTD1 und ARTD2 den Zellzyklus und die zelluläre Stressantwort, sowie andere biologische Prozesse im Nukleus durch verschiedene Mechanismen regulieren.

TABLE OF CONTENT

ABBREVIATIONS

aa	Amino acid
ADP	Adenosine diphosphate
ART	ADP-ribosyltransferase
ARTD	ADP-ribosyltransferase diphtheria toxin-like
ActD	Actinomycin D
ATP	Adenosine triphosphate
BER	Base excision repair
bp	Base pair
CAIX	Carbonic anhydrase IX
CAK	Cdk-activating kinase
Chk1	Serine/threonine-protein checkpoint kinase 1
Cdk	Cyclin-dependent kinase
ChIP	Chromatin immunoprecipitation
DAPI	4',6-diamidino-2-phenylindole
DDR	DNA damage response
DNA	Deoxyribonucleic acid
DNMT	DNA methyltransferase
DSB	Double-strand break
FCS	Fetal calf serum
γH2AX	gamma-histone 2A variant X (phosphorylated)
HDAC	Histone deacteylase
HIF	Hypoxia-inducible factor
H_2O_2	Hydrogen peroxide
IL6	Interleukin 6
LPS	Lipopolysaccharide
MEF	Mouse embryonic fibroblasts
miRNA	microRNA
MNNG	Methylnitronitrosoguanidine
NAD	Nicotinamide adenine dinucleotide
NAM	Nicotinamide
NF-κB	Nuclear factor of kappa light polypeptide gene enhancer in B-cells 1

NRH	Dihydronicotinamide ribosyl
PAR	Poly-ADP-ribose
PARG	Poly-(ADP-ribose)-glycohydrolase
PARP	Poly-(ADP-ribose)-polymerase
PARylation	Poly-ADP-ribosylation
PBS	Phosphate buffered saline
Pol I	RNA- Polymerase I
pRb	Retinoblastoma protein
PTM	Post-translational modification
rDNA	ribosomal DNA
RNA	Ribonucleic acid
rRNA	Ribosomal RNA
SSB	Single-strand break
snoRNP	small nucleolar ribonucleoprotein
TNFα	Tumor necrosis factor α
XRCC1	X-ray repair cross-complementing protein 1

1. INTRODUCTION

1.1 The nucleus

The nucleus is the central organelle of eukaryotic cells containing the genetic material – the DNA. It is the compartment where transcription, RNA processing and DNA replication take place, which all ensure the correct function of the cell. Throughout these processes, the DNA plays different roles: on one hand, the DNA needs to be well protected from damage or modification to ensure the correct inheritance of the genetic information. On the other hand, expression of this information as RNA or proteins allows the cell to react and respond immediately to internal (cellular) or external (environmental) changes. The accessibility of this information is ensured by an extensive protein network, which is comprised of a DNA-nucleoprotein-complex, the chromatin.

1.1.1 Chromatin

Chromatin structure

Chromatin is the complex structure of DNA and nucleoproteins, which guarantees the compaction of the DNA in the nucleus. Uncompact human DNA would reach a length of approximately 2 meters. Due to the compaction of the DNA by histone binding and the resulting condensation, the DNA can be packaged into cells with a diameter of 1 µm -100 µm (*1*). The smallest structural unit of the chromatin is called the nucleosome. A nucleosome is formed by the core histones – two stable H3-H4 histone dimers forming a tetramer, which is flanked by two H2A-H2B dimers (*2*). 147 bp of double stranded DNA are wound around this octamer forming a "beads on a string" fiber of 11 nm in diameter. Further compaction is induced by the addition of the linker histone H1, which binds the entry and exit sites of the linker DNA to the nucleosome and influences nucleosome positioning (*3*). The complex of core nucleosomes and linker histone together with DNA is known as chromatosome, a fiber of 30 nm in diameter (*4*). Further condensation by association with the chromosome scaffold leads to 300 nm and 700 nm diameter structures and eventually to the condensed metaphase chromosomes of the eukaryotic cells.

DNA methylation and posttranslational modifications of histones

Since the DNA is tightly compacted in eukaryotic cells, multifaceted mechanisms have evolved to regulate an easy accessibility. The chromatin is not a homogenous rigid structure; it is rather highly heterogeneous and contains different degrees of compaction, also referred as flavors. Major changes in this "open-close" conformation are induced by chemical modifications on the histones and the DNA. The DNA can for example be directly modified by DNA methyltransferases (DNMT) on cytosines (then named 5-methyl-cytosine) embedded in CpG dinucleotides. Theses CpG dinucleotides tend to cluster in regions that are called islands and the inheritance of this modification is termed epigenetics, which nowadays includes also the inheritance of posttranslational modifications (PTM) of histones (*5, 6*). The short amino-terminal domains of the histones (less than 40 amino acids) as well as the short protease-accessible carboxy-terminal domains (*2, 7*) are subject to different PTMs, which include methylation, acetylation, phosphorylation, SUMOylation, ubiquitination and ADP-ribosylation (*8, 9*). Many different proteins such as histone acetyltransferses (HAT), histone deacetylases (HDAC), histone methyltransferases (HMT), histone demethylases (HDM), and also ADP-ribosyltransferases (ART) are involved in the modification of histones (*10, 11*).

Different activities are assigned to distinct chromatin compaction degrees, which also correlate with different PTMs. There are regions of uncondensed chromatin occupied by lower amount of nucleosomes and which contains high levels of acetylation and also specific tri-methylated lysine sites (e.g., H3K4, H3K36 and H3K79). These regions indicate actively transcribed euchromatin (*12*). On the other hand, the highly compact and rather silent heterochromatin is characterized by low acetylation and enhanced methylation of lysines K9, K27, K20 on histone H3 (*13*). The chromatin compaction that can change quite rapidly is also referred to as chromatin plasticity.

Posttranslational modifications of histones and DNA methylation profiles are important marks that can be detected by chromatin immunoprecipitation (ChIP) to analyze the dynamic structure of the DNA. Inheritance of these modification profiles (epigenetics) is very important. Epigenetic deregulation occurs at various disease stages. Virtually all human cancers show epigenetic abnormalities, which often affects tumor suppressor genes leading to deregulation of regulatory pathways (*14*). Profiles of PTMs and DNA methylation are therefore also used as prognostic markers and even as therapeutic targets. However, only a few biomarkers are currently in clinical use and even less commercial tests are actually

available, since the identification of a single biomarker as well as the required specificity and sensitivity of a test is difficult to achieve (*15*).

Histone variants

Although histones are highly conserved proteins, their genes are repeated tens of times per genome and variably arranged in clusters (*16*). Not all histone genes encode a conserved histone type, allowing a certain diversity or variation among the histone proteins and their functions. For every canonical histone, different variants with distinct amino acid sequences are known. The histones H3 and H2A exhibit the most variations with specialized functions (*1*). For example, the human genome contains 10 genes encoding H2A1 variants. Six of these have identical sequences and four genes vary in 3 to 4 positions. Together with the H2A2 variants, these genes encode the bulk of mammalian H2A. In addition, there are five other H2A genes that encode amino acid sequences, which differ tremendously from the bulk H2A peptide and those variants might have different but important roles in cellular processes (*1*).

Core histone biosynthesis is largely restricted to the S phase, when DNA replication takes place (*17*). In contrast, histone variants are constantly expressed throughout the cell cycle as described for the H3.3 variant, which substantially differs in amino acid sequence from the major H3.1 (*18*). The variant H3.3 can replace H3.1 independently of DNA synthesis and marks active promoter sites (*19*). Thus, variants also appear to serve as markers for a distinct chromatin status. H2A.Z and H2A.X, discovered in the 1980s, are two other prominent examples (*20*). H2A can be substituted by H2A.Z at transcriptionally active start sites (*21*). H2A.X, when phosphorylated on serine 139 (called γ-H2A.X), appears at chromatin sites in close proximity of double strand breaks (DSB) and is thus used as a marker for DNA damage (*22*). It is interesting to note that only about 20 % of H2A.X in the distinct region of damage is phosphorylated during this process (*1*).

1.1.2 The nucleolus

Found in every eukaryotic cell, the nucleoli are specific, membrane-less, nuclear organelles and sites of rDNA transcription, rRNA maturation and ribosome production (*23, 24*). Mélèse *et al.* showed that the efficiency of ribosome biogenesis is dependent on the size and organization of the nucleoli (*25*). In cycling cells, the nucleoli are formed at the end of mitosis, functionally active throughout the interphase, and disassembled in the proceeding

prophase of the cell division (*26*). In terminal stages of differentiation (e.g., in lymphocytes or erythrocytes), the nucleoli are rather small or not formed, whereas in rapidly dividing cells (e.g., in cancer cells), the nucleoli represent dominant and highly productive structures (*27*). The nucleoli assemble around the nucleolar organizer regions (NOR) (*26*). These are located on the short arm of 5 acrocentric chromosomes, where multiple rDNA copies cluster in head-to-tail tandem repeats. The nucleolus is either built around a single NOR or around several active NORs that converge in a single nucleolus (*28*). The rDNA encodes the ribosomal RNA and each active rRNA gene is transcribed by the DNA-dependent RNA polymerase I (Pol I) to synthesize a 45S pre-rRNA. This 45S pre-rRNA is further processed to generate three ribosomal RNAs (18S, 5.8S, 28S), which are post-transcriptionally modified by small nucleolar ribonucleoproteins (snoRNP). These mature RNAs together with the 5S RNA, transcribed by Polymerase III (*24, 29, 30*), form together with the expressed ribosomal proteins the ribosomal subunits in the cytoplasm.

Even though the nucleolus is a transient compartment, it is highly structured and organized in different sub-regions (Figure 1). RNA polymerase I is highly enriched in the fibrillar center (FC) and at the edge of the dense fibrillar component (DFC), where rRNA transcription takes place. In the DFC, pre-ribosomal RNA is spliced and modified by snoRNPs. The final maturation and assembly with ribosomal proteins takes place in the granular component (*26*). Subsequently, the 40S and 60S ribosomal sub-units are transported to the cytoplasm, where they assemble into an active complex. Besides contributing to ribosome biogenesis, nucleoli serve additional functions. Nucleolar proteome analyses identified over 700 proteins in the nucleolus of human cells, of which only 30 % are designated to ribosome subunit production (*31-33*). The other proteins of the nucleolus were reported in part to play a role in cell cycle regulation (*34, 35*) and stress response (*36, 37*) and have been linked to various multiple genetic disorders such as the Werner syndrome or to the Diamond-Blackfan anaemia, which is characterized by aberrant ribosome biogenesis (*26, 38*).

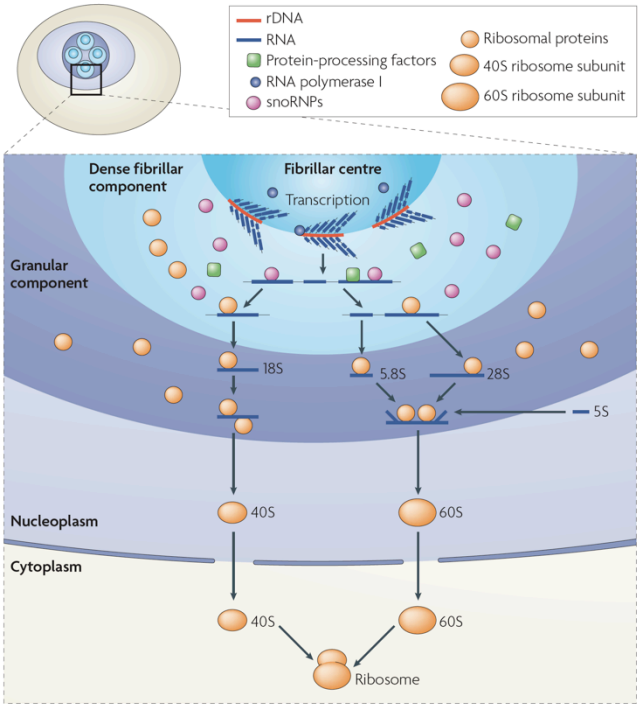

Figure 1: Compartmentalization and function of the nucleolus. The nucleolus is compartmentalized into different sub-regions shown here with their different functions – picture from (*26*)

RNA polymerase I

The DNA-dependent RNA polymerase I (Pol I) is exclusively found in the nucleolus. For the initiation of rRNA transcription, Pol I has to be part of a protein-multi-complex that includes factors like UBF, SL1, CK2, SIRT7, NM1, TTF-1 and TIF-IA (*39*). Pol I promoter specificity is mediated by TIF-IB/SL1, a complex containing the TAT-binding protein and five TATA binding protein-associated factors (TAF). UBF serves as a recruiter of Pol I and mediates the binding of Pol I to the DNA strand throughout the transcription process (*40*). Pol I was also found to interact with several DNA repair and replication factors, for example Topoisomerases I and IIα, Ku70/80 and PCNA (*39*).

rRNA genes

Somatic cells of higher eukaryotes contain several hundreds of rRNA genes with the same structure (Figure 2). A human diploid cell contains about 400 rRNA genes that are all organized in head-to-tail tandem repeats on five different chromosomes (*24*). However, also in highly active metabolic cells, only a subset of these genes (approximately 50 %) is transcribed (*41*). The remaining rRNA genes are silenced in a tissue- and cell type-specific

manner (*42*). These genes underlie the same epigenetic characteristics as any other gene of the chromosome and are regulated by post-translational modifications of histones and DNA methylation (as described in Chapter 1.1.2). RNA polymerase I can bind to the rRNA promoter (site of transcription initiation), but also binds to the highly homologous spacer promoter (*43*). The region of the repetitive enhancer elements is also called intergenic spacers (IGS). Transcripts from the spacer promoter are co-directed with the pre-mRNA and probably enhance transcription from the main rDNA promoter by directing Pol I (*44, 45*). The IGS is also relevant for the silencing of the rRNA genes since it gives rise to the dubbed promoter RNA (pRNA), important for the recruitment of the silencing complex (nucleolar remodeling complex, NoRC) (*41, 46, 47*).

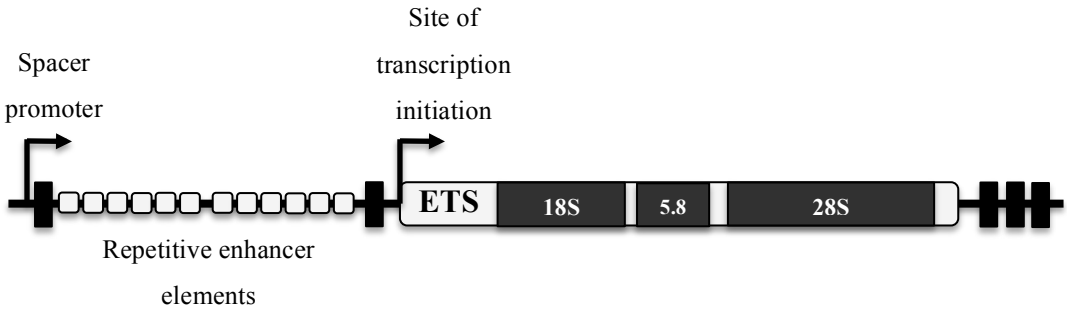

Figure 2: Structure of a rDNA gene. The diagram shows the structure of one copy of rDNA, which encodes for the 45S pre-mRNA. Black boxes indicate terminator elements, ETS indicates external transcribed sequence. The transcript of the ETS generates a non-functional RNA.

rRNA gene expression is influenced by diverse stress stimuli

The production of ribosome-subunits is heavily influenced by diverse stress stimuli and metabolic changes (*36*). The cell reacts to nutrient starvation, oxidative stress or inhibition of protein synthesis with a decrease of rRNA expression, whereas growth factors and proliferation stimulating agents increase the rRNA expression. A key regulator in this process is UBF, which enhances or represses rRNA production of active rDNA genes depending on its phosphorylation status (*48-50*). Furthermore, the down regulation of rRNA expression following different stress stimuli correlates with the binding ability of the transcription factor TIF-IA. It was shown that the phosphorylation of TIF-IA by JNK upon stress prevents the interaction between the TIF-IA and Pol I and hence inhibits rRNA expression (*37*).

Inhibition of rDNA transcription by Actinomycin D

Actinomycin D (ActD) or Dactinomycin is a cyclic polypeptide-containing antibiotic with DNA intercalating functions that is isolated from *Streptomyces* bacteria (*51, 52*). ActD intercalates in CG-rich regions of the DNA, thus stabilizing covalent topoisomerase I-DNA complexes and preventing RNA polymerase progression and RNA synthesis (*53*). The intercalation takes place downstream of rDNA transcription start sites, thus inhibiting transcription during elongation with the consequence that the RNA polymerase falls off the strand and synthesizes only a short RNA transcript (*54*). ActD treatment thus leads to an accumulation of short RNA transcripts over time (*55*). Nucleolar rRNA synthesis is particularly sensitive to ActD at a concentration of 50 ng/ml, while RNA polymerases II and III are only inhibited at higher concentrations (Pol II > 0.5 µg/ml, Pol III > 5µg/ml) (*56, 57*). In comparison, α-Amanitin is a potent Pol II and Pol III inhibitor that does not target RNA polymerase I (*58*). Upon ActD treatment, the nucleolar structure is reorganized. The different sub-components of the nucleolus segregate and nucleolar caps are formed around the nucleolar remnant (*59*). Nucleolar caps contain mainly RNA binding proteins, for instance the splicing factor PSF and pre-rRNA transcripts (*60*). ActD is a long known and established chemotherapeutic compound that is used to treat gestational trophoblastic cancer, testis cancer, Wilm's tumor, rhabdomyosarcoma and Ewing's sarcoma (*58*).

1.2 ARTD family

The ARTD (ADP-ribosyltransferases diphtheria toxin-like) family comprises a group of 18 proteins that share a common catalytic ART core domain. These enzymes have been formerly named PARPs (poly-ADP-ribose-polymerase), but were renamed based on structural and enzymatic evidences (*61*). The ARTD enzymes use NAD^+ as a substrate to modify target proteins by mono- or poly-ADP-ribosylation. The first discovery of a nuclear enzymatic activity able to synthesize an adenine-containing polymer was made in 1963 by the group of Mandel (*62*). The enzyme mainly responsible for the formation of this polymer and until now the most studied family member is ARTD1 (formerly PARP1) (*63, 64*). Over the last decades several additional family members have been identified and described. Some of these are also able to synthesize polymers of ADP-ribose (ARTD2, ARTD5, ARTD6), but contribute only little to polymer formation in the cell. Other family members exhibit only mono-ADP-ribosyltransferase activity (e.g., ARTD8 and ARTD10) or seem to be inactive, although containing the common catalytic domain (ARTD9 and ARTD13) (*61*).

Overall, the ARTD family members are involved in a variety of cellular functions such as genomic stability, transcriptional regulation, energy metabolism and cell death (*65-67*). However the mechanisms underlying these functions remain often unsolved and are the subject of a broad field of research.

1.2.1 Structure of ARTD1 and ARTD2

Mammalian ARTD1 is a 113.2 kDa protein consisting of different domains with distinct functions: an N-terminal DNA-binding domain comprised of three zinc-binding domains (Zn I, II and III) and a nuclear localization sequence (NLS), a central automodification domain containing a BRCA1 C-terminal (BRCT) phosphopeptide-binding motif, which was suggested to promote protein-protein interactions, a C-terminal catalytic domain containing the functionally uncharacterized tryptophan-, glycine-, and arginine-(WGR)-rich domain, a PARP regulatory domain which might be involved in polymer branching and the catalytic ART domain (*61*) (Figure 3). Recently, the group of Satoh showed that the WGR domain of ARTD1 was necessary for the enzymatic activation by RNA (*68*).
In comparison to ARTD1, ARTD2 was only discovered in 1990s as a result of the detection of residual poly-ADP-ribose forming activity in mouse embryonic fibroblasts (MEFs) lacking *ARTD1* (knockout) (*69*). Mammalian ARTD2 is a 66.2 kDA protein that shares the C-terminal domain of ARTD1. The catalytic domains of both enzymes show 69% similarity (*69*). ARTD2 lacks the N-terminal DNA-binding domain with the three zinc fingers and the central automodification domain, but has a SAF/Acinus/PIAS-DNA-binding domain, which comprises the nuclear localization sequence (Figure 3) (*70*). Haenni *et al.* could show that ARTD2 is able to auto-modify itself within the SAP domain (*71, 72*).

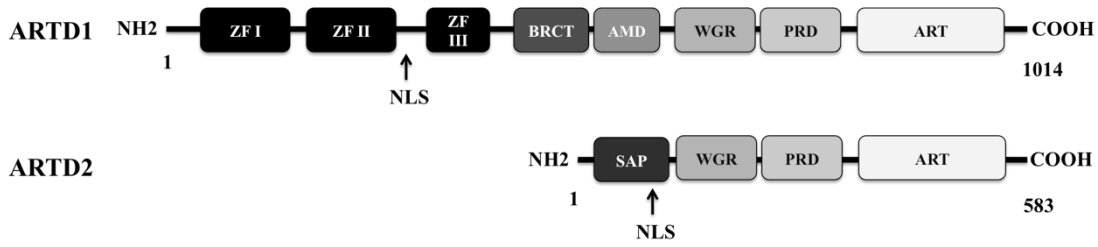

Figure 3: Structural overview of ARTD1 and ARTD2. ZF= zinc finger, BRCT= BRCA1 C-terminal (BRCT) phosphopeptide-binding motif, AMD= automodification domain, WGR= tryptophan-, glycine-, and arginine-(WGR)-rich domain, PRD=PARP regulatory domain, ART=catalytical domain, SAP= SAF/Acinus/PIAS-DNA-binding domain, NLS= Nuclear Localization Sequence.

1.2.2 ADP-ribosylation

Mono-ADP-ribosylation was originally identified as an activity of bacterial toxins such as *Corynebacterium diphtheria* toxin, which ADP-ribosylates the uncommon amino acid diphthamide (*73*). In contrast, poly-ADP-ribosylation (PARylation) is only found in higher eukaryotes, but not in yeast (*74*). The list of acceptor proteins is constantly growing and until now over 150 proteins have already been identified to be poly-ADP-ribose (PAR) acceptors. These proteins include ARTDs that are auto-modified as well as different DNA-binding proteins such as histones and topoisomerases that are trans-modified (*65, 66*). Furthermore, covalently modified PAR acceptors and non-covalently PAR binding protein modules have to be distinguished (*75*).

The detailed mechanistic process of ADP-ribose formation is depicted in Figure 4. In brief, the enzymes use nicotinamide adenine dinucleotide (NAD^+) as a substrate to transfer an ADP-ribose unit during initiation to an acceptor site of a target protein, generating nicontinamide (NAM) as a byproduct. The acceptor sites for mono-ADP-ribose are side chains of specific amino acid residues and so far the following acceptor amino acids in eukaryotic cells were reported to covalently bind ADP-ribose: lysine (K), arginine (R), glutamate (E), aspartate (D), cysteine (C), diphthamide (Dph), phospho-serine (pS) and asparagine (N) (*61*). The attached mono-ADP-ribose is further extended to oligomers and polymers of a length of 200 units *in vivo* and 400 units *in vitro* (*76*). Classical PAR antibodies can recognize only polymers over 10 ADP-ribose-units, which is a limiting factor for detecting PAR formation *in vivo* (*77*). The turnover of PAR formed upon cellular stress is

rather quick (*in vivo* half-life > 40s to 6min). Within the first 40s, 85% of polymers are degraded. The residual fraction is more slowly catabolized (*78-80*).

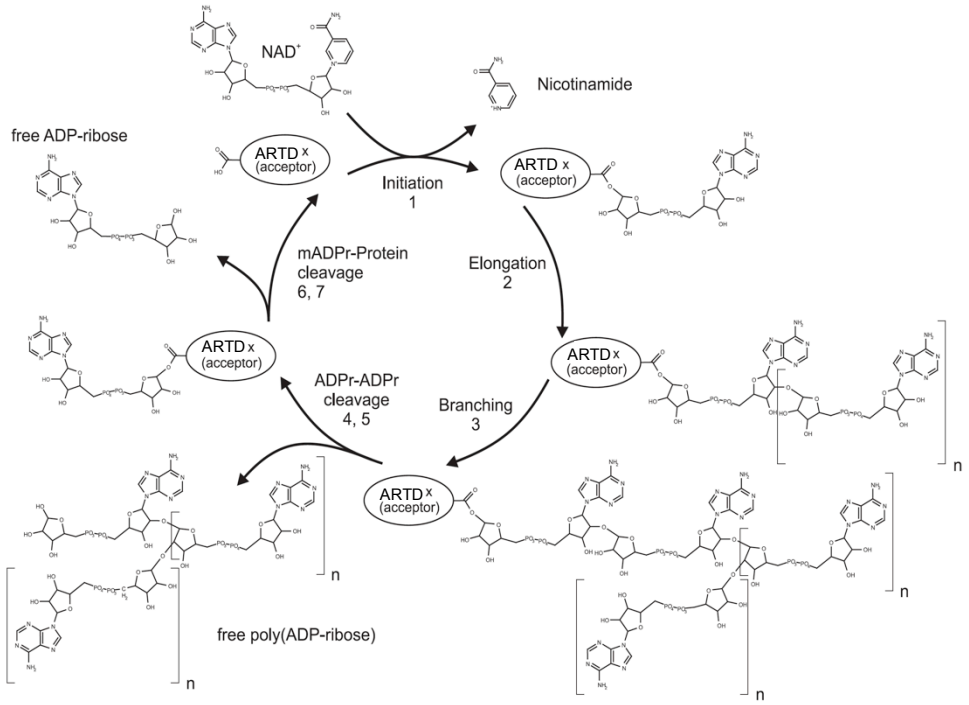

Figure 4: Poly- ADP-ribose metabolism. Different steps of initiation, elongation, branching and degradation of PAR formation are shown (modified from Hassa et. al (*65*)).

The rapid turnover of the polymers depends mainly on the activity of cellular ADP-ribose-protein hydrolases such as poly-(ADP-ribose)-glycohydrolase (PARG) or ADP-ribosyl hydrolase 3 (ARH3). These enzymes are able to hydrolyze the protein–ADP-ribose bonds between different ADP-ribose units (*81-84*). PARG is the major PAR-degrading enzyme. The knockout of PARG in mice leads to lethality in early embryogenesis, which hints at the importance of the enzyme and the regulation of PAR formation (*85*). PARG is an enzyme with exo-and endoglycosidase activity and generates large amounts of free ADP-ribose, but cannot cleave off the last ADP-ribose-moiety from the target protein (*86, 87*). Very recently, our group reported that some macrodomain-containing proteins are able to hydrolyze the mono-ADP-ribose modification catalyzed by ARTD10, providing strong evidence that ADP-ribosylation is a reversible PTM (*88*). Free ADP-ribose may for example function as a signal transducer in apoptosis signaling, DNA repair or cell cycle progression (*89*). Furthermore, poly-ADP-riboses can be non-covalently bound by PAR-binding proteins, which coordinate

several intracellular pathways (for detailed review see (*75*)). The major fraction of rapidly produced polymers plays a role in transient and dynamic cellular processes such as chromatin regulation and transcriptional response upon stress induction (*66*). PAR formation is not only stimulated by genotoxic stress, but also by mitogen induction (*90*). The contribution of ARTD2 to the total PAR synthesis upon genotoxic stress was shown to be approximately 15 %, which might be due to a lower abundance of ARTD2 or to lower enzymatic activity (*91, 92*). The highly negatively charged poly-ADP-ribose polymers lead to changes in physical and biochemical properties of the target proteins, which can result in the disruption of protein-DNA or protein-protein binding, as seen for ARTD1 and Topoisomerase I (*93-95*). Furthermore, the polymers can even inhibit the enzymatic activity of some DNA dependent enzymes such as Topoisomerase I and the ATPase Cockayne Syndrome group B (*96*). The activity of the enzyme is strictly dependent on the NAD^+ levels in cells (*66, 97*). The half-life of NAD^+ in proliferating cells is around 1-2h (*98-100*), but when ADP-ribose polymers are formed under strong stimulating conditions such as genotoxic stress, the cellular pool of NAD^+ is rapidly depleted and diminishes to 10-20% of the normal NAD^+ levels (*101, 102*). The NAD^+/ATP depletion after ARTD1 hyperactivation can lead to poly-ADP-ribosylation dependent translocation of apoptosis inducing factor (AIF) to the nucleus and consecutive cellular deregulation or programmed cell death (*103*).

1.2.3 Cellular processes regulated by ARTD1 and ARTD2

ARTD1 and ARTD2 are involved in several biological processes such as genome stability, chromatin regulation, genotoxic stress response, cell cycle regulation, cell death, inflammation and transcriptional regulation (*65-67*). Mice lacking *ARTD1* are healthy and fertile, but hypersensitive to ionizing radiation and alkylating agents (*104-106*). *ARTD2* knockout ($^{-/-}$) mice are also viable and hypersensitive to ionizing irradiation. Initial description of the *ARTD2* $^{-/-}$ phenotype provided evidence of an involvement of ARTD2 in different developmental processes, such as T-cell development or spermatogenesis (*107*). Double knockout mice (*ARTD1*$^{-/-}$ and *ARTD2* $^{-/-}$) are not viable and die at the onset of gastrulation, indicating that ARTD1 and ARTD2 play a crucial role during embryonic development and that the enzymes might be functionally redundant (*108*). However, ARTD2 is not as well studied as ARTD1 and besides some overlapping functions with ARTD1, a clear comprehension of its cellular function is still missing.

Genotoxic stress signaling

Originally, ARTD1 activity was described to play a role in the DNA damage response, particularly the base excision repair (BER) since it is strongly stimulated by genotoxic stress such as reactive oxygen species or alkylating agents (e.g., MNNG) (*109, 110*). ARTD1 was shown to be recruited to single-strand breaks (SSB) *in vivo* and thereby attracts X-ray repair cross-complementing I (XRCC1), a crucial scaffold protein that recruits other factors to SSBs and initiates base excision repair (BER) (*111*). Similarly, overexpressed ARTD2 was found to interact with XRCC1 and with other proteins of the DNA repair pathway, including DNA polymerase β and DNA ligase III (*112*). However, recent findings show that ARTD1 has only a minor function in BER and only participates in BER under conditions when the amount of unrepaired SSB exceeds the repair capacity of the cell (*110, 113-115*). Furthermore, it was suggested that ARTD1 is not only binding SSB, but also double strand breaks (DSB) as well as other DNA structures such as replication fork structures *in vitro* and might thus play a role in DNA damage repair at stalled replication forks (*116-118*). The diverse and sometimes contradictory observations reveal that the functions of ARTD1 and ARTD2 during DNA damage and repair processes are not yet completely understood. Ongoing research points more and more at functions of ARTD1 in non DNA damage response processes (*119*). Along this line, ARTD1 activity can be induced independent of DNA damage, most likely by phosphorylation via different kinases such as extracellular-signal regulated kinase 2 (ERK2) (*120*). Thus, posttranslational modification of ARTD1 and probably ARTD2 likely plays a significant role in the PAR-signaling process.

Chromatin regulation

ARTD1 is also known as an architectural nucleosome-binding factor and as a chromatin-modifying enzyme. Unmodified ARTD1 can bind to nucleosomes and lead to compaction, but upon automodification the structure is relaxed (*121, 122*). Histones can be poly-ADP-ribosylated as described earlier (see chapter 1.1.2) and thus, ARTD1 is involved in the regulation of higher-order chromatin structure. However, only a small fraction (less than 1%) of the histones were found to be modified *in vivo* (*123, 124*). Histone H1 is the main ADP-ribose acceptor in native chromatin, whereas in H1-depleted chromatin (open status), H2B is the preferential target of ARTD1 (*125*). Similar functions were also proposed for ARTD2 (*126*). However, ARTD2 is not able to modify histones *in vitro* (*127, 128*). As described above, genotoxic stress induces ADP-ribosylation, which consecutively leads to the

recruitment of different factors. Another model proposed that poly-ADP-ribosylation of histones might cause their dissociation from the DNA, thus giving distinct repair factors access to damaged DNA (*129, 130*). ADP-ribosylation of histones likely also takes place throughout other cellular processes such as transcription and remodeling, but the variation in polymer length may not be detectable by antibodies (as described earlier). Together, these models define ARTD1 rather as a chromatin remodeler, than a direct DNA damage repair enzyme (*10, 11*). In contrast, it was very recently shown that ARTD1 plays a major role during heterochromatin formation and interacts with pRNA – the non-coding RNA transcribed from a part of the intergenic spacers (*131*).

ARTD1 and ARTD2 have also other chromosome-related functions, since they both interact with the kinetochore proteins centromere protein A (CENPA), centromere protein B (CENPB) and with the mitotic spindle checkpoint protein BUB3 in a cell-cycle dependent manner (*132, 133*). *ARTD2* $^{-/-}$ male mice exhibit problems with accurate chromosome segregation, since the maintenance of centromeric heterochromatin structure and/or mitotic spindle integrity is disturbed (*108*). Moreover, ARTD2 has been implicated in the regulation of facultative heterochromatin integrity during X chromosome inactivation (Xi) (*108*).

Transcriptional regulation

ARTD1 influences transcriptional activation either as co-factor of the transcription complexes or via histone modifications and histone replacement. Hassa *et al*. could show for the first time that ARTD1 is a promoter-specific co-activator of nuclear factor kappaB (NF-κB) – a regulator of inflammation and the release of cytokines and inflammatory mediators (*134-137*). Moreover, ARTD1 was shown to physically interact with p300/CBP and with both subunits of NF-κB (p65 and p50) and to synergistically co-activate NF-κB-dependent target gene expression (*134, 136*). Ju *et al.* confirmed those observations with their report that ARTD1 forms a co-activator/co-repressor exchange complex with factors such as nucleolin, nucleophosmin and topoisomerase IIb (*66, 138-140*). Moreover, by modulating the chromatin environment, ARTD1 also influences the transcription of diverse genes (*141, 142*). ARTD1 was found to be enriched at promoter sites of actively transcribed genes, whereas histone H1 is absent from these sites (*67, 141*). It appears that ARTD1 can exclude H1 from certain promoters, suggesting an interplay between both proteins (*67, 143*). Moreover, ARTD1 activity is required for a nucleosome specific histone H1-high-mobility group B (HMGB1) exchange event and thus influences local chromatin structure (*144*). ARTDI was also

reported to maintain levels of H3K4me3 by inhibiting the recruitment of a lysine-specific demethylase KDM5B to sustain open chromatin (*142*). ADP-riboslyation of transcription factors has also been reported to have regulatory functions, as it regulates for example the CLOCK transcription factor, which is crucial for the maintenance of circadian rhythms of organisms (*145*).

Independent of ARTD1's function, ARTD2 was found to be involved in the modulation of several transcription factors, such as TTF-1and SIRT1 (*146*). Thereby, ARTD2 has a dual role, since it is a transcriptional repressor of SIRT1 and has activator functions together with TTF-1 for the expression of surfactant protein B (*147, 148*). ARTD2 was additionally reported to directly interact with topoisomerase I and IIβ and thus influences transcription indirectly by regulating the DNA structure (*149, 150*). As a modulator of the chromatin, ARTD2 was shown to regulate transcriptional intermediary factor (TIF)-1β and heterochromatin protein (HP)-1α (*151*). Furthermore, a recent publication inferred that ARTD2 acts as a co-repressor in an activity independent function by recruiting deacetlyases (HDACs) to active genes such as c-myc (*152*). Finally, Meder *et al.* analyzed the role of ARTD1 and ARTD2 in the nucleolus, showing that both enzymes colocalize with B23/nucleophosmin. No functional evidence of ARTD1 and ARTD2 on RNA polymerase I transcription was however described in that study (*153*). Another study showed that ribosomal biogenesis was influenced by ARTD1 at the post-transcriptional level and by pre-rRNA processing in *D. melanogaster* (*154*).

1.2.4 PARP inhibitors

The first PARP inhibitors were developed based on the benzamide structure to mimic NAD^+ - the substrate of the ARTDs. One of the first effective PARP inhibitors was 3-Aminobenzamide (3-AB), which functions as a competitive inhibitor (Figure 5). This rather simple structure is prone to bind not only to ARTDs but also to other NAD^+-consuming enzymes. Furthermore, its solubility and efficiency is poor (*155, 156*). Due to the homology of the catalytic active domain of the different ARTDs (especially ARTD1 and ARTD2), PARP inhibitors are not isoform specific, but rather inhibit several family members (*156, 157*). The basic compound 3-AB was improved and second and third generation PARP inhibitors have emerged. An inhibitor of the second generation is *N*-(5,6-Dihydro-6-oxo-2-phenanthridi-nyl)-2-acetamide hydro-chloride, also known as PJ-34 (Figure 5), which is a

potent PARP inhibitor (EC_{50}=20nM), but lacks specificity as described above (*157, 158*). Furthermore, it was recently shown that PJ-34 binds to Pim kinases, which are proteins that are unrelated to ARTD (*159*). However, PJ-34 is still widely used in different fields of research (*160*) (see later).

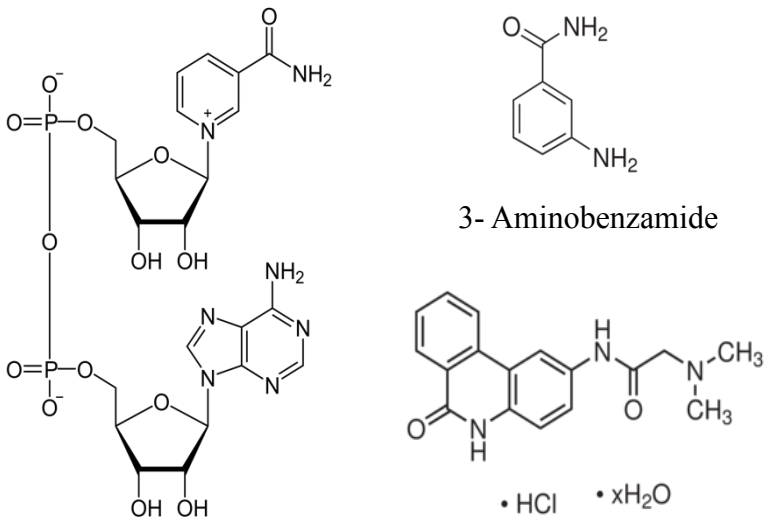

Figure 5: Structure of nicotinamide adenine dinucleotide and two PARP inhibitors.
3-Aminobenzamide – a first-generation PARP inhibitor and PJ-34 – a second-generation PARP inhibitor.

The third generation of PARP inhibitors comprises competitive inhibitors binding tightly to the active site of ARTDs. Olaparib and Veliparib seem to specifically inhibit ARTD1 and ARTD2 with high efficiency (Olaparib IC_{50} for ARTD1= 5nM, for ARTD2= 1nM; Veliparib IC_{50} for ARTD1=5.2 nM for ARTD2= 2.9nM; Figure 6), but also bind ARTD3, which however was not confirmed to be active *in vivo* (*157*). PARP inhibitors recently reached great attention due to their beneficial effect as therapies for patients with breast or ovarian cancer with genetic defects in the *BRCA1/2* gene (*161-164*), which later was shown not to be a requirement for sensitivity to PARP inhibitors (*155*). There are currently ongoing clinical trials with PARP inhibitors also in combination with radiation or chemotherapeutics, including the treatment of other cancer types such as advanced solid tumors and lymphoma (Figure 6) (*155, 161, 165*). However, none of the PARP inhibitors has so far been approved for clinical use.

Interestingly, these inhibitors might have a broader application spectrum, for instance in inflammatory or ischemia-reperfusion-associated diseases (*161*). Preliminary experiments for this kind of application have however only been tested in animal models. Especially PJ-34 was shown to be an effective inhibitor in angiogenesis (*166, 167*) and to improve endothelial and cardiac dysfunction associated with aging in mice (*168, 169*). This wide range of applications raises the question to which extent the effect is indeed due to inhibition of ARTD1 and 2. Thus, their specific mode of action remains to be further investigated.

Drug	Industry-Sponsor	Cancer	Association	Phase
Ku-0059436	National Cancer	BRCA1/2 mutated breast/ovarian	Carboplatin	I
AZD2281	Institute (NCI)	cancers TNBC	(Alkylating agent)	
Olaparib	NCI	Mixed muellerian, cervical, ovarian, breast, primary peritoneal, fallopian, endometrial cancers and	Carboplatin	I
IC_{50} = 5 nM PARP1				
IC_{50} = 1 nM PARP2		Carcinosarcoma		
IC_{50} = 1.5 μM TNKS	Astra Zeneca	Advanced solid tumors	Topocetan (Topoisomerase I inhibitor)	I
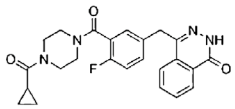		Melanoma neoplasms	Dacarbazine (Alkylating agent)	I
		Pancreatic neoplasms	Gemcitabine (Nucleoside analog)	I
		Breast/Ovarian neoplasms BRCA1/2 mutated	Single	II
	Cancer Research UK	Glioblastoma	Temozolomide (Alkylating agent)	I
	NCI	Neoplasms	Cisplatin/Gemcitabin	I
CEP-9722 (prodrug)	Cephalon	Advanced and metastatic solid tumors	Single	I/II
IC_{50} = 20 nM PARP1		Solid tumors or mantle cell lymphoma	Gemcitabine/Cisplatine	I
IC_{50} = 6 nM PARP2		Solid tumors	Single + Temozolomide	I
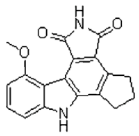				
ABT-888/Veliparib	Abbott	Solid tumors Lymphomas	Topocetan (Topoisomerase inhibitor)	I
	Abbott			
K_i = 5.2 nM PARP1		Colorectal cancer	Temozolomide	II
K_i = 2.9 nM PARP2		Multiple myeloma	Bortezomib (proteasome inhibitor) Dexamethasone (corticosteroide)	I
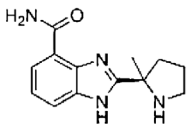		Colorectal cancer	Folfiri = Folinic acid + Fluorouracil + Irinotecan	I
INO-1001	Inotek pharmaceuticals	Acute myocardial infarction	Single	II
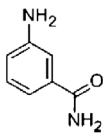				
Rucaparib	Clovis-Hoosier Oncology	TNBC	Cisplatin	II
AG-014699		with BRCA1/2 mutations		
PF-0136738	Cancer research UK	BRCA1/2 mutated breast and ovarian cancers	Single	II
K_i = 1.4 nmol/L	Clovis Oncology	Advanced solid tumors	Carboplatin	I
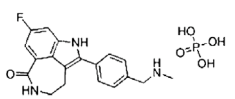				
BMN 673	Biomarin Pharmaceuticals	Solid tumors	Single	I
ND		Hematological malignancies		

Figure 6: Overview of third generation of PARP inhibitors in clinical trials (*165*)

1.3 The cell cycle

The term “cell cycle” refers to the process of cell division and the duplication of DNA, which is one of the most fundamental processes in biology (*170*). To ensure a proper cell division, a tremendous network of proteins and checkpoints tightly controls this process.
The cell cycle is divided into two parts, the interphase and mitosis, and takes on average 24 h for a normal cycling human cell (*171*). The interphase is further divided into the G_1, S and G_2 phases. During G_1, which is in most cases the longest cell cycle phase, the cell is growing and preparing itself for DNA synthesis. In S phase, DNA duplication takes place and by the end of the S phase, the cell contains the double amount of chromatids. The replicated copy of each chromatid is still connected to the original copy. During G_2 phase the proteins required for mitosis are synthesized. Moreover, the cell ensures that the DNA was replicated correctly before entering into mitosis. Mitosis is the stage of cell division, which is further divided into Pro-, Meta-, Ana- and Telophase (*172*). The sister chromatids are separated and two daughter cells arise. If extracellular conditions are disadvantageous, cells delay their progression through G_1 phase and may even enter a quiescent stage known as G_0 phase, in which they can remain for days, weeks or years before resuming proliferation (*172*). The aspects described above relate mainly to mammalian cells, since the cell cycle of yeast and plant cells functions slightly differently, although there are many homologous cell cycle factors (*173*).

1.3.1 Control of the cell cycle

The key-class of proteins responsible for a correct cell division are the Cyclins and the Cyclin-dependent kinases (Cdks) (*174*). The Cyclins received their names due to the cyclic fluctuation of their protein levels throughout the cell cycle (Figure 7). The Cyclins (the regulatory subunits) form a complex with Cdks (the catalytic subunit) and thus form active enzyme-complexes. The Cdks themselves are expressed constantly during the cell cycle and have only very little activity in the Cyclin-unbound state. The kinases are phosphorylated by Cdk activating kinases (CAK) after interacting with Cyclins, an event which turns them into active serine-threonine kinases that phosphorylate different target proteins in a cell cycle phase specific manner (*174*). The activity of the Cyclin-Cdk-complex is regulated by different events such as the induction and degradation of the Cyclin subunit, the phosphorylation of the Cdk subunit by CAK, the inhibition of the active complex by Cdk inhibitors and the spatial distribution of these factors in different cellular compartments (*175*).

At least 29 genes were found to encode related Cyclin proteins that share a conserved amino acid sequence termed the "Cyclin box". This domain is responsible for protein-protein interactions with different enzymes, including the Cdks (*176*). The best-known Cyclins are those directly regulating the cell cycle: Cyclin A, B, D and E. For other Cyclins (e.g., Cyclin F, G, I, J) it is not even known if they interact with Cdks (*176*).

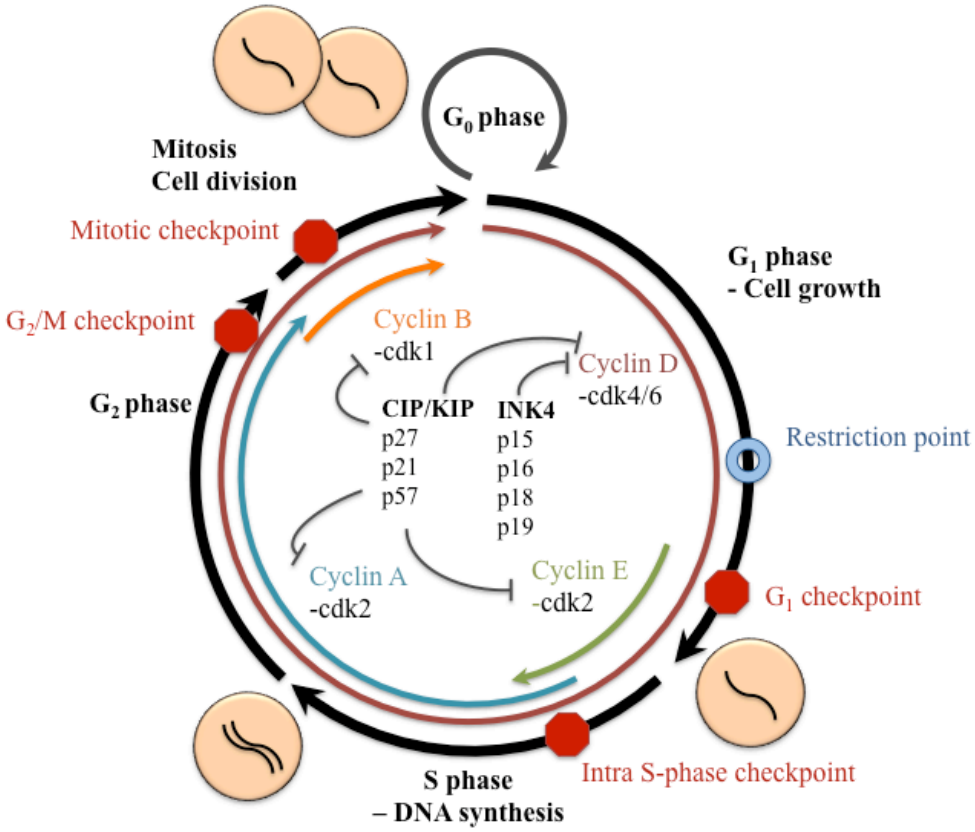

Figure 7: Scheme of the cell cycle. The different cell cycle phases are indicated and a cell division is schematically depicted. The cyclin-Cdk complexes of the different cell cycle phases are indicated and the possible Cyclin-cdk- inhibitors are shown (CIP/KIP and INK4 family). The restriction point in mid-G_1 phase is labeled in blue and cell cycle checkpoints are shown in red.

Cyclin A forms a complex with Cdk2 during the S-phase and exists in two isoforms. While Cyclin A1 is only expressed during embryogenesis, Cyclin A2 is active throughout cell progression of somatic cells (*177*). Cyclin B interacts with Cdk1 and regulates the entry into mitosis. There are three Cyclin B isoforms, which differ in their subcellular localization. However, Cyclin B1 is the most studied one (*178*). Cyclin D appears in three isoforms, which are expressed as long as growth factors are present in the extracellular matrix and forms an active complex with Cdk4 or 6 throughout the G_1 phase (*179*). The three different Cyclin D

isoforms are very similar, but are expressed in a tissue-specific or developmental-stage dependent manner (*180*). Cyclin E forms a complex with Cdk2 to enable G_1-S phase transition. The Cyclin E1 isoform is the major isoform, whereas Cyclin E2 is usually expressed at low levels, but more strongly expressed in various cancer cells (*181*).

1.3.2 Progression from G_0 phase to S phase

In regard to the results of the thesis, a detailed explanation of G_0 phase, G_0-G_1 phase transition and G_1-S-phase transition is presented here. Detailed explanations of the later cell cycle phases are descried elsewhere (*172, 177, 182-184*).

G_0 phase

Cells enter the G_0 phase because of growth inhibition or when they are terminally differentiated. During this process, transcription is reduced by the dREAM complex, which is responsible for the repression of many cell-cycle-regulating genes (over 800 genes) (*185*). The dREAM complex is composed of E2F-4, p130, DP and MuvB (*185*). When E2F-4 is removed from this complex, uncontrolled cellular proliferation is induced (*186*). In addition, E2F-4 can interact with HDAC and other chromatin-remodeling factors, which are important for repression of the G_1 phase genes (*187*). Furthermore, p27 – a Cyclin-Cdk-Inhibitor – is strongly induced in resting, quiescent cells. p27 is an important factor for establishing the G_0 phase, because its depletion prevents the exit from the cell cycle and entering into the G_0 phase (*188*). In certain circumstances, cells can rest in the G_0 phase until they die, but in most cases it is a transient state (*172*). For instance, liver cells neither grow nor divide, but keep the capacity to start cell division and to regenerate the tissue upon damage (*172*). Under favorable conditions, such as growth factor induction, cells are able to re-enter the cell cycle. In contrast, differentially terminated cells are insensitive to mitogens and rest permanently in the G_0 phase (*189*). Very often, the resting/re-entry of the cells is defective in tumor cells, which makes it an interesting subject to study, although the G_0 phase is still not very well understood (*190*).

G_0-G_1 phase transition

Because of the reduced transcriptional activity, it is assumed that transcription factors are repressed in G_0 phase and re-activated after mitogen induction. Several studies implicate that the E2F transcription factor family is involved in regulating cell cycle re-entry. For example, cells lacking E2F-1 show a delayed cell cycle re-entry (*191*). Furthermore, it has been recently shown that Cdk3, which is structurally similar to Cdk1 and Cdk2, binds Cyclin C during G_0-G_1transition and stimulates the phosphorylation of pRb during this transition in some human tumor cells (*192*). The inactivation of pRb seems to be sufficient for cell cycle re-entry (*189*). During the process of re-entry, p27 is exported from the nucleus to the cytoplasm and targeted for degradation. This process is mediated by Cyclin D2 (*193*).

Furthermore, microRNAs should be considered as important cell cycle regulators, especially for the re-entry from G_0 phase. Levels of several miRNAs are decreasing during the transition from G_0 to G_1 phase. For example, miR-503, an extended member of the miR-16 family, was shown to be highly expressed in G_0 phase, but immediately decreases when cells enter G_1hase. Although its function is not yet clear, the increased expression points to its importance during cell cycle entry (*194*).

G_1-S phase progression

pRb is one of the key players of the early cell cycle phases and part of a protein family of three members (pRb= p110, p130, p107) (*195*). pRb functions as a classical tumor suppressor gene and is absent or mutated in one third of all tumors (*196, 197*). A specific mutation of the *Rb* gene leads to a rare pediatric eye tumor, retinoblastoma, which gave the protein its name (*198*). Especially in human bladder carcinoma, pRb was found to be hyper-phosphorylated in asynchronous cells, which hints at a disruption of p16 function or an overexpression of Cyclin D1 (*199*). pRb protein is normally hypo-phosphorylated in G_0 phase and thus able to repress transcription by binding E2F-1. The most prominent candidates bound by pRB are the E2F proteins, but also histone deacetylases and chromatin remodeling complexes (*200*). The large pocket region of pRb binds to E2F, the small pocket binds proteins with an LXCXE motif (e.g., HDAC or Cyclin D1) (*195*). The D-type Cyclins are induced in early G_1 phase after mitogen induction and interact with Cdk4 and/or Cdk6. The active complex phosphorylates the members of the retinoblastoma protein family, which all contain multiple phosphorylation sites (e.g., pRb has 16), of which only some are recognized by the Cyclin D-Cdk4/6 complex.

E2F proteins are a family of transcription factors of which three are activators (E2F-1 to 3) and five are repressors (E2F-4 to 8) (*201*). E2F target genes are Cyclin E, A, D1, Cdc2, Cdc25A, DNA polymerase α, Cdc6 and minichromosome maintenance (MCM) proteins (*202*). E2F is also involved in apoptosis and thus responsible for transcription of apoptosis protease-activating factor 1, p73 and ARF (*203*). The active E2F transcription factor is a heterodimeric complex of E2F protein and a member of the DP family (*204, 205*). For transcriptional activity, the E2F-1 complex interacts with the histone acetyltransferase (HAT) p300/CBP co-activator proteins (Figure 8). p300 is bridging the E2F-1 complex to the basal transcriptional machinery and thus facilitates the assembly of multiprotein cofactor complex (*206*). The intrinsic HAT activity can loosen the chromatin by acetylating histones. Furthermore, the acetyltransferase is able to directly acetylate E2F-1, which increases its DNA binding activity and protein stability (*207*).

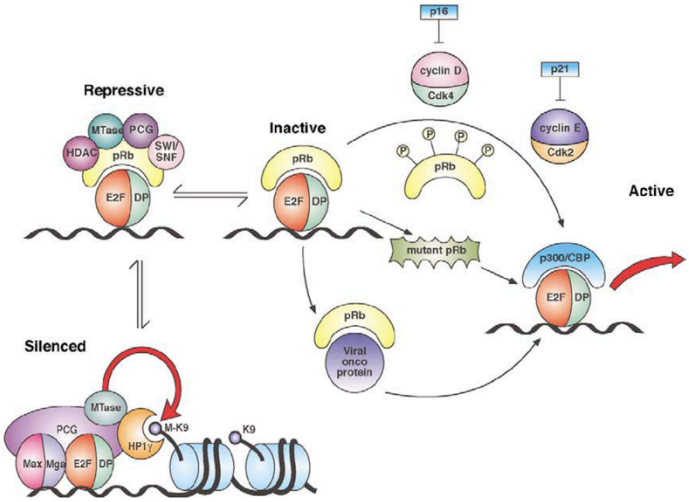

Figure 8: Regulation of E2F-1 activity (from Stevens et al. (*203*)).
pRb= Retionblastoma protein, HDAC= histone deacetylase, PCG= polycomb group proteins, SWI/SNF= SWItch/Sucrose Non Fermentable nucleosome remodeling complex, MTase= methyltransferase, p= phosphorylation.

The main driver of G_1-S phase progression is Cyclin E in complex with Cdk2. Cyclin E is a downstream target of E2F-1/DP1. Upon phosphorylation by Cyclin D-Cdk4/6, the pRb protein-binding pocket undergoes a conformational change and the bound protein (such as E2F-1) is released (*208*). Free E2F-1 binds to the promoter of the Cyclin E gene and thus Cyclin E expression is increased in late G_1 phase. Via a positive feedback loop, newly

formed Cyclin E/Cdk2 complexes further phosphorylate pRb to fully inactivate the protein and release all bound E2F (*195*). Moreover, Cyclin E-Cdk2 kinase activity is essential for the initiation of DNA replication by facilitating the loading of MCM chromosome maintenance proteins onto origins of replication (*209*). During early S phase the active Cyclin A-Cdk2-complex interacts with E2F-1, which leads to the loss of DP-1 and thus inactivates E2F-1 transcription factor during S phase progression (*203*).

1.3.3 Cyclin-dependent kinase inhibitors

Important regulators of the Cyclin-Cdk-complex are Cdk inhibitors, which bind transiently to the complex and inhibit its activity (*210, 211*). The Cdk inhibitors are divided into two main families, whose members share structural and functional homologies – the INK4 family and the CIP/KIP family (*210, 211*). The INK4 family comprises four members: $p16^{INK4a}$, $p15^{INK4b}$, $p18^{INK4c}$ and $p19^{INK4d}$, which are all specific for Cdks 4 and 6 and hence play a role during early G_1 phase (*175*). The key representative of the family is p16, which is one of the most commonly inactivated tumor suppressors in cancer (*212*). p16 is also used as a senescence marker, since it is not up regulated in quiescent or differentiated cells, but only in senescent cells (*213, 214*). Particularly interesting is, that the p16 gene CDKN2A can be transcribed from two distinct promoters, which leads to two structurally and functionally different proteins – p16INK4a and p14ARF (*215*). Both of these proteins are tumor suppressors. ARF is induced upon mitogen stimulation and involved in the DNA damage response of MDM2/p53 signaling, but also acts as an inhibitor of ribosome biogenesis in the nucleolus (*216, 217*). The second Cdk inhibitor family is named CIP/KIP family and comprises three proteins: $p21^{CIP1}$, $p27^{KIP1}$ and $p57^{KIP2}$. These inhibitors share a broad concentration-dependent specificity towards most of the Cyclin-Cdk-complexes through binding to Cyclins and Cdks by a conserved N-terminal domain (*210*). At low concentration, they mainly inhibit the Cyclin D-Cdk-complex, while at higher concentration also other Cyclin-Cdk-complexes are targeted. Interestingly, the CIP/KIP inhibitors may also function as adaptors to promote Cyclin-Cdk-complex assembly and programming them for certain functions (*218*). CIP/KIP Cdk inhibitors are regulators of apoptosis in various ways depending on the cellular context (*210*). Although they share broad specificity, each of the three family members also has specific biological functions. p21 is an important transcriptional target of p53 during DNA-damage induced cell cycle arrest (*210*). p27 is usually elevated in mitogen-starved cells and

other quiescent states and it is rapidly down regulated when cells resume the cell cycle in the G_1 phase (*219, 220*). p57 is the least studied family member, but it was shown to play a role during embryonic development (*219, 221, 222*).

1.3.4 Cell cycle checkpoints

High accuracy and fidelity are required throughout each phase of the cell cycle to ensure a correct cell division. Therefore, the cell cycle is controlled by several cell cycle checkpoints and the restriction point. The restriction point in the mid-G_1 phase is the is the moment when the cell commits to cell division if the environmental conditions (presence of growth factors) are favorable (*196*). The key regulatory event during this stage is the phosphorylation of pRb, which abrogates the binding to E2F-1 and subsequently leads to activation of E2F-1 and the expression of its target genes. As described in the previous section, Cdk-inhibitors (e.g., p16, p21 and p27) are important regulators of the Cyclin-Cdk- complexes, which in turn control the interaction of pRb with E2F-1 and thus are themselves also of great importance for this restriction point (*223*).

The checkpoints (Figure 7) are mostly activated upon DNA damage and induce growth arrest to gain time for the repair of the damaged DNA in order to prevent mutated DNA from being replicated. Hence, regulators of these checkpoints are very often mutated in cancer cells, leading to impaired cell division and uncontrolled cell growth. Beside the restriction point in G_1, a G_1 checkpoint exists, which is activated upon DNA damage and leads to a sustained sometimes even permanent arrest of cells in late G_1. This checkpoint is driven by the ATM/ATR-Chk2/Chk1-p53/MDM2-p21-pathway (*224-226*). Upon DNA damage, ATM/ATR phosphorylates p53 and its ubiquitin ligase MDM2, which usually targets p53 for degradation. Upon DNA damage, MDM2 is not only phosphorylated and thus inactivated by ATM/ATR, but also by Chk1/Chk2, which leads to p53 stabilization (*227*). p53 is the main transcription factor for the $p21^{CIP1}$ gene – a Cdk inhibitor of the G_1 phase, which itself arrests the cell cycle by blocking pRb phosphorylation and subsequently allowing complex formation with E2F-1 (*224, 226*). Another pathway that is activated during DNA damage is regulated by CDC25a, which usually is an important phosphatase to positively regulate the Cyclin E-Cdk2 complex. The phosphorylation of CDC25a is increased upon DNA damage and leads to enhanced degradation of CDC25a. Consequently, the Cyclin E-Cdk2 complex is not dephosphorylated and thus activated, and cells do not progress into S phase. This

pathway is activated much faster upon DNA damage than the rather slow p53 pathway (*228, 229*).

The intra-S-phase checkpoint can be activated in response to double strand breaks, which lead to a reduced DNA synthesis rate (*229*). On the other hand, DNA damage or depletion of deoxyribonucleotides can cause stalling of the replication fork to prevent replication of the damaged DNA and to allow the cell to recover after DNA repair (*229*). This checkpoint is additionally controlled in two ways by the ATM/ATR signaling machinery (*229*). On one hand and as described before, the phosphatase CDC25a influences Cdk2 activity. Destabilization of CDC25a upon DNA damage leads to a failure to activate Cdk2, thus prevents CDC45 loading and consecutively impairs recruitment of the DNA polymerase. Alternatively, NBS1, a member of the Mre11-Rad50-NBS1 (MRN) complex, is phosphorylated by ATM, which in turn phosphorylates H2A.X (yH2A.X) (*22, 230*) and recruits other factors of the DNA repair machinery to DNA double strand breaks (*231*).

The G_2/M checkpoint before mitosis prevents the segregation of defective chromosomes, which might be induced by DNA damage at earlier stages of the cell cycle (*232*). An important player at the G_2 checkpoint is the mitosis-promoting activity of the Cyclin B-Cdk1 kinase. ATM/ATR, Chk1/Chk2 and p38-kinase perturb Cyclin B-Cdk1 activity after stress by degrading the activation-promoting CDC25 family of phosphatases (*182*). Under normal conditions, CDC25 phosphorylates maturation promoting factor (MPF), which subsequently phosphorylates Cdk1.

The last checkpoint is the mitotic or spindle assembly checkpoint, which is active during metaphase and blocks the transition to anaphase by inhibition of the CDC20 activator anaphase-promoting complex (APC). This checkpoint is induced by wrongly attached kinetochores (*233*).

1.3.5 Role of microRNA expression in cell cycle regulation

An additional level of cell cycle regulation is exerted by microRNAs (miRNAs). miRNAs are a class of non-coding RNAs with a length of 18-25 nucleotides that bind to and partially silence complementary sequences in target mRNAs by inducing mRNA degradation or via translational repression (*234*). miRNAs are often found in clusters throughout the genome that are transcribed simultaneously. Recent evidences suggest that miRNAs may also control the levels of diverse cell cycle factors since they show dynamic expression patterns in a

tissue- or stage-specific manner (*235*). In fact, the deregulation of miRNAs was shown to alter protein levels of critical cell cycle-related genes and is thus implicated in various cancer types (*236, 237*). *In silico* analyses suggest that more than 30% of the human genome may be regulated by miRNAs (*238, 239*). Most of the cell-cycle-targeting miRNAs modulate the re-entry into the cell cycle or the G_1-S phase progression (*240*). The anti-proliferative potential of the miR-15a-16-1 cluster provided the first insight into miRNAs and cell cycle regulation (*240*). This cluster encodes two mature miRNAs, miR-15a and mir-16 (*240*), which target Cdk1, Cdk2, Cdk6 as well as Cyclin D1, D3 and E (*241-243*), but several other miRNAs regulate the expression of these same cell cycle factors. For example, the level of Cyclin D is also affected by let-7, miR-17, -19a, -20a and -34 (*240*). It was shown that miR-15 and -16 are specifically and directly target Cyclin E transcription and that these miRNA are strongly up regulated by E2F-1. Thus, E2F-regulated miRNAs participate in a feedback loop to restrict and control E2F-1 activity (*244*). miRNA may also play a major role in cell cycle re-entry from the quiescent G_0 phase, since there is evidence that cell-cell contact in quiescent cells globally activates miRNA biogenesis due to increased processing and more efficient incorporation of miRNAs into RNA-induced silencing complex (RISC) (*245*). As a consequence, fewer mRNAs are translated. The whole complexity of cell cycle regulation by miRNAs is not yet fully understood, but should be considered to better understand the regulatory processes.

1.3.6 Role of the ARTD proteins in the cell cycle – a focus on G1 progression

The ARTD protein family is involved in a variety of biological functions (chapter 1.2). Among these are also cell-cycle related processes such as heterochromatin formation during late S-phase (*131*) or the localization of ARTD1 to the centrosome and the chromosomes during cell division (*246*). Furthermore, overexpressed ARTD3 is localized at centrosomes and interferes with G_1 to S phase progression (*247*) and ARTD5 (tankyrase 1) is involved in the separation of sister telomeres during mitosis (*248*). Recently, it was shown that *progestin* gene regulation involves the activation of ARTD1 via Cdk2-dependent phosphorylation, leading to H1 displacement (*141, 249*). This is essential for the effect of progestin on cell cycle progression in breast cancer.

There is also evidence indicating that ARTD1 might play a role during the early cell cycle phases. ARTD1 interacts with the C-terminal binding protein (CtBP) to form a co-repressor complex for *p21* transcription. ARTD1 enzymatic activity was also reported to be necessary for p21 expression after genotoxic stress (*250*). Simbulan-Rosenthal *et al*. reported that ARTD1 interacts with E2F-1 *in vitro* and *in vivo* and up regulates E2F-1expression during early S phase (*251, 252*). PAR formation was also detected during G_0-G_1 transition after mitogen induction, suggesting that ADP-ribosylation is involved in growth factor signaling and the induction of immediate-early genes (*90*). However, this study faced the problem that PAR can be induced already during synchronization with chemical agents or by serum starvation and subsequent growth factor addition (Vetmed Dissertation of Sandra Bäckert, 2009), raising concerns about the physiological relevance of such findings.

2 AIM OF THE THESIS

The intracellular ADP-ribosyltransferase family (ARTD family) consists of 18 members. Some of these enzymes were described to synthesize polymers of ADP-ribose (PAR), while others are only able to catalyze mono-AD-ribosylation or may even be enzymatically inactive. ARTD1 and ARTD2 are both chromatin-associated enzymes and therefore localized in the nucleus. Both proteins were described to synthesize polymers of ADP-ribose (PAR) upon exposure of cells to genotoxic stress. Single ARTD1 or ARTD2 knockout mice are viable, but the double knockout is lethal, indicating that at least one allele of either ARTD1 or ARTD2 is required for development. In most cellular processes that are regulated by ADP-ribosylation, ARTD1 is the main contributor to PAR formation. However, there are indications that ARTD2 regulates distinct processes independent of ARTD1, but molecular details and mechanistic insight are still scarce. Previous biochemical analyses of our laboratory provide evidence that the catalytic domains of ARTD1 and ARTD2 are not interchangeable, suggesting that these enzymes have different roles. Furthermore, the two enzymes have very distinct N-termini, which also hints at different activation mechanisms. Based on these observations, we hypothesized that ARTD1 and ARTD2 regulate different cellular processes or use different mechanisms to regulate common processes.

This hypothesis was experimentally verified by studying the function of ARTD1 and ARTD2 in cell cycle regulation, in particular during G_0 to G_1 progression, and for PAR formation in response to oxidative stress.

3 RESULTS

3.1 Overview of published and submitted manuscripts

3.1.1 ARTD2 activity is stimulated by RNA

Authors: **Karolin Léger**, Natasa Savic, Raffaela Santoro, Michael O. Hottiger

Journal: Manuscript submitted

Contribution: Planning, performing and evaluating the experiments. Preparation of the figures and revision of the manuscript.

3.1.2 ARTD1 and ARTD2 differentially regulate cell-cycle re-entry and progression in T24 bladder carcinoma cells

Authors: **Karolin Léger**, Michael O. Hottiger

Journal: Manuscript submitted

Contribution: Planning, performing and evaluating the experiments. Preparation of the figures and revision of the manuscript.

3.1.3 PKC signaling prevents irradiation-induced apoptosis of primary human fibroblasts

Authors: A. Bluwstein, N. Kumar, **K. Léger**, J. Traenkle, J. van Oostrum, H. Rehrauer, M. Baudis and M.O. Hottiger

Journal: Cell Death Dis., 2013 Feb 14

Contribution: Performing and evaluation of qPCR analyses (Supplementary Figure 1e, 3c, 3d), performing of flow cytometry analyses (Supplementary Figure 2a, 2d, 3a, 13e)

ARTD2 activity is stimulated by RNA

Karolin Léger[1,2], Natasa Savic[1,2], Raffaella Santoro[1], Michael O. Hottiger[1*]

[1]Institute of Veterinary Biochemistry and Molecular Biology, University of Zurich, Winterthurerstrasse 190, 8057 Zurich, Switzerland

[2]Life Science Zurich Graduate School, University of Zurich, 8057, Switzerland

*Corresponding author: Email: hottiger@vetbio.uzh.ch

Running title: ARTD2 activation by RNA

Key words: ADP-ribosylation, ARTD1, ARTD2, PARP-1, PARP-2, genotoxic stress response, nucleolus, rRNA

Abstract

ADP-ribosyltransferases (ARTs) are important enzymes that regulate the genotoxic stress response and the maintenance of genome integrity. ARTD1 (PARP1) and ARTD2 (PARP2) are homologous proteins that modify themselves and target proteins by the addition of mono- and poly-ADP-ribose moieties. Although both enzymes were described to be involved in the genotoxic stress response, only ARTD1 is strongly activated by double stranded DNA *in vitro*, opening the question whether other molecules than DNA can regulate ARTD2 activity. Here, we characterize cellular poly-ADP-ribose (PAR) formation upon hydrogen peroxide (H_2O_2) or N-methyl-N'-methyl-nitro-N-nitrosoguanidine (MNNG) stress in combination with application of the RNA polymerase I inhibitor Actinomycin D (ActD). Combined treatment with ActD and H_2O_2 or MNNG substantially increased the number of PAR forming cells and enhanced the overall PAR content. This enhancement was mediated by ARTD2 but not by ARTD1 *in vivo*. Further elucidation revealed that ActD treatment lead to the accumulation of short RNA polymerase I-dependent rRNA transcripts. *In vitro* experiments confirmed that ARTD2, in contrast to ARTD1, is strongly activated by RNA but not by double-stranded DNA. Our findings identify a new activator for ARTD2-dependent ADP-ribosylation, which has important implications for the future analysis of the biological role of ARTD2 in the nucleus.

Introduction

Cells have evolved a complex and diverse arsenal of mechanisms to overcome genotoxic stress and to guarantee genome integrity (1). Depending on the type of stress, different response mechanisms are activated in order to prevent the inheritance or repair of damaged DNA (2,3). In addition to factors that directly bind and replace incorrect bases and repair DNA strand breaks, a variety of proteins are indirectly involved in the genotoxic stress response by regulating the levels and activities of other proteins or by modulating chromatin structure. ADP-ribosyltransferases (ARTs) are prominent members of this group of enzymes. ARTs use nicotinamide adenine dinucleotide (NAD^+) as a substrate for the synthesis of mono- and poly-ADP-ribose modifications on target proteins (4). The ART protein family is divided into diphtheria toxin-like ARTs (ARTDs) and cholera toxin-like ARTs (ARTCs) (5). In human, the ARTD family currently comprises 18 nuclear and cytoplasmic mono- and poly-ADP-ribosyltransferases, while ARTCs are mainly extracellular enzymes that only transfer one ADP-ribose unit to their target proteins (5).

Proteins of the ARTD family have been implicated in a plethora of cellular functions (6,7). Research during the last years has documented numerous functions of ARTD1 and of ADP-ribosylation in general that are not directly linked to DNA repair or the DNA damage response (8,9). The function of ARTD1 in DNA repair is substantiated by the strong activation of ARTD1 activity by DNA *in vitro*, as well as by the strong induction of poly-ADP-ribosylation upon treatment of cells with DNA damaging agents. Nevertheless, a direct involvement of DNA damage in the activation of ARTD1 *in vivo* is still largely based on correlations. PAR formation is dependent on the severity of the genotoxic stress and can even lead to cell death due to NAD^+ and ATP depletion (10). The functional involvement of ADP-ribosylation in the DNA damage response has provided the incentive to generate PARP inhibitors as anti-tumour drugs, which are being developed and tested as novel therapies (11-

14). The closest homolog of ARTD1 is ARTD2, which is also able to mono- and poly-ADP-ribosylate itself and target proteins. Although ARTD1 was discovered several decades ago, ARTD2 was only discovered in the 1990s as a result of the detection of residual PAR forming activity in ARTD1 knockout mouse embryonic fibroblasts (MEFs) (15). Like ARTD1, ARTD2 has also been implicated in various cellular functions, which include genome and chromosome stability, heterochromatin integrity, cell death, differentiation and inflammation (16). Mammalian ARTD2 is a 66.2 kDA protein with a C-terminal catalytic domain that is 69% similar to the homologous domain in ARTD1 (15) (17). Despite this common domain, ARTD2 is much less active than ARTD1, suggesting that it may be activated by different and yet unknown stimuli, which would interact with the other domains found in these proteins. While the DNA binding domain of ARTD1 contains two Zn-fingers and a Zn-binding domain, the DNA binding element of ARTD2 is represented by the SAF/Acinus/PIAS-DNA-binding (SAP) domain. In addition, ARTD2 seems to modify different proteins, suggesting that both enzymes might indeed regulate distinct biological functions (18,19). Thus, the identification of such new ARTD2 activators will likely also reveal novel biological phenomena that are regulated specifically by ARTD2.

The nucleoli are sites of ribosomal RNA (rRNA) genes transcription, rRNA maturation and ribosome production and assemble around the nucleolar organizer regions (NOR) (20,21). A human diploid cell contains about 400 rRNA genes that are all organized in head-to-tail tandem repeats on five different chromosomes (21). However, also in highly active metabolic cells, only a subset of these genes (approximately 50 %) is actively transcribed (22,23). The remaining rRNA genes are silenced in a tissue- and cell type-specific manner (24). Active rRNA genes are transcribed by RNA polymerase I (Pol I) to synthesize a 45S pre-rRNA. For the initiation of rRNA transcription, Pol I has to be part of a protein-multi-complex that includes factors like UBF, SL1, and TIF-IA (25). The production

of ribosome-subunits is heavily influenced by diverse stress stimuli and metabolic changes (26). The cell reacts to nutrient starvation, oxidative stress or inhibition of protein synthesis with a decrease of rRNA transcription, whereas growth factors and proliferation stimulating agents increase the rRNA transcription. rRNA synthesis is particularly sensitive to ActD at a low concentration of 50 ng/ml, while RNA polymerases II (Pol II) and III (Pol III) are only inhibited at higher concentrations (Pol II > 1 μg/ml, Pol III > 5 μg/ml) (27,28). ActD intercalates with CG-rich regions of the DNA and thus stabilizes covalent topoisomerase I-DNA complexes that prevent RNA polymerase progression and consequently inhibit RNA synthesis (29). The intercalation takes mainly place downstream of rDNA transcription start sites, thus inhibiting transcription during elongation and leading to an immense accumulation of short RNA transcripts over time (30,31). In *Drosophila*, ARTD1 was reported to regulate ribosomal biogenesis on the post-transcriptional and pre-rRNA processing level (32). Furthermore, ARTD1 and ARTD2 have been both shown to co-localize with B23/nucleophosmin and nucleolin, nucleolar proteins involved in several processes including rRNA transcription and elongation, ribosome assembly, and rRNA processing (33,34). No direct effect of ARTD1 and ARTD2 on Pol I transcription was, however, described in these studies. More recently, ARTD1 has been linked to heterochromatin formation and specifically to silencing of rRNA genes in the nucleolus (35,36).

Here, we characterize the nucleolar function of ARTD2 upon different stresses. H_2O_2 or MNNG treatment induced PAR formation in the nucleolus of different cell lines. Co-treatment with low doses of ActD enhanced PAR formation. Surprisingly, this co-treatment activated mainly ARTD2 but not ARTD1 *in vivo*. ActD treatment is known to enhance the formation of short rRNA products. *In vitro* experiments confirmed that ARTD2 is strongly activated by this RNA as well as other single stranded RNA but not by double-stranded DNA

through its SAP domain. Our findings thus reveal a new activator of ARTD2, which opens new possible implications for the future analysis of the biological role of ARTD2.

Methods

Cell culture

T24 cells were cultivated in McCoy's 5A medium (Gibco, Invitrogen, CA, California, USA) at 37°C. NIH/3T3, HeLa cells as well as MEFs were cultivated in Dulbecco's Modified Eagle's Medium (DMEM) (PAA, Pasching, Austria). 231-MD-MBA cells were cultivated in Roswell Park Memorial Institute medium (RPMI) (Gibco, Invitrogen, CA, California). All media were supplemented with 1% (v/v) Penicillin/Streptavidin and 10% (v/v) fetal calf serum (Gibco, Invitrogen, CA, California, USA).

siRNA transfection

Negative control allstars (siMock), human siPARP1 #6, human siPARP2 #6, human siPARG #2, mouse siPARP1 #7, mouse siPARP2 # 8 were ordered from Qiagen (Hilden, Germany). Cells were seeded 1 day before transfection ($5x10^5$ cells per 6cm plate) and transfection was carried out with 40 nmol siRNA per plate and RNAi MAX lipofectamine (Invitrogen, Carlsbad, CA, USA).

Antibodies

Following antibodies were used: From Santa Cruz Biotechnology, Inc (Dallas, TX, USA): PARP1/ARTD1 (H-250, rabbit), Pol I (rabbit). From Active motif (Carlsbad, CA, USA): PARP2 (rabbit). From Sigma Aldrich (St. Louis, MO, USA): tubulin (mouse). From Cell Signaling (Danvers, MA, USA): fibrillarin. From Jackson ImmunoResearch Laboratories (Suffolk, UK): secondary FITC-conjugated AffiniPure Goat Anti-mouse, secondary Cy3™ -conjugated AffiniPure Goat Anti-mouse. Homemade: PAR 10H (mouse).

RNA extraction with TRIzol® reagent and qPCR analysis

TRIzol® RNA Isolation Reagent (500 µl, Life Technologies, CA, California, USA) was applied directly to the plates and the supplier's protocol was followed. DNase treatment was performed using the TURBO DNA-freeTM Kit (Life Technologies, Carlsbad, CA, USA). RNA was quantified with a NanoDrop (ThermoFisherScintific, Waltham, MS, USA) and reverse transcribed according to the supplier's protocol (High Capacity cDNA Reverse Transcription Kit, Applied Biosystems, Foster City, CA, United States).

Quantitative-real-time polymerase chain reactions (qPCR) were performed with SYBR® green SensiMix SYBR Hi-ROX Kit (Bioline Reagents Ltd, London, UK) and a Rotor-Gene Q 2plex HRM System (Qiagen, Hilden, Germany).

Cell lysis, SDS-PAGE and Western blot analysis

Whole cell lysis was performed either with trypsinized cells or directly on plates by using a Tris-lysis buffer (50 mM Tris pH 8, 500 mM NaCl, 1% Triton X-100, 1 µg/ml pepstatin, 1 µg/ml bestatin, 1 µg/ml leupeptin, 2 mM PMSF; 10 min, 4°C). Bradford assay (Bio-Rad laboratories, Hercules, CA, USA) was performed and, if not otherwise indicated, 30 µg of protein extract was loaded and separated on an 10% or 12% SDS-polyacrylamide gel (120V). The gel was blotted on a PDVF membrane and analyzed by using protein specific antibodies.

Immunofluorescence microscopy

Cells were seeded on cover slips ($10x^5$ cells per well in a 24-well-plate) and grown overnight. After H_2O_2 (1 mM in FCS-free medium, 10 min), MNNG (500 µM in FCS-free medium, 30 min) or medium-only treatment, cells were fixed (methanol: acetic acid 3:1, 5 min on ice), washed twice with PBS, and incubated with 10H PAR antibody (1:350) in PBS (containing 5% milk and 0.05% Tween, 1 h at room temperature or overnight at 4°C). Cover slips were

incubated with secondary Cy3-Antibody (1 h at room temperature in the dark). After washing with PBS, cover slips were mounted with Vectashield containing DAPI (Vector Laboratories, Burlingame, CA, USA) and sealed with nail polish. For quantification, at least 100 cells per condition were analyzed.

Conventional microscopy was carried out using a Leica DMI 6000B light microscope (Leica microsystems GmbH, Wetzlar, Germany). Confocal laser scanning microscopy was carried out with a Leica SP 5 resonant APD system (Leica microsystems GmbH, Wetzlar, Germany).

In vitro RNA transcription

Linearized vectors containing rRNA sequences (from -16 to +130 and pRNA -232 to -1) and control sequences (hKCNA from +1 to +237) were used to *in vitro* transcribe RNA using T7 polymerase. After DNase I treatment, transcripts were double purified using TRIzol reagent (Invitrogen, Carlsbad, CA, USA) according to the manufacturer's protocol.

In vitro ARDT1 or ARTD2 activity assay

10 pmol baculo-virus purified MYC-hARTD1(wt)-HIS or purified human ARTD2(fl)-HIS were incubated with NAD^+ in the reaction buffer (250 mM Tris-HCl pH 8, 20 mM $MgCl_2$, 1.25 mM DTT, 5 µg/ml P/B/L – proteinase inhibitors, 30°C, 10 min). 5 pmol of EcoRI linker or different concentrations as indicated of short RNA transcripts were added to the reaction. For ADP-ribosylation reactions, radioactive NAD^+ (^{32}P, final concentration 100 nM) and non-radioactive NAD^+ (final concentration 1.6 µM) was added unless stated otherwise. Reactions were terminated by adding Laemmli buffer and subsequent boiling of the samples (5 min, 95°C). SDS-PAGE was performed; gels were stained with coomassie, de-stained, and subjected to film exposure.

In vitro PARG assay

ARTD1 auto-ADP-ribosylation was carried out as described before and the reaction mix was purified over illustra MicroSpin G-50 Columns (GE Healthcare GmbH Europe, Freiburg, Germany). Equal amounts of reaction mix were added to pre-chilled tubes containing baculo-purified hPARG-(fl) (2 pmol). Reactions were carried out in the presence or absence of the indicated PARG inhibitors.

Results

H_2O_2 treatment induces nucleolar PAR formation.

To investigate the localization and molecular mechanism of PAR formation, T24 cells were treated with H_2O_2 (1 mM for 10 min). PAR formation was analysed by immunofluorescence (IF) using anti-PAR antibodies and data were obtained by conventional or confocal fluorescence microscopy. The PAR signal was localized to regions of the nucleus that were weakly stained by DAPI, indicating that nucleoli are sites of PAR formation (Figure 1A). The PAR signal in T24 cells treated with H_2O_2 co-localized with ARTD1, which suggests that ARTD1 is at least partly responsible for PAR synthesis in response to oxidative stress in T24 cells (Figure 1B). The partial co-localization with Pol I and the nucleolar Fibrillarin protein confirmed that PAR formation occurs predominantly in the nucleolus of H_2O_2-treated NIH/3T3 cells (Figure 1C,D). A similar nucleolar PAR signal was observed in H_2O_2 treated NIH/3T3 cells, HeLa cells and mouse embryonic fibroblasts (MEFs), suggesting that the nucleoli are the main location for the cellular PAR formation during oxidative stress (Figure S1A).

ActD treatment enhances nucleolar PAR formation upon H_2O_2 and MNNG stimulation.

Although PAR formation has been mostly studied in the context of DNA damage, which can be induced by H_2O_2 and MNNG, a link between PAR synthesis and Pol I-dependent transcription has not been documented. To investigate the link between Pol I-dependent transcription and stress-induced PAR formation, we optionally pre-treated cells with a low dose of the transcription inhibitor ActD for 20 hours and then exposed them to H_2O_2 or MNNG (28). Unexpectedly, treatment with ActD and H_2O_2 or MNNG increased the number of PAR-positive cells and the intensity of the PAR signal in comparison to cells that were not

pre-treated with ActD (Figure 2A,B). The analysis of 45S pre-rRNA levels confirmed that ActD was effective in impairing pre-rRNA synthesis (>90%), while H_2O_2 or MNNG reduced pre-rRNA levels only by 25-40% (Figure S1B). ActD enhanced PAR formation also in NIH/3T3, HeLa and MDA-MB-231 cells co-treated with H_2O_2 or MNNG (Figure S1C,D and S2A), indicating that the observed ActD effect is generally conserved. Quantification of the number of responsive cells and the intensity of PAR formation per cell revealed that only a pre-treatment of at least 4 hours was able to enhance PAR formation, while short pre-treatment of only 30 min had no effect. Furthermore, PAR formation seemed to be enhanced stronger in MNNG treated cells as compared to H_2O_2 treated cells (Figure 2C and D). Since PAR formation could be inhibited by Olaparib, an inhibitor of ARTD1 and ARTD2 (Figure S2B and S1B, (37)), these data suggested the involvement of either ARTD1 or ARTD2 and provided evidence for a synergistic effect between oxidative stress and the interference of 45S pre-rRNA synthesis for PAR accumulation in the nucleolus.

ARTD2, but not ARTD1 is responsible for the ActD-dependent enhancement of PAR formation after H_2O_2 or MNNG treatment.

To investigate whether ActD exerts its synergistic effect through ARTD1 or ARTD2, T24 cells were depleted of ARTD1 or ARTD2 by siRNA (Figure S2C) and subsequently treated with H_2O_2. Knockdown of ARTD1, but not of ARTD2, almost completely abolished PAR formation in T24 cells treated with H_2O_2, confirming that ARTD1 strongly contributes to H_2O_2-induced PAR formation (Figure 3A,C). Co-treatment of siARTD1 cells with H_2O_2 and ActD revealed that ActD did not affect the numbers of PAR positive T24 cells after 30 min, but started to enhance PAR formation after 4 hours of ActD treatment (50 ng/ml) and even stronger (up to PAR positive cells to 90%) after 20 hours (Figure 3B). These results indicated that the synergistic effect between oxidative stress and the inhibition of 45S pre-

rRNA synthesis on PAR accumulation in the nucleolus was not mediated by ARTD1. In contrast, no increase in PAR formation was observed in ARTD2 depleted T24 cells that were treated with H_2O_2 and ActD (Figure 3D), indicating that the stimulatory ActD effect on PAR formation was mainly regulated by ARTD2. The presence of ARTD2, but not of ARTD1, seemed similarly responsible for the increased PAR formation observed after co-treatment of ActD and MNNG in T24 cells (Figure 3E-H). H_2O_2 or MNNG treatment in combination with ActD in NIH/3T3 cells and subsequent quantification of the PAR formation by IF or visualisation by Western blot furthermore confirmed that ARTD2 is also responsible for the stimulatory ActD effect in mouse cells (Figure S3A-G for H_2O_2 or S4A-C for MNNG). Together, these results indicated that ARTD2 is involved in PAR formation in response to H_2O_2- or MNNG-treatment in combination with ActD in T24 and NIH/3T3 cells.

ARTD2 activity is stimulated by rRNA *in vitro*.

The described synergistic effect between ActD and H_2O_2 or MNNG on PAR formation could either be due to an inhibition of PAR degradation or a stimulation of PAR synthesis. The former was studied by determining whether ActD affects the activity of the poly-ADP-ribose-glycohydrolase (PARG), the primary enzyme responsible for degrading protein-bound poly-ADP-ribose (Figure 4A). *In vitro* ^{32}P-labeled PARylated ARTD1 was incubated with PARG in the absence or presence of ActD and PARylated ARTD1 levels were monitored by autoradiography. Treatment with ActD did not prevent degradation of PAR moieties of ARTD1, indicating that ActD does not affect PARG activity.

The results described above indicated that H_2O_2 induces PAR formation in the nucleoli (Figure 1). Inhibition of 45S pre-rRNA synthesis by ActD prevents Pol I elongation at the rDNA coding region, leading to an accumulation of short RNA transcripts after 20h (Figure 4B) (30,31). We described above that only prolonged treatment with ActD (4 and 20 h)

enhanced formation of PAR in cells treated with H_2O_2 and MNNG (Figure 2C,D). Since PAR formation correlated with the inhibition of 45S pre-rRNA synthesis (Figure S5A), we hypothesized that the known enhancement of short rRNA transcripts induced by ActD treatment might potentially stimulate ARTD2 activity. To test this hypothesis, we investigated *in vitro* the ability of ARTD2's automodification in the presence of transcribed rRNA (corresponding to rDNA sequences from -16 to +130bp). The basal automodification of ARTD2 was strongly stimulated by the addition of this rRNA transcript, while equal amounts of double-stranded DNA induced only a moderate activation effect (Figure 4C). This effect did not seem to be mediated by specific rRNA sequences, as other non nucleolar RNA transcripts were able to stimulate ARTD2 activity to similar levels (Figure S5D). The RNA mediated stimulatory effect was also observed under low NAD^+ levels that only lead to mono-ADP-ribosylation of ARTD2 (Figure S5B). In contrast to ARTD2, ARTD1 was strongly activated by double-stranded DNA and, as previously described (36), only to a lower extent by RNA (Figure 4D). ARTD1 mono-ADP-ribosylation levels were not affected by RNA (Figure S5C).

Since the ActD effect was only observed in the presence of a genotoxic stress, we tested whether the activation of ARTD2 by RNA depends on DNA. Addition of DNA did not enhance the stimulatory effect of RNA on ARTD2, confirming that RNA is stimulating ARTD2 independent of DNA (Figure 4E). To define which domain of ARTD2 is responsible for the RNA mediated activation, we compared the RNA effect on the activities of human $ARTD2_{FL}$ (full length) and $ARTD2_{\Delta SAP}$ (aa 95-583), a mutant that is deleted of the SAP domain and that displays similar basal activity as $ARTD2_{FL}$. While $ARTD2_{FL}$ was stimulated by RNA, the deletion of the SAP domain impaired the RNA mediated activation (Figure 4F). The additional deletion of the WGR domain (aa 231-583, $ARTD2_{\Delta S\Delta W}$) or removal of the WGR domain alone (deletion of aa 116-193, $ARTD2_{\Delta WGR}$) showed, beside the loss of the

stimulation by RNA, a strong reduction of the general ARTD2 activity (Figure 4F). Together, these results suggested that RNA, but not DNA, is a potent activator of ARTD2 enzymatic activity through the SAP domain and that the WGR domain is an important structural element for the overall activity of the enzyme.

Discussion

ADP-ribosylation has been implicated in several nucleolar processes such as ribosome biogenesis, formation of rDNA heterochromatin and stress sensing (32,34,36,38-40). Here, we show that H_2O_2 or MNNG induced PAR formation in the nucleoli of both mouse and human cells. Combination of these treatments with low doses of ActD revealed a synergistic effect on PAR formation that is mediated by ARTD2 and not by ARTD1. It was well known before that ActD treatment leads to the accumulation of short rRNA transcripts, which might be responsible for the enhancement of PAR formation. Indeed, purified short rRNA transcripts were able to strongly stimulate ARTD2 activity via the SAP/WGR domain, while double-stranded DNA did not have this effect. Our findings thus reveal a new activator for ARTD2-dependent ADP-ribosylation, which has important implications for the future analysis of the biological role of ARTD2 in the nucleus.

ADP-ribosylation and in particular the homologous enzymes ARTD1 and ARTD2 have been traditionally implicated in the response to DNA damage. An important cornerstone for this model is the strong activation of ARTD1 by DNA *in vitro* and the detection of PAR upon treatment of cells with genotoxic compounds. In these DNA damage-dependent processes, ARTD2 displays much less activity than ARTD1, questioning whether other molecules than DNA are able to regulate ARTD2 function. Our results strongly suggest that instead to bind to sites of DNA damage, ARTD2 associates with RNA, providing an alternative cue to identify and respond to DNA damage. In support of this, recent data implicated site-specific Dicer and Drosha RNA moieties in the control of DNA damage (41). Furthermore, the activation of ARTD2 by RNA may also be part of an intricate network of RNA surveillance and repair mechanisms to preserve RNA quality (42-44). The identification of the strong ARTD2 activation by RNA is a new and unexpected result that may indicate an additional mean for monitoring not only genome integrity but also other

processes that are specific for ARTD2. Indeed, genetic disruption of ARTD2, but not of ARTD1, affects various differentiation processes in mice, including spermatogenesis (45), adipogenesis (46), and the survival of thymocytes (47).

Interestingly, the stimulation of ARTD2 *in vivo* was dependent on the co-stimulation with ActD and H_2O_2 or MNNG, indicating that additional stress signals are required for the activation of ARTD2 by RNA. These signals might include the damage of RNA. Indeed, oxidative damage in RNA is usually higher than in DNA (48). Future studies of the nucleolar ADP-ribose acceptors and the effect of ADP-ribosylation on the response to RNA damage are needed to reveal and define these functions in detail. Alternatively, the treatment of cells with genotoxic compounds might induce signalling cascades that lead to the post-translational modification of ARTD2, which is required for the stimulation with RNA. Interestingly, the ActD effect was observed in human and mouse cells, suggesting that the stimulation of ARTD2 is a conserved effect.

PAR formation was predominantly observed in the nucleoli, which might be due to the elevated occupancy of ARTD1 and ARTD2 in the nucleoli and/or to a high sensitivity of the nucleolus for the effects of genotoxic stress. Growing evidence indicates that the nucleolus plays a key role in monitoring and responding to cellular stress. After exposure to extra- or intracellular stress, signal pathways induce rapid down-regulation of 45S pre-rRNA synthesis that is followed by perturbation of nucleolar structure, cell cycle arrest and stabilization of p53 (49). The formation of high levels of PAR in nucleoli under genotoxic stress conditions might be part of this nucleolus-dependent signalling. Whether and how PAR formation is due to a high accessibility of nucleolar DNA and RNA to chemical agents remains further to be investigated.

Previous studies determined that RNA is a key regulator of ARTD1 in the nucleolus (36). Nucleolar localization of ARTD1 is dependent on RNA and ARTD1 binds *in vivo* and

in vitro to the nucleolar non-coding pRNA, an intergenic transcript implicated in the establishment of rDNA heterochromatin (50). pRNA associates with the zinc-finger DNA binding domain of ARTD1 and stimulates ARTD1 activity, although to a lesser degree than double-stranded DNA ((36) and Figure 4D).

In this work, we provide strong evidence that RNA is a key regulator of ARTD2's enzymatic activity. Although the lack of good antibodies prevented us from determining how RNA affects nucleolar occupancy of ARTD2, we could demonstrate that RNA regulates ARTD2 activity. In contrast to ARTD1, RNA strongly activated ARTD2, while double stranded DNA displayed no stimulatory effect, suggesting that the structure and the nature of nucleic acid is an important determinant for the regulation of ARTD2 function. Consistent with this, recent analyses with several DNA structures mimicking intermediates of different DNA metabolizing processes revealed that ARTD2 activation efficiency did not correlate with K(d) values for DNA (51). ARTD2 displayed the highest affinity for flap-containing DNA, but was more efficiently activated by 5'-overhang DNA, suggesting that single-stranded nucleic acid might be in general a stimulator of ARTD2. As for ARTD1, the stimulation did not seem sequence specific, since other tested RNAs were also able to strongly stimulate ARTD2 (36). We identified the SAP domain to be mainly responsible for the stimulation by RNA. The SAP (after SAF-A/B, Acinus and PIAS) motif is a putative DNA/RNA binding domain found in diverse nuclear and cytoplasmic proteins (52,53). Based on the presented findings, it is thus possible that other proteins with a SAP motif similarly bind RNA and are thereby regulated. Interestingly, deleting only the WGR domain abolished the RNA stimulation but also the overall activity of ARTD2, indicating that the structural arrangement of the SAP and the CAT motif is functionally relevant.

Together, the strong activation of ARTD2 by RNA, as opposed to the activation of ARTD1 by double-stranded DNA, is likely the underlying cause for the distinct and

complementary functions of these two homologous ARTDs. The fact that RNA stimulates PAR formation by ARTD2 has not only mechanistic implications, but also sheds new light on the function of ARTD2 and poly-ADP-ribosylation during the genotoxic stress response.

Supplementary data statement

Supplementary Data are available at NAR Online. This manuscript is accompanied by one supplementary pdf file containing five supplementary figures.

Author Contributions

The authors declare that they have no conflict of interest.

K.L. designed and performed experiments; N.S. produced synthetic RNA; R.S. and M.O.H. supervised the work and M.O.H. wrote the manuscript.

Funding

This work was supported in part by the Forschungskredit of the University of Zurich (to K.L.), the Swiss National Science Foundation [31-122421, PDMFP3_127315] as well as the Kanton of Zurich (to M.O.H.).

Acknowledgements

P.O.Hassa is acknowledged for providing the 10H antibody, M.Stucki (University of Zurich, Switzerland) is acknowledged for providing the T24 cell line. Monika Fey and Dominik Bär are acknowledged for technical support. F.Freimoser (University of Zurich, Switzerland) provided editorial assistance and critical input during the writing.

References

1. Harper, J.W. and Elledge, S.J. (2007) The DNA damage response: ten years after. *Mol Cell*, **28**, 739-745.
2. Zhou, B.B. and Elledge, S.J. (2000) The DNA damage response: putting checkpoints in perspective. *Nature*, **408**, 433-439.
3. Dianov, G.L. and Hubscher, U. (2013) Mammalian base excision repair: the forgotten archangel. *Nucleic Acids Res*.
4. Hassa, P.O., Haenni, S., Elser, M. and Hottiger, M.O. (2006) Nuclear ADP-ribosylation reactions in mammalian cells: where are we today and where are we going? *Microbiol Mol Biol Rev*, **70**, 789-829.
5. Hottiger, M.O., Hassa, P.O., Lüscher, B., Schüler, H. and Koch-Nolte, F. (2010) Toward a unified nomenclature for mammalian ADP-ribosyltransferases. *Trends Biochem Sci*, **35**, 208-219.
6. Luo, X. and Kraus, W.L. (2012) On PAR with PARP: cellular stress signaling through poly(ADP-ribose) and PARP-1. *Genes Dev*, **26**, 417-432.
7. Schreiber, V., Dantzer, F., Ame, J.-C. and De Murcia, G. (2006) Poly(ADP-ribose): novel functions for an old molecule. *Nat Rev Mol Cell Biol*, **7**, 517-528.
8. Hassa, P.O. and Hottiger, M.O. (2008) The diverse biological roles of mammalian PARPs, a small but powerful family of poly-ADP-ribose polymerases. *Front Biosci*, **13**, 3046-3082.
9. Kraus, W.L. and Hottiger, M.O. (2013) PARP-1 and gene regulation: Progress and puzzles. *Mol Aspects Med*.
10. David, K.K., Andrabi, S.A., Dawson, T.M. and Dawson, V.L. (2009) Parthanatos, a messenger of death. *Front Biosci*, **14**, 1116-1128.

11. Banerjee, S. and Kaye, S. (2011) PARP inhibitors in BRCA gene-mutated ovarian cancer and beyond. *Curr Oncol Rep*, **13**, 442-449.

12. Bryant, H., Schultz, N., Thomas, H., Parker, K., Flower, D., Lopez, E., Kyle, S., Meuth, M., Curtin, N. and Helleday, T. (2005) Specific killing of BRCA2-deficient tumours with inhibitors of poly(ADP-ribose) polymerase. *Nature*, **434**, 913-917.

13. Telli, M.L. (2011) PARP inhibitors in cancer: moving beyond BRCA. *Lancet Oncol*, **12**, 827-828.

14. Underhill, C., Toulmonde, M. and Bonnefoi, H. (2010) A review of PARP inhibitors: from bench to bedside. *Ann Oncol*, **22**, 268-279.

15. Amé, J., Rolli, V., Schreiber, V., Niedergang, C., Apiou, F., Decker, P., Muller, S., Höger, T., Ménissier-de Murcia, J. and de Murcia, G. (1999) PARP-2, a novel mammalian DNA damage-dependent poly(ADP-ribose) polymerase. *J Biol Chem*, **274**, 17860-17868.

16. Yelamos, J., Schreiber, V. and Dantzer, F. (2008) Toward specific functions of poly(ADP-ribose) polymerase-2. *Trends Mol Med*, **14**, 169-178.

17. Oliver, A.W., Ame, J.C., Roe, S.M., Good, V., de Murcia, G. and Pearl, L.H. (2004) Crystal structure of the catalytic fragment of murine poly(ADP-ribose) polymerase-2. *Nucleic Acids Res*, **32**, 456-464.

18. Yelamos, J., Farres, J., Llacuna, L., Ampurdanes, C. and Martin-Caballero, J. (2011) PARP-1 and PARP-2: New players in tumour development. *Am J Cancer Res*, **1**, 328-346.

19. Troiani, S., Lupi, R., Perego, R., Depaolini, S.R., Thieffine, S., Bosotti, R. and Rusconi, L. (2011) Identification of candidate substrates for poly(ADP-ribose) polymerase-2 (PARP2) in the absence of DNA damage using high-density protein microarrays. *FEBS J*, **278**, 3676-3687.

20. Brown, D.D. and Gurdon, J.B. (1964) Absence of ribosomal RNA synthesis in the anucleolate mutant of Xenopus laevis. *Proc Natl Acad Sci USA*, **51**, 139-146.

21. Hadjiolov, A.A. (1985) In Beerman, A. M., Goldstein, L., Portrer, K. R. and Sitte, P. (eds.), *Cell Biology Monographs*, New York, pp. 1-263.
22. Santoro, R. (2005) The silence of the ribosomal RNA genes. *Cell Mol Life Sci*, **62**, 2067-2079.
23. Santoro, R. (2011) In Olson, M. J. (ed.), *The Nucleolus*. Springer, pp. 57-82.
24. Haaf, T., Hayman, D.L. and Schmid, M. (1991) Quantitative determination of rDNA transcription units in vertebrate cells. *Exp Cell Res*, **193**, 78-86.
25. Drygin, D., Rice, W.G. and Grummt, I. (2010) The RNA polymerase I transcription machinery: an emerging target for the treatment of cancer. *Annu Rev Pharmacol Toxicol*, **50**, 131-156.
26. Olson, M.O. (2004) Sensing cellular stress: another new function for the nucleolus? *Sci STKE*, **2004**, pe10.
27. Perry, R.P. and Kelley, D.E. (1970) Inhibition of RNA synthesis by actinomycin D: characteristic dose-response of different RNA species. *J Cell Physiol*, **76**, 127-139.
28. Sobell, H.M. (1985) Actinomycin and DNA transcription. *Proc Natl Acad Sci USA*, **82**, 5328-5331.
29. Trask, D.K. and Muller, M.T. (1988) Stabilization of type I topoisomerase-DNA covalent complexes by actinomycin D. *Proc Natl Acad Sci USA*, **85**, 1417-1421.
30. Sentenac, A., Simon, E.J. and Fromageot, P. (1968) Initiation of chains by RNA polymerase and the effects of inhibitors studied by a direct filtration technique. *Biochim Biophys Acta*, **161**, 299-308.
31. Hadjiolova, K.V., Hadjiolov, A.A. and Bachellerie, J.P. (1995) Actinomycin D stimulates the transcription of rRNA minigenes transfected into mouse cells. Implications for the in vivo hypersensitivity of rRNA gene transcription. *Eur J Biochem*, **228**, 605-615.

32. Boamah, E.K., Kotova, E., Garabedian, M., Jarnik, M. and Tulin, A.V. (2012) Poly(ADP-Ribose) polymerase 1 (PARP-1) regulates ribosomal biogenesis in Drosophila nucleoli. *PLoS Genet*, e1002442.

33. Leitinger, N. and Wesierska-Gadek, J. (1993) ADP-ribosylation of nucleolar proteins in HeLa tumor cells. *J Cell Biochem*, **52**, 153-158.

34. Meder, V.S., Boeglin, M., de Murcia, G. and Schreiber, V. (2005) PARP-1 and PARP-2 interact with nucleophosmin/B23 and accumulate in transcriptionally active nucleoli. *J Cell Sci*, **118**, 211-222.

35. Guetg, C. and Santoro, R. (2012) Formation of nuclear heterochromatin: the nucleolar point of view. *Epigenetics*, **7**, 811-814.

36. Guetg, C., Scheifele, F., Rosenthal, F., Hottiger, M.O. and Santoro, R. (2012) Inheritance of silent rDNA chromatin is mediated by PARP1 via noncoding RNA. *Mol Cell*, **45**, 790-800.

37. Wahlberg, E., Karlberg, T., Kouznetsova, E., Markova, N., Macchiarulo, A., Thorsell, A.G., Pol, E., Frostell, A., Ekblad, T., Oncu, D. *et al.* (2012) Family-wide chemical profiling and structural analysis of PARP and tankyrase inhibitors. *Nat Biotechnol*, **30**, 283-288.

38. Tulin, A., Stewart, D. and Spradling, A. (2002) The Drosophila heterochromatic gene encoding poly(ADP-ribose) polymerase (PARP) is required to modulate chromatin structure during development. *Genes Dev*, **16**, 2108-2119.

39. Guerrero, P.A. and Maggert, K.A. (2011) The CCCTC-binding factor (CTCF) of Drosophila contributes to the regulation of the ribosomal DNA and nucleolar stability. *PLoS ONE*, **6**, e16401.

40. Rancourt, A. and Satoh, M.S. (2009) Delocalization of nucleolar poly(ADP-ribose) polymerase-1 to the nucleoplasm and its novel link to cellular sensitivity to DNA damage. *DNA Repair (Amst)*, **8**, 286-297.
41. Francia, S., Michelini, F., Saxena, A., Tang, D., de Hoon, M., Anelli, V., Mione, M., Carninci, P. and d'Adda di Fagagna, F. (2012) Site-specific DICER and DROSHA RNA products control the DNA-damage response. *Nature*, **488**, 231-235.
42. Wurtmann, E.J. and Wolin, S.L. (2009) RNA under attack: cellular handling of RNA damage. *Crit Rev Biochem Mol Biol*, **44**, 34-49.
43. Li, Z., Wu, J. and Deleo, C.J. (2006) RNA damage and surveillance under oxidative stress. *IUBMB Life*, **58**, 581-588.
44. Aas, P.A., Otterlei, M., Falnes, P.O., Vagbo, C.B., Skorpen, F., Akbari, M., Sundheim, O., Bjoras, M., Slupphaug, G., Seeberg, E. *et al.* (2003) Human and bacterial oxidative demethylases repair alkylation damage in both RNA and DNA. *Nature*, **421**, 859-863.
45. Dantzer, F., Mark, M., Quenet, D., Scherthan, H., Huber, A., Liebe, B., Monaco, L., Chicheportiche, A., Sassone-Corsi, P., de Murcia, G. *et al.* (2006) Poly(ADP-ribose) polymerase-2 contributes to the fidelity of male meiosis I and spermiogenesis. *Proc Natl Acad Sci USA*, **103**, 14854-14859.
46. Bai, P., Houten, S.M., Huber, A., Schreiber, V., Watanabe, M., Kiss, B., de Murcia, G., Auwerx, J. and Menissier-de Murcia, J. (2007) Poly(ADP-ribose) polymerase-2 [corrected] controls adipocyte differentiation and adipose tissue function through the regulation of the activity of the retinoid X receptor/peroxisome proliferator-activated receptor-gamma [corrected] heterodimer. *J Biol Chem*, **282**, 37738-37746.
47. Yelamos, J., Monreal, Y., Saenz, L., Aguado, E., Schreiber, V., Mota, R., Fuente, T., Minguela, A., Parrilla, P., de Murcia, G. *et al.* (2006) PARP-2 deficiency affects the survival of CD4+CD8+ double-positive thymocytes. *EMBO J*, **25**, 4350-4360.

48. Hofer, T., Badouard, C., Bajak, E., Ravanat, J.L., Mattsson, A. and Cotgreave, I.A. (2005) Hydrogen peroxide causes greater oxidation in cellular RNA than in DNA. *Biol Chem*, **386**, 333-337.

49. Boulon, S., Westman, B.J., Hutten, S., Boisvert, F.M. and Lamond, A.I. (2010) The nucleolus under stress. *Mol Cell*, **40**, 216-227.

50. Mayer, C., Schmitz, K.M., Li, J., Grummt, I. and Santoro, R. (2006) Intergenic transcripts regulate the epigenetic state of rRNA genes. *Mol Cell*, **22**, 351-361.

51. Kutuzov, M.M., Khodyreva, S.N., Ame, J.C., Ilina, E.S., Sukhanova, M.V., Schreiber, V. and Lavrik, O.I. (2013) Interaction of PARP-2 with DNA structures mimicking DNA repair intermediates and consequences on activity of base excision repair proteins. *Biochimie*.

52. Aravind, L. and Koonin, E.V. (2000) SAP - a putative DNA-binding motif involved in chromosomal organization. *Trends Biochem Sci*, **25**, 112-114.

53. Iida, T., Kawaguchi, R. and Nakayama, J. (2006) Conserved ribonuclease, Eri1, negatively regulates heterochromatin assembly in fission yeast. *Curr Biol*, **16**, 1459-1464.

Figure Legends

Figure 1. H_2O_2 treatment induces mainly nucleolar PAR formation. Confocal IF microscopy of PAR (red) was performed after H_2O_2 treatment (1 mM, 10 min). A) Z-Stack-resolution of T24 cells, bar= 10 µM. B) Double-staining of T24 cells: PAR (red), ARTD1 (green), bar= 10µM. C) Double-staining of T24 cells: PAR (red), RNA Pol 1 (green), bar= 10µM. D) Double staining of NIH/3T3 cells after H_2O_2 treatment (1 mM, 10 min): PAR (red) and fibrillarin (green), bar= 10 µM, lower panel: 2.5x zoom.

Figure 2. ActD treatment enhances nucleolar PAR formation upon H_2O_2 and MNNG stimulation. A) IF microscopy of T24 cells was examined after H_2O_2 (1 mM, 10 min) and/or ActD treatment (50 ng/ml, 20 h) and stained for PAR formation (red), DAPI (blue). B) IF microscopy of T24 cells after MNNG (500 µM, 30 min) and/or ActD treatment (50 ng/ml, 20 h) was examined. C) Quantitative analysis of PAR positive T24 cells was performed after treatment with 50 ng/ml ActD for different incubation times (30 min, 4 h, 20 h) in combination with H_2O_2 treatment (1 mM, 10 min). Cells were analyzed for exhibiting no PAR formation (white), low PAR formation (grey bar, example: grey arrow in A and high PAR formation (black bar, example: white arrow in A). D) Quantitative analysis of the fraction of PAR positive T24 cells shown in B and analyzed as described in C).

Figure 3. ARTD2, but not ARTD1 is responsible for the ActD-dependent enhancement of PAR formation after H_2O_2 and MNNG treatment. Quantitative analysis of PAR positive T24 cells of A) siMock and siARTD1-treated cells after H_2O_2 treatment B) siARTD1-treated cells after treatment with 50 ng/ml ActD for different incubation times (30 min, 4 h, 20 h) in combination with H_2O_2 treatment (1 mM, 10 min). C) siMock and

siARTD2-treated cells after H_2O_2 treatment. D) siARTD2-treated cells after treatment with 50 ng/ml ActD for different incubation times (30 min, 4 h, 20 h) in combination with H_2O_2 treatment (1 mM, 10 min). E) F) G) H) same as in A) B) C) D) only MNNG treated (500 µM, 30 min).

Figure 4. ARTD2 activity is stimulated by rRNA *in vitro*. A) *In vitro* radioactive PARG assay carried out with *in vitro* modified ARTD1. PARG was added to each reaction in presence or absence of ActD (1 µg/ml). The reaction was performed for 15 min at 4°C. B) 45S rRNA levels and 45S rRNA fragment levels (+25/+146 bp of the pre-mature 45S transcript) were measured after ActD treatment (20h, 50 ng/ml). C) *In vitro* radioactive ARTD2 activity assay was performed with 1.6 µM NAD^+ (^{32}P) and *in vitro* transcribed rRNA fragment (146 bp) or DNA linker. CB= coomassie blot. D) *In vitro* ARTD1 radioactive activity assay was performed under the same conditions as in C) with 16 µM NAD^+ (^{32}P). E) *In vitro* radioactive ARTD2 activity assay was performed with 1.6 µM NAD^+ (^{32}P) and *in vitro* transcribed rRNA fragment (146 bp) of different amounts (0.5 pmol, 5 pmol, 10 pmol) and in presence or absence of 0.5 pmol DNA linker. Reaction was carried out at 30°C, 10min. F) *In vitro* radioactive ARTD2 activity assay with ARTD2 mutants was performed with 1.6 µM NAD^+ (^{32}P) in presence or absence of 5 pmol rRNA fragment (146 bp). FL/wt= full length human ARTD2, ARDT2 ΔSAP mutant 95-583aa, ARTD2 ΔSΔW mutant 231-583aa, ARTD2 ΔWGR mutant without WGR domain (deleted aa 116-193).

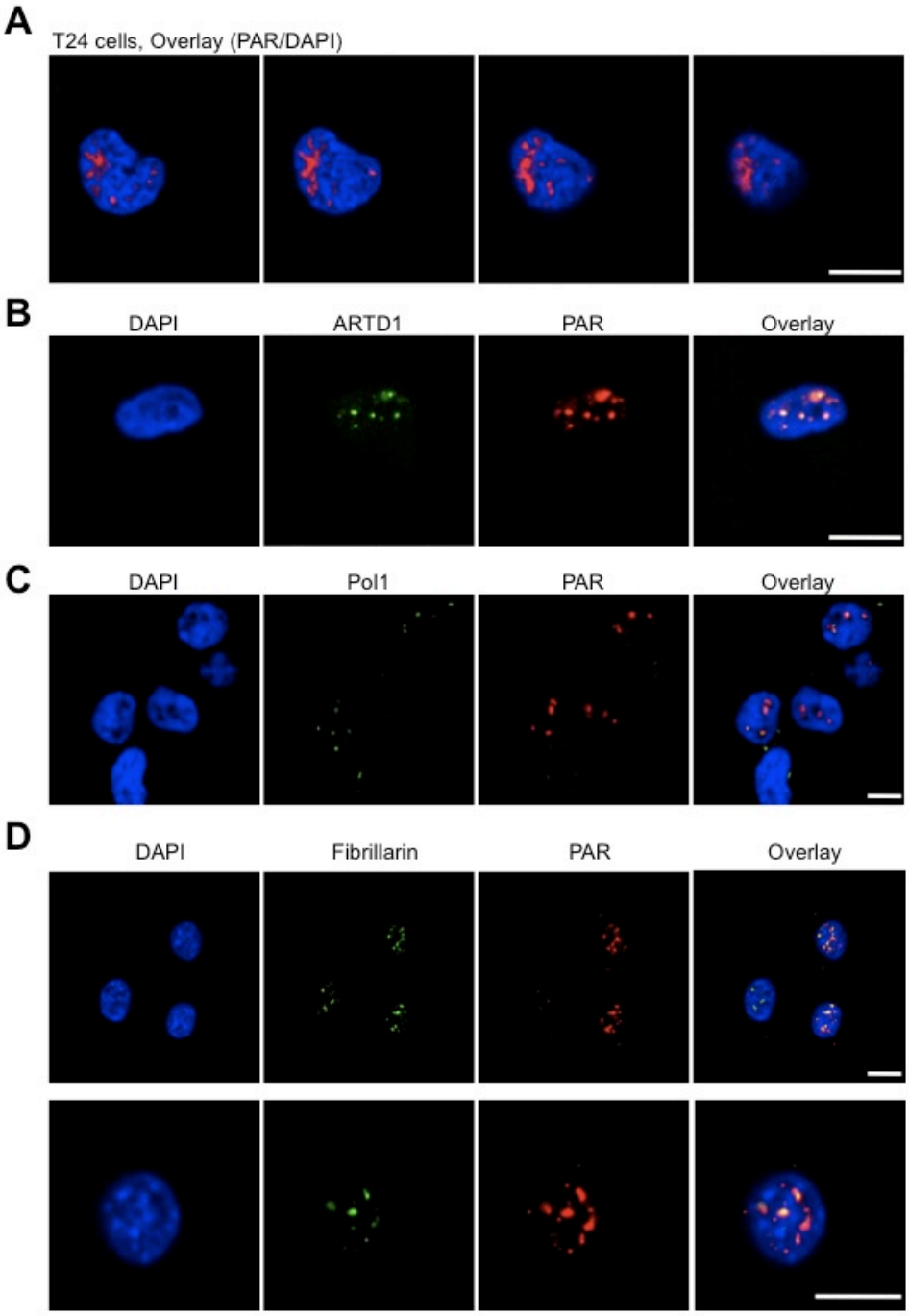
A
T24 cells, Overlay (PAR/DAPI)
B
DAPI
ARTD1
PAR
Overlay
C
DAPI
Pol1
PAR
Overlay
D
DAPI
Fibrillarin
PAR
Overlay

1

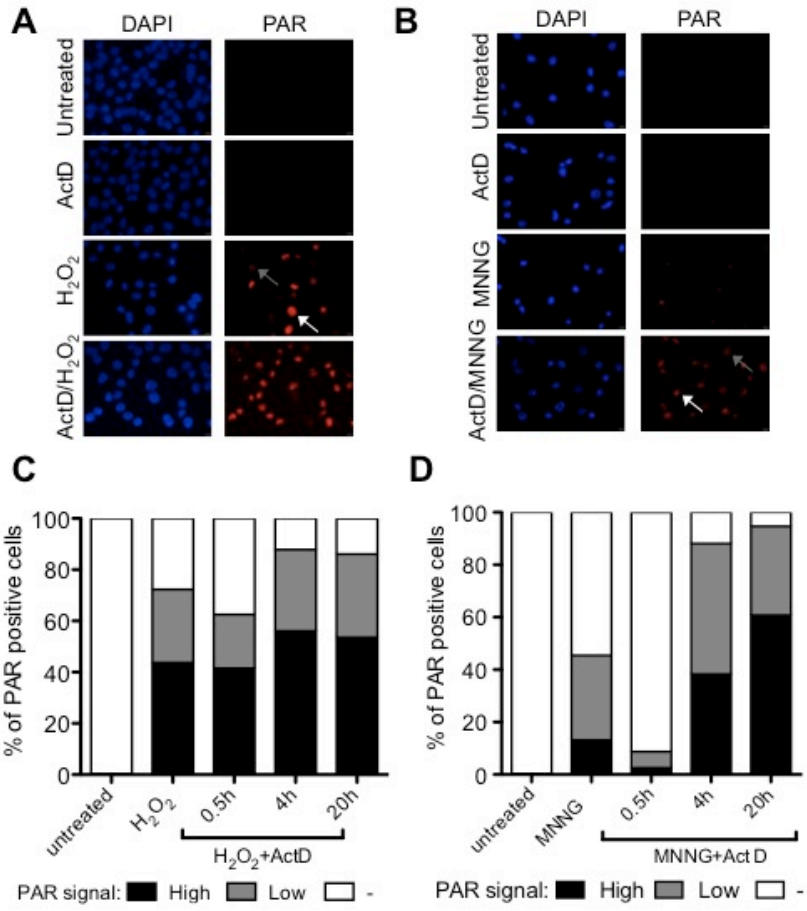
A
DAPI
PAR
Untreated
ActD
H2O2
ActD/H2O2
B
DAPI
PAR
Untreated
ActD
MNNG
ActD/MNNG
C
% of PAR positive cells
100
80
60
40
20
0
untreated
H2O2
0.5h
4h
20h
H2O2+ActD
PAR signal: High Low -
D
% of PAR positive cells
100
80
60
40
20
0
untreated
MNNG
0.5h
4h
20h
MNNG+Act D
PAR signal: High Low -

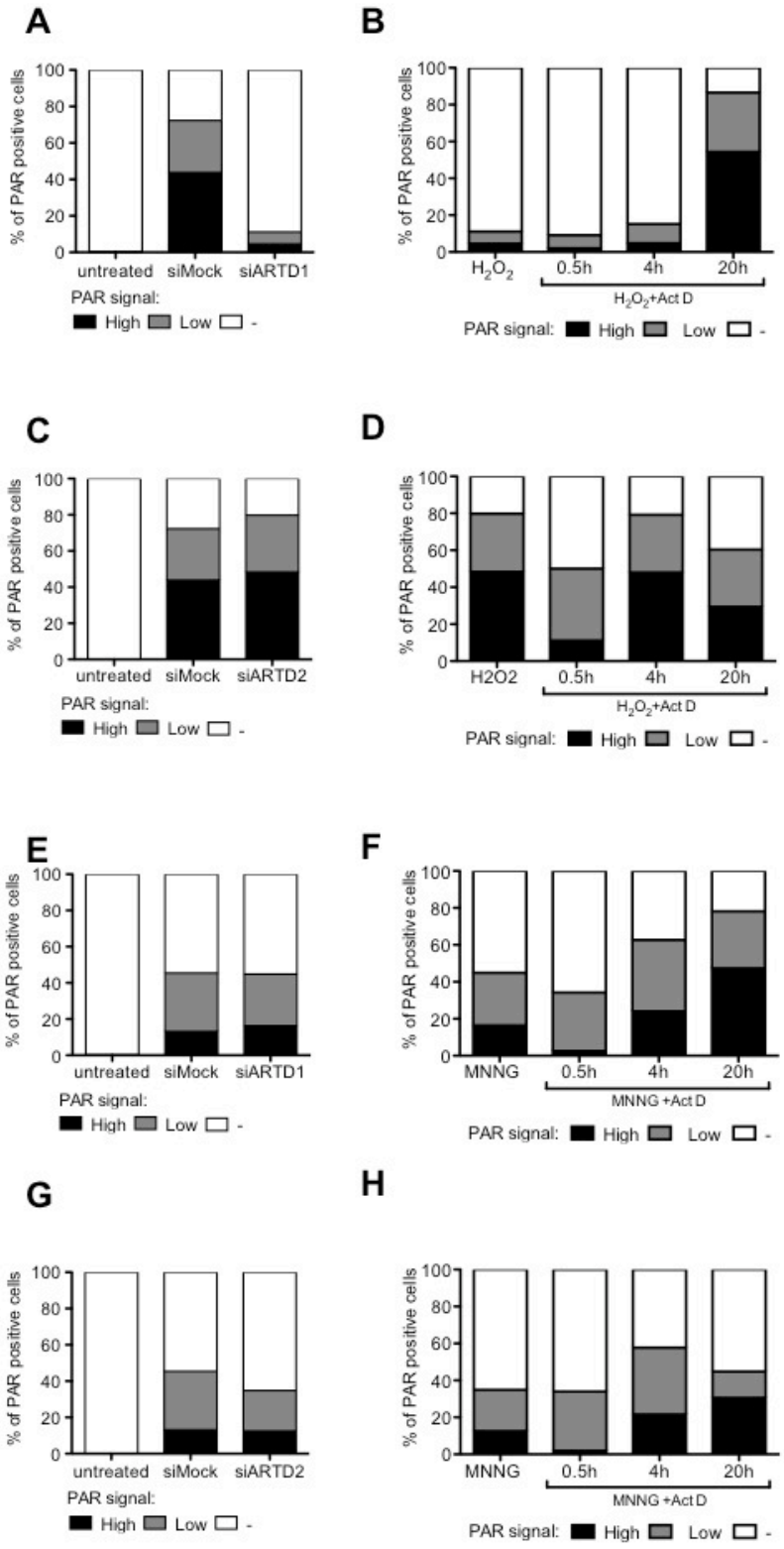
A
% of PAR positive cells
100
80
60
40
20
0
untreated
siMock
siARTD1
PAR signal:
High
Low
-
B
% of PAR positive cells
H_2O_2
0.5h
4h
20h
H_2O_2+Act D
PAR signal:
High
Low
-
C
% of PAR positive cells
untreated
siMock
siARTD2
PAR signal:
High
Low
-
D
% of PAR positive cells
H2O2
0.5h
4h
20h
H_2O_2+Act D
PAR signal:
High
Low
-
E
% of PAR positive cells
untreated
siMock
siARTD1
PAR signal:
High
Low
-
F
% of PAR positive cells
MNNG
0.5h
4h
20h
MNNG +Act D
PAR signal:
High
Low
-
G
% of PAR positive cells
untreated
siMock
siARTD2
PAR signal:
High
Low
-
H
% of PAR positive cells
MNNG
0.5h
4h
20h
MNNG +Act D
PAR signal:
High
Low
-

3

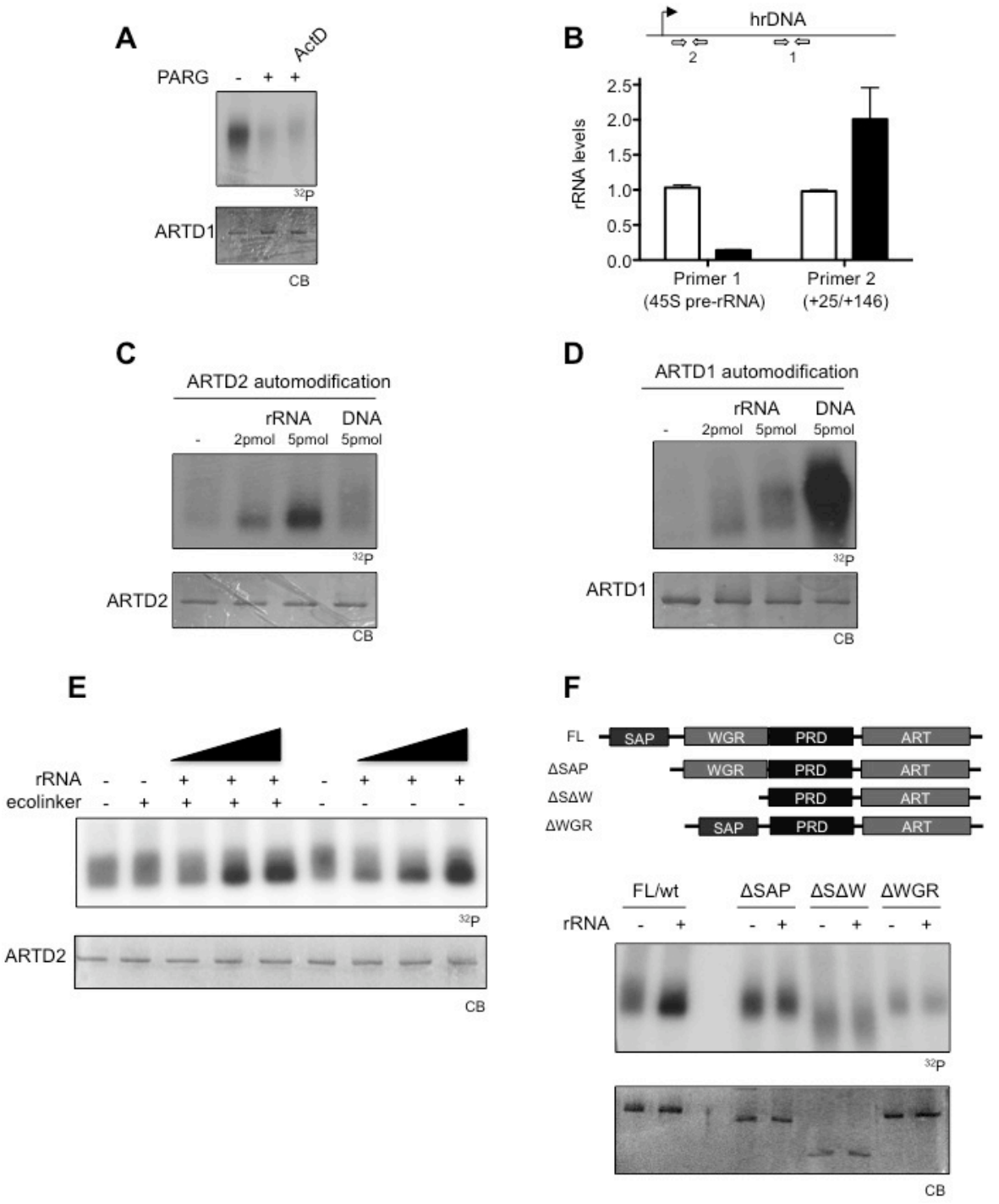
A
ActD
PARG - + +
32P
ARTD1
CB
B
hrDNA
2
1
rRNA levels
2.5
2.0
1.5
1.0
0.5
0.0
Primer 1
(45S pre-rRNA)
Primer 2
(+25/+146)
C
ARTD2 automodification
rRNA
DNA
- 2pmol 5pmol 5pmol
32P
ARTD2
CB
D
ARTD1 automodification
rRNA
DNA
- 2pmol 5pmol 5pmol
32P
ARTD1
CB
E
rRNA - - + + + - + + +
ecolinker - + + + + - - - -
32P
ARTD2
CB
F
FL SAP WGR PRD ART
ΔSAP WGR PRD ART
ΔSΔW PRD ART
ΔWGR SAP PRD ART
FL/wt ΔSAP ΔSΔW ΔWGR
rRNA - + - + - + - +
32P
CB

Supplementary Figures

ARTD2 activity is stimulated by RNA

Karolin Léger[1,2], Natasa Savic[1,2], Raffaella Santoro[1], Michael O. Hottiger[1*]

[1]Institute of Veterinary Biochemistry and Molecular Biology, University of Zurich, Winterthurerstrasse 190, 8057 Zurich, Switzerland

[2]Life Science Zurich Graduate School, University of Zurich, 8057, Switzerland

*Corresponding author: Email: hottiger@vetbio.uzh.ch

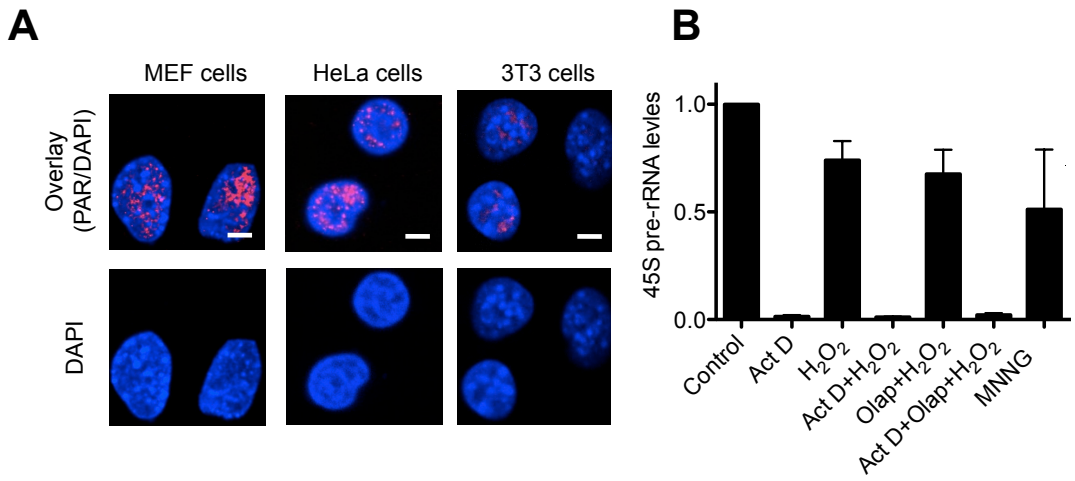
A
MEF cells
HeLa cells
3T3 cells
Overlay (PAR/DAPI)
DAPI
B
45S pre-rRNA levles
1.0
0.5
0.0
Control
Act D
H2O2
Act D+H2O2
Olap+H2O2
Act D+Olap+H2O2
MNNG

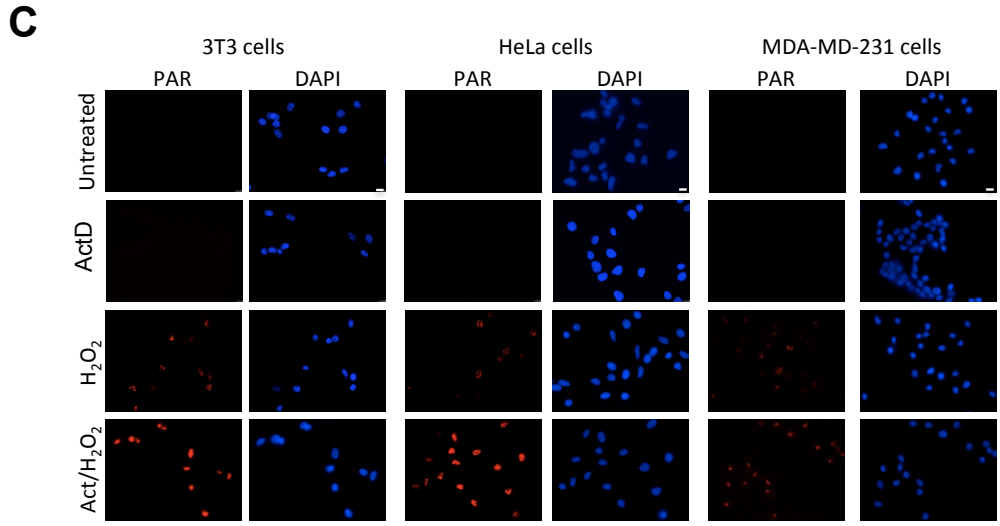
C
3T3 cells
HeLa cells
MDA-MD-231 cells
PAR
DAPI
Untreated
ActD
H2O2
Act/H2O2

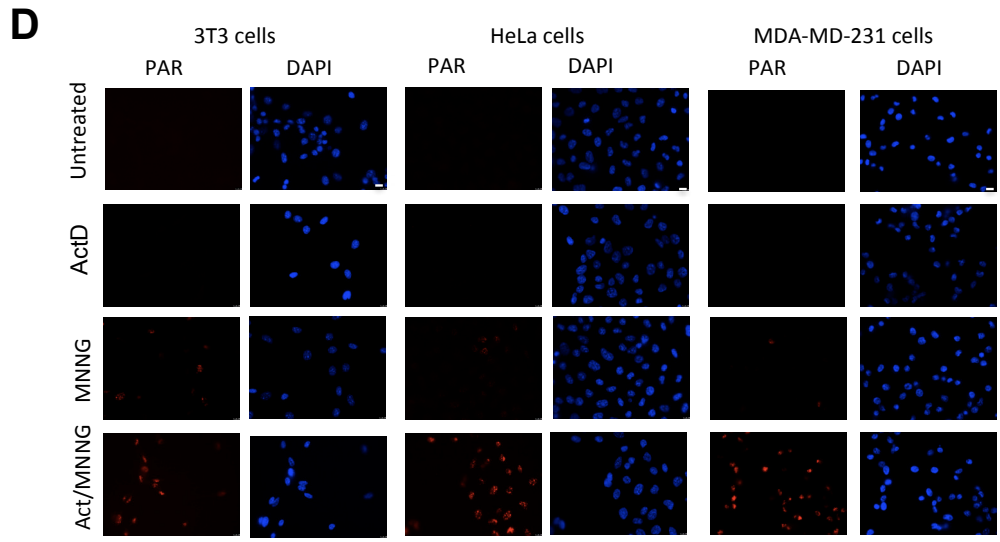
D
3T3 cells
HeLa cells
MDA-MD-231 cells
PAR
DAPI
Untreated
ActD
MNNG
Act/MNNG

Supplementary Figure 1. H_2O_2 treatment induces nucleolar PAR formation. A) Confocal IF microscopy of PAR (red) after H_2O_2 treatment (1 mM, 10 min) was analyzed in MEF cells, HeLa cells and NIH/3T3 cells, bar= 10 µM. B) 45S tanscription in T24 cells was measured by qPCR after ActD treatment (50 ng/ml, 20 h); Olaparib treatment (10 µM, 3 h); H_2O_2 treatment (1 mM, 10 min) or MNNG treatment (500 µM, 30 min). C) IF microscopy of different cell lines after H_2O_2 (1 mM, 10 min) and/or ActD treatment (50 ng/ml, 20 h) was performed. Cells were stained with DAPI (blue) and for PAR (red). D) IF microscopy of different cell lines after MNNG (500 µM, 30 min) and/or ActD treatment (50 ng/ml, 20 h) was performed. Cells were stained with DAPI (blue) and for PAR (red).

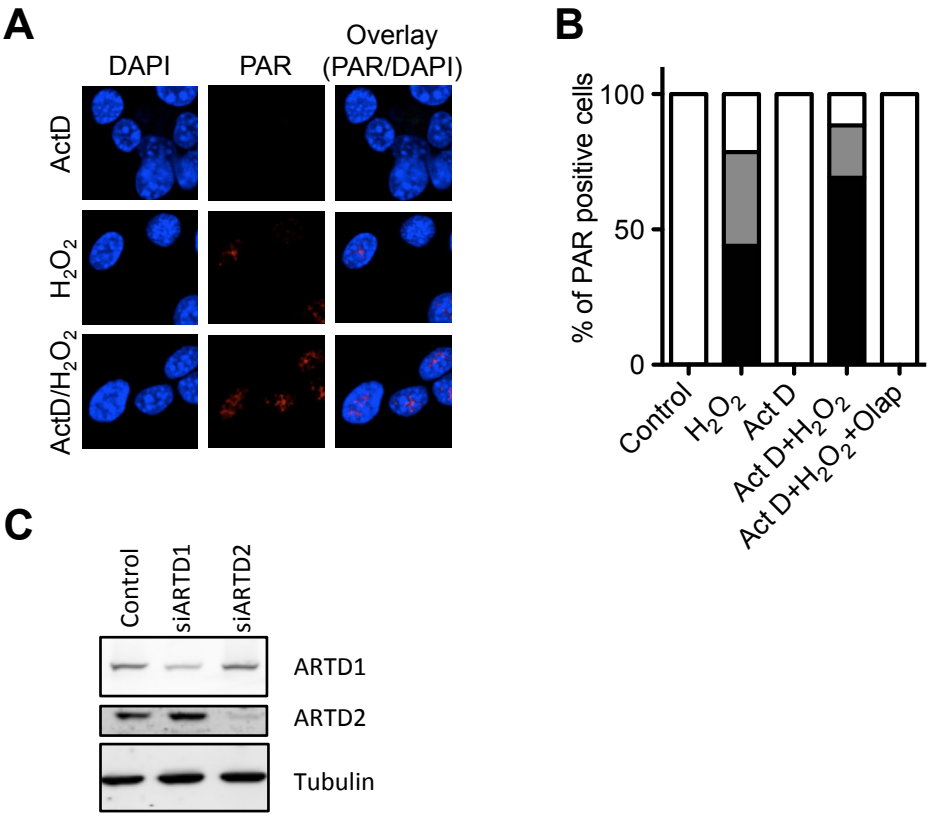

Supplementary Figure 2. ActD treatment enhances nucleolar PAR formation. A) Confocal IF microscopy of NIH/3T3 cells was performed after H_2O_2 (1 mM, 10 min) and/or ActD treatment (50 ng/ml, 20 h) to detect PAR (red). B) Quantitative PAR analysis of NIH/3T3 cells in presence or absence of ActD (50 ng/ml, 20 h), H_2O_2 (1 mM, 10 min) treatment and Olaparib treatment (10 µM, 1 h). C) Western blot analysis of T24 cells treated with siMock, siARTD1 or siARTD2.

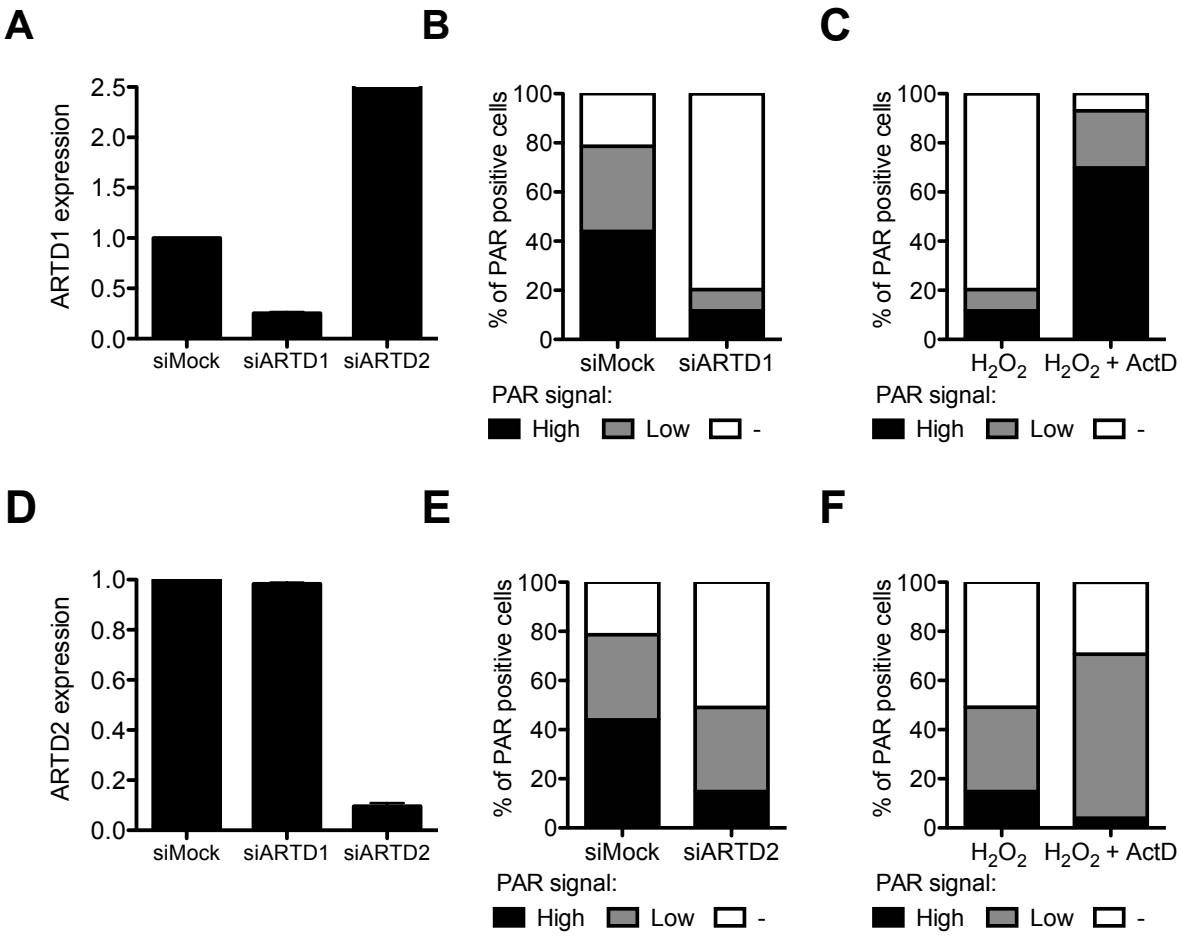
A
B
C
ARTD1 expression
2.5
2.0
1.5
1.0
0.5
0.0
siMock
siARTD1
siARTD2
% of PAR positive cells
100
80
60
40
20
0
siMock
siARTD1
PAR signal:
High
Low
-
H_2O_2
H_2O_2 + ActD
D
E
F
ARTD2 expression
1.0
0.8
0.6
0.4
0.2
0.0
siMock
siARTD1
siARTD2
siARTD2
G
shMock
shARTD1
ActD
H_2O_2
Olaparib
PAR-10H
250 kDa –
130 kDa –
100 kDa –
ARTD1
Tubulin
Control

Supplementary Figure 3. ActD treatment increases nuclear PAR formation upon H_2O_2 in siARTD1 and siARTD2 treated NIH/3T3 cells. A) Knockdown efficiency of siARTD1 treatment was measured by qPCR in NIH/3T3 cells. B) Quantitative analysis of IF microcopy of PAR positive NIH/3T3 cells in siARTD1 background was measured after H_2O_2 treatment (1 mM, 10 min). C) Same as in B) but additionally ActD treated (50 ng/ml, 20 h). D) Knockdown efficiency of siARTD2 treatment was measured by qPCR in NIH/3T3 cells. E) Quantitative analysis of immunofluorescence microcopy of PAR positive NIH/3T3 cells in siARTD2 background was measured after H_2O_2 treatment (1 mM, 10 min). F) Same as in E) but additionally Act D treated (50 ng/ml, 20 h). G) Western blot analysis of stably transfected NIH/3T3 cells with shMock or shARTD1 was performed, treated with ActD (50 ng/ml, 20 h), H_2O_2 (1 mM,10 min) and Olaparib (10 μM, 3 h).

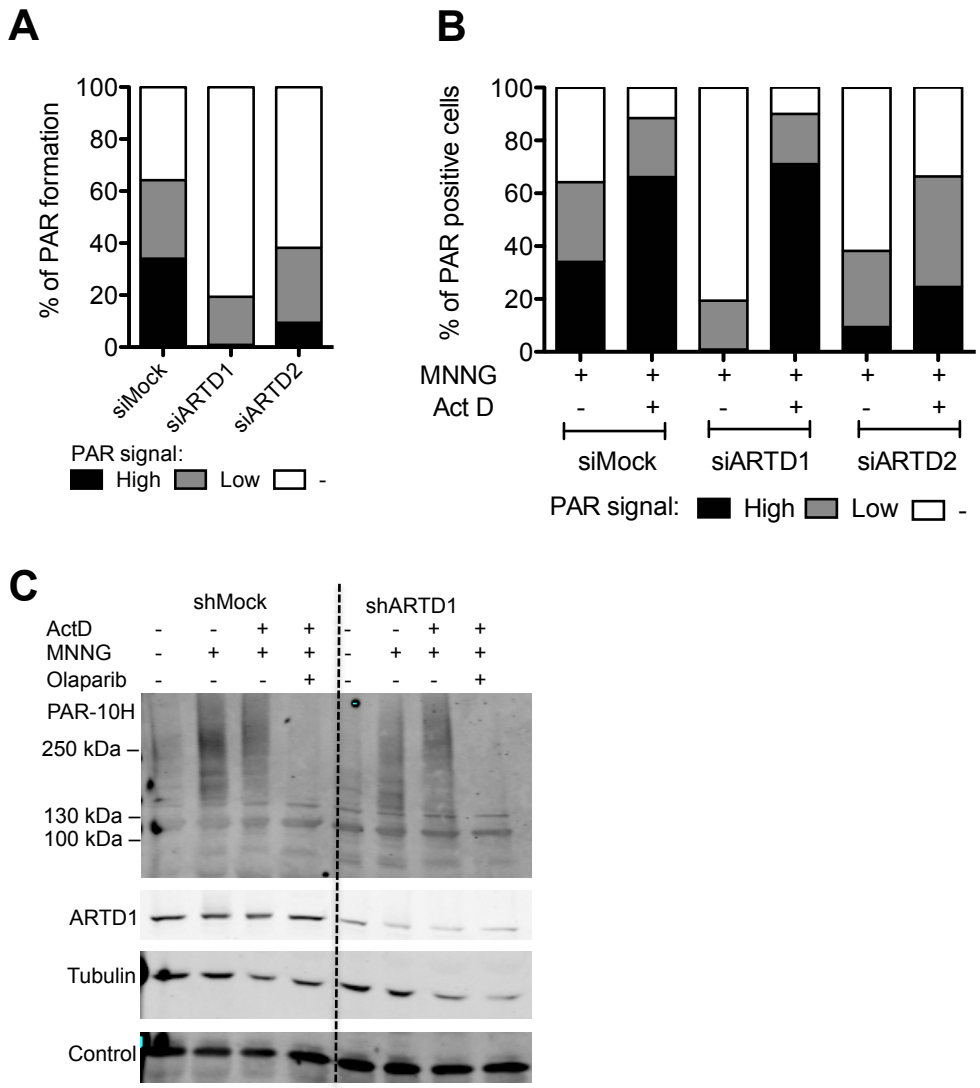

Supplementary Figure 4. ARTD2 is responsible for ActD induced nuclear PAR formation upon MNNG stimulation in NIH/3T3 cells. A) Quantification of the fraction of PAR positive, siARTD2 or siARTD1 transfected NIH/3T3 cells was measured by analyzing IF microscopy pictures obtained after MNNG treatment (500 µM, 30 min). B) as in A) but additionally ActD treated (50 ng/ml, 20 h). C) Western blot analysis of stably transfected NIH/3T3 cells with shMock or shARTD1 was performed, treated with ActD (50 ng/ml, 20 h), MNNG (500 µM, 30 min) and Olaparib (10 µM, 3 h).

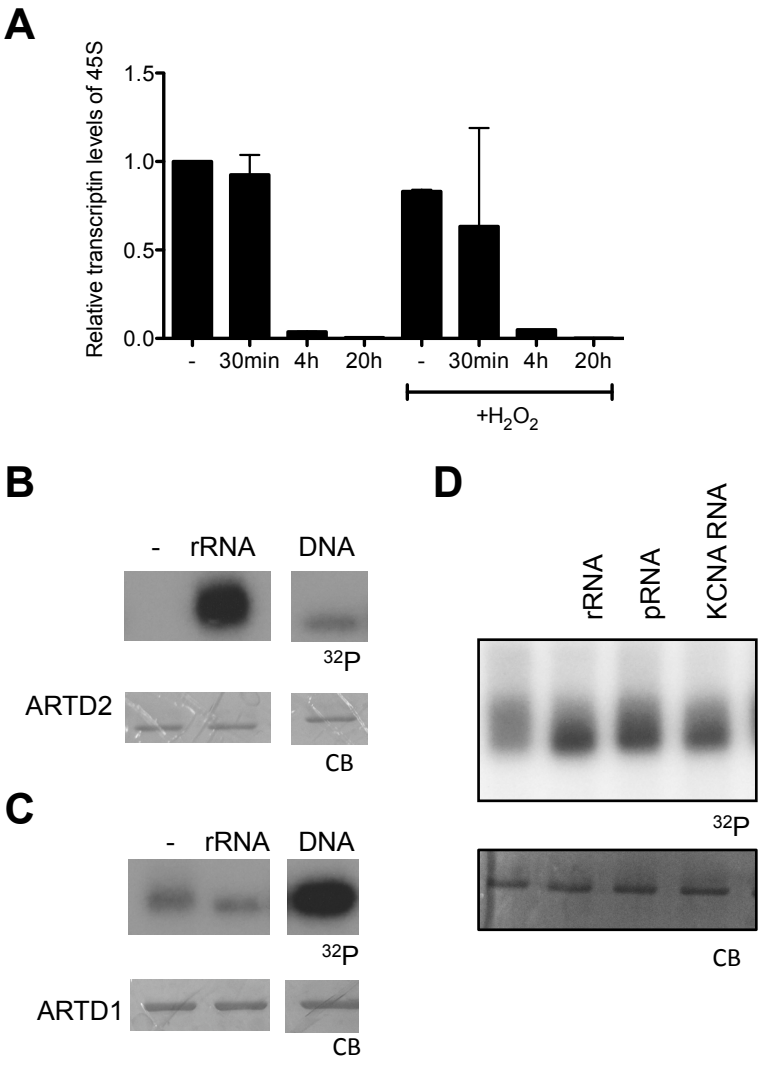

Supplementary Figure 5. ***In vitro*** **ARTD2 activation by RNA.** A) 45S rRNA transcription was measured of T24 cells treated with ActD (50 ng/ml) for 30 min, 4h or 20h in combination with H_2O_2 treatment for the last 10min (1mM). B) *In vitro* radioactive ARTD2 activity assay was performed with 100 nM NAD^+ (^{32}P) and an *in vitro* transcribed rRNA fragment (146 bp, 2pmol) or ecolinker DNA (5pmol). CB= coomassie blot. C) *In vitro* radioactive ARTD1 activity assay was performed as in A. D) *In vitro* radioactive ARTD2 activity assay was performed with 1.6 μM NAD^+ (^{32}P) and *in vitro* transcribed rRNA fragment (146 bp), KCNA RNA (237 bp), pRNA (232 bp).

ARTD1 and ARTD2 differentially regulate cell-cycle re-entry and progression in T24 bladder carcinoma cells

Karolin Léger[1,2], Michael O. Hottiger[1*]

[1]Institute of Veterinary Biochemistry and Molecular Biology, University of Zurich, Winterthurerstrasse 190, 8057 Zurich, Switzerland

[2]Life Science Zurich Graduate School, University of Zurich, 8057, Switzerland

*Corresponding author: Email: hottiger@vetbio.uzh.ch

Running title: *ARTD cell cycle regulation*

Key words: PARP1, PARP2, cell cycle, regulation, E2F-1, cyclin E, p27, gene expression

Abstract

Under favorable conditions, arrested cells are able to re-enter the G_1 phase and to progress through the cell cycle. Among the molecular factors that are involved in cell cycle re-entry are for example transcription factors of the E2F family, cyclin-dependent kinases, cyclins or microRNAs. ARTD1 (PARP1) and ARTD2 (PARP2) have recently been described to co-regulate the expression of proteins involved in different cellular processes. Here we investigated the functional contribution of ARTD1 and ARTD2 for cell cycle re-entry and cell-cycle progression. For this analysis, ARTD1 and ARTD2 were down-regulated in T24 urinary bladder carcinoma cells using an siRNA approach and cell cycle re-entry and progression of synchronous cells was studied. We describe that siARTD1 treatment of T24 cells caused specific down-regulation of *Cyclin E* but not of other E2F-1 target genes and thereby lead to a decelerated cell cycle re-entry and progression. In absence of ARTD1, the *Cyclin E* promoter was enriched for H1 and reduced for H4 acetylation and H2A.Z, indicating at a rather compact chromatin. In contrast, down-regulation of ARTD2 by siRNA treatment specifically affected *p27*, but not *p21* expression and rendered T24 unable to re-enter the cell cycle. Lack of ARTD2 lead to an increase of the activating marks H3K4me3 as well as H4 acetylation and a decrease of the repressory mark H3K27me3. Together, our results provide evidence for novel, non-redundant functions in cell cycle re-entry and progression for both, ARTD1 and ARTD2.

Introduction

The G_0 phase is a transcriptionally silent stage of the cell cycle that cells enter upon growth inhibition[1]. If the conditions change and become favorable for cell growth again, cells are able to re-enter the G_1 phase and progress through the cell cycle. Among the molecular factors that are involved in cell cycle re-entry are for example transcription factors of the E2F family (e.g., E2F1, E2F4), cyclin-dependent kinases (e.g., Cdk2, Cdk3, Cdk4, Cdk6)[2], cyclins, the retinoblastoma protein (pRb)[3], or microRNAs[4]. pRb is one of the key players of the early cell cycle phases whose inactivation (phosphorylation) seems sufficient for cell cycle re-entry[5]. It binds transcription factors (e.g., E2F) of downstream targets involved in cell proliferation and thus functions as a classical tumor suppressor gene. pRb is absent or mutated in one third of all tumors[6, 7]. For example, pRb is hyperphosphorylated in asynchronous human bladder carcinoma cells and should thus favor cell cycle progression[8]. The most prominent factors regulated by pRb are E2F proteins, histone deacetylases and chromatin remodeling complexes[9]. E2F proteins are a family of transcription factors of which three are activators (E2F-1 to 3) and five are repressors (E2F-4 to 8). E2F targets include Cyclin E, A, D1, Cdc2, Cdc25A, DNA polymerase, Cdc6 and minichromosome maintenance (MCM) proteins[10]. Cyclin E, in complex with Cdk2, is the main driver of G_1-S phase progression. A further level of cell cycle regulation is carried out by cell cycle inhibitors such as the CIP/KIP family proteins p21 and p27. These two homologous proteins bind to cyclin - Cdk complexes and inhibit their activity, but have also been implicated in cyclin-independent functions in the nucleus as well as in the cytoplasm[11, 12].

ADP-ribosylation is a post-translational protein modification (PTM) that consists of ADP-ribose units that are transferred to specific residues on target proteins. The protein family of the ADP-ribosyltransferases comprises 18 members, which are divided into cholera toxin and diphtheria toxin like ADP-ribosyltransferases (ARTCs and ARTDs, respectively).

The ARTD subgroup comprises only intracellular proteins that transfer the ADP-ribose moiety from NAD^+ and thereby catalyze mono- or poly-ADP-ribosylation of acceptor proteins. The best-studied members are ARTD1 (formerly PARP1) and its close homologue ARTD2 (PARP2). Both, ARTD1 and ARTD2 are nuclear proteins that poly-ADP-ribosylate target proteins or themselves. Experimental evidence so far indicates that ARTD1 is the most active cellular ADP-ribosyltransferase and that ARTD2 only contributes 5-10 % of PAR synthesis[13]. However, ARTD1 and ARTD2 must also exhibit distinct functions, since the deletion of both genes causes synthetic lethality [14]. This is also emphasized by the fact that in particular the DNA binding domains of ARTD1 and ARTD2 differ[15], which may hint at distinct activation mechanisms and cellular functions. Furthermore, the carboxy-terminal catalytic domains of ARTD1 and ARTD2 are not able to compensate for each other[16].

ADP-ribosylation is involved in a variety of biological processes, many of which are chromatin dependent and linked to important functions during the cell cycle. For example, ARTD1 localizes to and modifies centromeric proteins[17-19], was described to regulate the mitotic chromosomal protein kinase Aurora B by PARylation[20] and modifies chromatin-associated proteins[21]. Importantly, depletion of ARTD1 or inhibition of ADP-ribosylation has also lead to a cell cycle arrest in prophase or prolongation of the G_2-M phase transition, suggesting that it is required for chromosomal functions during mitosis[22-26]. Recently, it was also shown that progestin gene regulation involves the activation of ARDT1 via Cdk2-dependent phosphorylation and consecutive modification and displacement of histone H1 [27]. This is essential for the effect of progestins on cell cycle progression in breast cancer. There are also various reports that implicate functions of ARTD1 in early cell cycle phases. For example, ARTD1 and the C-terminal binding protein (CtBP) form a co-repressor complex for p21 repression and ARTD1 activity is necessary for p21 activation after genotoxic stress[28]. Simbulan-Rosenthal et al. showed that ARTD1 up regulates the promoter activity of E2F-1

during the early S phase and that ARDT1 interacts with E2F-1 *in vitro* and *in vivo* in immortalized fibroblasts that were synchronized by serum deprivation or aphidicolin treatment[29, 30]. Another study detected PAR formation during G_0-G_1 transition after mitogen induction and thus implicated ARTD1 in growth factor signaling and the induction of immediate-early genes[31]. Deletion of ARTD2 rendered mouse embryonic fibroblasts sensitive to DNA base damage and consecutively prevented resumption of cell cycle progression[14]. ADP-ribosylation in general is involved in spindle formation, the assembly of spindle poles[32, 33], heterochromatin formation[34], and the maintenance of an ATR and Chk1-dependent S-phase checkpoint[35].

Any study on ADP-ribosylation and the cell cycle faces the problem that synchronization with chemical agents or by serum starvation and subsequent growth factor addition already activates ADP-ribosylation[36]. In the study described here, we used T24 urinary bladder carcinoma cells, which represent a well-characterized exemplary bladder cancer cell line[37, 38]. Importantly, T24 cells synchronously re-enter the cell cycle after splitting without any additional stimuli and are therefore an ideal model to study cell cycle regulation. However, the molecular mechanism responsible for this characteristic cell cycle regulation is not known.

Here, ARTD1 and ARTD2 were down-regulated in T24 cells using an siRNA approach and cell cycle re-entry and progression were studied. Our results indicated distinct functions in cell cycle progression for ARTD1 and ARTD2. siARTD1 treatment of T24 cells caused down-regulation of Cyclin E expression and thereby lead to decelerated cell cycle entry and progression. Interestingly, the expression of other E2F-1 target genes was not affected or even enhanced. In contrast, down-regulation of ARTD2 by siRNA treatment specifically enhanced p27 expression, but not p21, and rendered T24 unable to re-enter the cell cycle. Furthermore, ChIP experiments revealed that lack of ARTD1 lead to an increase

of H1 recruitment and a reduction of H4 acetylation as well as H2A.Z content at the Cyclin E promoter, while the absence of ARTD2 lead to a reduction of the H3K27me3 and an increase of the H3K4me3 mark at the p27 promoter. These molecular analyses of cell cycle regulatory factors and promoter marks in siARTD1 and siARTD2 treated T24 cells thus confirm novel, non-redundant functions in cell cycle regulation of these two ARTD family members.

Results

Down regulation of ARTD1 in T24 cells leads to decelerated cell cycle re-entry and cell cycle progression, while knocking down ARTD2 maintains cells in G_0.

In order to elucidate the role of ARTD1 and ARTD2 and their enzymatic activity on cell cycle re-entry and progression, the urinary bladder carcinoma cell line T24 was studied. T24 cells have the characteristic of arresting in the G_0 phase of the cell cycle upon reaching confluence and synchronously re-enter the cell cycle after splitting, without additional stimuli[39, 40]. These cells are thus an ideal model, because synchronization does not require chemical agents or stimuli that may activate these enzymes. T24 cells are characterized by strong, cell-cycle dependent retinoblastoma (Rb) phosphorylation[8], which is indicated by the comparison with U2OS cells (Fig. 1A). The cell cycle effects that can be studied in T24 cells are thus down-stream of Rb phosphorylation. To assess the role of ARTD1 and ARTD2, both proteins were down-regulated by siRNA treatment of T24 cells in G_0 (Fig. 1B). To specifically assess cell cycle re-entry and progression downstream of Rb, siRNA treated cell were synchronously released into the cell cycle by splitting the cells (Fig. S1A). The expression of ARTD1 was confirmed to remain knocked down during the whole analysis (Fig. S1B).

Flow-cytometry analysis of siMock and siARTD1 T24 cells indicated a delayed cell cycle re-entry and progression for siARTD1 cells that became apparent 16 h after splitting, which suggests a decelerated S-phase transition (Fig. 1C, D). This finding was confirmed by reduced bromodeoxyuridine (BrdU) incorporation in siARTD1 cells (Fig. S1C) and stably knocking down ARTD1 in T24, which similarly caused a delay in S-phase (Fig. S1D). In contrast, siARTD2 treatment caused an almost complete inability to re-enter the cell cycle (Fig. 1C, D), indicating that both ARTD1 and ARTD2 regulated cell-cycle re-entry and

progression, although through a different molecular mechanism. Treatment of T24 cells in G_0 with the PARP inhibitors Olaparib or Veliparib and subsequent release into the cell cycle also caused an increase in the cell population in S-phase and a reduction in the G_2/M-phase cells indicated that ADP-ribosylation by ARTD1 and ARTD2 is not required for the above described cell cycle phenotypes, but that it is required for normal cell cycle progression of T24 cells through S phase (most likely ARTD1 enzymatic activity, Fig. S1E). Based on these results it was concluded that ARTD1 and ARTD2 play important, non-redundant functions in cell cycle progression of T24 urinary bladder carcinoma cells.

ARTD1 down regulation causes down-regulation of Cyclin E expression.

Since ARTD1 was implicated in DNA repair, siARTD1 treatment of T24 may induce DNA damage and subsequently lead to cell cycle arrest. Western blot analysis of siMock and siARTD1 treated cells at different time points after release indicated that down-regulation of ARTD1 had no effect on protein 53 (p53), p21, p27 and p57 levels or on replication protein A (RPA) and Chk-1 phosphorylation (Fig. 2A and S2A-E), suggesting that the observed deceleration was not the results of an activated DNA damage response.

In order to characterize and mechanistically understand the function of ARTD1 for cell cycle progression of T24 cells, the expression levels of the important cell cycle regulator E2F-1 were further assessed in siMock and siARTD1 treated cells throughout the cell cycle. E2F-1 transcript levels were only slightly elevated in siARTD1 treated cells in comparison to control cells and only at distinct time-points (0-4 h; 24 h), furthermore this change was not observed at the protein level (Fig. 2B, C), indicating that E2F-1 was not altered under the tested conditions. Moreover, ARTD1 depletion neither affected cyclin-dependent kinase 2 (Cdk2) transcription, while the protein levels were slightly increased, which could however not account for the observed deceleration (Fig. S2F). Interestingly, when analyzing different

cyclins in siARTD1 treated T24 cells, mRNA and protein levels of the E2F-1 target *Cyclin E* were, at all measured time-points, lower and particularly in S-phase significantly reduced (Fig. 2D, E). In contrast, the Cyclin A, B and D transcript and protein levels were not or rather slightly increased upon knockdown of ARTD1 (Fig. S3A, B). The reduced *Cyclin E* expression could not be attributed by a lack of E2F-1 (Fig. 1A and 2B) or the inability of E2F-1 to activate genes, since the E2F target gene *c-myc* as well as *miR-15* and *miR-16* were up-regulated upon siARTD1 treatment (Fig. S3C-E). Repeating the *Cyclin E* expression analysis during the cell cycle in the presence of the PARP inhibitor Olaparib confirmed that the enzymatic activity of ARTD1 is dispensable for the effect on *Cyclin E* expression (Fig. 2F). Again, Cyclin E reduction was similarly observed in stable shARTD1 knock-down cells (Fig. S3F), indicating that the deceleration can be induced also upon permanent knock-down of ARTD1. Based on these results it was concluded that ARTD1 down-regulation in T24 cells mainly affected cell cycle re-entry and progression by reducing *Cyclin E* expression.

Knocking down ARTD1 reduces H4 acetylation and H2A.Z, but increases H1 levels at the *Cyclin E* promoter.

In order to investigate how ARTD1 down-regulation affects *Cyclin E* expression, repressory and activatory marks at the *Cyclin E* promoter were analyzed. In agreement with the previous findings, ARTD1 recruitment to the *Cyclin E* promoter, analyzed by chromatin immune-precipitation, was significantly increased upon entry of siMock-treated T24 cells into G_1-phase (Fig. 3A). In siARTD1 cells, no recruitment was detectable, confirming the specificity of the assay and suggesting that ARTD1 might render the *Cyclin E* promoter permissive and therefore transcriptionally active. siARTD1 treatment did not affect histone H3 during cell cycle re-entry (compare G_0 to G_1), since neither H3 levels at the *Cyclin E* promoter nor H3 lysine 4 trimethylation (H3K4me3), which is a mark for actively transcribed genes, were

influenced (Fig. 3B, C). However, histone H4 acetylation (H4ac), another mark of active transcription, was strongly reduced in siARTD1 T24 cells as compared to siMock treated cells (Fig. 3D). Additionally, another mark that is associated with promoters of actively transcribed genes, the presence of the histone H2A variant H2A.Z[41], did change significantly in response to ARTD1 down-regulation. H2A.Z was highly enriched at the *Cyclin E* promoter and significantly declined upon the depletion of ARTD1 by siRNA treatment (Fig. 3E). In contrast, the linker histone variant H1.2 strongly increased at the *Cyclin E* promoter upon siARTD1 treatment in both the G_0 and the G_1 phase (Fig. 3F). In summary, knocking down ARTD1 changed the histone marks at the *Cyclin E* promoter in such a manner that the compaction of this chromatin region seems to be enhanced (loss of H4 acetylation, increase of H1 recruitment), subsequently also negatively affecting the transcription of *Cyclin E* (loss of H2A.Z).

ARTD2 regulates p27 transcription at the chromatin level.

Our initial findings (Fig. 1C) hinted at distinct, non-redundant functions of ARTD1 and ARTD2 for cell cycle progression of T24 cells. Additional analysis of the ARTD2 levels confirmed that ARTD2 was as well down regulated, during the whole time period (Fig. S4A). Western blot analysis of ARTD1, revealed that ARTD1 was cleaved under these conditions, indicating that knock-down of ARTD2 is inducing apoptosis (Fig. 4SB). Interestingly, this seemed not to be mediated by p53, since neither p53 nor p21 levels were altered (Fig. 4A, S4B). Surprisingly, p27 were very strongly up regulated under the tested conditions, providing an explanation for the strong cell cycle arrest and the observed induction of apoptosis (Fig. 4A,S4B).

In order to elucidate the molecular mechanism by which ARTD2 affects p27 expression, the transcription levels of p27 and of p21 as a control were analyzed by qRT-PCR. While p21

expression levels were not affected, p27 levels were strongly enhanced, indicating that ARTD2 is regulating p27 expression mainly at the transcriptional level. This result was confirmed by a promoter analysis, which detected significantly increased activatory H3K4me3 levels and decreased repressory H3K27me3 marks at the p27 promoter in siARTD2 treated T24 cells, while total H3 occupancy or acetylation of H4 was minimally affected (Fig. 4B, 4D). Comparable analysis at the p21 promoter revealed that knocking down ARTD2 did not affect this chromatin region and indicated that the observed changes are p27 specific (Fig. 4C, 4D). Moreover, the observed chromatin changes were limited to the p27 promoter region, since these chromatin changes were not observed in a region of the p27 nor the p21 gene body (Fig. S4C). Together, these results suggest that ARTD2 affects the cell cycle in synchronized T24 cells via modulating the expression of the cyclin-dependent kinase inhibitor p27, which represents a distinct and different mechanism in comparison to ARTD1.

Discussion

ARTD1 and ARTD2 are the most homologous members of the ARTD protein family and often thought to fulfill similar functions. However, ARTD1 has been studied much more extensively and is in general a more active enzyme. This is one of the reasons why it has proven difficult to identify specific functions of ARTD2. T24 bladder carcinoma cells re-enter the cell cycle and divide synchronously after splitting and are therefore an ideal model to study cell cycle regulation without the addition of toxins or stimulatory factors. Using a siRNA approach to down-regulate ARTD1 and ARTD2 in T24 cells and an analysis of cell cycle re-entry and progression of synchronous cells revealed non-redundant functions for both, ARTD1 and ARTD2. The work described here suggests down-regulated *Cyclin E* as the cause for decelerated cell cycle entry and progression in siARTD1 treated cells, while ARTD2 was shown to specifically affect *p27* expression levels. The molecular analyses of marks at the promoter sites of *Cyclin E* and *p27* in siARTD1 and siARTD2 treated T24 cells revealed that both proteins affect the promoter structure through different mechanisms. These results therefore confirm non-redundant functions in cell cycle re-entry and progression of ARTD1 and ARTD2.

Our results indicate that ARTD1 is required for the correct regulation of *Cyclin E* expression during cell cycle re-entry and G_1 – S phase progression. The increased recruitment of ARTD1 to the *Cyclin E* promoter during G_0 - G_1 phase transition indicates that ARTD1 might affect the initiation of *Cyclin E* transcription. Interestingly, this effect was independent of ARTD1 enzymatic activity, since no cell cycle deceleration could be observed in PARP inhibitor (e.g., Olaparib) treated cells. The *Cyclin E* promoter state was thus not regulated via the ADP-ribosylation of histone modifiers such as the demethylase KDM5B[42], and the levels of H3K4me3 were not changed upon siARDT1 treatment. Beside a reduced acetylation of H4, the main observed changes in siARTD1 treated cells included an increase in H1.2 and a

reduction of the H2A.Z levels at the *Cyclin E* promoter. Increased H1 recruitment as well as decreased H2A.Z were both reported to coincide with a restrictive chromatin state and reduced gene expression [41, 43]. While replacement of H1 by ARDT1 has been documented before for many promoters of actively transcribed genes[43], changes of H2A.Z were not described before. It remains to be investigated whether the alterations of H2A.Z and H1 are regulated by separate mechanisms, or whether the H2A.Z changes are a consequence of the observed H1 changes. Moreover, it is not clear by which mechanism ARTD1-dependent regulation is confined to *Cyclin E* expression without affecting other E2F-1 target genes. It will be interesting to study if the recruitment of ARTD1 to promoters is fine-tuned and regulated by posttranslational modifications of ARTD1 (e.g., acetylation, mono-ADP-ribosylation, phosphorylation, sumoylation or ubiquitylation) as previously suggested[44].

In contrast to *Cyclin E* expression, our studies also revealed that the expression levels of two other E2F-1-induced miRNAs (*microRNAs 15* and *16*) are strongly enhanced after siARTD1 treatment, indicating that ARTD1 is able to regulate gene expression within the same cell in two different manners. This could be due to differential affinities of ARTD1 for different E2F-1 target genes would thus lead to an unequal chromatin distribution of ARTD1 upon knock down and subsequently affect chromatin composition, the recruitment of transcription factor complexes, and gene expression. On a cellular level, these differential regulatory effects of reduced *Cyclin E* expression and enhanced *microRNA15/16* levels would, however, both lead to reduced Cyclin E protein levels, since the miRNAs negatively regulate *Cyclin E* expression[45]. Interestingly, stably transduced shARTD1 T24 cells overcame the observed cell cycle delay after only 3 passages (not shown), suggesting that in these cells other cell cycle regulatory factors such as Cyclin D or Cyclin A could functionally compensate for the loss of Cyclin E, as it was speculated to be the case in *Cyclin E* knockout mice [46] or that the induced permissive chromatin changes are over-ruled by the plasticity of

the chromatin (i.e. compensatory mechanisms).

siARTD2 treated T24 cells exhibited an even stronger phenotype than cells with reduced ARTD1 levels and were arrested early during the cell cycle at the G_0 - G_1 transition and subsequently induced apoptosis. The G_0 - G_1 phase arrest was not observed in asynchronous siARTD2 treated cells, indicating that ARTD2 is particularly important for G_0 phase progression. Our data indicate that ARTD2 regulates *p27* by enhancing the activatory mark H3K4me3 and reducing the inhibitory histone modification H3K27me3 at the promoters of *p27*, but not in the gene body or at the promoter of *p21*, suggesting that ARTD2 is specifically recruited to the transcription start site of defined genes. ARTD2 thus likely regulates the recruitment of chromatin regulators such as histone methylases, as it has been recently shown for the expression of *MYC* [47] and SIRT1 [48, 49].

Interestingly, PARP inhibitors (e.g., Olaparip) did not inhibit progression of cells from G_0 to G_1, but rather decelerated cell cycle progression during late S phase, indicating that ADP-ribosylation is not required for the above-described functions during re-entry or early G_1 progression in T24 cells. This observation is in contrast to earlier reports on serum-stimulated, quiescent fibroblasts and lectin-stimulated, peripheral, mononucleated blood cells[31]. These opposing findings thus highlight the importance of studying cellular processes in undisturbed systems, because stimuli such as serum or lectin treatment likely induce cellular stress and consequently ADP-ribosylation. The functional contribution of ADP-ribsoylation during late S phase was already reported in a recent publication providing evidence that ARDT1 interacts with pRNA and TIP5 during late S phase in an activity-dependent manner and that this interaction is important during the formation of heterochromatin [34]. Treatment with PARP inhibitors would lead to disrupted or unstable heterochromatin, which results, amongst other things, in sister chromatid exchange formation.

The CIP/KIP family members p21 and p27 are highly homologous and therefore

believed to function similarly [50] and both proteins have been implicated in the regulation of cellular processes such as apoptosis and transcriptional activation [11, 51]. p21 and p27 were reported to repress transcription indirectly by inhibiting cyclin-Cdk complexes and the consecutive phosphorylation of Rb-family proteins (p107, p110, and p130). In turn, hypophosphorylated Rb-related proteins sequester E2F family members and thereby repress the transcriptional targets of this transcription factor family[52]. The here described and observed increase of *p27* was, however, unlikely mediated through E2F, since ARTD2 knockdown in T24 cells did not change the phosphorylation status of pRB (data not shown).

ARTD2 down-regulation in T24 cells not only up-regulated *p27*, but also induced apoptosis, which was observed by ARTD1 cleavage and increased PAR formation. Interestingly, this event was not dependent on p53, indicating that the DNA damage response was not activated. This fits the observation that ARTD2 knockout mice do not show the propensity for the development of spontaneous tumors [14], but have a reduced thymic cellularity associated with increased apoptosis in thymocytes[53]. It therefore remains to be elucidated whether p27 mediates apoptosis or if the apoptotic program is initiated independent of *p27* up regulation. Given the fact that p27 has been described as a tumor suppressor [54], the function of p27 and the mechanistic link to ADP-ribosylation and ARTD2 might be further evaluated and reveal new potential therapeutic approach for specific cancer types.

Together, we describe the regulation of *Cyclin E* and *p27* in T24 cells by ARTD1 and ARTD2, respectively. Since the down-regulation of ARTD2 had a more dramatic effect on cell cycle re-entry and progression than siARTD1 treatment, these results are an example where ARTD2 plays a more prominent role than ARTD1, despites is significantly lower enzymatic activity. The results presented here thus confirm novel, non-redundant functions in cell cycle regulation for ARTD1 and ARTD2.

Materials and Methods

Cell culture

T24 cells were cultivated in McCoy's 5A medium (Gibco, Invitrogen, CA, California, USA) at 37°C. All media were supplemented with 1% (v/v) Penicillin/Streptavidin and 10% (v/v) fetal calf serum (Gibco, Invitrogen, CA, California, USA).

siRNA transfection

Negative control allstars (siMock), human siPARP1 #6 and human siPARP2 #6 were ordered from Qiagen (Hilden, Germany). Cells were seeded 1 day before transfection ($5x10^5$ cells per 6 cm plate) and transfection was carried out with 40 nmol siRNA per plate and RNAi MAX lipofectamine (Invitrogen, Carlsbad, CA, USA).

Antibodies

Following antibodies were used: From Santa Cruz Biotechnology, Inc (Dallas, TX, USA): PARP1/ARDT1 (H-250, rabbit); PCNA (PC10. mouse); p53 (FL-393,rabbit); p27 (C-19, rabbit), p21 (C-19, rabbit), cyclin E (HE12, mouse), E2F-1 (C-20-rabbit), PARP-1 (C2-10, mouse). From Active motif (Carlsbad, CA, USA): PARP2 (rabbit). From Sigma Aldrich (St. Louis, MO, USA): tubulin (mouse). From Millipore (MS, USA): H3K4me3 (rabbit); phospho-Histone H2A.X (mouse); trimethyl-HistoneH3K27 (rabbit), H2A (rabbit); acetyl-Histone H4 (rabbit). From Abcam pls (Cambridge, UK): Histone H2A.Z (rabbit), H1.2 (rabbit); Histone H3 (rabbit). From Cell Signaling Technology, Inc. (MS, USA): P-Chk1 (S345, rabbit). From NeoMarkers (Fremont, CA, USA): RPA / p34 (9H8, mouse). From Roche AG (Basel, Switzerland): BrdU. homemade: PAR 10H (mouse). Jackson ImmunoResearch Laboratories: CyTM3-conjugated AffiniPure Goat Anti-Rabbit (Suffolk, UK).

Cell cycle analysis by flow cytometry

Cells were harvested with trypsin and washed once with PBS. Cells (at least $3.5x10^5$) were fixed (70% ethanol, at least 30 min on ice or overnight at 4°C), washed once with 1ml PBS and centrifuged (865 g, 4°C, 8min). Cells were stained with a Propidium iodide solution (Sigma Aldrich, St. Louis, MO, USA), final concentration of 20 µg/ml in PBS with the addition of 100 µg/ml RNase A (37°C, 30 min in the dark). Flow cytometry analysis was performed with the CyANTM ADP 9 Analyzer (Beckman Coulter, Fullerton, CA, USA).

RNA extraction and qPCR analysis

Cells were harvested either by trypsin or directly lysed on the plate in lysis buffer. RNA extraction was performed with the NucleoSpin® RNA II kit (Macherey-Nagel, Düren, Germany). RNA was quantified with a NanoDrop (ThermoFisherScintific, Waltham, MS, USA) and reverse transcribed according to the supplier's protocol (High Capacity cDNA Reverse Transcription Kit, Applied Biosystems, Foster City, CA, United States).

Quantitative-real-time polymerase chain reactions (qPCR) were performed with SYBR® green SensiMix SYBR Hi-ROX Kit (Bioline Reagents Ltd, London, UK) and a Rotor-Gene Q 2plex HRM System (Qiagen, Hilden, Germany).

Cell lysis, SDS-PAGE and Western blot analysis

Whole cell lysis was performed either with trypsinized cells or directly on plates by using a Tris lysis buffer (50 mM Tris pH 8, 500 mM NaCl, 1% Triton X-100, 1 µg/ml pepstatin, 1 µg/ml bestatin, 1 µg/ml leupeptin, 2 mM PMSF; 10 min, 4°C). Bradford assay (Bio-Rad laboratories, Hercules, CA, USA) was performed and, if not otherwise indicated, 30 µg of protein extract was loaded and separated on a 10% or 12% SDS-polyacrylamide gel (120V). The gel was blotted on a PDVF membrane and analyzed by using protein specific antibodies.

BrdU Incorporation assay

Cells were seeded on cover slips ($1x10^5$ per well in a 24-well-plate) prior to the experiment as indicated. Cells were treated with 10 μM BrdU for 30 min, fixed with ice-cold methanol (10 min, 4°C), washed with PBS and denatured with 2 M HCl (60 min, 37°C). The reaction was neutralized by adding 0.1 M borate buffer (pH 8.5, 10 min). Cover slips were incubated with BrdU Antibody in PBS/BSA (60 min, room temperature) and after washing with PBS; the secondary antibody was applied (60 min, room temperature, in the dark). Cover slips were mounted and analyzed by immunofluorescence microscopy. For quantification, at least 300 cells per condition were analyzed.

Chromatin Immunoprecipitation

ChIP analysis was performed as previously described (Santoro *et al.*, 2002) using magnetic Dynabeads® (Life Technologies, Carlsbad, CA, USA).

Conflict of interest

The authors declare no conflict of interest.

Author Contributions

K.L. designed and performed experiments, M.O.H. supervised the work, and both authors wrote the manuscript.

Acknowledgements

We are grateful to R. Santoro (University of Zurich) for providing the BrdU antibody and for support in the course of the BrdU and ChIP experiments, to S. Ferrari (University of Zurich, Switzerland) for support and the Cdk2, Cyclin A and Cyclin B antibody, to A. Groth (University of Copenhagen, Denmark) for technical support. M. Fey is acknowledged for support in the course of the experiments. M. Stucki (University of Zurich, Switzerland) is acknowledged for providing the T24 cell line. F. Freimoser (University of Zurich, Switzerland) provided editorial assistance and critical input during the writing. This work was supported in part by the Swiss National Science Foundation Grants 31-122421, and PDMFP3_127315 as well as the Forschungskredit Universität Zürich (to K.L.) and Kanton of Zurich (to M.O.H.).

References

1. Murray AH, Hunt T. The cell cycle: an introduction. New York: Oxford University Press, 1993.
2. Takahashi Y, Rayman JB, Dynlacht BD. Analysis of promoter binding by the E2F and pRB families in vivo: distinct E2F proteins mediate activation and repression. Genes Dev 2000; 14:804-16.
3. Ren S, Rollins BJ. Cyclin C/cdk3 promotes Rb-dependent G0 exit. Cell 2004; 117:239-51.
4. Rissland OS, Hong SJ, Bartel DP. MicroRNA destabilization enables dynamic regulation of the miR-16 family in response to cell-cycle changes. Mol Cell 2011; 43:993-1004.
5. Sage J. Cyclin C makes an entry into the cell cycle. Dev Cell 2004; 6:607-8.
6. Sherr CJ. Cancer cell cycles. Science 1996; 274:1672-7.
7. Weinberg RA. The retinoblastoma protein and cell cycle control. Cell 1995; 81:323-30.
8. Chatterjee SJ, George B, Goebell PJ, Alavi-Tafreshi M, Shi SR, Fung YK, et al. Hyperphosphorylation of pRb: a mechanism for RB tumour suppressor pathway inactivation in bladder cancer. J Pathol 2004; 203:762-70.
9. Cobrinik D. Pocket proteins and cell cycle control. Oncogene 2005; 24:2796-809.
10. Dyson N. The regulation of E2F by pRB-family proteins. Genes Dev 1998; 12:2245-62.
11. Coqueret O. New roles for p21 and p27 cell-cycle inhibitors: a function for each cell compartment? Trends Cell Biol 2003; 13:65-70.
12. Besson A, Dowdy SF, Roberts JM. Cdk inhibitors: cell cycle regulators and beyond. Dev Cell 2008; 14:159-69.

13. Amé J, Rolli V, Schreiber V, Niedergang C, Apiou F, Decker P, et al. PARP-2, a novel mammalian DNA damage-dependent poly(ADP-ribose) polymerase. J Biol Chem 1999; 274:17860-8.
14. de Murcia JM, Ricoul M, Tartier L, Niedergang C, Huber A, Dantzer F, et al. Functional interaction between PARP-1 and PARP-2 in chromosome stability and embryonic development in mouse. EMBO J 2003; 22:2255-63.
15. Yelamos J, Schreiber V, Dantzer F. Toward specific functions of poly(ADP-ribose) polymerase-2. Trends Mol Med 2008; 14:169-78.
16. Altmeyer M, Messner S, Hassa PO, Fey M, Hottiger MO. Molecular mechanism of poly(ADP-ribosyl)ation by PARP1 and identification of lysine residues as ADP-ribose acceptor sites. Nucleic Acids Res 2009; 37:3723-38.
17. Kanai M, Uchida M, Hanai S, Uematsu N, Uchida K, Miwa M. Poly(ADP-ribose) polymerase localizes to the centrosomes and chromosomes. Biochem Biophys Res Commun 2000; 278:385-9.
18. Saxena A, Wong LH, Kalitsis P, Earle E, Shaffer LG, Choo KH. Poly(ADP-ribose) polymerase 2 localizes to mammalian active centromeres and interacts with PARP-1, Cenpa, Cenpb and Bub3, but not Cenpc. Hum Mol Genet 2002; 11:2319-29.
19. Saxena A, Saffery R, Wong LH, Kalitsis P, Choo KH. Centromere proteins Cenpa, Cenpb, and Bub3 interact with poly(ADP-ribose) polymerase-1 protein and are poly(ADP-ribosyl)ated. J Biol Chem 2002; 277:26921-6.
20. Monaco L, Kolthur-Seetharam U, Loury R, Murcia JM, de Murcia G, Sassone-Corsi P. Inhibition of Aurora-B kinase activity by poly(ADP-ribosyl)ation in response to DNA damage. Proc Natl Acad Sci USA 2005; 102:14244-8.

21. Ryu H, Al-Ani G, Deckert K, Kirkpatrick D, Gygi S, Dasso M, et al. PIASy mediates SUMO-2/3 conjugation of poly (ADP-ribose) polymerase1 (PARP1) on mitotic chromosomes. J Biol Chem 2010.
22. Caiafa P, Guastafierro T, Zampieri M. Epigenetics: poly(ADP-ribosyl)ation of PARP-1 regulates genomic methylation patterns. FASEB J 2009; 23:672-8.
23. Wesierska-Gadek J, Schloffer D, Gueorguieva M, Uhl M, Skladanowski A. Increased susceptibility of poly(ADP-ribose) polymerase-1 knockout cells to antitumor triazoloacridone C-1305 is associated with permanent G2 cell cycle arrest. Cancer Res 2004; 64:4487-97.
24. Tanuma S, Kanai Y. Poly(ADP-ribosyl)ation of chromosomal proteins in the HeLa S3 cell cycle. J Biol Chem 1982; 257:6565-70.
25. Tentori L, Muzi A, Dorio AS, Scarsella M, Leonetti C, Shah GM, et al. Pharmacological inhibition of poly(ADP-ribose) polymerase (PARP) activity in PARP-1 silenced tumour cells increases chemosensitivity to temozolomide and to a N3-adenine selective methylating agent. Curr Cancer Drug Targets 2010; 10:368-83.
26. Kashima L, Idogawa M, Mita H, Shitashige M, Yamada T, Ogi K, et al. CHFR protein regulates mitotic checkpoint by targeting PARP-1 protein for ubiquitination and degradation. J Biol Chem 2012; 287:12975-84.
27. Wright RH, Castellano G, Bonet J, Le Dily F, Font-Mateu J, Ballare C, et al. Cdk2-dependent activation of PARP-1 is required for hormonal gene regulation in breast cancer cells. Genes Dev 2012; 26:1972-83.
28. Madison DL, Lundblad JR. C-terminal binding protein and poly(ADP)ribose polymerase 1 contribute to repression of the p21(waf1/cip1) promoter. Oncogene 2010; 29:6027-39.
29. Simbulan-Rosenthal CM, Rosenthal DS, Luo R, Samara R, Espinoza LA, Hassa PO, et al. PARP-1 binds E2F-1 independently of its DNA binding and catalytic domains, and

acts as a novel coactivator of E2F-1-mediated transcription during re-entry of quiescent cells into S phase. Oncogene 2003; 22:8460-71.

30. Simbulan-Rosenthal CM, Rosenthal DS, Luo R, Smulson ME. Poly(ADP-ribose) polymerase upregulates E2F-1 promoter activity and DNA pol alpha expression during early S phase. Oncogene 1999; 18:5015-23.
31. Carbone M, Rossi MN, Cavaldesi M, Notari A, Amati P, Maione R. Poly(ADP-ribosyl)ation is implicated in the G0-G1 transition of resting cells. Oncogene 2008; 27:6083-92.
32. Chang P, Jacobson MK, Mitchison TJ. Poly(ADP-ribose) is required for spindle assembly and structure. Nature 2004; 432:645-9.
33. Chang P, Coughlin M, Mitchison TJ. Tankyrase-1 polymerization of poly(ADP-ribose) is required for spindle structure and function. Nat Cell Biol 2005; 7:1133-9.
34. Guetg C, Scheifele F, Rosenthal F, Hottiger MO, Santoro R. Inheritance of silent rDNA chromatin is mediated by PARP1 via noncoding RNA. Mol Cell 2012; 45:790-800.
35. Horton J, Stefanick D, Naron J, Kedar P, Wilson S. Poly(ADP-ribose) polymerase activity prevents signaling pathways for cell cycle arrest after DNA methylating agent exposure. J Biol Chem 2005; 280:15773-85.
36. Bäckert S. Involvement of PARP1 in NF-κB-dependent gene expression during the cell cycle. Vetsuisse-Fakultät Universität Zürich, Institut für Veterinärbiochemie und Molekularbiologie Zurich: University of Zurich, 2009.
37. Peng CC, Chen KC, Peng RY, Su CH, Hsieh-Li HM. Human urinary bladder cancer T24 cells are susceptible to the Antrodia camphorata extracts. Cancer Lett 2006; 243:109-19.
38. Cooper MJ, Haluschak JJ, Johnson D, Schwartz S, Morrison LJ, Lippa M, et al. p53 mutations in bladder carcinoma cell lines. Oncol Res 1994; 6:569-79.

39. Jin Y, Xu X, Yang M, Wei F, Ayi T, Bowcock A, et al. Cell cycle-dependent colocalization of BARD1 and BRCA1 proteins in discrete nuclear domains. Proc Natl Acad Sci USA 1997; 94:12075-80.
40. Chen Y, Farmer AA, Chen CF, Jones DC, Chen PL, Lee WH. BRCA1 is a 220-kDa nuclear phosphoprotein that is expressed and phosphorylated in a cell cycle-dependent manner. Cancer Res 1996; 56:3168-72.
41. Ku M, Jaffe JD, Koche RP, Rheinbay E, Endoh M, Koseki H, et al. H2A.Z landscapes and dual modifications in pluripotent and multipotent stem cells underlie complex genome regulatory functions. Genome Biol 2012; 13:R85.
42. Krishnakumar R, Kraus W. PARP-1 Regulates Chromatin Structure and Transcription through a KDM5B-Dependent Pathway. Mol Cell 2010; 39:736-49.
43. Krishnakumar R, Gamble M, Frizzell K, Berrocal J, Kininis M, Kraus W. Reciprocal binding of PARP-1 and histone H1 at promoters specifies transcriptional outcomes. Science 2008; 319:819-21.
44. Luo X, Kraus WL. On PAR with PARP: cellular stress signaling through poly(ADP-ribose) and PARP-1. Genes Dev 2012; 26:417-32.
45. Ofir M, Hacohen D, Ginsberg D. MiR-15 and miR-16 are direct transcriptional targets of E2F1 that limit E2F-induced proliferation by targeting cyclin E. Mol Cancer Res 2011; 9:440-7.
46. Lents NH, Baldassare JJ. Cdk2 and cyclin E knockout mice: lessons from breast cancer. Trends Endocrinol Metab 2004; 15:1-3.
47. Liang YC, Hsu CY, Yao YL, Yang WM. PARP-2 regulates cell cycle-related genes through histone deacetylation and methylation independently of poly(ADP-ribosyl)ation. Biochem Biophys Res Commun 2013; 431:58-64.

48. Bai P, Canto C, Brunyanszki A, Huber A, Szanto M, Cen Y, et al. PARP-2 Regulates SIRT1 Expression and Whole-Body Energy Expenditure. Cell Metab 2011; 13:450-60.
49. Bai P, Canto C, Oudart H, Brunyanszki A, Cen Y, Thomas C, et al. PARP-1 Inhibition Increases Mitochondrial Metabolism through SIRT1 Activation. Cell Metab 2011; 13:461-8.
50. Russo AA, Jeffrey PD, Patten AK, Massague J, Pavletich NP. Crystal structure of the p27Kip1 cyclin-dependent-kinase inhibitor bound to the cyclin A-Cdk2 complex. Nature 1996; 382:325-31.
51. Philipp-Staheli J, Payne SR, Kemp CJ. p27(Kip1): regulation and function of a haploinsufficient tumor suppressor and its misregulation in cancer. Exp Cell Res 2001; 264:148-68.
52. Sherr CJ, Roberts JM. Cdk inhibitors: positive and negative regulators of G1-phase progression. Genes Dev 1999; 13:1501-12.
53. Yelamos J, Monreal Y, Saenz L, Aguado E, Schreiber V, Mota R, et al. PARP-2 deficiency affects the survival of CD4+CD8+ double-positive thymocytes. EMBO J 2006; 25:4350-60.
54. Slingerland J, Pagano M. Regulation of the cdk inhibitor p27 and its deregulation in cancer. J Cell Physiol 2000; 183:10-7.

Figure Legends

Figure 1. Down regulation of ARDT1 in T24 cells leads to decelerated cell cycle re-entry and cell cycle progression, while knocking down ARDT2 maintains cells in G_0. A) Western blot analysis of T24 and U2OS cell extracts was performed to compare the levels of Rb phosphorylation and E2F-1 levels. B) Western blot analysis was used to confirm the knockdown of ARTD1 and ARTD2 upon siRNA treatment of T24 cells. C) Flow cytometry analysis was performed of siMock, siARTD1 and siARDT2 treated, synchronized T24 cells. The cells were analyzed over 24 h starting from confluence (G_0) D) Quantification of the flow cytometry analysis shown in C.

Figure 2.ARTD1 depletion leads to decreased Cyclin E expression A) Western blot analysis was performed to investigate p53 and RPA after cell cycle re-initiation of siMock (M) or siARTD1 (A_1) treated T24 cells at different time points. B-C) qPCR (B) and Western blot (C) analysis of E2F-1 in siMock and siARTD1 treated T24 cells. D-E) qPCR (D) and Western blot (E) analysis of Cyclin E levels in siMock and siARTD1 treated cells. (F) qPCR analysis of Cyclin E expression in cells treated with the PARP inhibitor Olaparib. (n=3, t-test $p^* < 0.05$)

Figure 3. ARTD1 is recruited to the cyclin E promoter and keeps the chromatin in an open conformation. Chromatin immunoprecipitation (ChIP) analysis of the cyclin E promoter in siMock or siARDT1 treated T24 cells. ARTD1 binding (A), H3 occupancy (B), H3K4me3 during G1 phase (10h time point) (C), H4 acetylation during G1 phase (10h time point)(D), H2A and H2A.Z occupancy (E) and H1.2 occupancy (F) were analyzed.

Figure 4. ARTD2 is a repressor for p27 transcription. A) qPCR and western blot analysis of p21 and p27 in siMock and siARTD2 treated T24 cells. B) and C) ChIP analysis of H3, H3K4me3 and H3K27me3 were analysed in siMock and siARTD2 treated confluent cells for B) the p27 promoter and C) the p21 promoter D) ChIP analysis to assess H4 acetylation at the p21 and p27 promoter in siMock and siARTD2 treated cells.

Supplementary Figure Legends

Supplementary Figure 1. Inhibition of the enzymatic activity leads to an S-phase delay. A) Experimental setup of cell cycle analysis in T24 cells. T24 cells were seeded and transfected on the next day at 70%-80% confluence. After 3 days of growth, cells reached confluence and entered the G0 phase. Upon splitting, cells re-initiated the cell cycle and samples for flow cytometry analysis, western blot analysis, qPCR analysis and ChIP analysis were taken at the indicated time points. B) mRNA expression of ARTD1 was measured by qPCR analysis during the cell cycle in siMock and siARTD1-treated cells. C) BrdU incorporation assay was performed and quantified by cell counting in siMock or siARTD1 treated cells, at least 300 cells were counted for each condition and time point. D) Flow cytometry analysis for shMock and shARTD1 transduced T24 cells after viral transduction. E) Overlay of flow cytometry analyses of untreated, Olaparib (20h, 10μM) and Veliparib (20h, 10μM) treated T24 samples (20h time point).

Supplementary Figure 2. Cell cycle checkpoints and cdk-inhibitors are not affected upon siARTD1 treatment. A) Western blot analysis of Chk1- phosphorylation during the cell cycle re-initiation after siMock (M) or siARTD1 (A1) treatment was performed for the indicated time points. B-D) qPCR analyses of p21 (B), p27 (C) and p57 (D). E) The corresponding Western blot analysis of p27 in siMock (M) and siARTD1 (A1) treated cells. F) qPCR analysis of Cdk2 in siMock and siARTD1 treated cells (left panel), Western blot analysis of G0 time point of Cdk2 protein levels (right panel).

Supplementary Figure 3. A) qPCR analysis of cyclin A, B and D was performed in siMock and siARTD1 treated samples. (n=2). B) Western blot analysis was carried out of cyclin A and cyclin B in siMock and siARTD1 treated samples. C-F) qPCR analysis of c-myc (C), miR15 (D) and miR16 (E) expression levels in siMock and siARTD1 treated cells

(n=3). F) Western blot analysis was performed of shARTD1 and shMock treated T24 cells in the G_0 phase of the cell cycle to detect Cyclin E protein levels.

Supplementary Figure 4. A) mRNA expression of ARTD2 during the cell cycle after siMock and siARTD2 treatment was analyzed by qPCR . B) Western blot analysis of siMock and siARTD2 treated samples was performed and analyzed for PAR formation, cleavage of ARDT1, and p53 and p27 levels. C) ChIP analysis was carried out for H3, H3K4me3, H3K27m3 and H4ac analyzing the occupancy at the p27 gene body (+2 kb from TSS) and at the p21 gene body (+1.5 kb from TSS) in siMock and siARTD2 treated confluent cells.

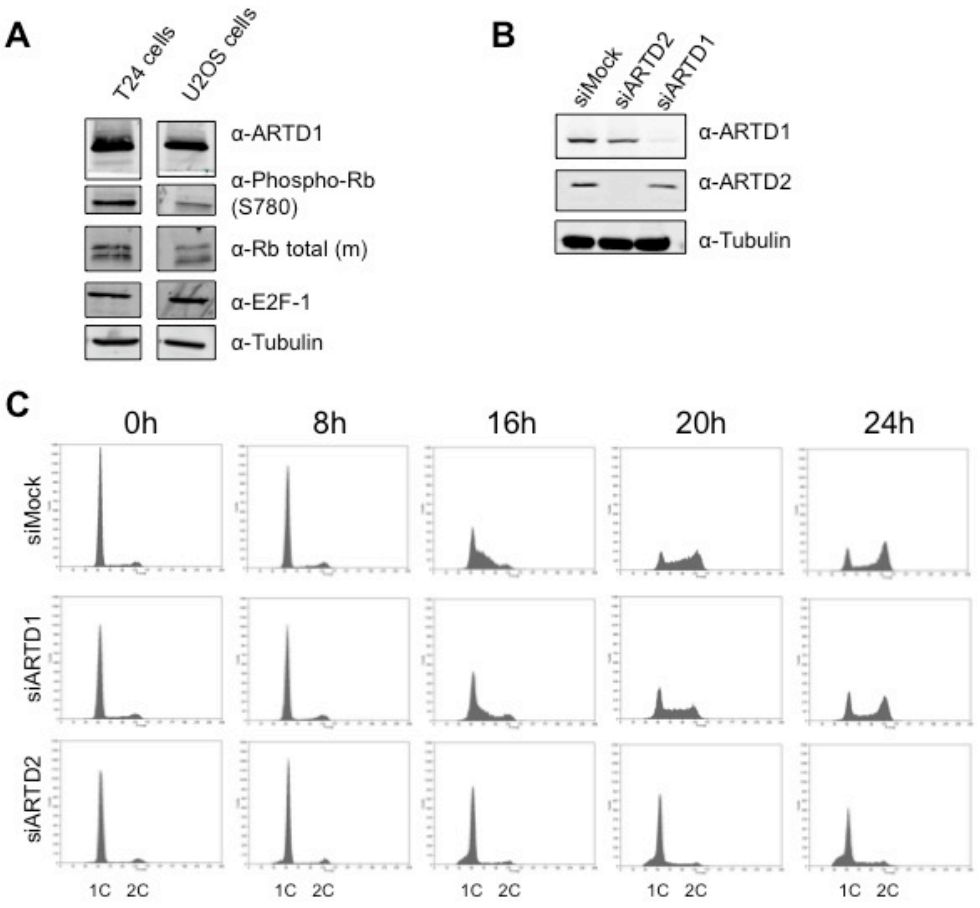

D

time point (h)	G1 phase			S phase			G2/M phase		
	M	A1	A2	M	A1	A2	M	A1	A2
0	87.2	82.2	89.1	8.5	13.0	3.6	4.5	4.7	7.2
8	87.8	81.1	84.1	6.4	13.3	5.2	5.8	5.5	8.1
16	65.8	74.0	76.7	29.9	20.0	8.1	6.2	6.9	5.4
20	34.3	57.7	69.1	55.6	35.6	16.6	11.3	7.5	5.3
24	26.5	42.1	63.8	52.2	37.4	19.2	23.7	20.2	7.5

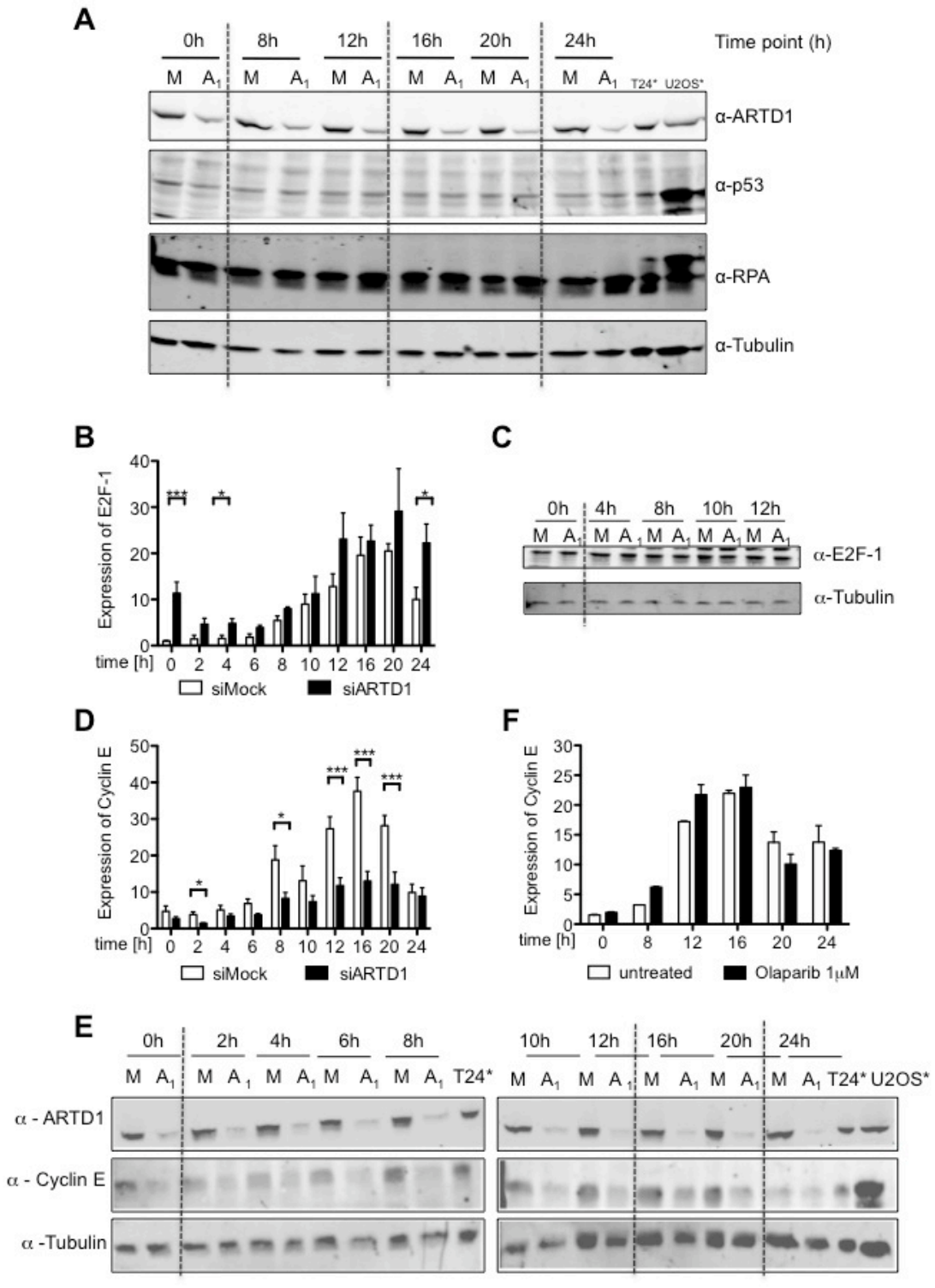
A
0h
8h
12h
16h
20h
24h
Time point (h)
M A1 M A1 M A1 M A1 M A1 M A1 T24* U2OS*
α-ARTD1
α-p53
α-RPA
α-Tubulin
B
Expression of E2F-1
time [h] 0 2 4 6 8 10 12 16 20 24
siMock
siARTD1
C
0h
4h
8h
10h
12h
α-E2F-1
α-Tubulin
D
Expression of Cyclin E
time [h] 0 2 4 6 8 10 12 16 20 24
siMock
siARTD1
F
Expression of Cyclin E
time [h] 0 8 12 16 20 24
untreated
Olaparib 1μM
E
0h
2h
4h
6h
8h
10h
12h
16h
20h
24h
M A1 M A1 M A1 M A1 M A1 T24* M A1 M A1 M A1 M A1 M A1 T24* U2OS*
α - ARTD1
α - Cyclin E
α -Tubulin

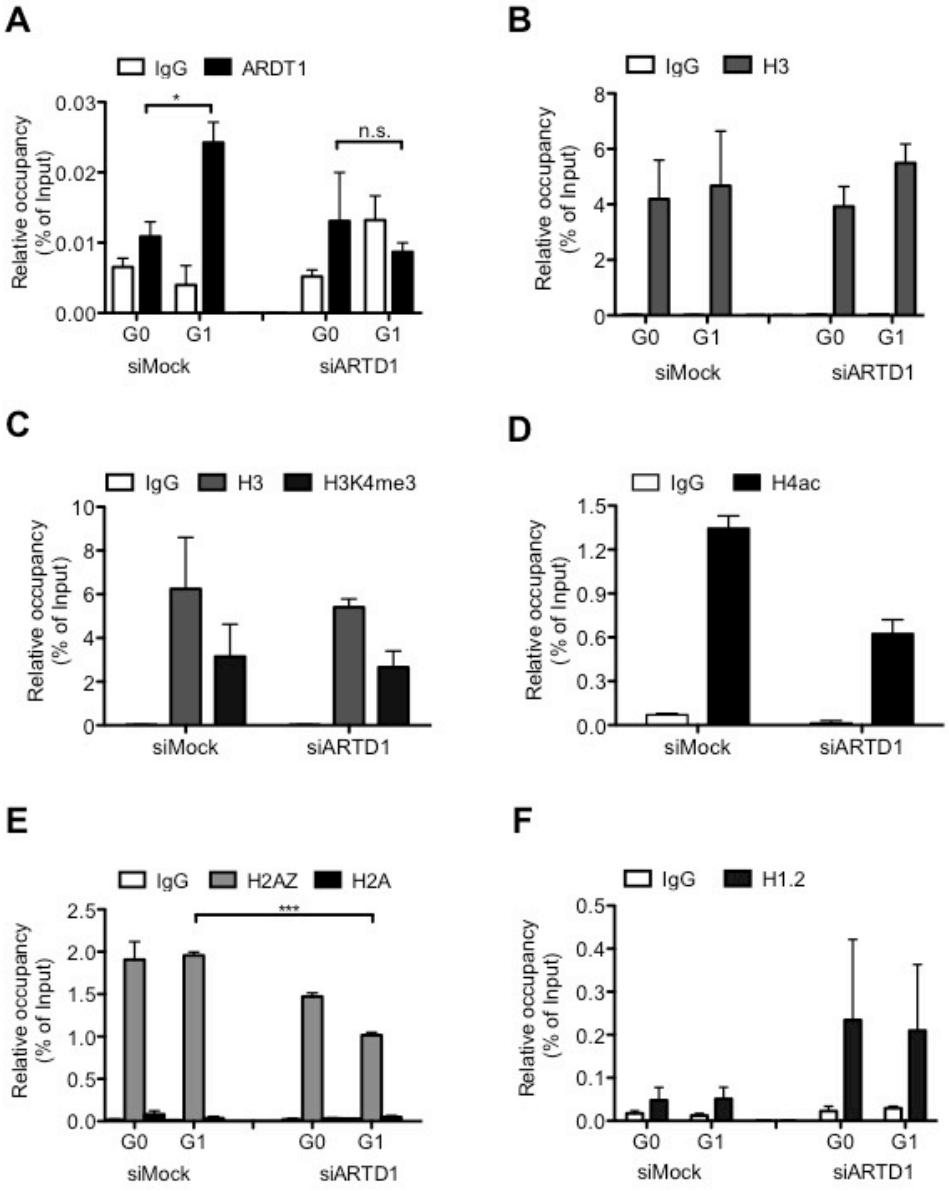
A
IgG
ARDT1
Relative occupancy (% of Input)
0.03
0.02
0.01
0.00
*
n.s.
G0
G1
G0
G1
siMock
siARTD1
B
IgG
H3
Relative occupancy (% of Input)
8
6
4
2
0
G0
G1
G0
G1
siMock
siARTD1
C
IgG
H3
H3K4me3
Relative occupancy (% of Input)
10
8
6
4
2
0
siMock
siARTD1
D
IgG
H4ac
Relative occupancy (% of Input)
1.5
1.2
0.9
0.6
0.3
0.0
siMock
siARTD1
E
IgG
H2AZ
H2A
Relative occupancy (% of Input)
2.5
2.0
1.5
1.0
0.5
0.0
***
G0
G1
G0
G1
siMock
siARTD1
F
IgG
H1.2
Relative occupancy (% of Input)
0.5
0.4
0.3
0.2
0.1
0.0
G0
G1
G0
G1
siMock
siARTD1

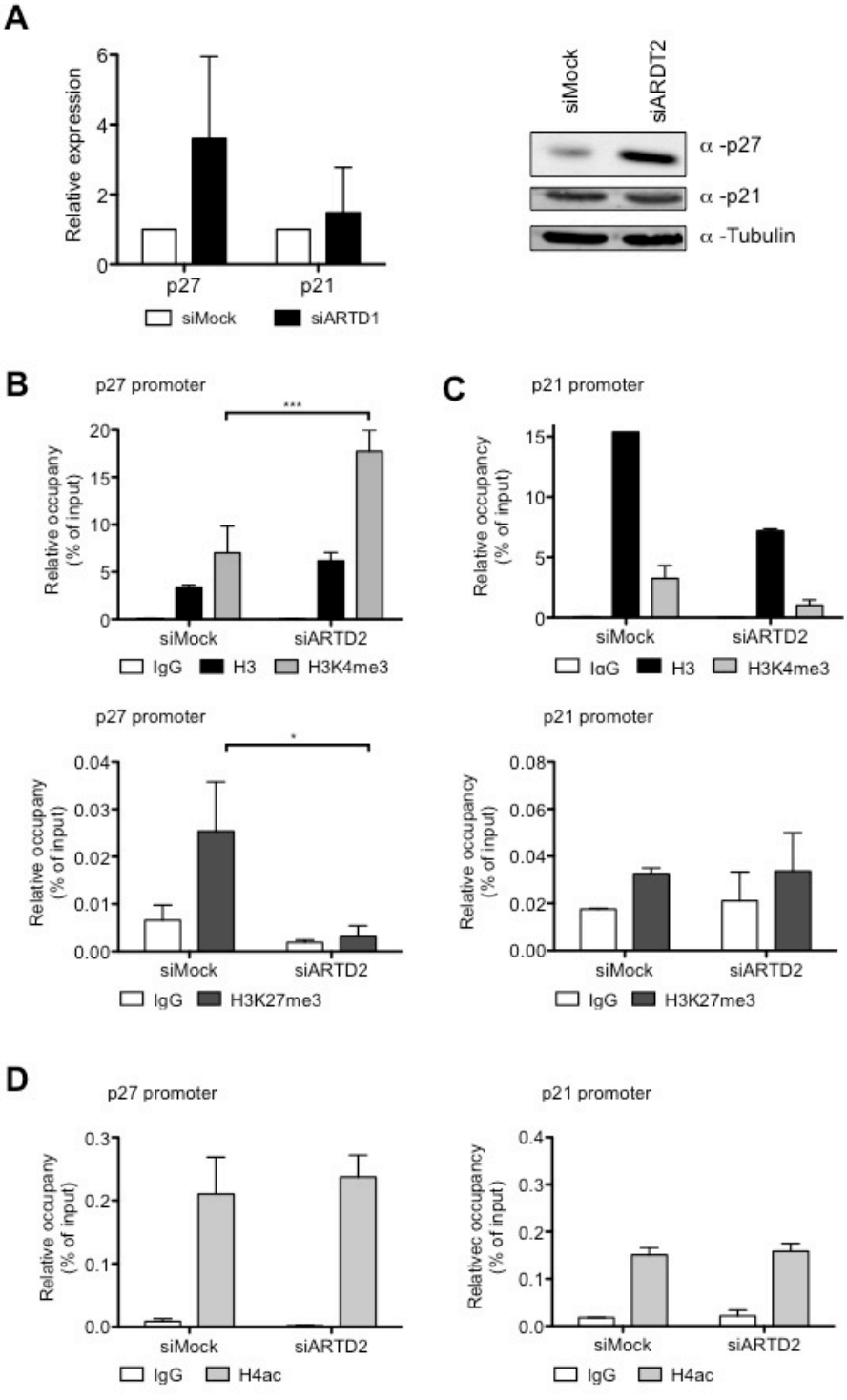
A
Relative expression
6
4
2
0
p27
p21
siMock
siARTD1
siMock
siARDT2
α -p27
α -p21
α -Tubulin
B
p27 promoter
***
Relative occupany (% of input)
20
15
10
5
0
siMock
siARTD2
IgG
H3
H3K4me3
C
p21 promoter
Relative occupancy (% of input)
15
10
5
0
siMock
siARTD2
IgG
H3
H3K4me3
p27 promoter
*
Relative occupany (% of input)
0.04
0.03
0.02
0.01
0.00
siMock
siARTD2
IgG
H3K27me3
p21 promoter
Relative occupancy (% of input)
0.08
0.06
0.04
0.02
0.00
siMock
siARTD2
IgG
H3K27me3
D
p27 promoter
Relative occupany (% of input)
0.3
0.2
0.1
0.0
siMock
siARTD2
IgG
H4ac
p21 promoter
Relativec occupancy (% of input)
0.4
0.3
0.2
0.1
0.0
siMock
siARTD2
IgG
H4ac

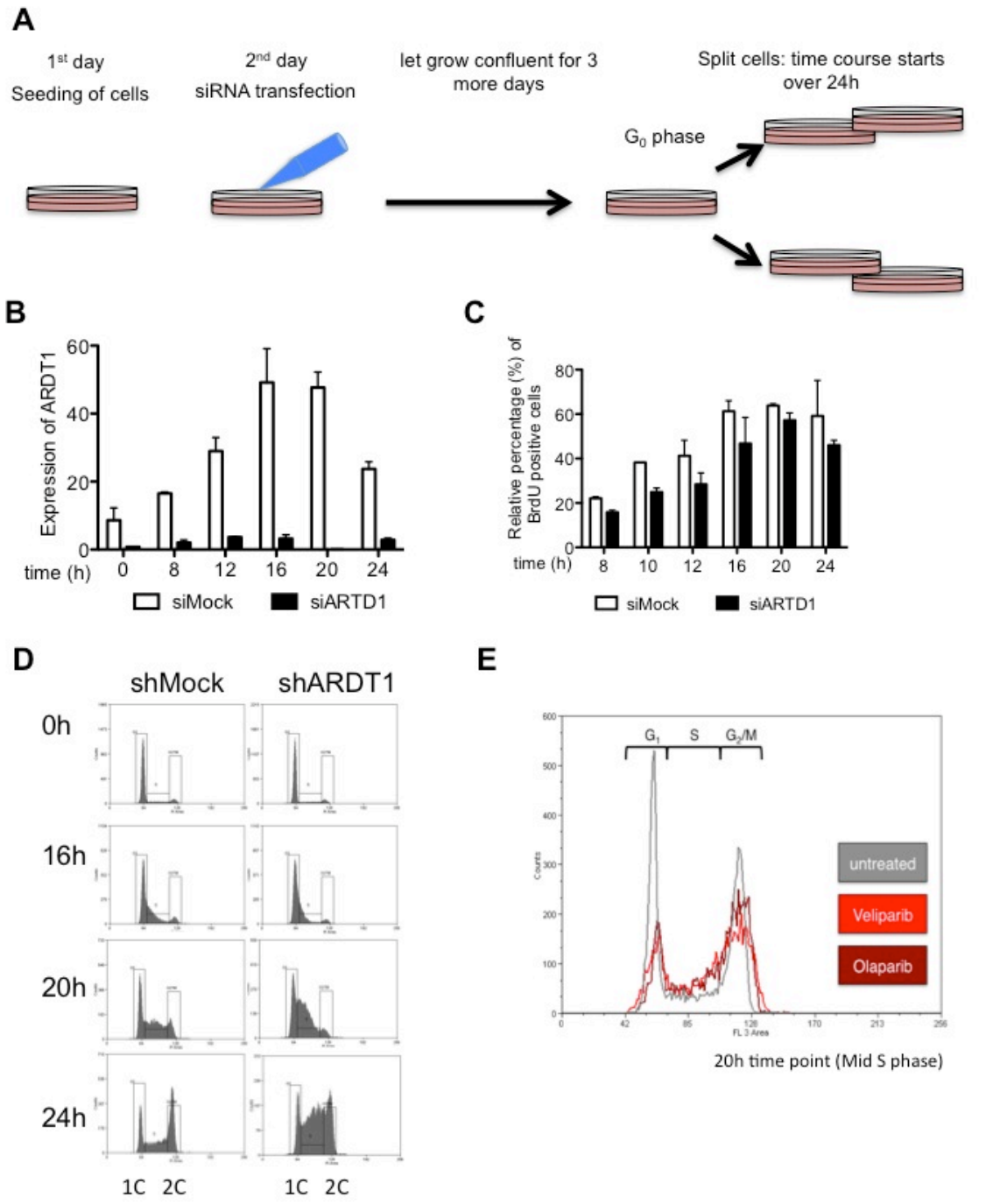
A
1st day
Seeding of cells
2nd day
siRNA transfection
let grow confluent for 3 more days
Split cells: time course starts over 24h
G0 phase
B
Expression of ARDT1
60
40
20
0
time (h) 0 8 12 16 20 24
siMock
siARTD1
C
Relative percentage (%) of BrdU positive cells
80
60
40
20
0
time (h) 8 10 12 16 20 24
siMock
siARTD1
D
shMock
shARDT1
0h
16h
20h
24h
1C 2C
1C 2C
E
G1 S G2/M
Counts
untreated
Veliparib
Olaparib
FL 3 Area
20h time point (Mid S phase)

1

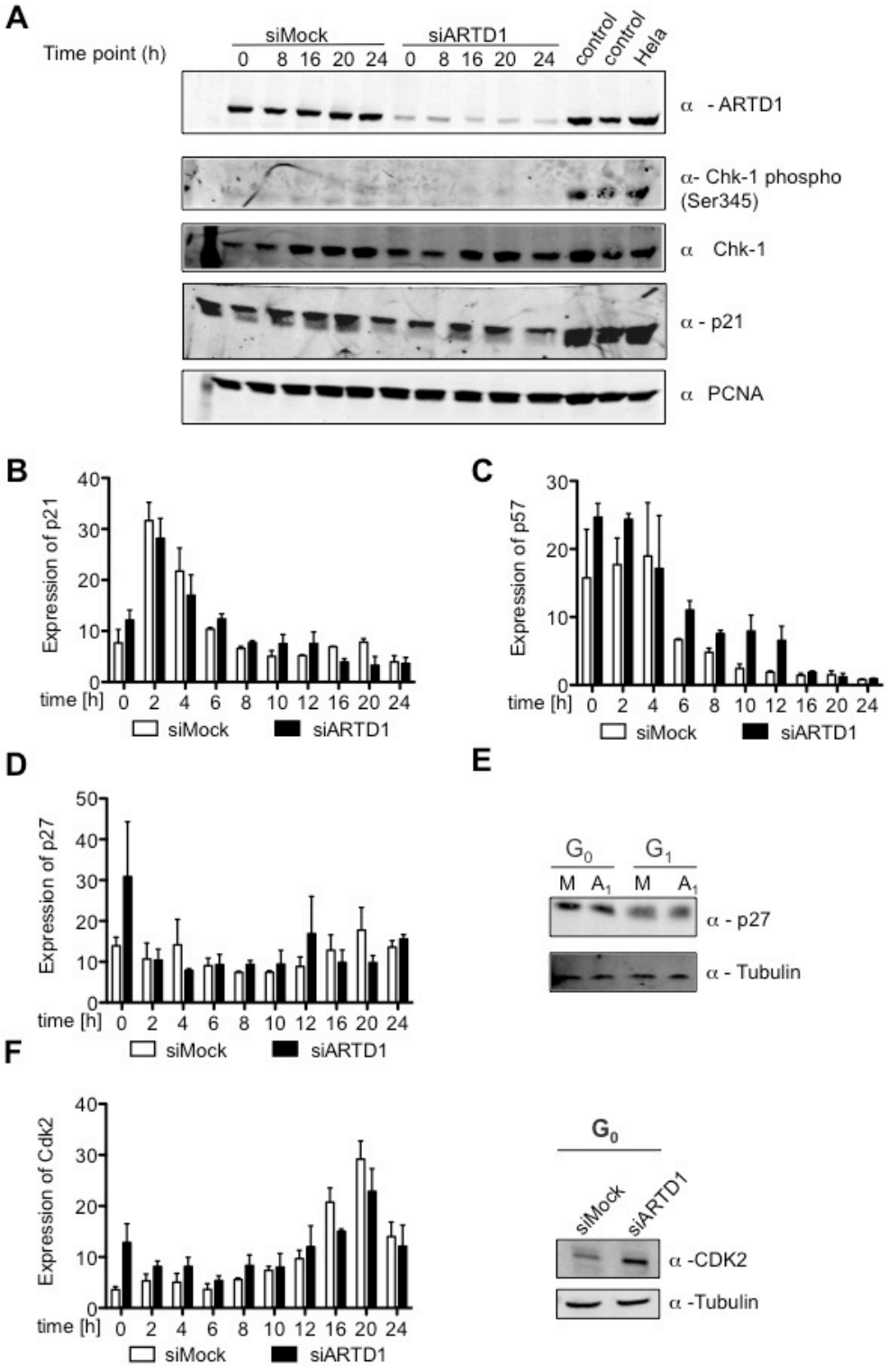
A
Time point (h)
siMock
siARTD1
0 8 16 20 24 0 8 16 20 24
control
control
Hela
α - ARTD1
α- Chk-1 phospho (Ser345)
α Chk-1
α - p21
α PCNA
B
Expression of p21
time [h] 0 2 4 6 8 10 12 16 20 24
siMock
siARTD1
C
Expression of p57
time [h] 0 2 4 6 8 10 12 16 20 24
siMock
siARTD1
D
Expression of p27
time [h] 0 2 4 6 8 10 12 16 20 24
siMock
siARTD1
E
G0
G1
M A1 M A1
α - p27
α - Tubulin
F
Expression of Cdk2
time [h] 0 2 4 6 8 10 12 16 20 24
siMock
siARTD1
G0
siMock
siARTD1
α -CDK2
α -Tubulin

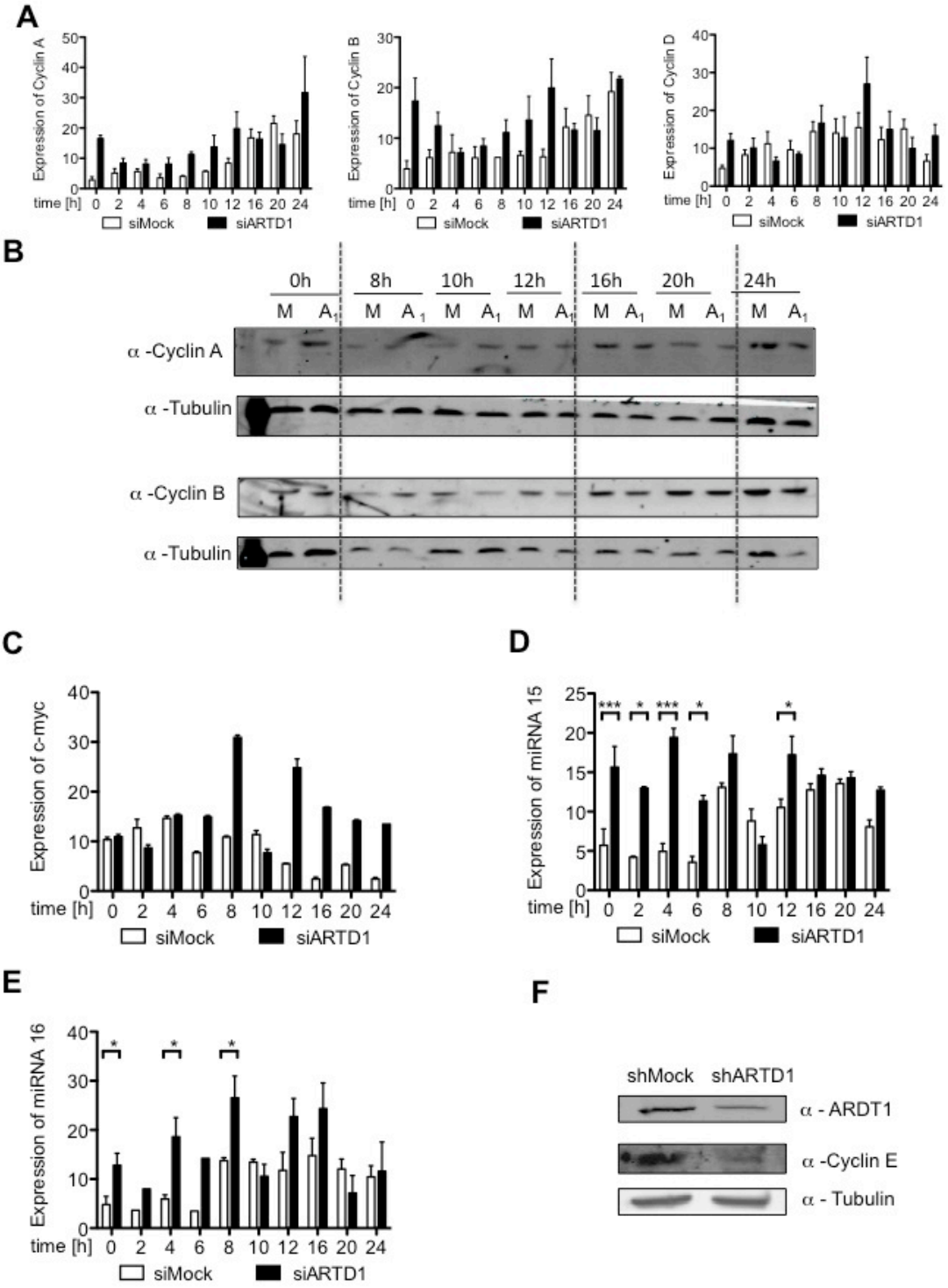
A
Expression of Cyclin A
Expression of Cyclin B
Expression of Cyclin D
time [h] 0 2 4 6 8 10 12 16 20 24
siMock
siARTD1
B
0h 8h 10h 12h 16h 20h 24h
M A1
α -Cyclin A
α -Tubulin
α -Cyclin B
α -Tubulin
C
Expression of c-myc
D
Expression of miRNA 15
E
Expression of miRNA 16
F
shMock shARTD1
α - ARDT1
α -Cyclin E
α - Tubulin

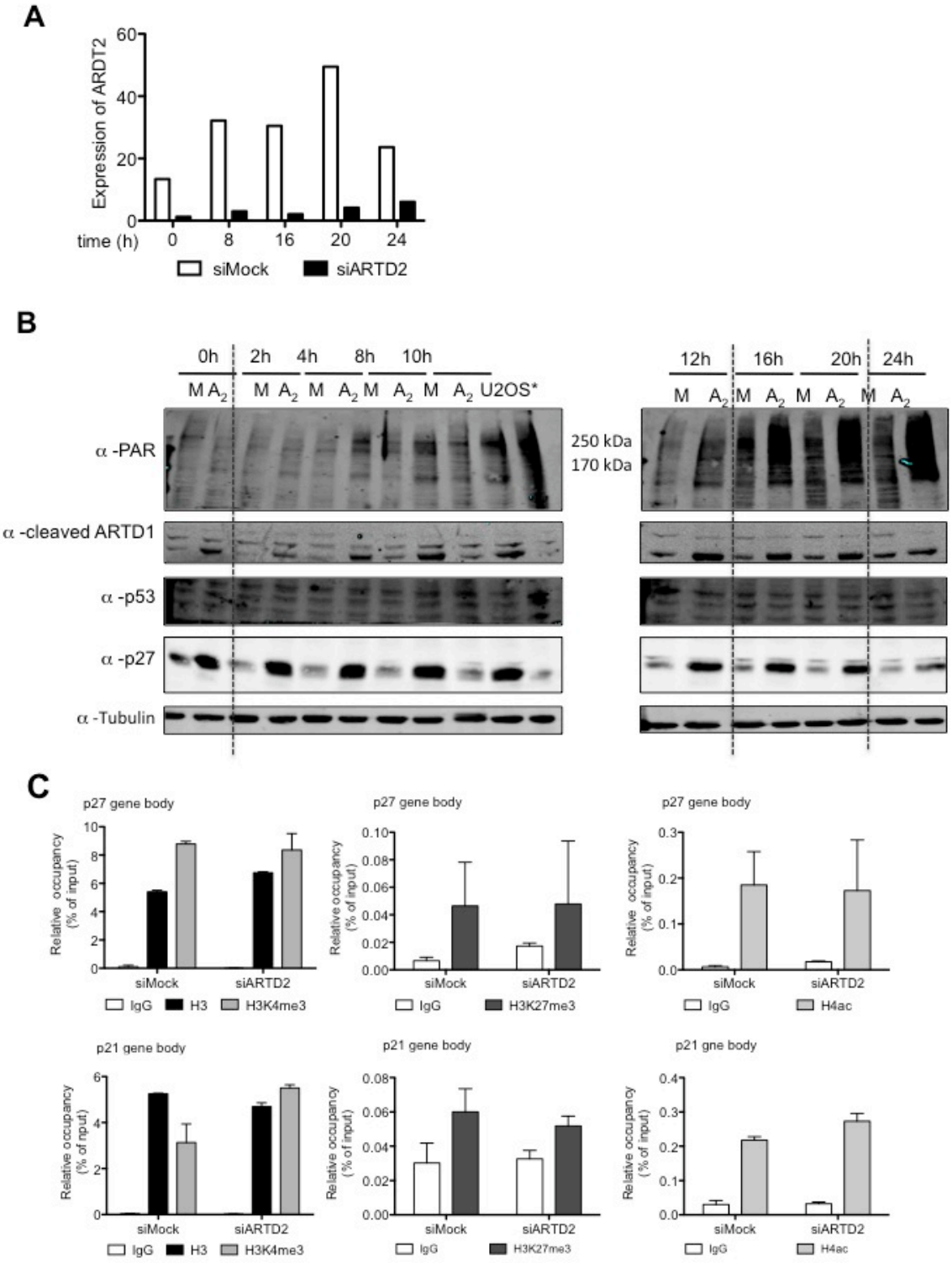
A
Expression of ARDT2
60
40
20
0
time (h)
0
8
16
20
24
siMock
siARTD2
B
0h
2h
4h
8h
10h
12h
16h
20h
24h
M A2 M A2 M A2 M A2 M A2 U2OS*
M A2 M A2 M A2 M A2
α -PAR
α -cleaved ARTD1
α -p53
α -p27
α -Tubulin
250 kDa
170 kDa
C
p27 gene body
Relative occupancy (% of input)
siMock
siARTD2
IgG
H3
H3K4me3
H3K27me3
H4ac
p21 gene body
p21 gne body

Citation: Cell Death and Disease (2013) 4, e498; doi:10.1038/cddis.2013.15

www.nature.com/cddis

PKC signaling prevents irradiation-induced apoptosis of primary human fibroblasts

A Bluwstein[1,2], N Kumar[3], K Léger[1,2], J Traenkle[4], J van Oostrum[5], H Rehrauer[6], M Baudis[3] and MO Hottiger*[,1]

Primary cells respond to irradiation by activation of the DNA damage response and cell cycle arrest, which eventually leads to senescence or apoptosis. It is not clear in detail which signaling pathways or networks regulate the induction of either apoptosis or senescence. Primary human fibroblasts are able to withstand high doses of irradiation and to prevent irradiation-induced apoptosis. However, the underlying regulatory basis for this phenotype is not well understood. Here, a kinetic network analysis based on reverse phase protein arrays (RPPAs) in combination with extensive western blot and cell culture analyses was employed to decipher the cytoplasmic and nuclear signaling networks and to identify possible antiapoptotic pathways. This analysis identified activation of known DNA damage response pathways (e.g., phosphorylation of MKK3/6, p38, MK2, Hsp27, p53 and Chk1) as well as of prosurvival (e.g., MEK-ERK, cAMP response element-binding protein (CREB), protein kinase C (PKC)) and antiapoptotic markers (e.g., Bad, Bcl-2). Interestingly, PKC family members were activated early upon irradiation, suggesting a regulatory function in the ionizing radiation (IR) response of these cells. Inhibition or downregulation of PKC in primary human fibroblasts caused IR-dependent downregulation of the identified prosurvival (CREB phosphorylation) and antiapoptotic (Bad phosphorylation, Bcl-2) markers and thus lead to a proliferation stop and to apoptosis. Taken together, our analysis suggests that cytoplasmic PKC signaling conditions IR-stressed MRC-5 and IMR-90 cells to prevent irradiation-induced apoptosis. These findings contribute to the understanding of the cellular and nuclear IR response and may thus eventually improve the efficacy of radiotherapy and help overcome tumor radioresistance.

Cell Death and Disease (2013) **4,** e498; doi:10.1038/cddis.2013.15; published online 14 February 2013
Subject Category: Cancer

Genotoxic stress such as ionizing radiation (IR) causes DNA damage and thereby induces diverse cellular responses such as cell cycle arrest and the activation of the DNA damage response (DDR) pathways to deal with this threat.[1] These complex DDRs are regulated by the PI3K-like kinases ATM, ATR and DNA-PK, which regulate downstream effectors that induce cell cycle checkpoints via phosphorylation of checkpoint kinases (Chk1/2), phosphatases (Cdc25) as well as stabilization of p53 and activation of the p16INK4a-Rb pathway to delay progression into the S phase or mitosis.[2] Following the detection of DNA breaks, ATM initiates a nuclear signaling cascade, leading to the phosphorylation of protein substrates such as histone H2A.X, which is thus modified into γH2A.X and sensitively marks individual DNA breaks.[3] Depending on the cell type, prolonged cell cycle arrest and extensive DNA damage leads to apoptosis or senescence,[4–6] but the molecular mechanism leading to either of these outcomes is not understood in detail. Recent large-scale network analyses have extended our understanding not only of genotoxic stress signaling and identified new phosphorylation but also of acetylation sites and target proteins mainly in the nucleus.[7–11] Reverse phase protein arrays (RPPA) represent a powerful technology for the sensitive detection and high-throughput quantification of protein changes at the single-cell level in a multiplex setting.[12,13] Protein arrays have already been applied to study changed expression levels or post-translational modification status of proteins in cellular stress conditions or in normal and cancerous prostate and ovarian tissue.[10,13–15]

Depending on the cell type, IR induces different responses and proteome changes. MRC-5 primary human lung fibroblasts were used in this study as a model cell strain, because these cells tolerate IR doses up to 80 Gy and do not induce apoptosis.[16,17] Here, we applied the RPPA technology to study IR-induced stress pathways in primary cells on a 'signalosome level' by analyzing cellular candidate markers. The RPPAs were probed with 165 different antibodies to quantify the major components and post-translational modifications of nuclear and cytoplasmic stress signaling events. Besides classical components of the DDR, such as protein level and phosphorylation changes in Chk1, p53, p21 and cyclin D1, as well as activation of the MEK-ERK, p38-Hsp27

[1]Institute of Veterinary Biochemistry and Molecular Biology (IVBMB), University of Zurich, Winterthurerstrasse 190, Zurich, Switzerland; [2]Cancer Biology PhD Program, Life Science Zurich Graduate School, University of Zurich, Winterthurerstrasse 190, Zürich, Switzerland; [3]Institute for Molecular Life Science (IMLS) and Swiss Institute of Bioinformatics (SIB), University of Zurich, Winterthurerstrasse 190, Zurich, Switzerland; [4]Bayer Technology Services GmbH, Zeptosens Platform, Leverkusen, Germany; [5]Luxembourg Clinical Proteomics Center, CRP-Santé, Strassen, Luxembourg and [6]Functional Genomics Center Zurich (FGCZ), University of Zurich, Zurich, Switzerland
*Corresponding author: MO Hottiger, Institute of Veterinary Biochemistry and Molecular Biology (IVBMB), University of Zurich, Winterthurerstrasse 190, Zurich 8057 Switzerland. Tel: +41 44 6355474; Fax: +41 44 6356840; E-mail: hottiger@vetbio.uzh.ch
Keywords: apoptosis; DNA damage response; PKC signaling; primary human fibroblast; radiation sensitivity; reverse phase protein array
Abbreviations: CREB, cAMP response element-binding protein; DDR, DNA damage response; DNA, deoxyribonucleic acid; IgG, immunoglobulin G; IR, ionizing radiation; NHF, normal human fibroblast; PKC, protein kinase C; RPPA, reverse phase protein array
Received 26.09.12; revised 21.12.12; accepted 02.01.13; Edited by A Stephanou

and LKB-AMPK pathways, the RPPA analysis described here also identified specific components of the cellular IR response involved in antiapoptotic and prosurvival signaling. Among these changes was also the activation of PKC family members. The PKC signaling pathway is known to integrate extracellular signals, calcium and secondary lipid messengers (diacylglycerol, phosphatidylserine), to regulate diverse cellular responses, including apoptosis or survival during genotoxic stress.[18–20] We found that experimental inhibition or downregulation of PKC led to downregulation of prosurvival (cAMP response element-binding protein (CREB) phosphorylation) and antiapoptotic (Bad phosphorylation, Bcl-2) markers upon IR treatment and thus lead to apoptosis in normal human MRC-5 and IMR-90 fibroblasts (normal human fibroblasts (NHFs)). These results thus implicated significantly changed kinetics of prosurvival (CREB phosphorylation) and antiapoptotic (Bad phosphorylation, Bcl-2) key determinants in the ability to prevent apoptosis upon severe DNA damage. IR-induced PKC signaling is thus defined as the mechanism that prevents IR-induced apoptosis.

Results

IR induces a DDR and senescence in MRC-5 fibroblasts. To induce DNA damage, primary human MRC-5 fibroblasts were irradiated with doses of 10 and 40 Gy. Both doses induced key components of the classical DDR, including phosphorylation of ATM at serine 1981 (pS1981), of Chk1 at serine 345 (pS345), of H2A.X at serine 139 (pS139) and stabilization of p53 protein levels (Figure 1a). The IR doses were chosen based on preliminary experiments and reflect the high capacity to repair IR-induced DNA damage of MRC-5 cells, which have been shown to efficiently remove DNA strand breaks (DSBs) up to IR doses of 80 Gy[16] and to enter the senescent state upon treatment with various stress stimuli.[21] In agreement with these findings, irradiation of MRC-5 cells with IR doses between 4 and 10 Gy induced a dose-dependent increase and time-dependent decrease of H2A.X pS139 that was mediated by ATM and DNA-PK (Figures 1b and c). The majority of DSBs was repaired within 8 h post-irradiation as indicated by the reduction of γH2AX foci and the remaining γH2AX foci continued to be repaired 24–48 h following IR treatment (Supplementary Figures S1a and b).

The strong reduction in colony formation of single cells after 10 days and the appearance of β-galactosidase-positive cells (MRC-5 and IMR-90) by 72 h after irradiation indicated growth arrest and induction of cell senescence (Supplementary Figures S1c and d), which was further supported by elevated p21 gene expression as well as p21 and p16 protein levels in MRC-5 and IMR-90 primary fibroblasts (Supplementary Figures S1e–g). Irradiation caused only a slight increase in the G2/M cell cycle population, but this effect was intensified upon ATM inhibition, suggesting that the efficient DDR prevented a more pronounced effect on cell cycle progression of irradiated MRC-5 cells (Supplementary Figures S2a–d). Cells did not exhibit elevated apoptosis even at the 8 h time point after 40 Gy irradiation, as indicated by the stable fraction of Annexin V-positive cells and undetectable expression of NOXA, PUMA and Bax (relative to a significant increase after staurosporine or cycloheximide treatment; Supplementary Figures S3a–d).

These results documented the suitability of 10 and 40 Gy IR to induce non-lethal, but senescence responses in primary fibroblasts.

IR induces significant proteome changes in MRC-5 fibroblasts. To quantify the kinetic proteome changes upon IR, MRC-5 fibroblasts were harvested at the 0.5, 2, 4 and 8 h time points after IR exposure (10 and 40 Gy) and RPPA analysis was performed (Figure 2a and Supplementary Figure S4). The time points were chosen based on the observed kinetics of γH2AX activation (Figure 1b) and were similar to those used in earlier studies.[7] The protein arrays were probed with 165 validated antibodies that specifically recognize the activation state of crucial proteins of all major signaling pathways. Only antibodies previously assessed and certified for commercial RPPA analysis services (identifying only one single band in a conventional western blot) were used and the spotted protein samples were diluted to increase the dynamic range for protein detection.[13] All quantitative RPPA data of three independent biological experiments (eight technical replicates) were subjected to stringent statistical analysis (ANOVA: $P<0.05$ and fold change cutoff: fold change $\geq 1.5 \times$ S.D.) (Supplementary Figures S5–9). Altogether, 90 unique proteome changes were either significant based on ANOVA and/or passed the $1.5 \times$ S.D. cutoff (Supplementary Figures S6 and 7 and Supplementary Table).

Clustering analysis identifies early cytoplasmic signals and subsequent activation of classical DDR proteins. The analysis described here identified distinct clusters based on the temporal up- and downregulation of specific proteins or protein modifications. In general, treatment of MRC-5 fibroblasts with 40 Gy induced more distinct clusters as compared with 10 Gy irradiation and three broad groups were apparent (Figures 2b and c and Supplementary Figures S10a and -b). The earliest changes affected many cytoplasmic proteins such as MEK1/2 (pS217/222, pS221/226), ERK1/2 (pT202/185, pY204/187), LKB (pS428) and cyclin D1 (pT286), which were sharply induced at 0.5 h after irradiation and relaxed to much lower and constant levels thereafter (cluster 1; Figure 2c and Supplementary Figure S10b). Following this first wave of protein changes, a cluster with a distinct maximum at 2 h after 40 Gy IR appeared (clusters 2 and 5). The protein changes that appeared at later time points after 40 Gy IR comprised changes that were upregulated throughout the entire IR response or specifically increased by the higher IR dose (clusters 3 and 4). The consecutive activation and inactivation of different groups of proteins indicated a signaling cascade that progresses from the cytoplasm (early activation of MEK1/2, ERK1/2, LKB) to the nucleus (delayed activation of classical nuclear DDR proteins such as Chk1, p53, p21, MAPKAP2, Hsp27).

Validation of RPPA analysis confirms upregulation of known DDR pathways and identifies pRb downregulation. The detection of many classical DDR proteome

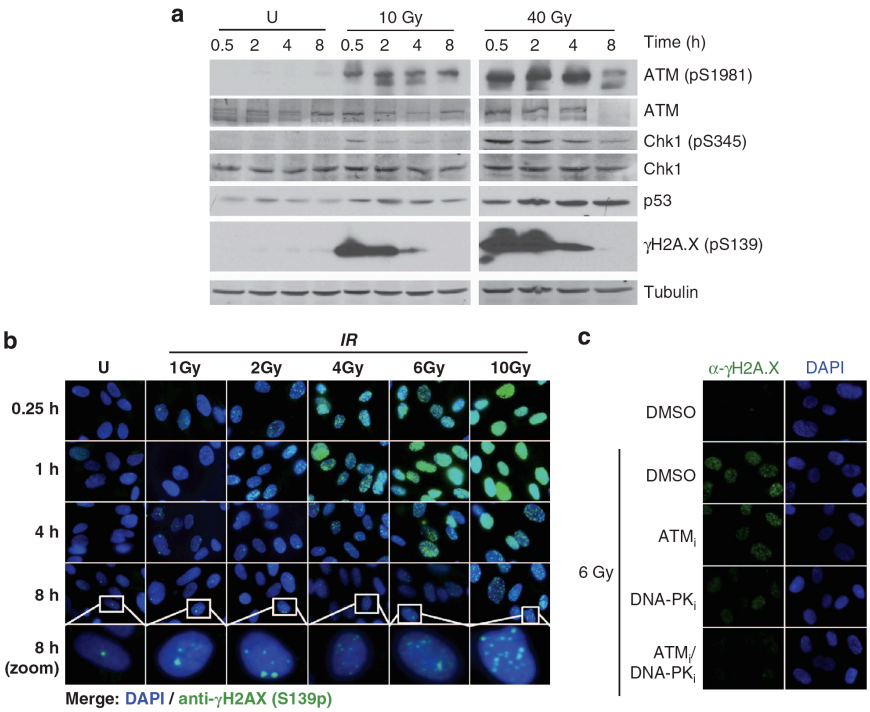

Figure 1 Induction of the DRR and efficient repair of IR-induced DNA breaks over 48 h in NHFs. (**a**) Western blot analysis of irradiated MRC-5 cells after recovery from IR for 0.5–8 h. (**b**) Immunofluorescence staining of MRC-5 cells irradiated with X-ray doses of 1–10 Gy or left untreated (U) and recovered for 15 min–8 h. (**c**) MRC-5 cells were pretreated with 10 μM KU-55933 (ATMi) and/or 10 μM Nu7441 (DNA-PKi) before irradiation with 6 Gy, or left untreated (U) as a control. Cells were stained with anti-γH2A.X (phospho-Ser139) 1 h post-irradiation. ATM, Ataxia-telangiectasia mutated; Chk, checkpoint kinase; DAPI, 4′,6-diamidino-2-phenylindole; DNA-PK, DNA protein kinase; DMSO, dimethyl sulfoxide

changes upon both 10 and 40 Gy IR validated the RPPA analysis of IR-treated MRC-5 fibroblasts. Known proteome changes of the DDR pathway included higher total amounts of p53 and p21 as well as increased levels of phosphorylated p38 MAPK (pT180, pY182), Hsp27 (pS78), p53 (pS15) and Chk1 (pS345) (clusters 1–3 for 10 Gy and clusters 2–5 for 40 Gy; Figures 2b and c and Supplementary Figures S10a and -b). In addition, Chk1 phosphorylation upon 10 and 40 Gy IR was confirmed by western blot analysis (Figure 1a and Supplementary Figure S10c). Levels of Chk1 phosphorylation determined by RPPA and western blot analysis showed similar kinetics (early increase after 30 min recovery from IR followed by a decline over the 8 h time course) and thus confirmed the validity of the RPPA approach. IR-induced Chk2 phosphorylation could only be shown by western blotting because of its poor antibody performance on the arrays (Supplementary Figure S10f). Even though ANOVA ($P<0.05$) and fold cutoff (S.D. = 1.5) analysis did not reveal significantly changed phosphorylation of the classical DDR marker H2A.X (pS139) in response to 10 Gy, at the 2 h time point, the Student's *t*-test showed a significantly increased H2A.X phosphorylation ($P<0.05$) (Supplementary Figures S7 and 8). The kinetics of H2A.X phosphorylation upon 10 and 40 Gy correlated well, but the higher dose resulted in a stronger fold induction (Supplementary Figures S8 and 9). In agreement with previously published studies,[22] activation of the cytoplasmic stress kinase p38 MAPK and its downstream effector, the small heat-shock protein Hsp27, were both ATM-dependent as confirmed by western blotting and ATM inhibitor studies (Supplementary Figure S10d). Other proteome changes that were also analyzed by western blotting similarly confirmed the RPPA results, albeit western blotting revealed higher fold changes. Temporarily increased levels of p53, which is the main target for ATM in response to IR,[2] correlated with delayed upregulation of p21 (clusters 1 and 2 for 10 Gy; Figure 2b). Surprisingly, the important cell cycle regulator retinoblastoma protein (pRb) was significantly downregulated upon 10 Gy irradiation (cluster 5; Figure 2b), representing a proteome change that has not been implicated in the IR response previously. The RPPA-based pRb quantification correlated strongly with results obtained by western blotting (Supplementary Figures S10e and f), supporting *in vivo* pRb downregulation upon IR in MRC-5 fibroblasts. In contrast to total pRb levels, the phosphorylation of pRb at S780 (relative to total pRb) increased upon 10 Gy after 8 h and already after 2 h following irradiation with 40 Gy (Supplementary Figure S10f). In line with this finding, a strong cell-cycle effect was not observed 24–48 h after irradiation compared with a clear accumulation of cells at the G1/S boundary upon hydroxyurea treatment (Supplementary Figure S2), suggesting that the pRb changes may be important for the maintenance of cell cycle progression during the immediate IR response.

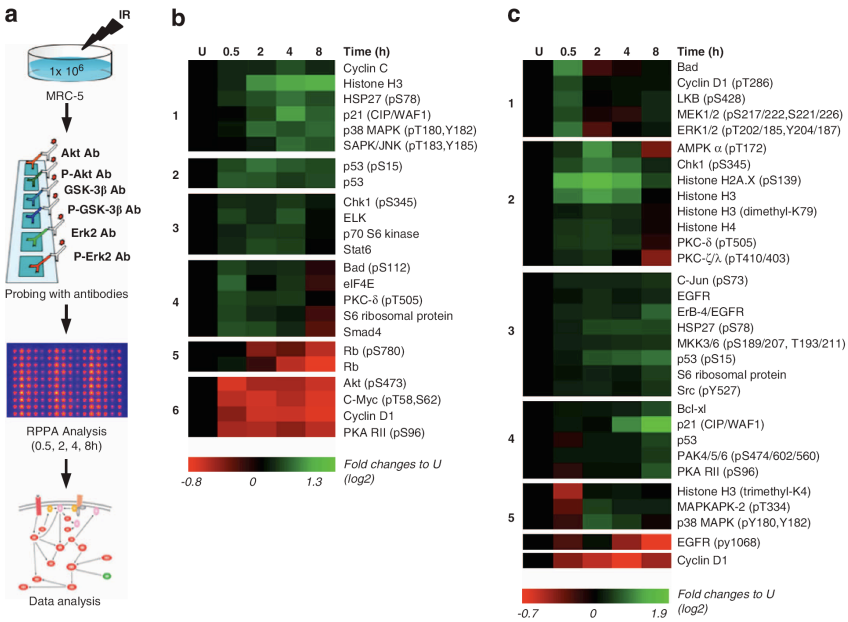

Figure 2 Identification of significant proteome changes in response to IR. (**a**) Workflow for the characterization of IR-induced proteome changes by RPPA. MRC-5 cells were left untreated (U) or irradiated in biological triplicates with 10 or 40 Gy. At different time points, cell lysates were prepared and spotted in equal amounts on hydrophobic glass slides. Each array was incubated with a different primary antibody, directed against a protein of interest and a secondary fluorophore-labeled antibody. Relative fluorescence intensities were quantified and used for statistical data analysis to identify significant proteome changes in response to irradiation. (**b** and **c**) Time-profile clustering of IR-dependent proteome changes (analysis of variance (ANOVA), $P<0.05$; 1.5 S.D. cutoff) using Self-Organizing Tree Algorithm (SOTA) showing protein expression and modification (e.g., phosphorylation) in green or downregulation and de-modification (e.g., de-phosphorylation) in red. (**b**) Clustering of proteome changes upon irradiation with 10 Gy. (**c**) Clustering analysis of IR-dependent proteome changes upon 40 Gy treatment. AMPK, AMP-activated protein kinase; Bad, Bcl2 antagonist of cell death; EGFR, epidermal growth factor receptor; eIF4E, Eukaryotic initiation factor eIF4E like protein; ERK, extracellular signal-regulated kinase; Hsp, heat-shock protein; JNK, c-Jun NH2-terminal kinase; MAPK, mitogen-activated protein kinase; MEK, MAPK/ERK kinase; PAK, p21-activated kinase; PKA RII, cAMP-dependent protein kinase type II regulatory subunit; PKC, protein kinase C; Rb, Retinoblastoma-associated protein; SAPK, stress-activated protein kinase; SMAD, Homolog of mothers against decapentaplegic homolog from *Drosophila* and SMA from *Caenorhabditis elegans*; Stat6, signal transducer and activator of transcription 6

The role of the p53 pathway in DDR and its function as a 'guardian of the genome'[23,24] is emphasized by the fact that it was significantly over-represented among the proteins responding to both 10 and 40 Gy IR (Figure 3a), and by its many interactions (more than 14 interactions) in the predicted protein network (Figure 3b and Supplementary Figure S10g). The agreement of the RPPA analysis with western blot quantifications, as well as the identification of the known key players in the DDR, confirmed the validity of the RPPA approach described here and proved that the IR-treated cells used in these experiments launched a classical DDR.

IR upregulates antiapoptotic and prosurvival markers in MRC-5 cells. The kinetic RPPA analysis described here also revealed many new cytoplasmic factors, which were further analyzed in more detail. The here identified changes included prosurvival signals CREB (pS133) as well as MEK1/2 (pS217/222, pS221/226), ERK1/2 (pT202/185, pY204/187) and AMPK (pT172) for 40 Gy only, antiapoptotic markers (Bad pS112 and pS136, Bcl-2 pS70 for 10 Gy only) as well as a cluster comprising protein kinase C (PKC) family members. The changes in PKC family members included the phosphorylation of the novel PKC-δ (pT505) and of the atypical PKCζ/λ (pT410/403) in the activation loop (Figures 2b and c), which marks the activated state of these two PKC isoforms.[25]

These analyses suggested that IR treatment of primary fibroblasts activates not only the classical DDR pathways MEK-ERK and p38-Hsp27 but that also the cytoplasmic PKC signaling and specific antiapoptotic and prosurvival factors were regulated. It is thus possible that PKC signaling is involved in mediating the high IR resistance of MRC-5 and IMR-90 cells by preventing apoptosis and stimulating prosurvival factors.

Inhibitor screen identifies PKC signaling as important for IR resistance. To elucidate whether PKC or other main signaling cascades regulate cell viability in NHFs upon IR treatment, a radiosensitivity screen with inhibitors specific for key components of the MEK-ERK, p38, JNK or PKC pathways was performed (Figure 4 and Supplementary Figures S11a–e). While JNK inhibitors had only a weak effect on cell viability, inhibition of MEK and p38 affected cell proliferation, but independent of IR (i.e., similar effect in treated and untreated cells). Interestingly, already 48 h after the cotreatment with either one of two PKC inhibitors (GF109203X or Ro-318220) and with IR, MRC-5 cells showed a significant reduction in cell viability compared with cells treated with DMSO (the solvent) or with IR alone (Figure 4 and Supplementary Figure S11). The NHF strain IMR-90 behaved similarly and showed a significant reduction

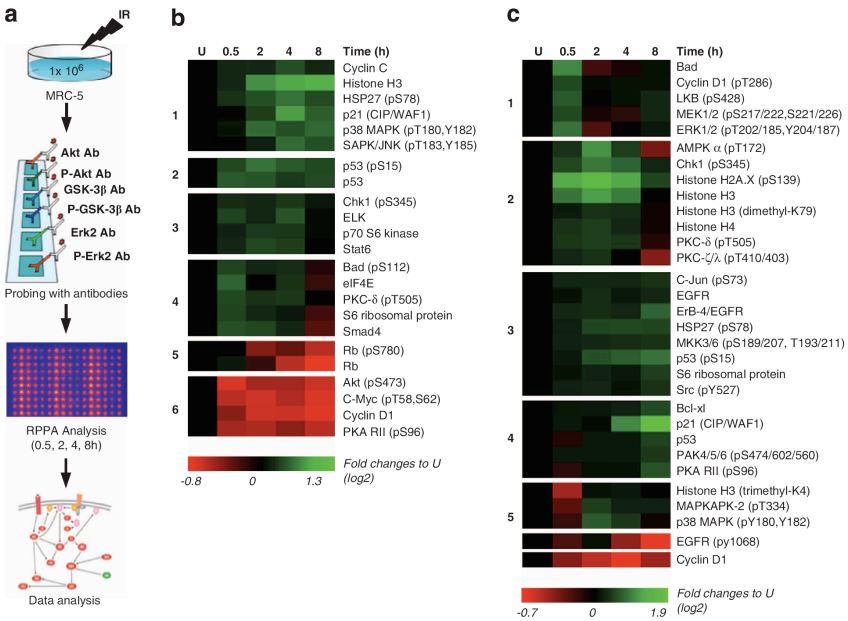

Figure 2 Identification of significant proteome changes in response to IR. (**a**) Workflow for the characterization of IR-induced proteome changes by RPPA. MRC-5 cells were left untreated (U) or irradiated in biological triplicates with 10 or 40 Gy. At different time points, cell lysates were prepared and spotted in equal amounts on hydrophobic glass slides. Each array was incubated with a different primary antibody, directed against a protein of interest and a secondary fluorophore-labeled antibody. Relative fluorescence intensities were quantified and used for statistical data analysis to identify significant proteome changes in response to irradiation. (**b** and **c**) Time-profile clustering of IR-dependent proteome changes (analysis of variance (ANOVA), $P<0.05$; 1.5 S.D. cutoff) using Self-Organizing Tree Algorithm (SOTA) showing protein expression and modification (e.g., phosphorylation) in green or downregulation and de-modification (e.g., de-phosphorylation) in red. (**b**) Clustering of proteome changes upon irradiation with 10 Gy. (**c**) Clustering analysis of IR-dependent proteome changes upon 40 Gy treatment. AMPK, AMP-activated protein kinase; Bad, Bcl2 antagonist of cell death; EGFR, epidermal growth factor receptor; eIF4E, Eukaryotic initiation factor eIF4E like protein; ERK, extracellular signal-regulated kinase; Hsp, heat-shock protein; JNK, c-Jun NH2-terminal kinase; MAPK, mitogen-activated protein kinase; MEK, MAPK/ERK kinase; PAK, p21-activated kinase; PKA RII, cAMP-dependent protein kinase type II regulatory subunit; PKC, protein kinase C; Rb, Retinoblastoma-associated protein; SAPK, stress-activated protein kinase; SMAD, Homolog of mothers against decapentaplegic homolog from *Drosophila* and SMA from *Caenorhabditis elegans*; Stat6, signal transducer and activator of transcription 6

The role of the p53 pathway in DDR and its function as a 'guardian of the genome'[23,24] is emphasized by the fact that it was significantly over-represented among the proteins responding to both 10 and 40 Gy IR (Figure 3a), and by its many interactions (more than 14 interactions) in the predicted protein network (Figure 3b and Supplementary Figure S10g). The agreement of the RPPA analysis with western blot quantifications, as well as the identification of the known key players in the DDR, confirmed the validity of the RPPA approach described here and proved that the IR-treated cells used in these experiments launched a classical DDR.

IR upregulates antiapoptotic and prosurvival markers in MRC-5 cells. The kinetic RPPA analysis described here also revealed many new cytoplasmic factors, which were further analyzed in more detail. The here identified changes included prosurvival signals CREB (pS133) as well as MEK1/2 (pS217/222, pS221/226), ERK1/2 (pT202/185, pY204/187) and AMPK (pT172) for 40 Gy only, antiapoptotic markers (Bad pS112 and pS136, Bcl-2 pS70 for 10 Gy only) as well as a cluster comprising protein kinase C (PKC) family members. The changes in PKC family members included the phosphorylation of the novel PKC-δ (pT505) and of the atypical PKCζ/λ (pT410/403) in the activation loop (Figures 2b and c), which marks the activated state of these two PKC isoforms.[25]

These analyses suggested that IR treatment of primary fibroblasts activates not only the classical DDR pathways MEK-ERK and p38-Hsp27 but that also the cytoplasmic PKC signaling and specific antiapoptotic and prosurvival factors were regulated. It is thus possible that PKC signaling is involved in mediating the high IR resistance of MRC-5 and IMR-90 cells by preventing apoptosis and stimulating prosurvival factors.

Inhibitor screen identifies PKC signaling as important for IR resistance. To elucidate whether PKC or other main signaling cascades regulate cell viability in NHFs upon IR treatment, a radiosensitivity screen with inhibitors specific for key components of the MEK-ERK, p38, JNK or PKC pathways was performed (Figure 4 and Supplementary Figures S11a–e). While JNK inhibitors had only a weak effect on cell viability, inhibition of MEK and p38 affected cell proliferation, but independent of IR (i.e., similar effect in treated and untreated cells). Interestingly, already 48 h after the cotreatment with either one of two PKC inhibitors (GF109203X or Ro-318220) and with IR, MRC-5 cells showed a significant reduction in cell viability compared with cells treated with DMSO (the solvent) or with IR alone (Figure 4 and Supplementary Figure S11). The NHF strain IMR-90 behaved similarly and showed a significant reduction

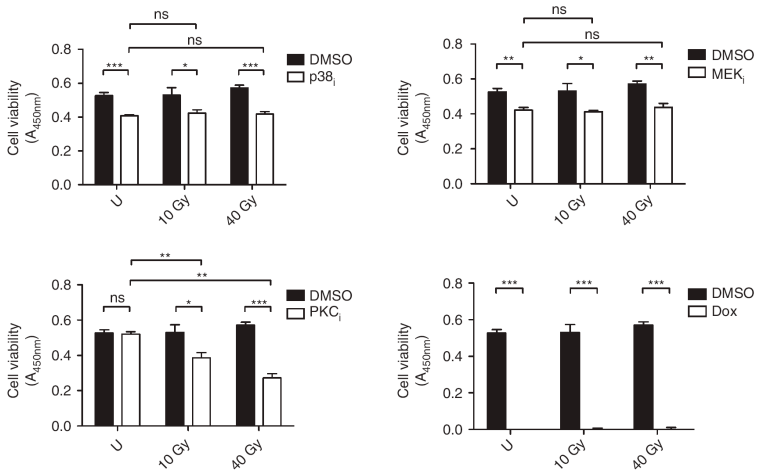

Figure 4 PKC inhibition sensitizes MRC-5 to 10 and 40 Gy after 48 h. Cell viability assay (WST-1) of MRC-5, pretreated with p38 (SB203580, 10 μM), MEK (PD98059, 20 μM) or PKC inhibitor (GF109203X, 10 μM) and as a positive control for cell death with doxorubicin (Dox, 1 μg/ml) for 2 h before IR and recovery for the indicated time points ($n=3$). DMSO, dimethyl sulfoxide; MEK, mitogen-activated protein kinase/extracellular signal-regulated kinase kinase; NS, nonsignificant; PKC, protein kinase C; U, untreated; *$p<0.05$; **$p<0.01$; ***$p<0.001$

in growth when treated with the PKC inhibitor GF109203X (2.5 μM) and either 10 or 40 Gy irradiation (Supplementary Figures S12a–c). These results implicated PKC activity and signaling in the radiosensitivity of MRC-5 and IMR-90 cells.

Inhibition or downregulation of PKC directs cells towards apoptosis. To confirm and validate PKC activation upon IR, western blot analyses were performed. In agreement with the RPPA results and the inhibitor studies, phosphorylation of PKCζ/λ (pT410/pT403) as well as of PKCβ (pT641) were confirmed to be increased upon IR (Figures 5a and b). To further characterize the mechanism of the PKC-dependent reduction in cell viability, one prosurvival (CREB phosphorylation)[26] and one antiapoptotic marker (phosphorylation of Bad)[27] was analyzed in more detail by western blotting (Figures 5c–e). In combination with IR treatment, PKC inhibition or downregulation caused strongly reduced phosphorylation of CREB (pS133) and Bad (pS136), while the total protein levels were only marginally affected (Figures 5c and d for MRC-5; Figure 5e for IMR-90). Interestingly, ATM (pS1981) was not affected by PKC inhibition (Figures 5c and e) and did not affect CREB phosphorylation or protein levels (Figure 5c), suggesting that the PKC pathway is activated independent of the classical DDR.

Although primary human fibroblasts are known to undergo senescence as a response to irradiation, the reduced phosphorylation of CREB and Bad, as well as the reduced cell viability, upon IR treatment and PKC inhibition or downregulation indicated the induction of apoptosis.[28,29] It was therefore assessed whether irradiation and PKC inhibition affects senescence and possibly induces apoptosis. Upon PKC inhibition and irradiation with 10 or 40 Gy, MRC-5 and IMR-90 cells both showed reduced β-galactosidase staining as compared with the DMSO-treated control, which is indicative of reduced senescence (Figure 5f and Supplementary Figure S13a). Using an alternative senescence marker, reduced p16 protein levels upon irradiation, in combination with PKC inhibition or downregulation, could be confirmed in MRC-5 cells (Figure 5h). The p16 levels were not significantly reduced in IMR-90 cells in response to IR and PKC inhibition; however; the significant reduction in p21 protein levels (Supplementary Figures S13b and c) was another alternative indicator for cellular senescence.[30] In contrast, in the presence of PKC inhibitors, IR treatment led to induced levels of the proapoptotic marker Bad and reduced amounts of the antiapoptotic marker Bcl-2, persistently increased p53 protein levels (in addition to the temporary p53 stabilization observed as a response to IR alone) and ARTD1 (PARP-1) cleavage (reduction in ARTD1 full-length levels and accumulation of the 89 kDa cleavage fragment), all suggestive of a switch from senescence to apoptosis, specifically upon IR in combination with PKC inhibitor treatment or PKC knockdown after 48 h of IR recovery (Figures 5g and h). Reduced ARTD1 levels and an increased sub-G1 cell population in the NHF strain IMR-90 also confirmed the findings with the MRC-5 strain (Supplementary Figures S13b–f), in addition to the reduced senescence and cell viability upon IR treatment in combination with PKC inhibition.

In summary, these results demonstrated the IR-dependent activation of cytoplasmic PKC signaling and discovered the consecutive PKC-dependent activation of prosurvival signaling mediated via CREB and Bcl-2 as well as the inactivation of proapoptotic pathways (Bad), which direct normal human MRC-5 and IMR-90 fibroblasts towards senescence and prevent IR-induced apoptosis (Figure 6). Activation of cytoplasmic PKC signaling upon IR is thus a novel mechanism that orchestrates the different IR-induced responses to ensure cell survival of primary human fibroblasts.

Discussion

Human primary fibroblasts such as MRC-5 cells are able to repair DNA damage induced by IR doses up to 80 Gy.[16,17] However, it was so far not clear how MRC-5 fibroblasts prevent

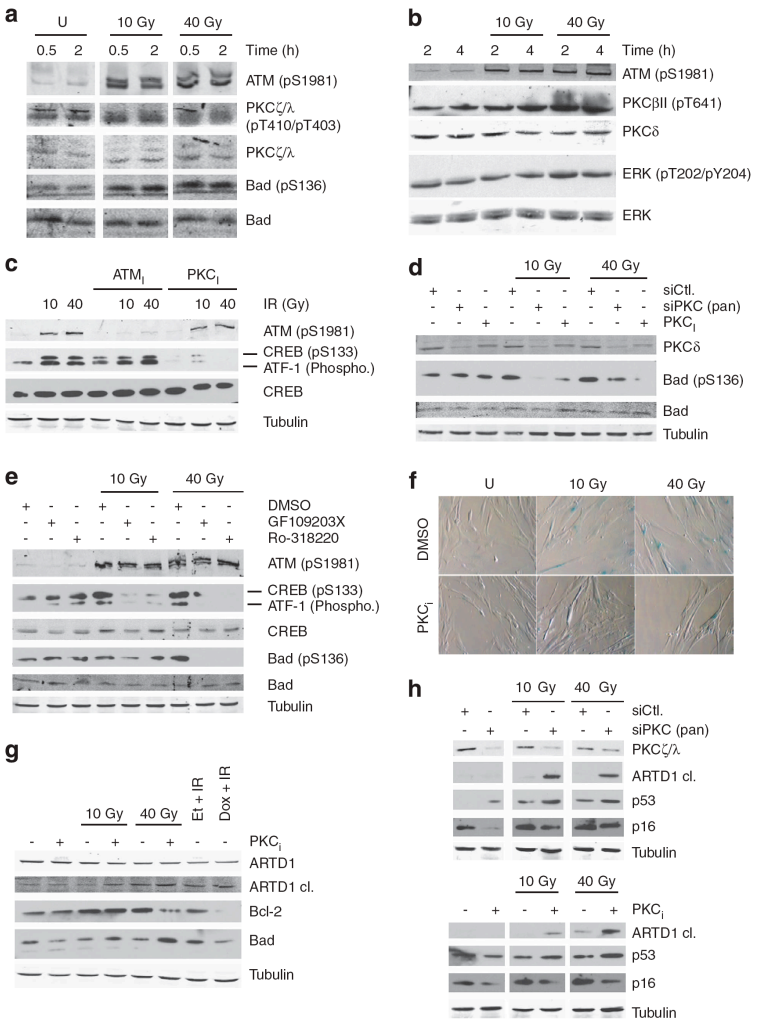

Figure 5 Inhibition or downregulation of PKC reduces prosurvival signaling in NHFs. Phosphorylation of PKCζ/λ and Bad (**a**) or PKCβII and ERK (**b**) in response to IR. Western blot analysis of irradiated MRC-5 cells after recovery for 0.5–2 or 2–4 h following IR. Total PKCζ/λ and Bad (**a**) or total PKCδ and ERK (**b**) were used as loading control. (**c**) Phosphorylation of CREB and ATF-1 is downstream of PKC activation in response to IR. Western blot analysis of irradiated MRC-5 cells (4 h recovery) that were treated either with the PKC-specific inhibitor Ro-318220 (5 μM, added before irradiation) or with the ATM inhibitor KU-55933 (10 μM, added before irradiation). Tubulin was used as loading control. (**d**) Phosphorylation of Bad is downstream of PKC activation in response to IR. Western blot analysis of irradiated MRC-5 cells (4 h recovery) that were exposed to the PKC-specific inhibitor GF109203X (5 μM, for 2 h) or siPKC pan. (**e**) Phosphorylation of CREB, ATF-1 and Bad is downstream of PKC activation in response to IR. Western blot analysis of irradiated IMR-90 cells (4 h recovery) that were treated with GF109203X or Ro-318220 (2.5 μM, 2 h pre-incubation before irradiation). Tubulin was used as loading control. (**f**) Pharmacological inhibition of PKC reduces senescence associated β-galactosidase (β-gal) staining. SA-β-gal staining of irradiated MRC-5 in presence of PKC inhibitor (GF109203X, 5 μM, 72 h recovery) with untreated (U) as control. (**g**) Pharmacological inhibition of PKC (GF109203X, 5 μM) leads to ARTD1 cleavage, Bcl-2 downregulation and Bad upregulation 48 h after IR. (**h**) Knockdown of PKC leads to increased p53 stabilization and reduced p16 protein levels as well as increased ARTD1 cleavage in response to 10 and 40 Gy at 48 h after IR. Western blot analysis of irradiated MRC-5, transfected either with siPKC pan or scrambled siRNA as control for 3 days before IR. Tubulin was used as loading control. ARTD1, ADP-ribosyltransferase diphtheria toxin-like 1; ATF, cyclic AMP-dependent transcription factor 1; ATM, ataxia–telangiectasia mutated; Bad, Bcl2 antagonist of cell death; Bcl-2, B-cell lymphoma 2; CREB, cAMP response element-binding protein; DMSO, dimethyl sulfoxide; ERK, extracellular signal-regulated kinase; Et, etoposide; PKC, protein kinase C

apoptosis, which is induced at much lower IR doses in other cell types.[31] Understanding the dynamics of *in vivo* signaling events in response to IR in human primary fibroblast may thus reveal medically relevant IR resistance mechanisms.

The network analysis of IR-induced proteome changes in MRC-5 fibroblasts presented here identified upregulation of known DDR factors (H2AX, p53, p21, MKK3/6, p38, MK2, Hsp27, Chk2) only 2–8 h after irradiation (Supplementary Table). In contrast, growth factor- and cytokine-dependent signaling pathways including members of the MAPK family (MEK/ERK), PKC family (PKCδ, PKCζ/λ, PKCβII) as well as anti- and proapoptotic Bcl-2 family members (Bcl-2, Bad) tended to respond with faster kinetics and thus indicated that cytoplasmic signaling events are upstream of the canonical DDR. Indeed, an increasing body of evidence implicates an IR-dependent cytoplasmic signaling network in regulating

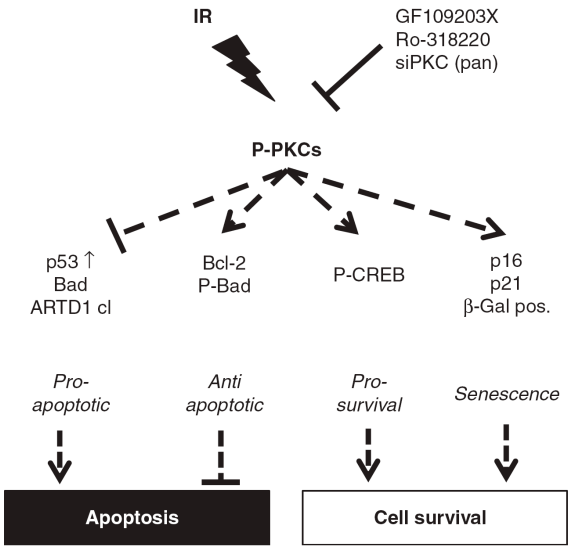

Figure 6 Model of PKC-dependent cellular prosurvival signaling in response to IR. IR-induced PKC signaling orchestrates cell survival via upregulation of Bcl-2 and phosphorylation of Bad and CREB. Hypersensitization with PKC inhibitors (GF109203X, Ro-318220) and genetic knock down (siPKC pan) leads to IR-induced activation of apoptosis mediated by p53 stabilization, upregulation of Bad and ARTD1 cleavage, as well as reduced senescence mediated via decrease in p21 protein levels and reduced β-galactosidase (β-Gal) activity in response to IR. ARTD1, ADP-ribosyltransferase diphtheria toxin-like 1; Bad, Bcl2 antagonist of cell death; Bcl-2, B-cell lymphoma 2; CREB, cAMP response element-binding protein

DNA break repair.[32] Although RPPA analysis is restricted by antibody performance and reduced dynamic range, western blotting confirmed the tested proteome changes discovered by RPPA analysis, supporting the stringent statistical analysis. However, western blotting indicated that RPPA analysis usually underestimated the IR-induced proteome changes.

Most proteome changes, in particular upon 40 Gy IR, affected mitogenic signaling events controlling cell survival (MKK3/6-p38-MK2 pathway, MEK-ERK pathway, LKB-AMPK pathway, PKC-Bad pathway). Previously published results have demonstrated p38-MK2 pathway activation and subsequent cell cycle arrest in G2/M in response to UV irradiation, thus protecting DNA damaged cell from entering mitosis, which would lead to a mitotic catastrophe and eventually to apoptosis.[33,34] In agreement with these findings, in response to 10 and even more pronounced upon 40 Gy, we could show activation of the major p38-MK2 pathway components, with phosphorylation of MKK3/6, p38, MAPKAP-2 (MK2) and Hsp27, besides the slight increase in the percentage of the G2/M cell cycle population 24–48 h after IR recovery (Supplementary Figures S2 and S7).

The most important finding of this systematic RPPA analysis is the identification of PKC as a key player that orchestrates the downstream signaling pathways regulating apoptosis and cell survival (Figure 6). IR-dependent PKC activation regulated Bad, Bcl-2 and CREB to prevent apoptosis and to induce prosurvival signaling. Whether PKC family members directly phosphorylate the identified downstream proteins or rather indirectly affect their activation is currently not known. Interestingly, PKCs are known to translocate to the nucleus[35] and all identified regulatory components (Bad, Bcl-2, CREB) contain putative target sites for phosphorylation by PKC.[36] PKC inhibitors, or PKC downregulation before IR treatment, downregulated antiapoptotic factors (Bad phosphorylation, Bcl-2) and induced apoptosis (ARTD1 cleavage, increased p53 stabilization, Bad upregulation, increased sub-G1 population and decline in cell number). Sensitization of primary fibroblasts by PKC inhibitors or downregulation thus induced an apoptotic program that is mediated by effects on CREB, Bad and proapoptotic genes. PKC-dependent regulation of cell survival, apoptosis as well as cell cycle progression is thus proposed as a part of the mechanism by which primary fibroblasts resist high IR doses and circumvent apoptosis, which is in agreement with the high DNA repair efficiency and the PKC-dependent regulation of p53 function.[16,37] The inhibitor and siRNA experiments described here imply PKC signaling in the prevention of apoptosis in human primary MRC-5 and IMR-90 fibroblasts. However, these analyses do not identify which PKC family member mediates the observed phenotypes. The RPPA analysis identified PKCδ activation, which was previously shown to be induced upon DNA damage[38] and linked to pro- and antiapoptotic functions (Basu and Pal[39] and many reference therein). Future studies on the upstream regulators relevant for PKC activation upon IR in MRC-5 and IMR-90 cells will identify the required cofactors and signaling components and thereby indicate which PKC subgroup mediates the antiapoptotic function. Taken together, our findings provide the cellular mechanism, which is responsible for this phenotype and may thus open up possiblities for new treatment schemes of highly IR-resistant tumors.

This result has not only important implications for our understanding of the IR response but also for the comprehension of nuclear regulatory events and supports the concept of the cellular, in contrast to the nuclear, radiation response.[40] Cellular stress such as IR is perceived at the plasma membrane and in the cytoplasm and initiates cytoplasmic signaling pathways that consecutively control nuclear events such as DNA repair. This is also suggested by the induction of IR-induced signaling in cells exposed to IR conditioned medium, which is termed the 'bystander effect'.[41] The classical DDR, comprised of nuclear events regulating cell cycle progression and DNA repair, is thus preceded and controlled by the cytoplasmic radiation response, which is mediated by the PKC signaling pathway as well as other signaling pathways such as the MEK-ERK pathway.

This RPPA network analysis of IR-induced signaling identified a new, cytoplasmic, PKC-dependent regulatory mechanism that conditions stressed cells by preventing apoptosis. The PKC-dependent induction of prosurvival signaling and evasion of apoptosis is thus a mechanism, which renders primary human fibroblasts resistant to high doses of IR, and may thereby protect the microenvironment and permit survival of tumors. Our results thus provide an explanation for the cellular response to severe irradiation stress and will therefore help optimize and improve radiotherapy.

Materials and Methods

Cell culture, IR treatment, siRNA transfection, lysis, viability and senescence assays. The MRC-5 and IMR-90 human lung fibroblast cell strains[42,43] were obtained from the American Type Culture Collection and cultured in supplemented MEM (Invitrogen; Life Technologies, Carlsbad, CA, USA). Cells were exposed to IR using an X-ray generator (Pantak Seifert X-ray System, Ahrensburg, Germany; 120 kV; 19 mA; aluminum filter, 3.11 Gy/min) and recovered for different time periods. Inhibitor treatment was performed as indicated in the figure legends before the exposure to IR. To reduce PKC expression, 1×10^5 MRC-5 cells were transfected using human siPKC pan (Santa Cruz Biotechnology, Dallas, TX, USA; sc-29449) over 3 and 4 days, before irradiation. Whole cell extracts were prepared with Zeptosens Cell Lysis Buffer CLB1 (Bayer Technology Services GmbH, Leverkusen, Germany) or RIPA lysis buffer and total protein concentration was determined using the standard Lowry method. Cell viability was determined by seeding 2×10^3 cells in 96-well plates overnight before irradiation or drug treatment. Cell viability was quantified using the WST-1 proliferation reagent (Roche, Basel, Switzerland) or alamarBlue cell viability assay (Invitrogen) and a plate reader (Tecan, Männedorf, Switzerland). The clonogenic and senescence assays were performed as described elsewhere.[44,45]

Reverse phase protein arrays. RPPA were prepared as described.[46] In brief, whole cell extracts were spotted onto hydrophobically coated Zeptosens Chips (Bayer Technology Services GmbH). Serially diluted lysates (100, 75, 50 and 25%) were arrayed in duplicates onto hydrophobic Zeptosens Chips using the Nanoplotter NP2.0 (GeSiM; Gesellschaft für Silizium-Mikrosysteme mbH, Grosserkmannsdorf, Germany), followed by blocking in an ultrasonic nebulizer (ZeptoFOG; Bayer Technology Services GmbH). Antibody incubation, microarray data acquisition (ZeptoREADER; Bayer Technology Services GmbH) and data analysis (ZeptoVIEW version 3.1.0.2; Bayer Technology Services GmbH) was performed exactly as described.[47] The eight data points (100, 75, 50 and 25% lysate amount in duplicates) were fitted using a weighted linear least-squares fit[48] and the relative fluorescence intensity determined by interpolating at the median protein concentration or modification. To correct for small variations in protein content, relative intensities were normalized to the signals of β-catenin, which did not show any significant variation (ANOVA, $P<0.05$; $1.5 \times$ S.D.) in response to IR over indicated time points.

Significance and clustering analysis. To identify significant proteome changes in response to IR, relative fluorescence intensities were imported to MeV version 4.6.[49] Relative fluorescence intensities were log 2 transformed and normalized, before performing statistical analysis using one-way ANOVA as described in Zar.[50] The mean transformed fluorescence intensities for group 1 (untreated: 0.5, 2, 4 and 8 h), group 2 (biological triplicates of 10 or 40 Gy at 0.5 h), group 3 (biological triplicates of 10 or 40 Gy at 2 h), group 4 (biological triplicates of 10 or 40 Gy at 4 h) and group 5 (biological triplicates of 10 or 40 Gy at 8 h) were compared using F-statistics with $P<0.05$. Owing to technical problems during preparation of the serial dilution of the whole cell extracts, two biological replicates for the 8 h time point of 10 Gy irradiated samples (10 Gy at 8 h) and one biological replicate for the 2 and 8 h time point of 40 Gy irradiated samples (40 Gy at 2 h and 40 Gy at 8 h) were excluded from the statistical analysis. For fold-change analysis, transformed means of the biological replicates were normalized to the untreated sample (set as 1) and proteome changes were filtered (cutoff set at $1.5 \times$ S.D. equal to $\log 2 > 0.27 / < -0.27$ for 10 Gy or $\log 2 > 0.29 / < -0.29$ for 40 Gy). Significant proteome changes in response to IR were selected, if significant by one-way ANOVA ($P<0.05$) and fold cutoff ($1.5 \times$ S.D.). Alternatively, significance analysis was performed using two-tailed Student's *t*-test ($P<0.05$). Similar profiles of the fold changes over time were identified by clustering analysis using the Self Organizing Tree Algorithm[51] and default parameters of MeV version 4.6.[49]

Pathway and network analysis. Gene pathway membership data were obtained from protein interaction database, PID[52] and KEGG.[53] A total of 200 and 211 pathways were obtained from PID and KEGG, respectively. For statistical analysis, all analyzed proteins in this study (unique IDs) were set as the background list and all pathways consisting of more than five proteins from the background list were considered for statistical analysis by Fisher's exact test, resulting in a total of 93 pathways from PID and 63 from KEGG. Fisher's exact test was performed to identify pathways significantly affected by proteins (modifications) altered in response to irradiation (significant by ANOVA and fold change) using the R statistical framework.[54] To account for multiple testing, *P*-values were corrected for false discovery rates (FDRs) using Benjamini–Hochberg correction. We have used an FDR-corrected *P*-value cutoff of 0.1 to identify pathways significantly affected by proteome changes.

Significant proteome changes, identified by statistical (ANOVA) and fold-change analysis (log 2 cutoff) were subjected to protein–protein interaction analysis using STRING (v. 9.0, http://www.string-db.org/).[55] Only interactions with a STRING score of 0.7 and above were further analyzed using Cytoscape (http://www.cytoscape.org/).[56]

Immunoblotting. For western blot analysis, proteins were separated by SDS-PAGE gel electrophoresis and bands were visualized by using either horseradish peroxidase-conjugated antibodies (1 : 5000; GE Healthcare, Life Sciences, Uppsala, Sweden) and ECL detection (GE Healthcare) or IR-dye-conjugated antibodies (1 : 15 000; LI-COR Biosciences) and detection by the Odyssey infrared imaging system (LI-COR Biosciences, Lincoln, NE, USA). For quantification, bands were analyzed by ImageJ 1.46 (ref. 57) and the Odyssey imaging software (LI-COR Biosciences).

Antibodies used for western blotting were anti-ATM (GeneTex, Irvine, CA, USA), anti-ATM Phospho (pS1981) (Epitomics-an Abcam Company, Burlingame, CA, USA), anti-Bad (CST), anti-Bad Phospho (pS136) (Cell Signaling Technology (CST), Danvers, MA, USA), anti-Chk1 (CST), anti-Chk1 Phospho (pS345) (1 : 500; CST), anti-Chk2 Phospho (pT68) (CST), anti-CREB (CST), anti-CREB Phospho (pS133)/anti-ATF-1 (phospho) (CST), anti-histone H2A.X Phospho (pS139) (Millipore, Billerica, MA, USA), anti-Hsp27 (CST), anti-Hsp27 Phospho (pS78) (1 : 500; CST), anti-PARP1 (Santa Cruz Biotechnology), anti-PARP1 cleaved (1 : 500; CST), anti-p16 (1 : 500; Santa Cruz Biotechnology), anti-p21 (Santa Cruz Biotechnology), anti-p38 (CST), anti-p38 Phospho (pThr180/Tyr182), anti-p44/42 Erk1/2 (CST), anti-p44/42 Erk1/2 Phospho (pThr202/Tyr204) (CST), anti-p53 (Santa Cruz Biotechnology), anti-Rb (1 : 500; Epitomics), anti-Rb (pS780) (CST), anti-tubulin (1 : 10 000; Sigma-Aldrich, St Louis, MO, USA), anti-PKCβII Phospho (pT641) (CST), anti-PKCδ (CST), anti-PKCζ/λ (CST) and anti-PKCζ/λ Phospho (pT410/pT403) (CST). Unless otherwise stated, antibody dilution was 1 : 1000.

Immunofluorescence microscopy. MRC-5 cells grown on cover slips over night ($\approx 1 \times 10^4$ cells) were irradiated and immunohistochemically stained with primary (1 : 500 mouse anti-histone H2A.X Phospho (S139) immunoglobulin G1 (IgG1) (Millipore) or 1 : 500 rabbit anti-53BP1 IgG1 (Santa Cruz Biotechnology)) and secondary antibodies (1 : 250 FITC- or cyanine 3-conjugated IgG anti-mouse IgG (Jackson ImmunoResearch Laboratories, West Grove, PA, USA) or 1 : 250 Alexa Fluor 488-conjugated anti-rabbit IgG (Invitrogen)).

Flow cytometry. Cell cycle analysis of IR-treated or -untreated MRC-5 cells was performed using standard ethanol fixation/PI-staining protocol and flow cytometry analysis (FACS) with a Dako CyAn ADP flow cytometer (Dako, North America, Carpinteria, CA, USA). For sub-G1 peak analysis of IMR-90, cell debris and necrotic cells were gated out according to the protocol of Riccardi and Nicoletti.[58] Annexin V staining was performed using the FITC Annexin V apoptosis detection kit (BD Biosciences, San Jose, CA, USA) and a Dako CyAn ADP flow cytometer (Dako).

RNA extraction and real-time PCR analysis. Total RNA was reverse transcribed using High-Capacity cDNA Reverse Transcription kit (Applied Biosystems; Life Technologies). Real-time PCR was performed using SYBR green premixed buffer and analyzed by the Rotor-Gene Q cycler (Qiagen, Hilden, Germany).

Conflict of Interest

JT was Zeptosens Technology Manager at Bayer Technology Services GmbH and is currently Group Head for Process Analytical Technologies at the same company. JvO was Head of Business Development at Zeptosens, a division of Bayer (Schweiz) AG. All the other authors declare no conflict of interest.

Acknowledgements. F Freimoser (University of Zurich) provided editorial assistance and critical input during the writing. We thank M Ehrat, G Balciunaite and J Grognux for technical assistance with protein arrays. This work was supported in part by the Kanton of Zurich (to MOH), Oncosuisse (KLS 02396-02-2009) and the UBS foundation.

Author contributions

AB, NK, JT and MOH designed the experiments; AB, NK and KM performed and analyzed the experiments; and JvO, HR, MB and MOH supervised the study. All authors contributed to the preparation of the manuscript.

1. Harper JW, Elledge SJ. The DNA damage response: ten years after. *Mol Cell* 2007; **28**: 739–745.
2. Shiloh Y. ATM and related protein kinases: safeguarding genome integrity. *Nate Rev Cancer* 2003; **3**: 155–168.
3. Bonner WM, Redon CE, Dickey JS, Nakamura AJ, Sedelnikova OA, Solier S *et al.* GammaH2AX and cancer. *Nat Rev Cancer* 2008; **8**: 957–967.
4. Surova O, Zhivotovsky B. Various modes of cell death induced by DNA damage. *Oncogene* 2012; E-pub ahead of print; doi: 10.1038/onc.2012.556.
5. Roos WP, Kaina B. DNA damage-induced cell death by apoptosis. *Trends Mol Med* 2006; **12**: 440–450.
6. Sabin RJ, Anderson RM. Cellular senescence – its role in cancer and the response to ionizing radiation. *Genome Integr* 2011; **2**: 7.
7. Bennetzen M, Larsen D, Bunkenborg J, Bartek J, Lukas J, Andersen J. Site-specific phosphorylation dynamics of the nuclear proteome during the DNA damage response. *Mol Cell Proteomics* 2010; **9**: 1314–1323.
8. Bensimon A, Schmidt A, Ziv Y, Elkon R, Wang SY, Chen DJ *et al.* ATM-dependent and -independent dynamics of the nuclear phosphoproteome after DNA damage. *Sci Signal* 2010; **3**: rs3.
9. Beli P, Lukashchuk N, Wagner SA, Weinert BT, Olsen JV, Baskcomb L *et al.* Proteomic investigations reveal a role for RNA processing factor THRAP3 in the dna damage response. *Mol Cell* 2012; **46**: 212–225.
10. Lee MJ, Ye AS, Gardino AK, Heijink AM, Sorger PK, MacBeath G *et al.* Sequential application of anticancer drugs enhances cell death by rewiring apoptotic signaling networks. *Cell* 2012; **149**: 780–794.
11. Tentner AR, Lee MJ, Ostheimer GJ, Samson LD, Lauffenburger DA, Yaffe MB. Combined experimental and computational analysis of DNA damage signaling reveals context-dependent roles for Erk in apoptosis and G1/S arrest after genotoxic stress. *Mol Syst Biol* 2012; **8**: 568.
12. van Oostrum J, Voshol H. Antibody-based proteomics to study cellular signalling networks. *Eur Pharmaceut Rev* 2008; **2**: 31–35.
13. Paweletz CP, Charboneau L, Bichsel VE, Simone NL, Chen T, Gillespie JW *et al.* Reverse phase protein microarrays which capture disease progression show activation of pro-survival pathways at the cancer invasion front. *Oncogene* 2001; **20**: 1981–1989.
14. Nishizuka S, Ramalingam S, Spurrier B, Washburn FL, Krishna R, Honkanen P *et al.* Quantitative protein network monitoring in response to DNA damage. *J Proteome Res* 2008; **7**: 803–808.
15. Hudson ME, Pozdnyakova I, Haines K, Mor G, Snyder M. Identification of differentially expressed proteins in ovarian cancer using high-density protein microarrays. *Proc Natl Acad Sci USA* 2007; **104**: 17494–17499.
16. Kuhne M, Riballo E, Rief N, Rothkamm K, Jeggo PA, Lobrich M. A double-strand break repair defect in ATM-deficient cells contributes to radiosensitivity. *Cancer Res* 2004; **64**: 500–508.
17. Lobrich M, Shibata A, Beucher A, Fisher A, Ensminger M, Goodarzi AA *et al.* gammaH2AX foci analysis for monitoring DNA double-strand break repair: strengths, limitations and optimization. *Cell Cycle* 2010; **9**: 662–669.
18. Yoshida K. Role for PKCδ on apoptosis in the DNA damage response. In: Chen CC (eds). *Selected Tpics in DNA Repair*. InTech: San Diego, USA, 2011. pp 293–304.
19. Newton AC. Protein kinase C: poised to signal. *Am J Physiol Endocrinol Metab* 2010; **298**: E395–E402.
20. Jackson DN, Foster DA. The enigmatic protein kinase Cdelta: complex roles in cell proliferation and survival. *FASEB J* 2004; **18**: 627–636.
21. Kosar M, Bartkova J, Hubackova S, Hodny Z, Lukas J, Bartek J. Senescence-associated heterochromatin foci are dispensable for cellular senescence, occur in a cell type- and insult-dependent manner and follow expression of p16(ink4a). *Cell Cycle* 2011; **10**: 457–468.
22. Cosentino C, Grieco D, Costanzo V. ATM activates the pentose phosphate pathway promoting anti-oxidant defence and DNA repair. *EMBO J* 2011; **30**: 546–555.
23. Meek DW. Tumour suppression by p53: a role for the DNA damage response? *Nat Rev Cancer* 2009; **9**: 714–723.
24. Lavin MF, Gueven N. The complexity of p53 stabilization and activation. *Cell Death Differ* 2006; **13**: 941–950.
25. Parekh DB, Ziegler W, Parker PJ. Multiple pathways control protein kinase C phosphorylation. *EMBO J* 2000; **19**: 496–503.
26. Lonze BE, Riccio A, Cohen S, Ginty DD. Apoptosis, axonal growth defects, and degeneration of peripheral neurons in mice lacking CREB. *Neuron* 2002; **34**: 371–385.
27. Datta SR, Dudek H, Tao X, Masters S, Fu H, Gotoh Y *et al.* Akt phosphorylation of BAD couples survival signals to the cell-intrinsic death machinery. *Cell* 1997; **91**: 231–241.
28. Adams JM, Cory S. The Bcl-2 apoptotic switch in cancer development and therapy. *Oncogene* 2007; **26**: 1324–1337.
29. Vogler M, Dinsdale D, Dyer MJ, Cohen GM. Bcl-2 inhibitors: small molecules with a big impact on cancer therapy. *Cell Death Differ* 2009; **16**: 360–367.
30. Lawless C, Wang C, Jurk D, Merz A, Zglinicki T, Passos JF. Quantitative assessment of markers for cell senescence. *Exp Gerontol* 2010; **45**: 772–778.
31. Torudd J, Protopopova M, Sarimov R, Nygren J, Eriksson S, Markova E *et al.* Dose–response for radiation-induced apoptosis, residual 53BP1 foci and DNA-loop relaxation in human lymphocytes. *Int J Radiat Biol* 2005; **81**: 125–138.
32. Meyn RE, Munshi A, Haymach JV, Milas L, Ang KK. Receptor signaling as a regulatory mechanism of DNA repair. *Radiother Oncol* 2009; **92**: 316–322.
33. Bulavin DV, Higashimoto Y, Popoff IJ, Gaarde WA, Basrur V, Potapova O *et al.* Initiation of a G2/M checkpoint after ultraviolet radiation requires p38 kinase. *Nature* 2001; **411**: 102–107.
34. Manke IA, Nguyen A, Lim D, Stewart MQ, Elia AE, Yaffe MB. MAPKAP kinase-2 is a cell cycle checkpoint kinase that regulates the G2/M transition and S phase progression in response to UV irradiation. *Mol Cell* 2005; **17**: 37–48.
35. Martelli AM, Evangelisti C, Nyakern M, Manzoli FA. Nuclear protein kinase C. *Biochim Biophys Acta* 2006; **1761**: 542–551.
36. Xue Y, Ren J, Gao X, Jin C, Wen L, Yao X. GPS 2.0, a tool to predict kinase-specific phosphorylation sites in hierarchy. *Mol Cell Proteomics* 2008; **7**: 1598–1608.
37. Yoshida K. Protein kinase C, p53, and DNA damage. In: Kazanietz MG (eds). *Protein Kinase C in Cancer Signaling and Therapy*. Springer: Berlin, 2010. pp 253–265.
38. Yoshida K, Miki Y, Kufe D. Activation of SAPK/JNK signaling by protein kinase Cdelta in response to DNA damage. *J Biol Chem* 2002; **277**: 48372–48378.
39. Basu A, Pal D. Two faces of protein kinase Cdelta: the contrasting roles of PKCdelta in cell survival and cell death. *Scientific World J* 2010; **10**: 2272–2284.
40. Schmidt-Ullrich RK, Dent P, Grant S, Mikkelsen RB, Valerie K. Signal transduction and cellular radiation responses. *Radiat Res* 2000; **153**: 245–257.
41. Baskar R, Balajee AS, Geard CR, Hande MP. Isoform-specific activation of protein kinase c in irradiated human fibroblasts and their bystander cells. *Int J Biochem Cell Biol* 2008; **40**: 125–134.
42. Jacobs JP, Jones CM, Baille JP. Characteristics of a human diploid cell designated MRC-5. *Nature* 1970; **227**: 168–170.
43. Nichols WW, Murphy DG, Cristofalo VJ, Toji LH, Greene AE, Dwight SA. Characterization of a new human diploid cell strain, IMR-90. *Science* 1977; **196**: 60–63.
44. Franken NA, Rodermond HM, Stap J, Haveman J, van Bree C. Clonogenic assay of cells *in vitro*. *Nat Protoc* 2006; **1**: 2315–2319.
45. Dimri GP, Lee X, Basile G, Acosta M, Scott G, Roskelley C *et al.* A biomarker that identifies senescent human cells in culture and in aging skin *in vivo*. *Proc Natl Acad Sci USA* 1995; **92**: 9363–9367.
46. Pawlak M, Schick E, Bopp MA, Schneider MJ, Oroszlan P, Ehrat M. Zeptosens' protein microarrays: a novel high performance microarray platform for low abundance protein analysis. *Proteomics* 2002; **2**: 383–393.
47. Voshol H, Ehrat M, Traenkle J, Bertrand E, van Oostrum J. Antibody-based proteomics: analysis of signaling networks using reverse protein arrays. *FEBS J* 2009; **276**: 6871–6879.
48. Bevington PR. *Data Reduction and Error Analysis for the Physical Sciences*. 3rd edn McGraw-Hill: New York, NY, 2002. p 352.
49. Saeed AI, Sharov V, White J, Li J, Liang W, Bhagabati N *et al.* TM4: a free, open-source system for microarray data management and analysis. *Biotechniques* 2003; **34**: 374–378.
50. Zar JH. *Biostatistical Analysis*. 5th edn Prentice-Hall: Upper Saddle River, NJ, 2009. p 960.
51. Herrero-Yraola A, Bakhit SM, Franke P, Weise C, Schweiger M, Jorcke D *et al.* Regulation of glutamate dehydrogenase by reversible ADP-ribosylation in mitochondria. *EMBO J* 2001; **20**: 2404–2412.
52. Schaefer CF, Anthony K, Krupa S, Buchoff J, Day M, Hannay T *et al.* PID: the Pathway Interaction Database. *Nucleic Acids Res* 2009; **37**: D674–D679.
53. Kanehisa M, Goto S, Furumichi M, Tanabe M, Hirakawa M. KEGG for representation and analysis of molecular networks involving diseases and drugs. *Nucleic Acids Res* 2010; **38**: D355–D360.
54. Ihaka R, Genleman RR. A language for data analysis and graphics. *J Comput Graph Stat* 1996; **5**: 299–314.
55. Szklarczyk D, Franceschini A, Kuhn M, Simonovic M, Roth A, Minguez P *et al.* The STRING database in 2011: functional interaction networks of proteins, globally integrated and scored. *Nucleic Acids Res* 2011; **39**: D561–D568.
56. Shannon P, Markiel A, Ozier O, Baliga NS, Wang JT, Ramage D *et al.* Cytoscape: a software environment for integrated models of biomolecular interaction networks. *Genome Res* 2003; **13**: 2498–2504.
57. Schneider CA, Rasband WS, Eliceiri KW. NIH Image to ImageJ: 25 years of image analysis. *Nat Methods* 2012; **9**: 671–675.
58. Riccardi C, Nicoletti I. Analysis of apoptosis by propidium iodide staining and flow cytometry. *Nat Protoc* 2006; **1**: 1458–1461.

Supplementary Information accompanies the paper on Cell Death and Disease website (http://www.nature.com/cddis)

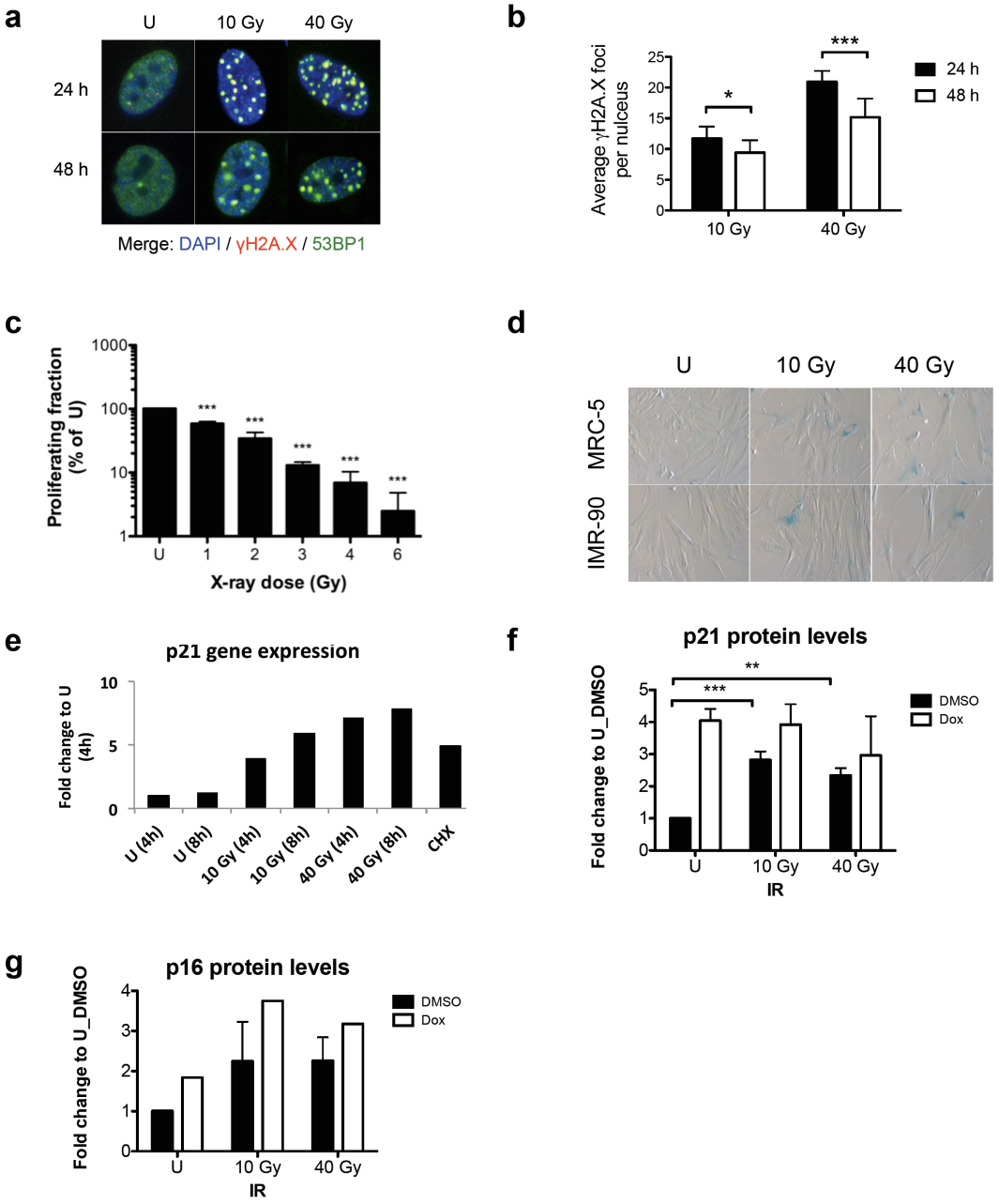

Figure S1. Irradiation increases senescence in response to 10 Gy or 40 Gy X-rays in NHFs. (a) Immunofluorescence staining of irradiated MRC-5 cells and of untreated control cells after 24 h and 48 h of recovery. Repair efficiency was determined using double staining with anti-γH2AX (Cy3) and 53BP1 (Alexa Fluor 488), which are recruited to particular foci (co-localization), marking sites of DNA double strand breaks. **(b)** Quantification of (a). The average number of γH2AX foci per cell was quantified with the spot detection function of Imaris (Bitplane) and identical image acquisition and foci detection parameters (n > 100 cell nuclei quantified per condition, n=5). **(c)** Colony forming assay of MRC-5 cells irradiated with X-ray doses of 1-6 Gy or left untreated (U) and recovered for 10 days (n=3). **(d)** SA-β-Gal staining of irradiated MRC-5 or IMR-90 after 72 h IR recovery with untreated (U) as control. **(e)** Gene expression analysis of senescence marker (p21) in MRC-5 in response to irradiation following 4-8 h IR recovery or cyclohexamide (CHX, 200 µM for 16 h). Quantification of WB analysis in IMR-90 of p21 **(f)** and p16 **(g)** protein level changes upon IR following 48 h recovery. Doxorubicin (0.5 µg/ml, 48 h) was used as positive control for induction of DNA damage (n=2-3). Statistical analysis was performed by Student's t-test, * p<0.05, ** p<0.01, *** p<0.001.

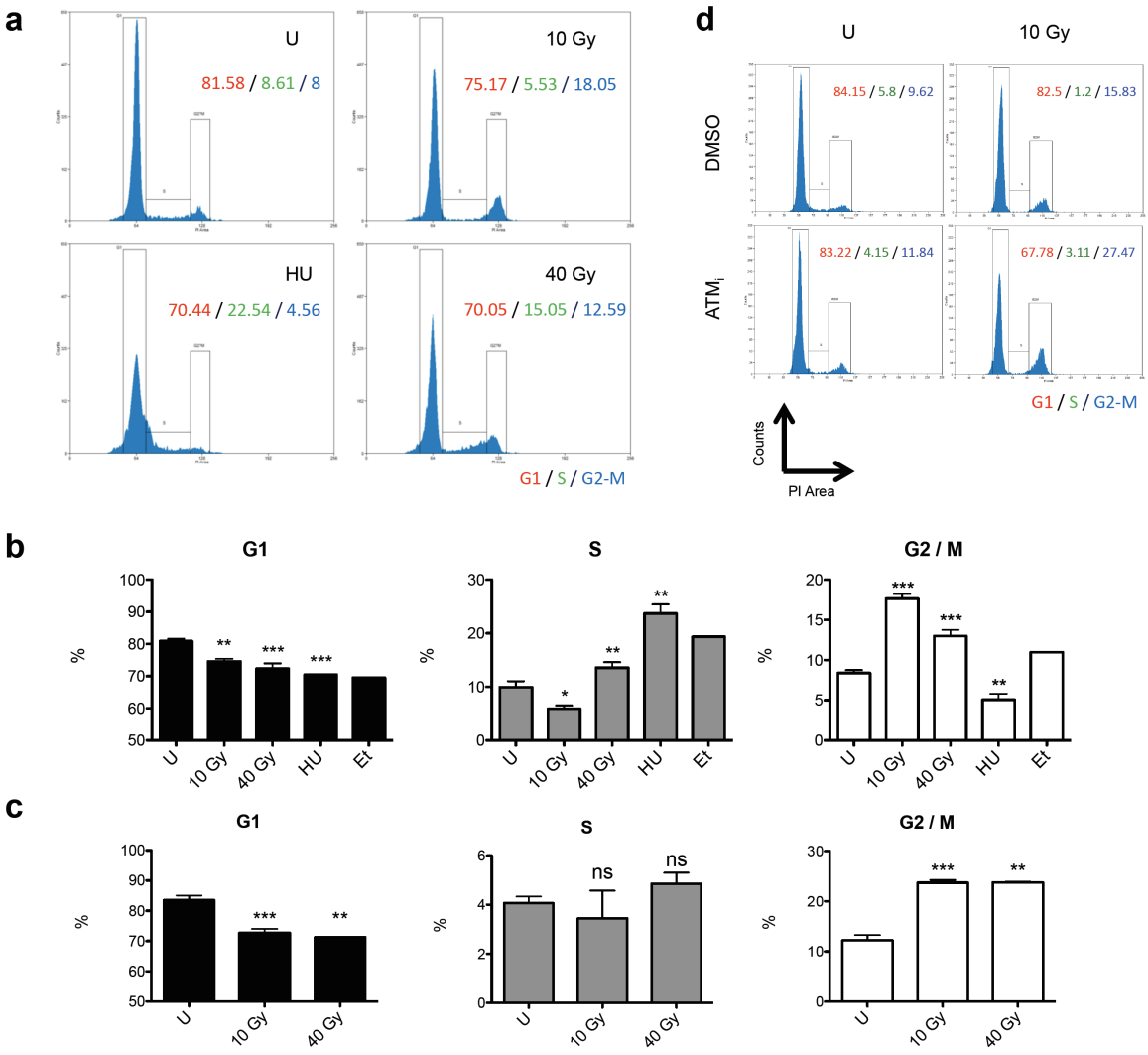

Figure S2. Irradiation increases the the G2/M cell cycle population 24-48 h after IR recovery in NHFs (a) Cell cycle analysis of irradiated MRC-5 by FACS analysis 24 h after irradiation (representative). To induce early S-phase arrest 2 mM hydroxyurea (HU) were incubated for 24 h prior to FACS analysis. **(b)** Quantification of cell cycle population changes in either G1, S or G2 / M 24 h after IR recovery or treatment with either hydroxyurea (2 mM) or etoposide (50 µM) (n=2-4). **(c)** Quantification of cell cycle population changes in either G1, S or G2 / M 48 h after IR recovery or treatment with either hydroxyurea (2 mM) or etoposide (50 µM) (n=2-4). **(d)** ATM-dependent cell cycle analysis in MRC-5. Cells were pretreated for 2h with ATM-specific inhibitor (KU-55933, 10 µM) prior to IR and FACS analysis 24 h after irradiation. Statistical analysis was performed by Student's t-test, * p<0.05, ** p<0.01, *** p<0.001.

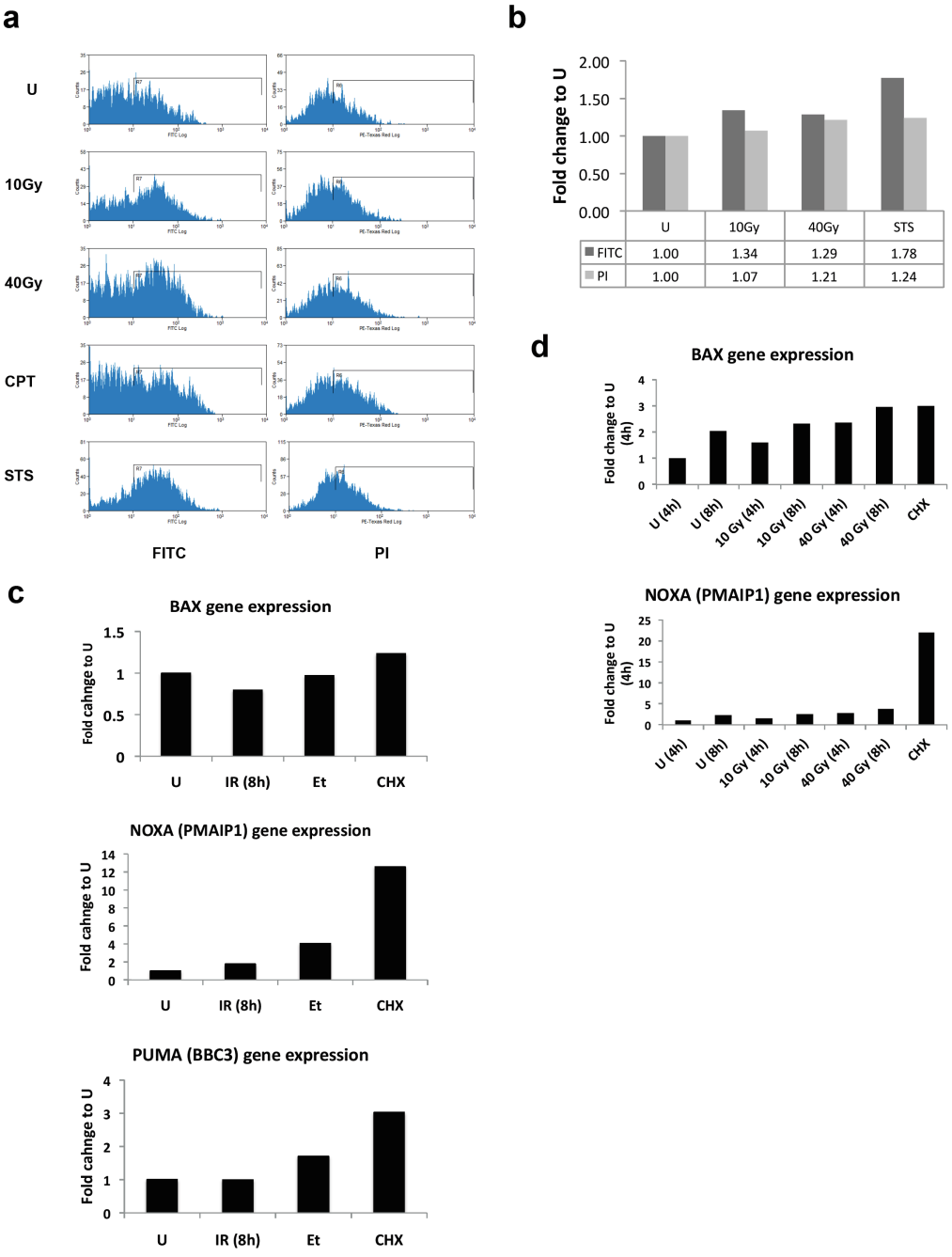

Figure S3. Irradiation does not induce early apoptosis in response to 10 Gy or 40 Gy X-rays in MRC-5. (a) Annexin V staining of MRC-5 irradiated (recovered for 8 h) or treated with camptothecin (CPT, 4 μM for 8 h) or staurosporin (STS, 1 μM, 2 h), prior to Annexin V staining and FACS analysis. **(b)** Quantification of Annexin V positive population (FITC) corresponding to early apoptosis and propidium iodide positive population (PI) corresponding to necrosis from (a). **(c)** Gene expression analysis of pro-apoptotic genes in response to irradiation (10 Gy, 8 h recovery), etoposide (Et, 50 μM for 8 h) or cyclohexamide (CHX, 200 μM for 16 h) with untreated (U) as control. **(d)** Gene expression analysis of pro-apoptotic genes in response to irradiation (4-8 h recovery) or cyclohexamide (CHX, 200 μM for 16 h) with untreated as control.

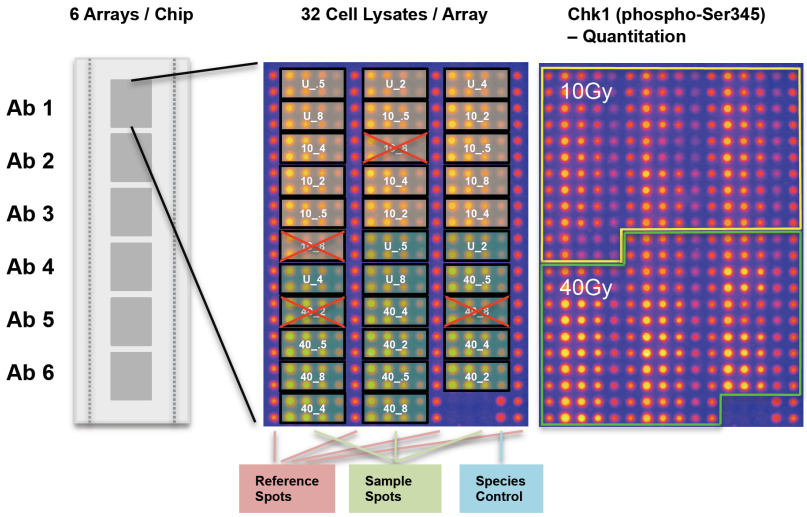

Figure S4. Arrangement of whole cell extracts on chips showing representative microarray image of Chk1 phosphorylation (pS345) in response to 10 Gy and 40 Gy. Equal amounts of whole cell extract were spotted on hydrophobic glass slides and replicated on 6 arrays on one chip. Each chip contains all samples (replicates of U, 10 Gy and 40 Gy), while each condition (e.g. U after 30 min = U_.5) is serially diluted (0.25, 0.5, 0.75 and 1) and spotted in technical duplicates (8 technical replicates in total). 10 Gy samples (highlighted in yellow) are spotted on position 1-16, 40 Gy samples (highlighted in green) are spotted on position 17-32. Samples placed on position 7 (10_8 # 1), position 16 (10_8 # 3), position 22 (40_2 # 1) and position 24 (40_8 # 1) were excluded from significance analysis due technical problems during serial dilution of the samples and subsequent spotting.

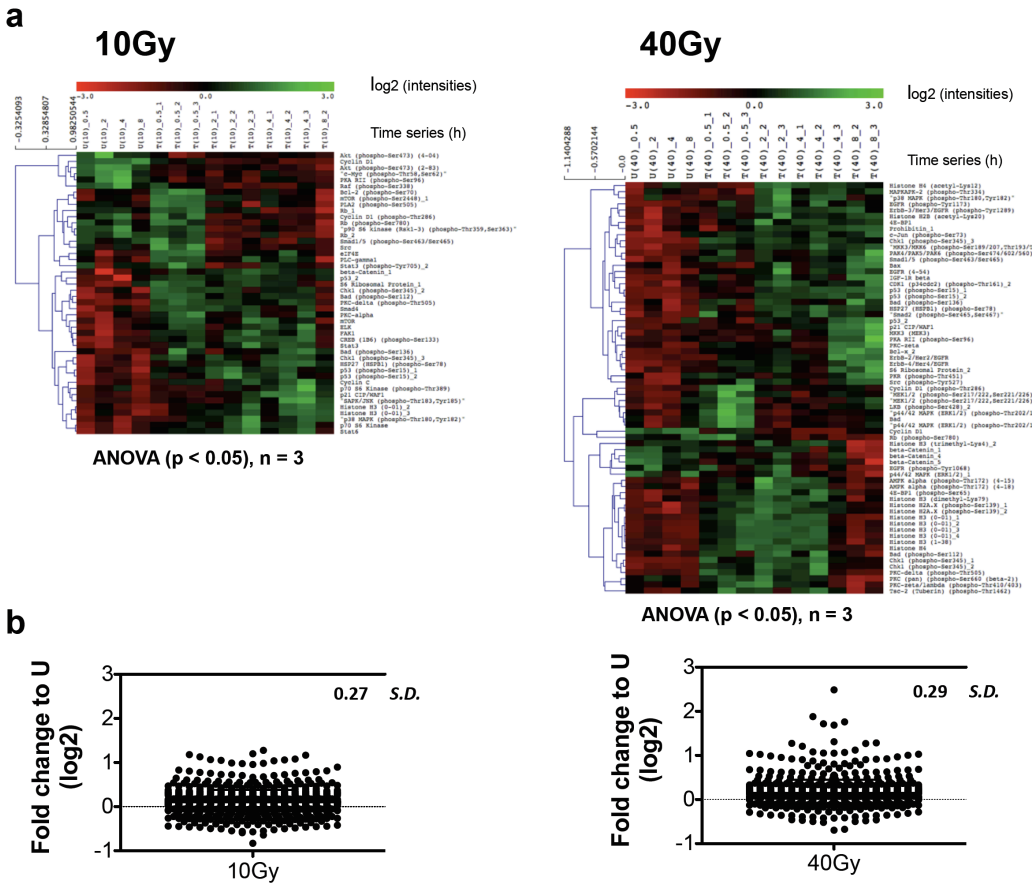

Figure S5. Significance analysis of IR-dependent proteome changes. (a) Relative fluorescence intensities (RFIs) (log2) for group 1 (untreated (U)_0.5 h, 2 h, 4 h, and 8 h), group 2 (biological triplicates of 10, T(10) or 40 Gy, T(40)_0.5 h), group 3 (biological triplicates of 10, T(10) or 40 Gy, T(40)_2 h), group 4 (biological triplicates of 10, T(10) or 40 Gy, T(40)_4 h) and group 5 (biological triplicates of 10, T(10) or 40 Gy, T(40)_8 h) were compared using F-statistics with $p < 0.05$. **(b)** Means of RFIs (replicates) were log2 transformed and fold changes (to U, group 1) were plotted individually for 10 and 40 Gy to determine the standard deviation, resulting in 0.27 S.D for 10 Gy and 0.29 for 40 Gy.

a

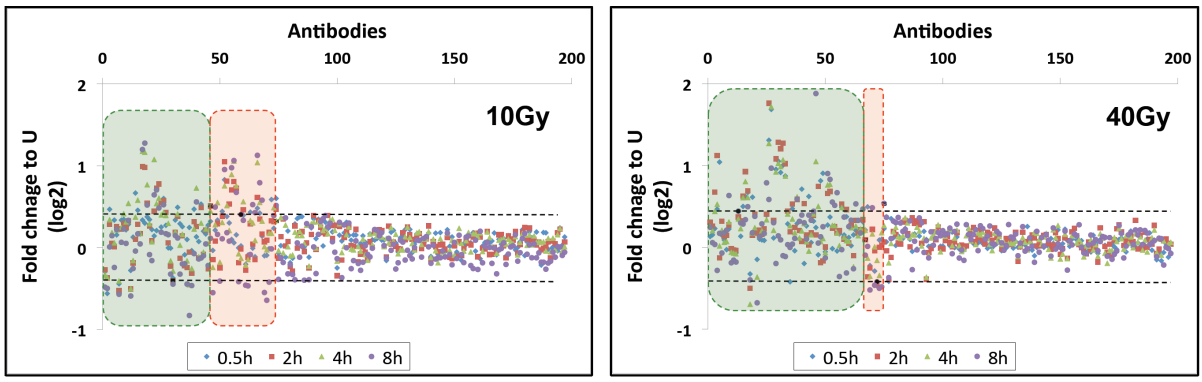

b

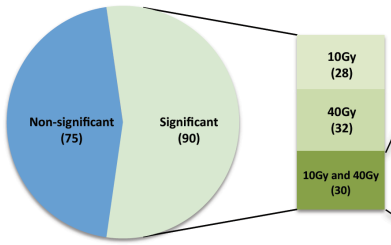

10 and 40Gy	
Canonical	**Non-canonical**
Chk1 (pS345)	Bad (pS112)
Cyclin D1	HSP27 (HSPB1) (pS78)
p21 CIP/WAF1	p38 MAPK (pT180,pTyr182)
p53	PKC-delta (pT505)
p53 (pS15)	PKA RII (p-Ser96)
…	…

Figure S6. Identification of significant proteome changes in response to X-rays. (a) Statistical and fold change analysis of significant proteome changes in response to IR using ANOVA ($p < 0.05$, $n = 3$) (green) and cut off (1.5 S.D.) (dashed line). Proteome changes, which only passed the strong cut off filter (1.5 S.D.), are highlighted in red. **(b)** Proportion of significant proteome changes, unique (ANOVA, $p < 0.05$, $n = 3$ or 1.5 cut off) in response to IR induced by 10 Gy only (light green), 40 Gy only (green) or unique for both doses (dark green). The table represents examples of canonical and non-canonical proteome changes significantly induced by 10 and 40 Gy.


Akt (phospho−Ser473) (2−83)
Akt (phospho−Ser473) (4−04)
Bad (phospho−Ser112)
Bad (phospho−Ser136)
Bcl−2 (phospho−Ser70)
beta−Catenin (phospho−Ser33,Ser37,Thr41)
beta−Catenin_1
beta−Catenin_3
beta−Catenin_4
beta−Catenin_5
c−Jun (phospho−Ser73)
c−Myc (phospho−Thr58,Ser62)
Caspase 9
Caspase 9 (cleaved−Asp330)
Chk1 (phospho−Ser345)_1
Chk1 (phospho−Ser345)_2
Chk1 (phospho−Ser345)_3
CREB (1B6) (phospho−Ser133)
Cyclin C
Cyclin D1
eIF4E
ELK
FAK1
Histone H2A.X (phospho−Ser139)_1
Histone H3 (0−01)_2
Histone H3 (0−01)_3
Histone H3 (0−01)_4
HSP27 (HSPB1) (phospho−Ser78)
IRS−1
mTOR
mTOR (phospho−Ser2448)_1
p21 CIP/WAF1
p38 MAPK (phospho−Thr180,Tyr182)
p53 (phospho−Ser15)_1
p90 S6 kinase (Rsk1−3) (phospho−Ser380)
p90 S6 kinase (Rsk1−3) (phospho−Thr359,Ser363)
p53 (phospho−Ser15)_2
p53_1
p53_2
p70 S6 Kinase
p70 S6 Kinase (phospho−Thr389)
PKA RII (phospho−Ser96)
PKC−alpha
PKC−delta (phospho−Thr505)
PLA2 (phospho−Ser505)
PLC−gamma1
PKC−alpha
PKC−delta (phospho−Thr505)

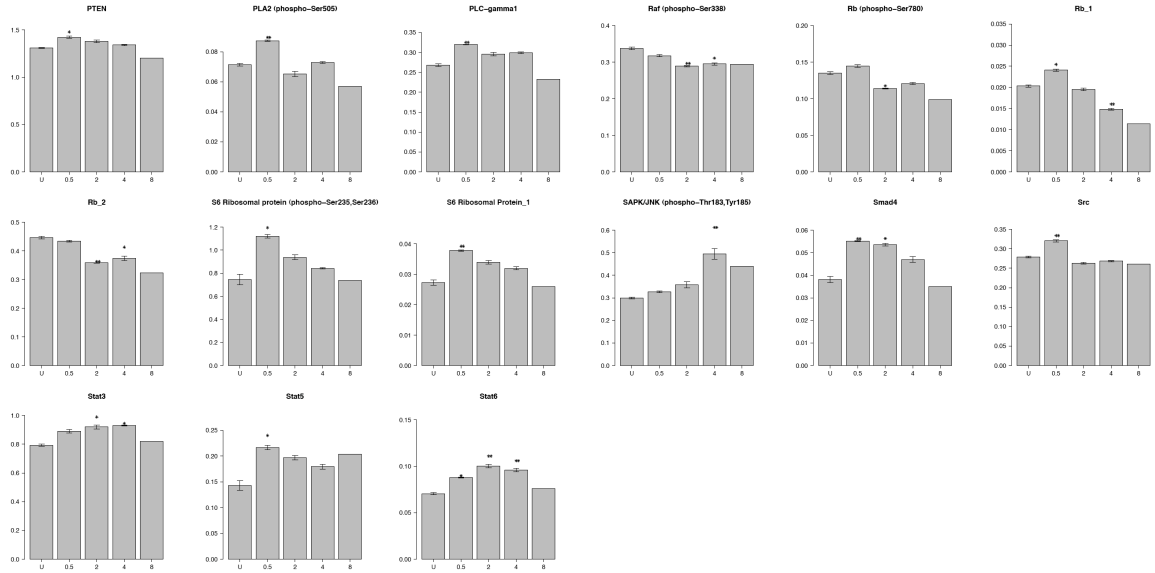

Figure S8. Significant proteome changes in response to 10Gy IR. Bar plots from Figure S7 (Student's t-test, n=3, * = p < 0.05; ** = p < 0.01; *** = p < 0.001).

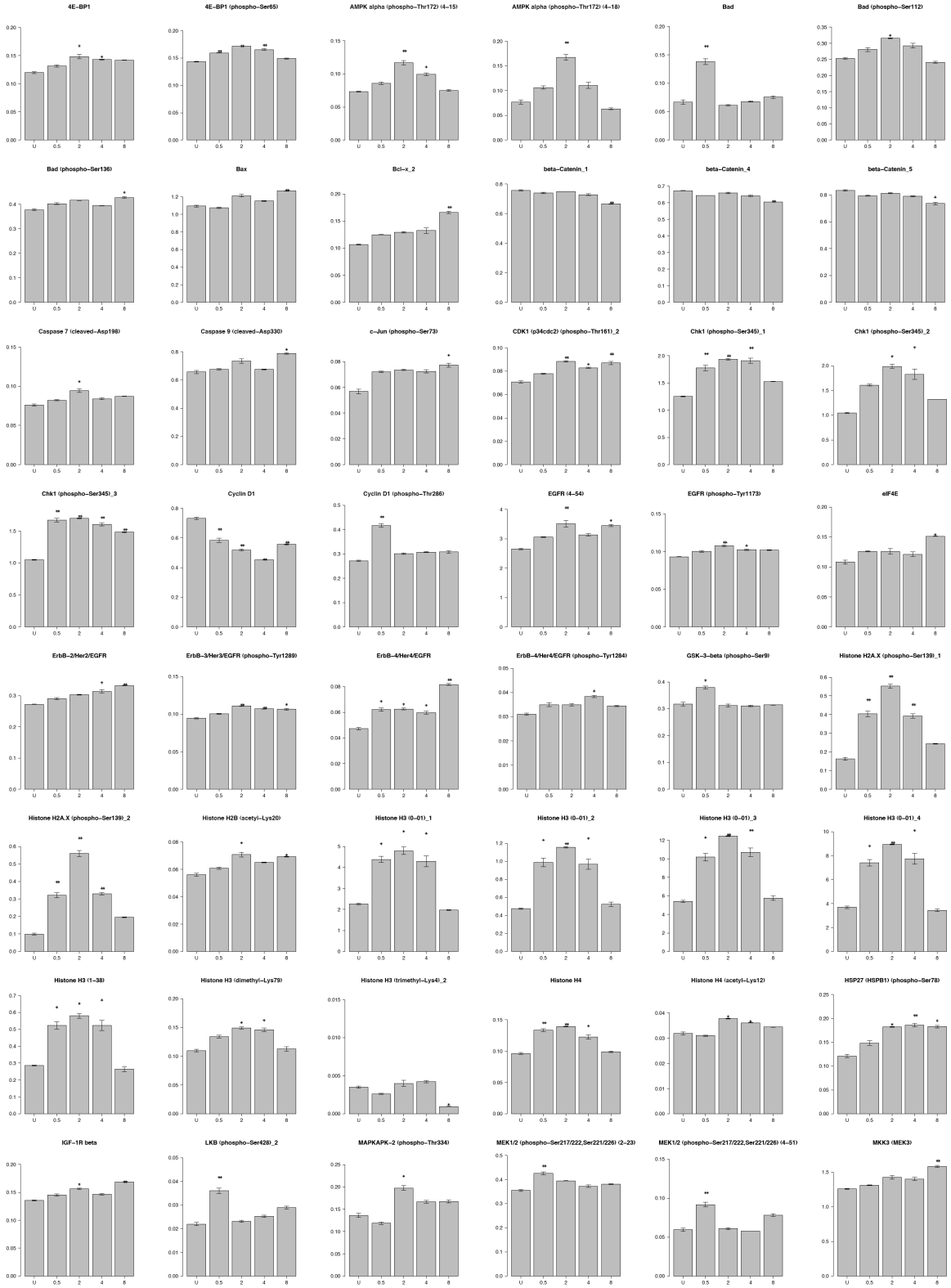
4E−BP1
4E−BP1 (phospho−Ser65)
AMPK alpha (phospho−Thr172) (4−15)
AMPK alpha (phospho−Thr172) (4−18)
Bad
Bad (phospho−Ser112)
Bad (phospho−Ser136)
Bax
Bcl−x_2
beta−Catenin_1
beta−Catenin_4
beta−Catenin_5
Caspase 7 (cleaved−Asp198)
Caspase 9 (cleaved−Asp330)
c−Jun (phospho−Ser73)
CDK1 (p34cdc2) (phospho−Thr161)_2
Chk1 (phospho−Ser345)_1
Chk1 (phospho−Ser345)_2
Chk1 (phospho−Ser345)_3
Cyclin D1
Cyclin D1 (phospho−Thr286)
EGFR (4−54)
EGFR (phospho−Tyr1173)
eIF4E
ErbB−2/Her2/EGFR
ErbB−3/Her3/EGFR (phospho−Tyr1289)
ErbB−4/Her4/EGFR
ErbB−4/Her4/EGFR (phospho−Tyr1284)
GSK−3−beta (phospho−Ser9)
Histone H2A.X (phospho−Ser139)_1
Histone H2A.X (phospho−Ser139)_2
Histone H2B (acetyl−Lys20)
Histone H3 (0−01)_1
Histone H3 (0−01)_2
Histone H3 (0−01)_3
Histone H3 (0−01)_4
Histone H3 (1−38)
Histone H3 (dimethyl−Lys79)
Histone H3 (trimethyl−Lys4)_2
Histone H4
Histone H4 (acetyl−Lys12)
HSP27 (HSPB1) (phospho−Ser78)
IGF−1R beta
LKB (phospho−Ser428)_2
MAPKAPK−2 (phospho−Thr334)
MEK1/2 (phospho−Ser217/222,Ser221/226) (2−23)
MEK1/2 (phospho−Ser217/222,Ser221/226) (4−51)
MKK3 (MEK3)

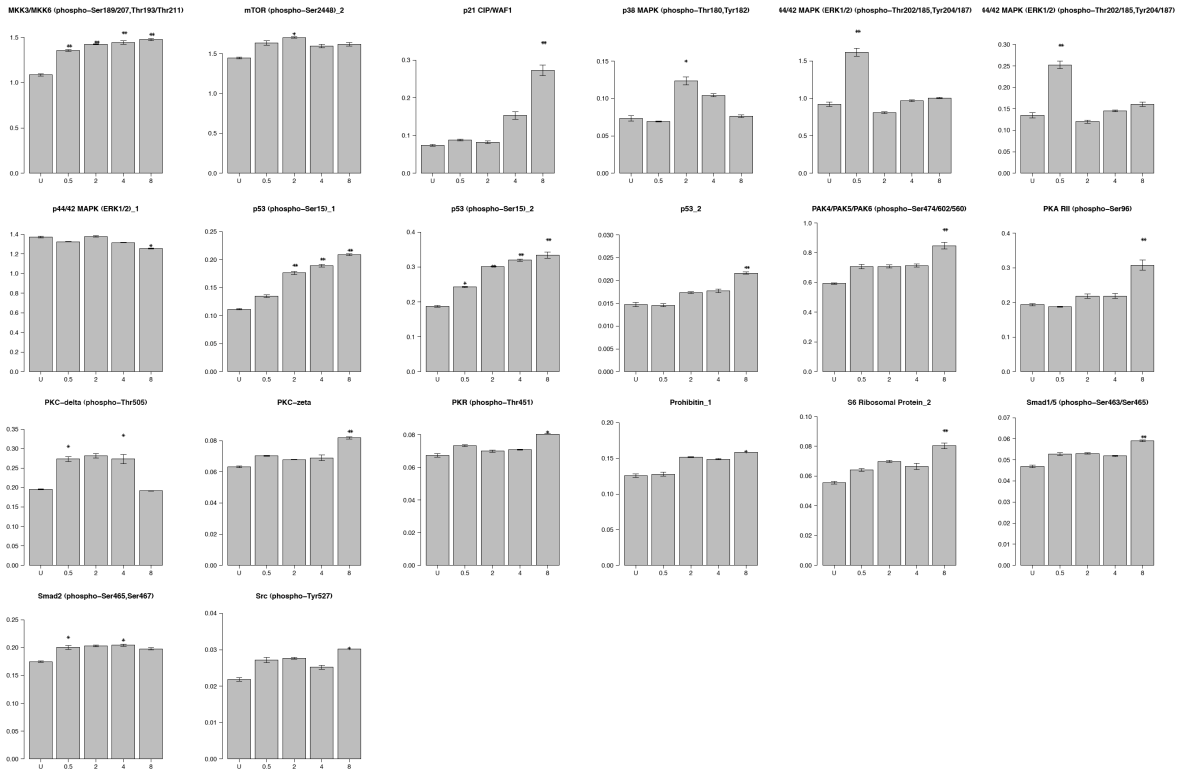

Figure S9. Significant proteome changes in response to 40Gy IR. Bar plots from Figure S7 (Student's t-test, n=3, * = p < 0.05; ** = p < 0.01; *** = p < 0.001).

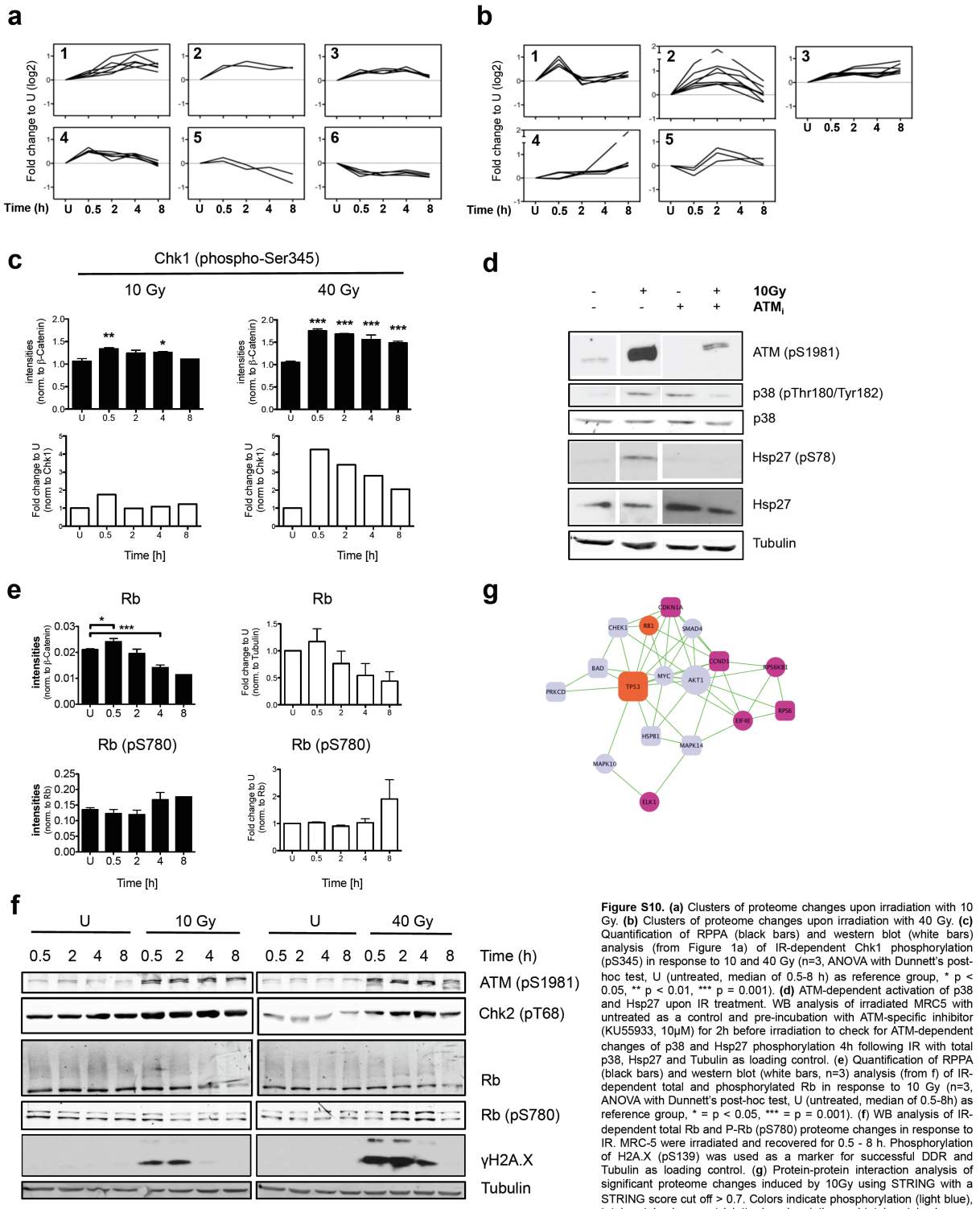

Figure S10. (a) Clusters of proteome changes upon irradiation with 10 Gy. **(b)** Clusters of proteome changes upon irradiation with 40 Gy. **(c)** Quantification of RPPA (black bars) and western blot (white bars) analysis (from Figure 1a) of IR-dependent Chk1 phosphorylation (pS345) in response to 10 and 40 Gy (n=3, ANOVA with Dunnett's post-hoc test, U (untreated, median of 0.5-8 h) as reference group, * $p < 0.05$, ** $p < 0.01$, *** $p = 0.001$). **(d)** ATM-dependent activation of p38 and Hsp27 upon IR treatment. WB analysis of irradiated MRC5 with untreated as a control and pre-incubation with ATM-specific inhibitor (KU55933, 10μM) for 2h before irradiation to check for ATM-dependent changes of p38 and Hsp27 phosphorylation 4h following IR with total p38, Hsp27 and Tubulin as loading control. (**e**) Quantification of RPPA (black bars) and western blot (white bars, n=3) analysis (from f) of IR-dependent total and phosphorylated Rb in response to 10 Gy (n=3, ANOVA with Dunnett's post-hoc test, U (untreated, median of 0.5-8h) as reference group, * = $p < 0.05$, *** = $p = 0.001$). (**f**) WB analysis of IR-dependent total Rb and P-Rb (pS780) proteome changes in response to IR. MRC-5 were irradiated and recovered for 0.5 - 8 h. Phosphorylation of H2A.X (pS139) was used as a marker for successful DDR and Tubulin as loading control. (**g**) Protein-protein interaction analysis of significant proteome changes induced by 10Gy using STRING with a STRING score cut off > 0.7. Colors indicate phosphorylation (light blue), total protein changes (violet), phosphorylation and total protein changes (orange). Circle represent unique changes and squares overlapping changes. Large symbols indicate proteins that interact with more than 14 members.

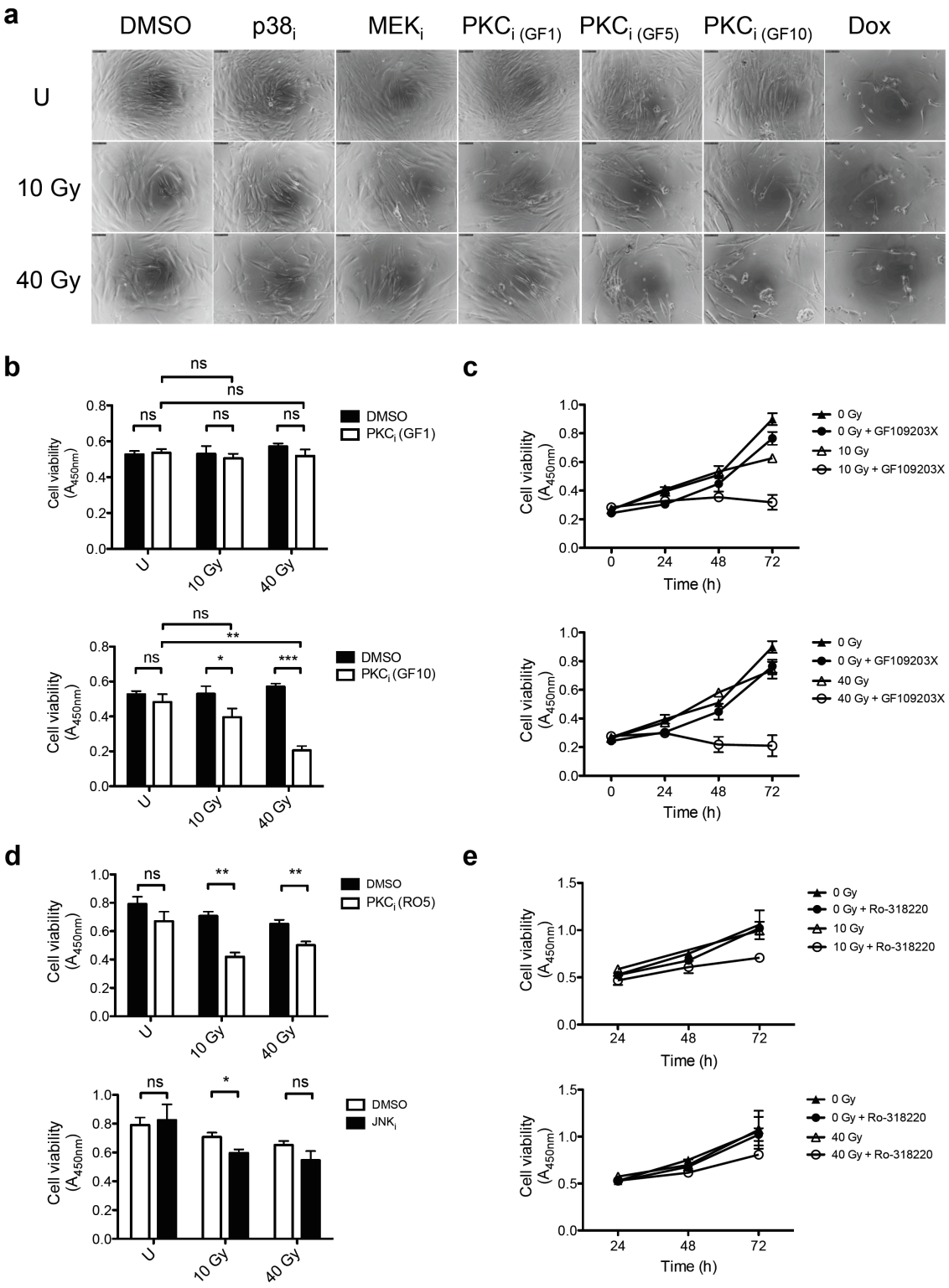

Figure S11. Radiosensitization of MRC-5 by pharmacological inhibition of PKC in response to IR. (a) PKC inhibition sensitizes MRC-5 to 10 and 40 Gy after 48 h. Phase contrast images of samples from (Figure 4), taken after 48 h recovery from IR. **(b)** Cell viability assay (WST-1) of MRC-5 (n=3) pretreated with PKC inhibitor (GF109203X, 1 or 10 μM) for 2 h before IR and recovery for the indicated time points (n=3). **(c)** Quantification of radiosensitization of MRC-5 by PKC inhibition (GF109203X, 10 μM) upon 10 and 40 Gy from (a). (**d)** Cell viability assay (WST-1) of MRC-5 (n=3) pretreated with PKC inhibitor (Ro-318220, 5 μM) or JNK inhibitor (SP600125, 10 μM) for 2 h before IR and recovery for the indicated time points (n=3). **(e)** Quantification of radiosensitization of MRC-5 by PKC inhibition (Ro-318220, 5 μM) upon 10 and 40 Gy from (d). Statistical analysis was performed by Student's t-test, * p<0.05, ** p<0.01, *** p<0.001, ns = not significant.

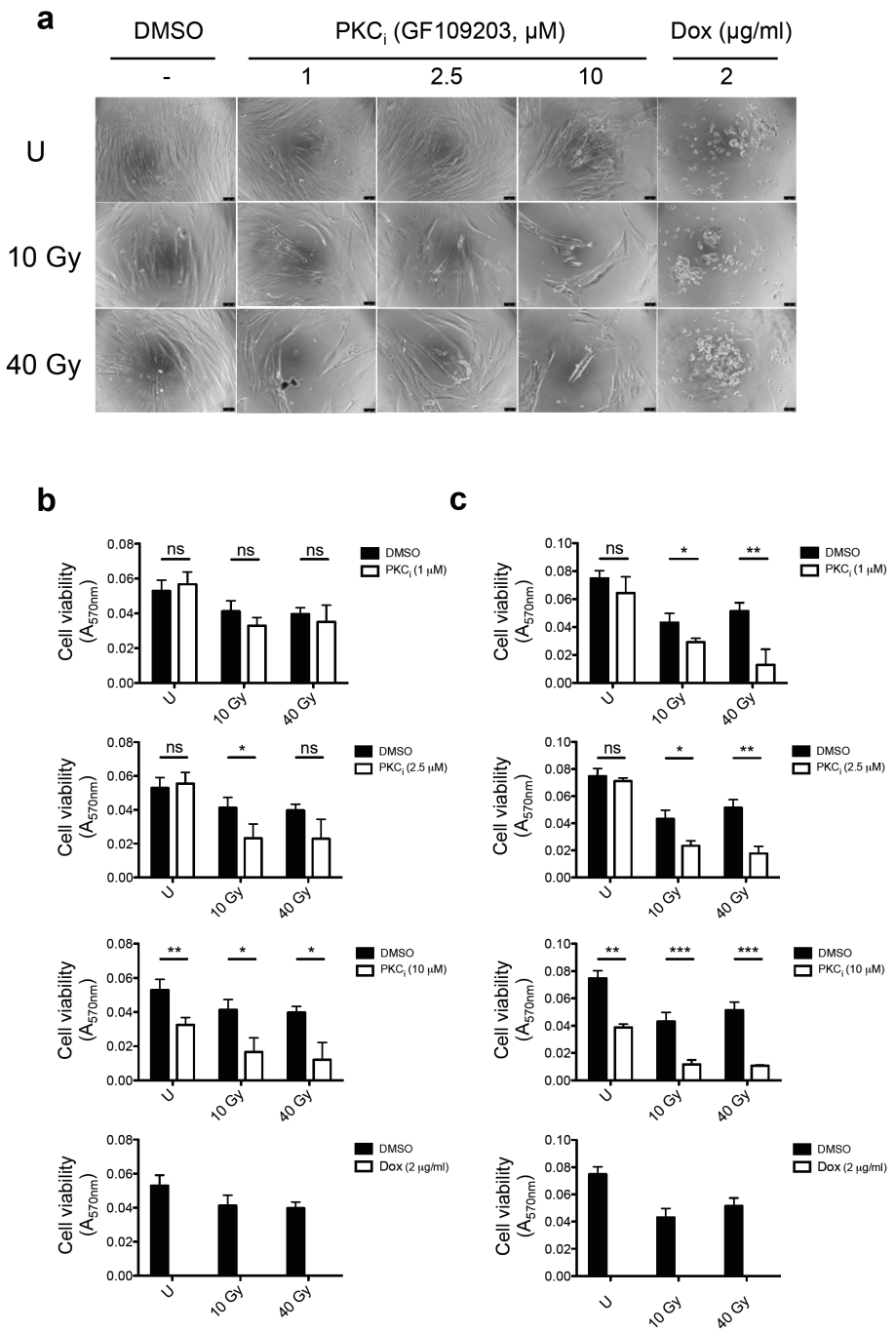

Figure S12. Radiosensitization of IMR-90 by pharmacological inhibition of PKC in response to IR. PKC inhibition sensitizes IMR-90 to 10 and 40 Gy after 48-72 h. **(a)** Phase contrast images of samples from (c), taken after 72 h recovery from IR. Cell viability assay (WST-1) of IMR-90 (n=3) pretreated with PKC inhibitor (GF109203X, 1, 2.5 and 10 μM) for 2 h before IR and recovery for 48 h **(b)** or 72 h **(c)** (n=3). Statistical analysis was performed by Student's t-test, * p<0.05, ** p<0.01, *** p<0.001), ns = not significant.

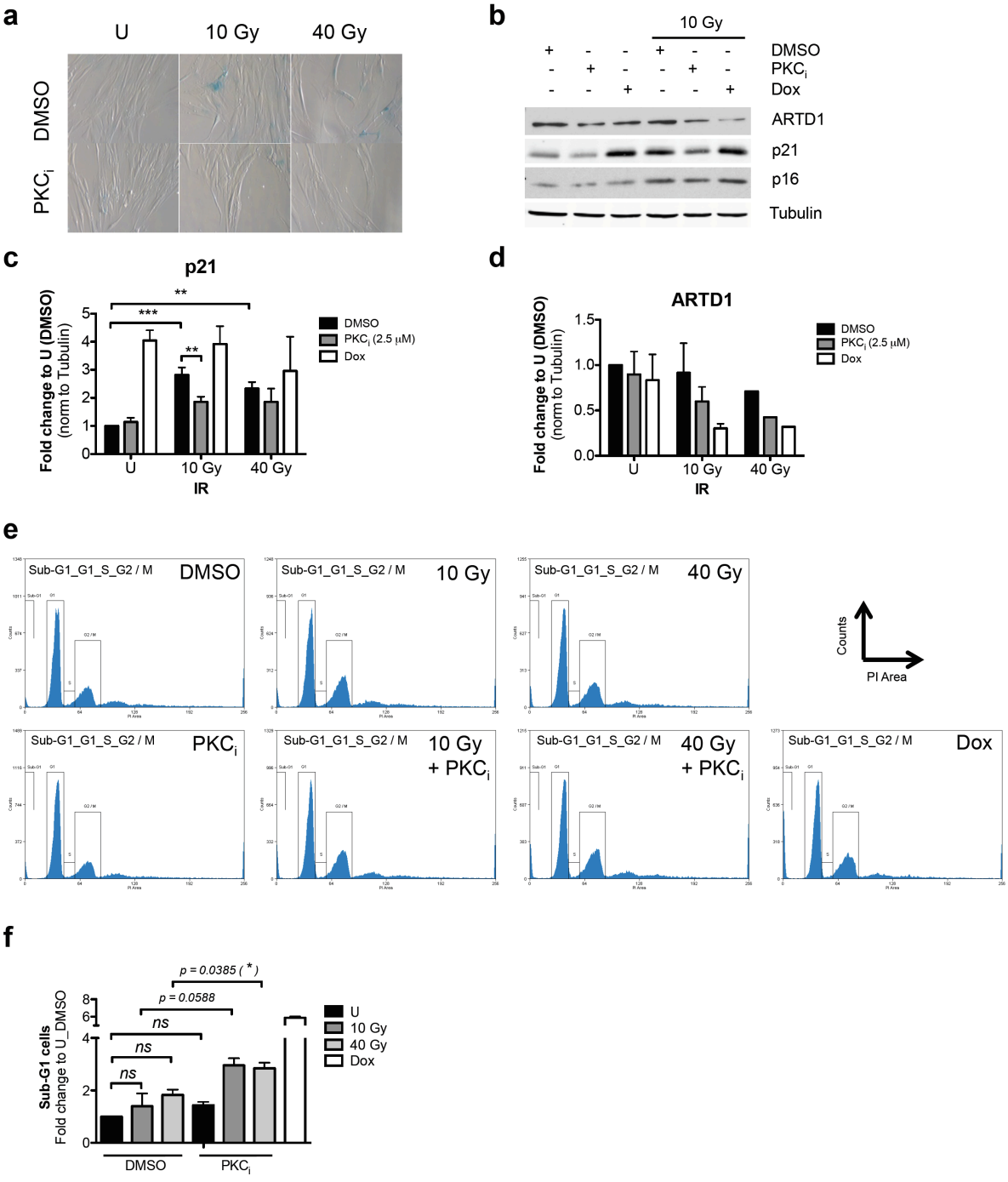

Figure S13. PKC inhibition reduces senescence and increases apoptosis in IMR-90 upon IR. (a) SA-β-Gal staining of irradiated IMR-90 in presence of PKC inhibitor (72 h recovery) with untreated (U) as control. **(b)** WB analysis of irradiated IMR-90 (48 h recovery) in presence of PKC inhibitor (GF109203X, 2.5 μM) or doxorubicin (0.5 μg/ml). Tubulin was used as loading control. Quantification of p21 protein **(c)** and ARTD1 levels **(d)** levels from (b) (n=2-3). **(e)** Sub-G1 peak analysis of irradiated IMR-90 (recovery for 48 h) in presence of PKC inhibitor (GF109203X, 2.5 μM) or DMSO as control. **(f)** Quantification from (e) (n=2). Statistical analysis was performed by Student's t-test, * p<0.05, ** p<0.01, *** p<0.001, ns = not significant.

3.2 Unpublished Results

3.2.1 Role of ARTD1 during immortalization of primary mouse embryonic fibroblasts

A primary cell that is isolated from a tissue undergoes a definite number of divisions until it enters senescence, which is a state of growth arrest, even though cells may still be metabolically active (*253*). While normal human cells in culture will stop dividing after several passages and are not able to overcome senescence without additional treatment to immortalize them, some rodent cells are able to recover from senescence by recombination-dependent mechanisms to maintain telomeres and by spontaneous mutations of cell cycle regulatory genes (*254, 255*). The most prominent genes, which are often mutated are the p16 and p53 tumor suppressor genes (*256*).

ARTD1 -/- MEF cells grow slower after outgrowth from senescence

We were interested, whether ARTD1 plays a similar role during outgrowth from senescence as during cell cycle re-entry from the G_0 phase of T24 cells (see 3.1.2). Primary wild type (WT) or *ARTD1* $^{-/-}$ mouse embryonic fibroblasts (MEFs) were isolated from 14.5 days old embryos, passaged every third day, and their growth behavior was monitored until they became immortalized (knockout analysis Figure 1A). After passage six, cell growth started to slow down and a large fraction of the cells died. The culture medium was replaced every third day and residual cells started to form colonies. Detectable colony formation occurred earlier in WT than in *ARTD1* $^{-/-}$ cells (Figure 1C). Directly after immortalization (around passage 15), *ARTD1* $^{-/-}$ cells grew slower and were mainly arrested in G_0/G_1 phase as determined by FACS analysis (Figure 1B). After another 10 passages, cell cycle analysis and cell counting revealed that *ARTD1* $^{-/-}$ cells grew as fast as WT cells (Figure 1C). Together, these experiments indicated that ARTD1 plays an important role during the transformation of MEFs, although the cells overcame this dependency after extended time in culture.

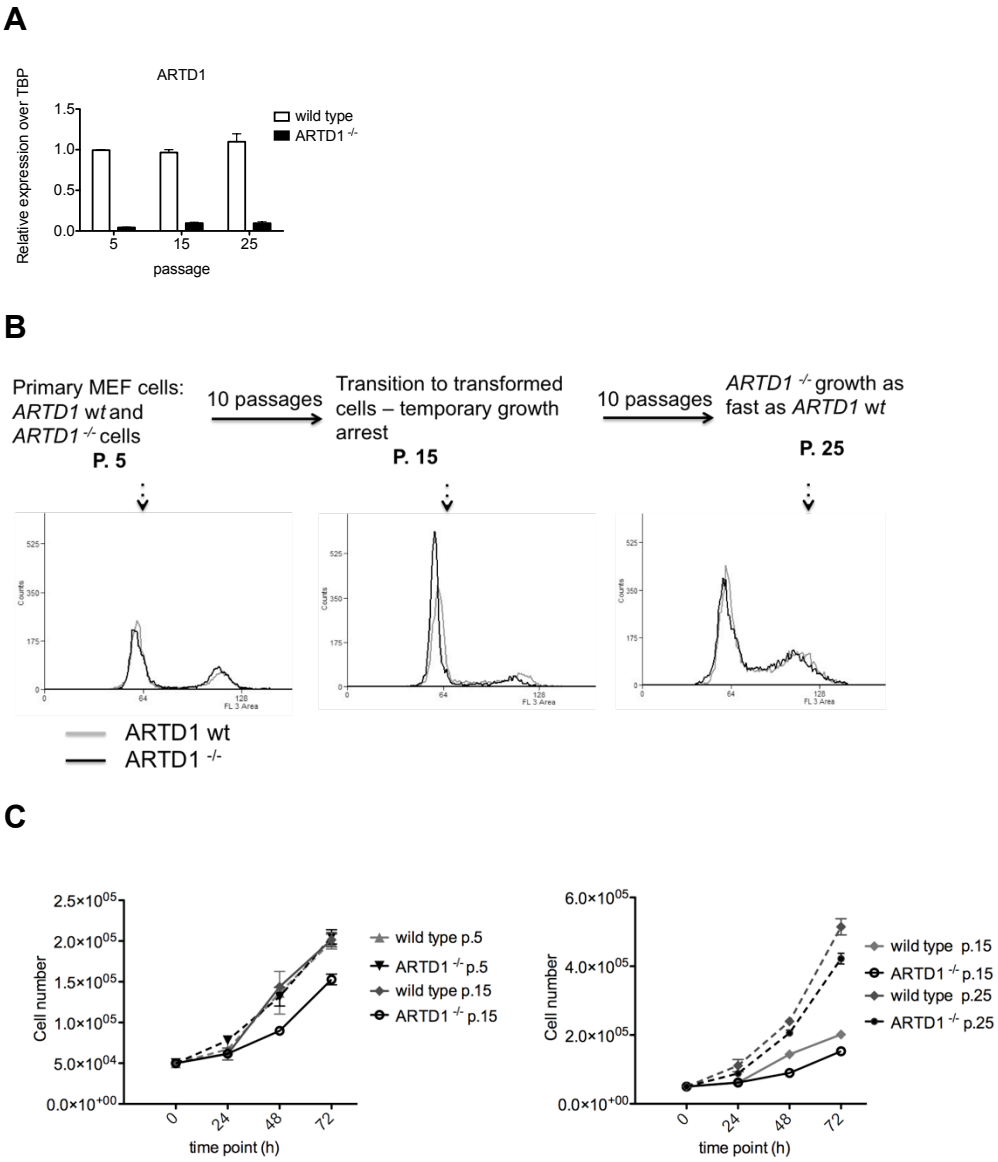

Figure 1: *ARTD1* $^{-/-}$ cells show a different cell cycle distribution shortly after cell immortalization but regain cell growth comparable to wild type cells after 25 passages. A) qPCR expression levels of ARTD1 in wild type and *ARTD1* $^{-/-}$ MEF cells at different passages were performed to confirm ARTD1 knockout. (Average + SEM, n=2) B) Scheme and FACS analysis of wild type and *ARTD1* $^{-/-}$ MEFs at different cell passages are displayed. C) Growth curve of wild type and *ARTD1* $^{-/-}$ MEFs before immortalization and shortly after immortalization were analyzed (left panel). Growth curve was analyzed of cells shortly after immortalization as in left panel compared to cells after 10 passages after immortalization (right panel). (Average + SEM, n=2), P.5= before immortalization P.15= early after immortalization P.25= late after immortalization.

After outgrowth from senescence Cyclin E levels are down regulated in ARTD1$^{-/-}$ cells

Since we observed a cell cycle delay for *ARTD1*$^{-/-}$ MEFs that was comparable to the cell cycle effect observed in siARTD1 treated T24 cells after cell cycle re-entry (G_0 to G_1 phase), we analyzed whether the Cyclin E levels are also changed during the immortalization of primary MEFs.

Western blot analysis revealed that Cyclin E protein levels increased early after transformation (passage 15) in WT MEFs. In *ARTD1* $^{-/-}$ cells, such an increase of Cyclin E protein levels was not observed. qPCR analysis of *Cyclin E* levels in MEFs of different passages confirmed a reduced Cyclin E expression in *ARTD1*$^{-/-}$ MEFs after immortalization (compared to WT cells (Figure 2)). These results indicated, that ARTD1 might indeed be involved in the regulation of Cyclin E during the immortalization process.

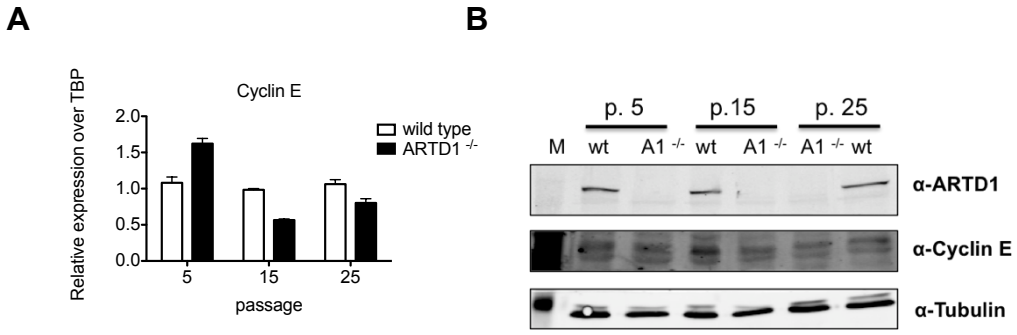

Figure 2: Cyclin E levels are diminished in ARTD1 $^{-/-}$ cells shortly after transformation. A) qPCR analysis of MEFs at different passages was performed (average + SEM, n=2). B) Western blot analysis of MEFs at different passages was performed. p.5= before immortalization p.15= early after immortalization n p.25= late after immortalization. M=protein marker.

E2F-1 and Cyclin A expression levels are decreased in ARTD1$^{-/-}$ MEFs in the early stages after immortalization

Next, we investigated whether the lack of ARTD1 affects other cell cycle factors during immortalization. E2F-1 and Cyclin A transcript levels were reduced in *ARTD1* $^{-/-}$ MEFs as compared to WT MEFs shortly after immortalization, whereas pRb expression was increased (Figure 3A). The p53 and p16 expression levels remained unchanged (Figure 3B). These results differed from our previous observation for T24 cells (chapter 3.1.2), where only Cyclin E expression was decreased upon ARTD1 knockdown.

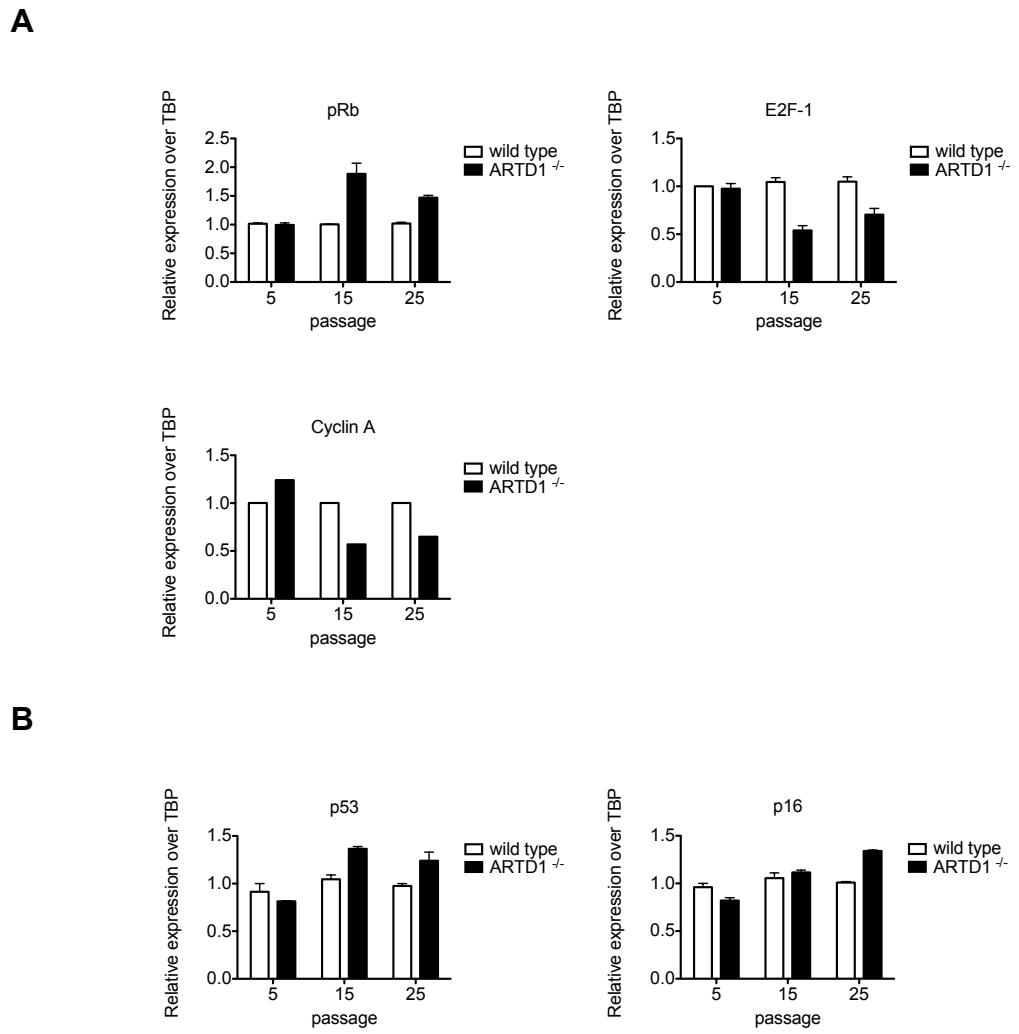

Figure 3: Expression levels of cell cycle regulatory factors are differently affected during immortalization. A) qPCR analysis of pRb, E2F-1and Cyclin A was performed of wild type and *ARTD1* $^{-/-}$ MEFs at different passages. B) qPCR analysis of p53 and p16 was performed as in A). (Average + SEM, n=2) p.5= before immortalization p.15= early after immortalization p.25= late after immortalization.

In conclusion, ARTD1 seemed to positively regulate cell immortalization. However, several passages after immortalization, *ARTD1* $^{-/-}$ MEFs grow as fast as their wild type counterpart, suggesting a primarily beneficial role of ARTD1 during escape from senescence. Similar to our cell cycle studies with T24 cells, Cyclin E expression was dependent on the presence of ARTD1, but the general mechanism seems to be different, since also E2F-1 and Cyclin A levels were negatively affected by the lack of ARTD1, which was not observed for T24 cells. A western blot analysis of these genes should clarify whether the observed expression changes also affect the protein levels.

3.2.2 ARTD1 does not interact with Cyclin E or retinoblastoma protein in T24 cells

ARTD1 was observed to influence Cyclin E expression in T24 cells upon cell cycle re-entry (chapter 3.1.2). To understand this regulation, initial experiments were performed to analyze a possible interaction of ARTD1 with Cyclin E, but also with Retinoblastoma protein pRb, as a key player of early cell cycle progression. Total pRb, Cyclin E or Cdk2 (as control for Cyclin E interaction) were immunoprecipitated from T24 cells harvested in G_0 phase (in confluence) and, immunoprecipitated complexes were resolved by SDS-PAGE and analyzed by western blot analysis using antibodies against ARTD1, Cyclin E, total pRb and Cdk2 (Figure 4).

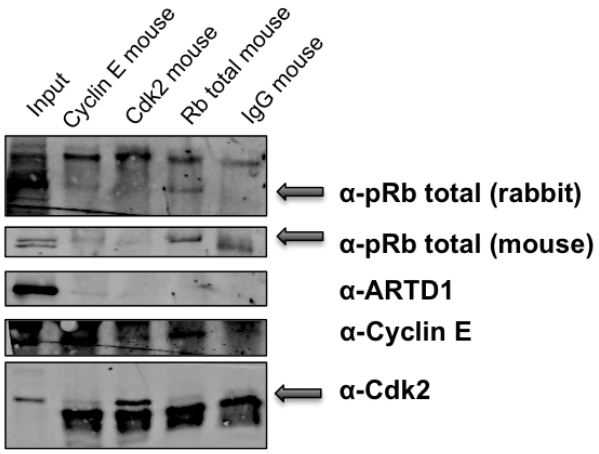

Figure 4: ARTD1 does not interact with Cyclin E or retinoblastoma protein. pRb, Cyclin E or Cdk2 were immunoprecipitated from T24 cells harvested in G_0 phase (in confluence). Western blot analysis was performed and possible interactions were detected by using antibodies against pRb, ARTD1, Cyclin E and Cdk2.

ARTD1 interacted neither with immunoprecipitated pRb nor with Cyclin E or Cdk2. A similar result was observed when ARTD1 was immunoprecipiated and analyzed for complex formation with pRb and Cyclin E (data not shown). The already described interaction of Cyclin E with Cdk2 and of pRb with Cyclin E served as positive controls for these experiments. Together, the analyses indicate that pRb and Cyclin E do not interact with ARTD1. If ARTD1 is still able to modify one of these targets and regulate them, has to be further experimentally evaluated by *in vitro* PARylation assays of pRb and Cyclin E.

3.2.3 Actinomycin D treatment affects mitochondrial gene expression, while H_2O_2 treatment has no effect

Mitochondria are important organelles of the cell since they are the main supplier of ATP (*257*). A notable characteristic is that mitochondria contain their own DNA of approximately 16.6 kbp, which encodes for 2 rRNAs, 22 mitochondrial tRNAs and 13 proteins in human cells (*257*). Most mitochondrial proteins are therefore encoded in the nucleus and have be transported to the mitochondria (*258*). The homeostasis of mitochondria is tightly regulated by mitochondrial chaperones, which assist proteins to fold correctly. Different factors such as mitochondrial biogenesis, production of reactive oxygen species (ROS), as well as other environmental stress conditions, affect the mitochondrial protein-folding environment (*259*). When the load of unfolded or incorrectly folded proteins in mitochondria exceeds a certain limit, the mitochondrial unfolded protein response (UPR^{mt}) is activated to re-establish homeostasis (*260*). The UPR^{mt} is a mitochondria-to-nucleus signaling pathway, which leads to the expression of mitochondrial protective genes (e.g., chaperones and proteases) (*261*). Given the link of ARTD activity and the consumption of NAD^+, we were wondering whether H_2O_2 stimulated PAR formation influences mitochondrial homeostasis and trigger the UPR^{mt}. Therefore, T24 cells were treated with H_2O_2 (1 mM, 60 min) and/or the PARP inhibitor Olaparib (1 μM, 3 h). Usually, PAR formation peaks after 10-15 minutes of H_2O_2 treatment and cannot be detected anymore after 60 minutes, although the generation of early PAR might influence downstream processes such as RNA transcription of e.g., mitochondrial gene expression. RNA was isolated from each condition and qPCR analysis was performed. To follow possible changes of mitochondrial gene expression, the NADH-dehydrogenase subunit 1 (ND1) and cytochrome C oxidase I (CO-1) were examined. These genes were used to investigate the direct effect of the different treatments on mitochondrial gene expression (mtDNA). Additionally, the expression of mitochondrial genes encoded in the nucleus (succinate dehydrogenase complex, subunit B (SDHB), and NADH dehydrogenase (ubiquinone) 1 alpha subcomplex, 2 (NDUFA2)) was analyzed. Furthermore, genes of the UPR^{mt} pathway were investigated, namely mitochondrial heat shock protein 70 (mtHsp70) and caseinolytic peptidase (ClpP), which is a quality control protease. qPCR analysis of theses genes revealed that neither H_2O_2 treatment alone, nor additional Olaparib treatment had a significant effect on the expression of mitochondrially encoded genes, nuclear encoded mitochondrial genes and genes involved in the UPR^{mt} (Figure 5). When cells are treated with

H_2O_2 in combination with Actinomcyin D (ActD), PAR formation is still detectable after 1 h of H_2O_2 treatment (data now shown) Since it was shown that additional ActD treatment enhanced PAR formation in the nucleus after H_2O_2 or MNNG treatment, we investigated whether ActD treatment affects the mitochondrial homeostasis in presence or absence of H_2O_2 or PARP inhibitor. T24 cells were treated with ActD (20 h, 50 ng/ml) and/or H_2O_2 (1 mM, 60 min) and/or Olaparib (1 μM, 3 h). qPCR analyses for the same genes as described above were performed (Figure 5). Mitochondrial gene expression (mtDNA) increased upon ActD treatment, while co-treatment with additional H_2O_2 and/or Olaparib treatment did not have a significant effect. Interestingly, ActD had no uniform effect on the expression levels of nuclear encoded mitochondrial genes (nDNA). SDHB was down regulated after ActD treatment, whereas NDUFA2 was strongly increased (Figure 5). The same was observed for genes of the mitochondrial unfolded protein response pathway. mtHsp70 expression was decreased after ActD treatment, while ClpP expression did not significantly change.

In conclusion, ActD increased gene expression of mitochondria encoded genes (mtDNA), while it had differential effects on the expression levels of genes encoded in the nucleus. H_2O_2 treatment and/or PAR inhibition by Olaparib treatment had no significant effect on the analyzed genes. Thus, increased PAR formation after ActD treatment in combination with H_2O_2 cannot be responsible for the disruption of mitochondrial homeostasis.

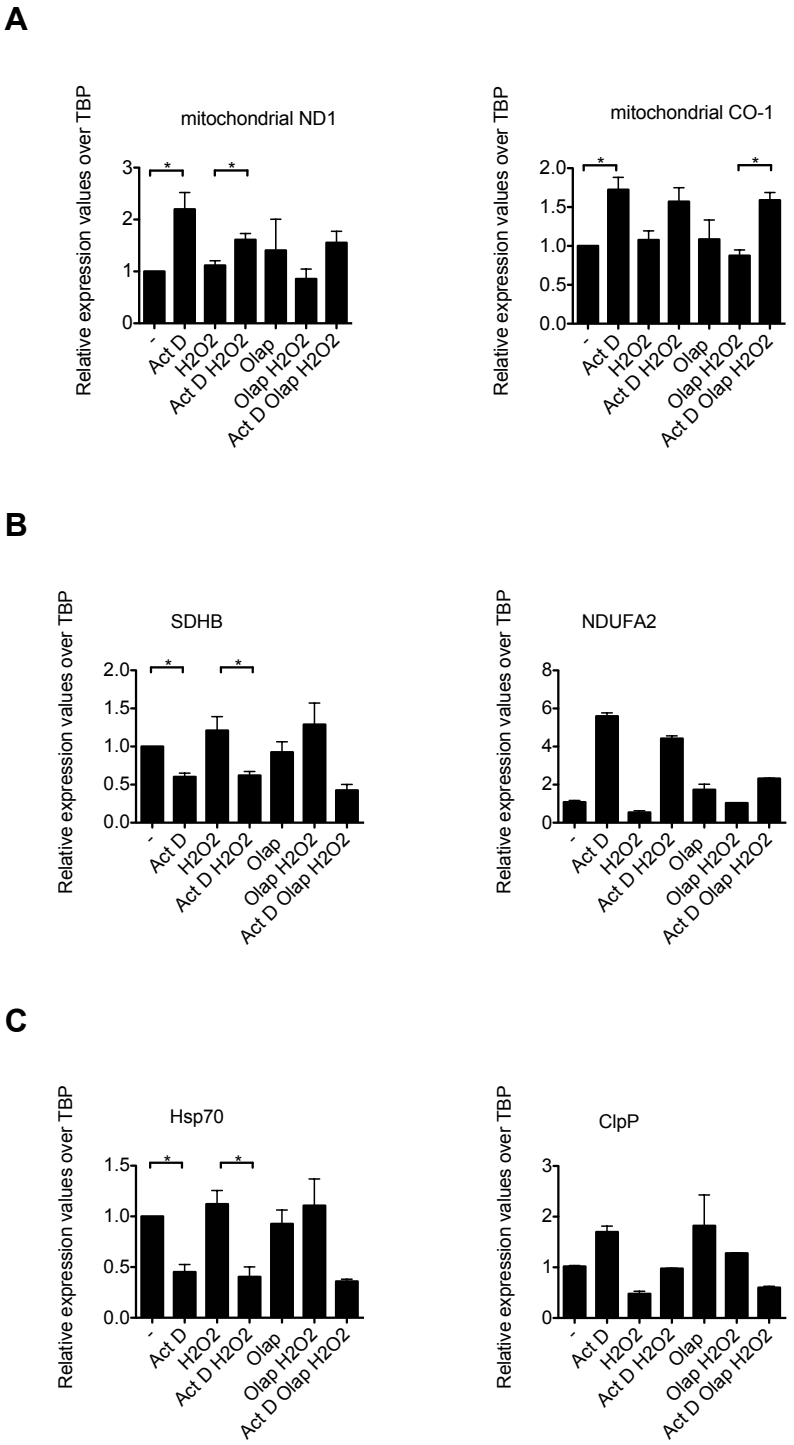

Figure 5: Actinomycin D treatment has an impact on the expression of mitochondrial genes, independent of H_2O_2 or Olaparib co-treatment. T24 cells were treated with Actinomycin D (20 h, 0.05 µg/ml) and/or H_2O_2 (1 h, 1 mM) and/or Olaparib (3 h, 1 µM). RNA was isolated from 2 independent experiments and expression levels were measured by qPCR analysis. A) Gene expression of mitochondrial encoded ND1 and CO-1. B) Gene expression of nuclear encoded mitochondrial proteins SDHB and NDUFA2. C) Gene expression of genes involved in the UPR^{mt}: Hsp70 and ClpP. (average + SEM, n=2, t-test, p* < 0.05).

3.2.4 NQO1 and NQO2 are potential off-targets of PJ-34

NQO1 (NAD(P)H: quinone oxidoreductase 1) and NQO2 (NRH: quinone oxidoreductase 2) are cytosolic flavoproteins catalyzing the oxygen independent two-electron reduction of quinone to hydroquinone by using NAD(P)H or dihydronicotinamide ribosyl (NRH) as electron donors (*262, 263*). This is a protective and detoxifying mechanism, since these enzymes prevent the formation of reactive oxygen species (ROS) by counteracting the one-electron reduction of quinone (*264, 265*) (Figure 6).

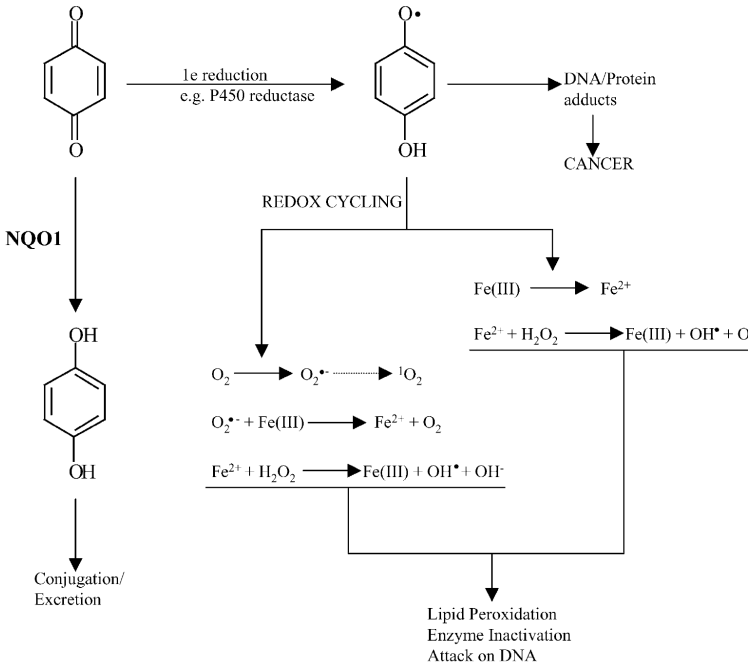

Figure 6: Quinone metabolism. A reaction scheme of a simple quinone is shown. $1e^-$ reduction by e.g., P450 reductase leads to the radical semi-quinone, which in turn leads to ROS production. $2e^-$ reduction by NQO1 results in the stable, less toxic hydroquinone formation (from Nioi *et al.* (*265*)).

NQO1 is highly expressed in diverse cancer types (e.g., in breast cancer, colon cancer, pancreatic cancer and non-small cell lung cancer) probably as an adaptation to an increased metabolic activity (*266*). NQO1 is therefore often used as a marker of early carcinogenesis, but is also an interesting target for cancer therapy. The overexpression of NQO1 in cancer cells can be exploited by using special quinone derivatives. These derivatives are reduced to toxic hydroquinone, which are able to induce cell death through ROS formation. Different compounds are currently tested in pre-clinical trials (e.g., mitomycin C or β-lapachone) (*267*). Another approach used for cancer therapy is the direct inhibition of NQO1. Dicumarol, a natural compound, is known to inhibit NQO1 more specifically than other NADPH

oxidoreductase and was shown to have growth inhibitory effects in pancreatic cancer cells (*268*). In comparison to NQO1, NQO2 is less studied. It is 49 % homologous to NQO1 and uses another electron donor (NRH) (*269*). Consequently, NQO2 is resistant to the typical NQO1 inhibitors such as Dicumarol (*269*) and specific NQO2 inhibitors are currently being developed (*270*).

Previous results of our laboratory and of other groups indicated that treatment with the PARP inhibitor PJ-34 leads to growth deficiencies and cell death (unpublished results and (*160*)). Madison *et al.* even observed that the growth inhibitory effects of PJ-34 was due to a mitotic arrest independent of ARTD1 (*271*), indicating that an off-target of PJ-34 is likely responsible for the observed growth arrest.

A drug-profiling screen with PJ-34 in a yeast-based system was performed to identify PJ-34 interacting proteins. Besides ARTD1, PJ-34 bound specifically to NQO2, but not to NQO1 (unpublished data). To further investigate the functional relevance of this interaction, T24 cells and NIH 3T3 cells were transiently transfected with siMock, siARTD1, siNQO1 (both as controls) and siNQO2. After plating equal amounts of cells ($5x10^5$ cells), cell growth was measured after 48 h (Figure 7B). siARTD1, siNQO1 as well as siNQO2 treatment led to a decrease in proliferation. The knockdown cells were additionally treated with PJ-34 (10 µM) for 48 h and cell growth was measured again (Figure 7C). PJ-34 treatment alone induced reduced cell growth of siMock treated T24 and NIH 3T3 cells. A similar effect was observed in siARTD1 treated samples, excluding ARTD inhibition as the reason for reduced cell growth after PJ-34 treatment. Treatment of siNQO1 cell with PARP inhibitors, in both cell lines did not further inhibit cell growth. A similar effect was also observed for siNQO2 treated T24 cell, but was not observed in NIH 3T3 cells, indicating that PJ-34 induced growth defects were likely due to NQO1 and NQO2 inhibition, although the cell type or species might be important for the observed effect.

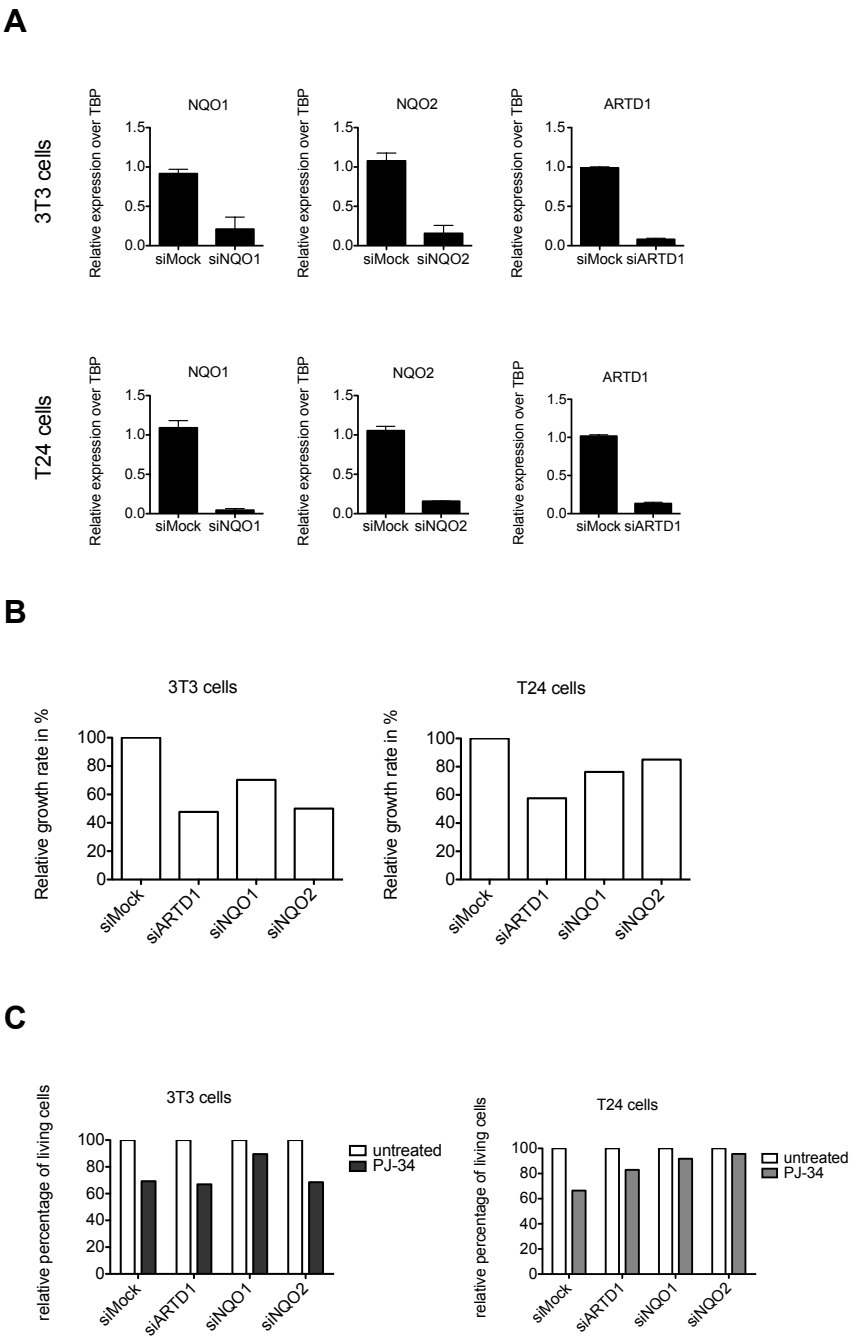

Figure 7: PJ-34 induces growth reduction, which is diminished by siNQO1 and NQO2 knockdown. A) qPCR analysis was carried out to measure the knockdown efficiency in NIH 3T3 and T24 cells. B) and C) Cell counting was performed after 48 h of siRNA transfected T24 cells or NIH 3T3 cells. Starting cell number was $5x10^5$ cells for each condition. C) Cells were additionally treated with PJ-34 (10 μM). Cell numbers are shown relative to the untreated cells of each condition. siMock was set as 100 % as arbitrary unit.

Since PJ-34 seemed to have an effect on NQO1 independent on the cell type and species, we decided to further analyze this effect in NQO1 overexpressing MBA-MD 231 breast cancer cells and H596 lung cancer cells (kindly provided by the Boothman laboratory). Bentle *et al.* previously reported that overexpression of NQO1 reduced ROS production, ARTD1

hyperactivation, cell death and DNA damage (*272*). Furthermore, it was shown that NQO1 stabilizes p53 protein by protein-protein interaction independent of its enzymatic function (*273, 274*). NQO1 and vector-only overexpressing MBA-MD 231 and H596 cells were treated with PJ-34 (10 µM, 1 h) and/or H_20_2 (1 mM, 10 min) and PAR formation was subsequently analyzed by western blot analysis (Figure 8B). NQO1 overexpressing cells showed indeed reduced PAR formation after H_2O_2 treatment (also observed by immunofluorescence microscopy, data not shown). Hence, it could be confirmed that PAR formation is reduced in NQO1 overexpressing 231 and H596 cells. PJ-34 treatment completely inhibited PAR formation. Additionally, colony formation assays were performed with these two cell lines. Cells were treated with different concentrations of PJ-34 (0-10 µM) and after 7 days (231 cells) and 12 days (H596 cells), colonies were stained and counted (Figure 8C and 8D). In general, NQO1 overexpressing cells generated more colonies compared to cells complemented with a control vector, but the number of colonies was reduced for all cell lines to a similar extend by PJ-34. At a PJ-34 concentration of 5 µM, the number of colonies was markedly reduced and a concentration of 7.5 µM almost completely inhibited colony formation. In conclusion, PJ-34 treatment induced a comparably growth inhibition in all tested cell lines independent of the overexpression of NQO1.

To test a direct effect of PJ-34 on the enzymatic activity of NQO1, the commercially available WST-1 assay was used. In living cells, cellular dehydrogenases convert WST-1 to formazan, which leads to a color change that can be quantified spectrophotometrically. The WST-1 assay is usually used as a cell viability assay, but since the conversion of NADH to NAD^+ involves oxidoreductases such as NQO1, it is rather a metabolic assay and thus can be used to indirectly measure the effect of PJ-34 treatment on NQO enzymes. Should PJ-34 inhibit the NQOs, the conversion of WST-1 to formazan should be reduced. In the 231 breast cancer cell line, a reduced WST-1 conversion was indeed detected (Figure 8C). The reaction was controlled with Dicumarol, which is a direct inhibitor of NQO1. The sensitivity of this readout was rather low, since high concentrations of PJ-34 and Dicumarol had to be used. The effect in H596 overexpressing NQO1 cells was not very prominent, although Dicumarol inhibited the WST-1 conversion slightly stronger (Figure 8D). Together, our experiments provide evidence that PJ-34 indeed inhibits other NAD^+ related enzymes in the cell. However, further investigations are required to strengthen the point, that PJ-34 can specifically inhibit NQO1 and/or NQO2.

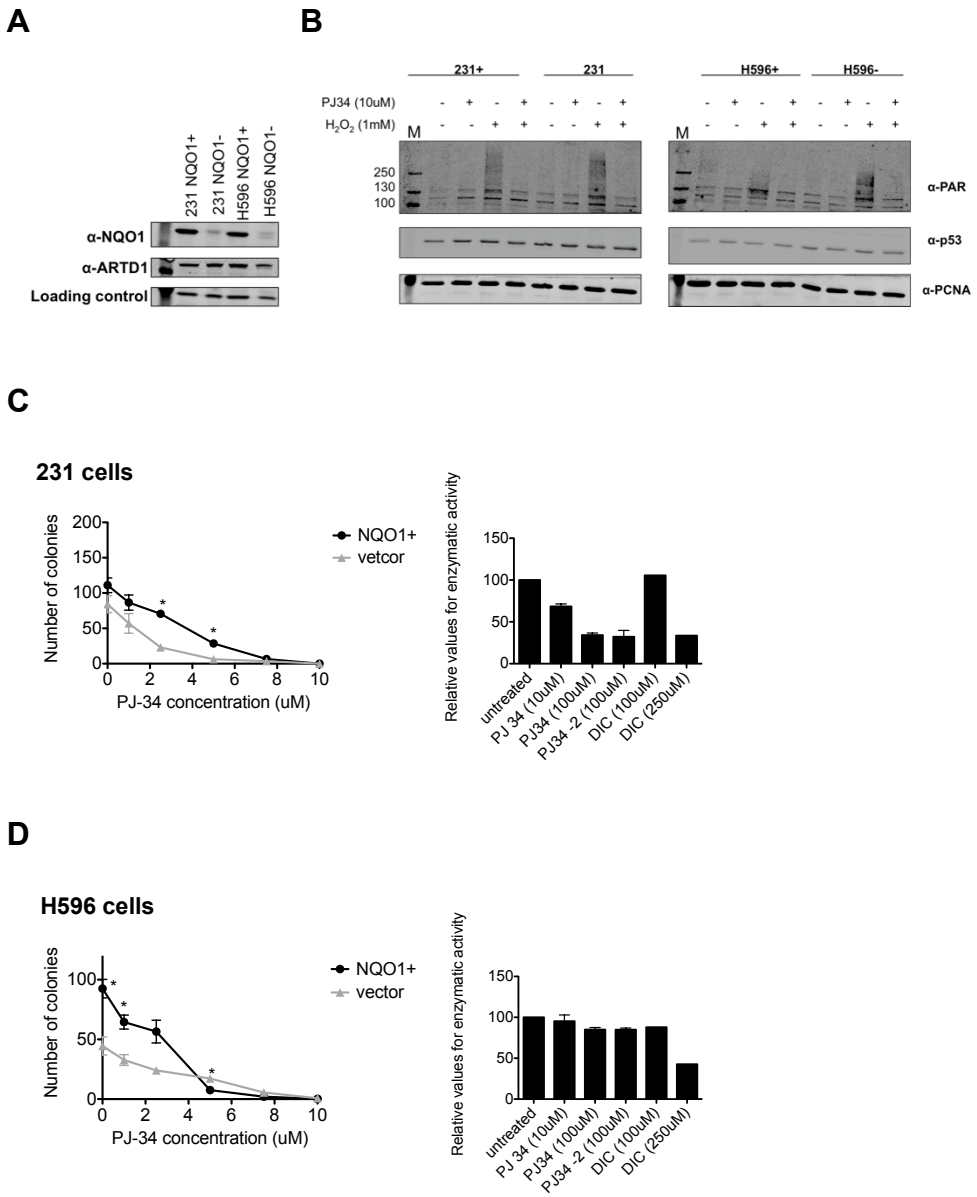

Figure 8: PJ-34 treatment strongly reduces cell growth in NQO1 overexpressing 231 cells and H596 cells. A) Western blot analysis of 231 and H596 cells stably transfected with vector-only (vector) or NQO1 over expressing vector (NQO1+) was performed. B) Western blot analysis of PAR formation was performed after H_2O_2 treatment (1 mM, 10min) and/or treated with PJ-34 (1 h, 10 µM) of 231cells and H596 cells. C) Colony forming assay of 231 cells NQO1 overexpressed or vector-only (n= 2, left panel), WST-1 assay of NQO1 overexpressing 231 cells. D) Colony forming assay and WST-1 assay for NQO1 overexpressed or vector-only H596 cells (as in C). PJ-34_2 is a duplicate measurement for PJ-34, uM= µM, DIC= Dicumarol, t-test *p<0.05.

3.2.5 Functional role of p65, ARTD1 and ARTD2 during LPS-induced inflammatory signaling in the colon cancer cell line MC-38

Colorectal cancer is the 3rd most common malignancy and responsible for every 4th death due to cancer (*275*). Inflammation and hypoxia are common features of solid tumor development. Risk factors such as chronic intestinal inflammation and pathogens increase colon cancer formation dramatically, as seen in patients with bowel diseases (*276*). This cancer type exhibits increased expression of cytokines and often displays constitutive activity of NF-κB (*276*). NF-κB is a hetero-dimeric complex of p65 and p50, which is induced by inflammatory signals leading to its translocation to the nucleus where it acts as a transcription factor of inflammatory response genes. NF-κB activity supports tumorigenesis by inducing cell proliferation and angiogenesis, which were both shown to promote cell invasion and metastasis (*277*). Moreover, tumor cells with induced NF-κB are often resistant to chemotherapeutics (*278*). Increased levels of TNFα and IL6 in patient serum samples were described to correlate with an increased risk for colorectal adenoma (*279*). Colon cancer cells are known to highly metastasize into the lung, promoted by immune and inflammatory cells (*280*). Previous data of our laboratory revealed that NF-κB-dependent gene expression after TNFα or LPS treatment is heavily impaired in *ARTD1*$^{-/-}$ MLFs (*137*). It was therefore the goal of this sub-project to identify new target genes of p65 in MC38 cells (murine colon tumor cells, isolated from a chemically induced grade III adenocarcinoma of a C57BL/6 female mouse) and to clarify the role of ARTD1 and ARTD2 during NF-κB-dependent gene expression after LPS treatment. Since hypoxia is an important aspect of tumors, we investigated the inflammatory response after LPS treatment under normoxic and hypoxic conditions in microtissues by RNA deep sequencing. Upon intracaecal injection, MC38 cells form primary tumors in the colon and secondary metastases in the liver. Borsig *et al.* established a MC38 cell line, stably transfected with GFP, to analyze and study the metastasis formation *(281)*. For the induction of the cellular inflammatory response, cells were treated with bacterial lipopolysaccharide (LPS) from *Escherichia coli* 055:B5. Pathogens like *E.coli* are often involved in colorectal cancer formation (*282, 283*).

In comparison to 2D cell cultures, microtissues show an increased inflammatory response after LPS stimulation

The LPS-induced gene expression in MC38 cells was first analyzed under normal 2D cell culture conditions. Stimulation of MC38 cells in the presence of 10 % fetal calf serum (FCS) induced NF-κB target genes such as IP-10 only to a very low extent (approx. two fold, Figure 9). Also other inducers of NF-κB such as IL-12 and TNFα did not cause a strong induction of IP-10 (data not shown). The expression could be enhanced up to 6 fold by starving cells over night (medium with 0 % FCS) (Figure 9).

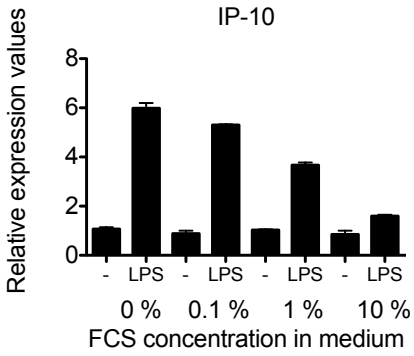

Figure 9: FCS in medium quenches the inflammatory response. shMock MC38 cells were cultured overnight in medium with different FCS concentrations (as indicated). Upon LPS stimulation (1 µg/ml, 1h) IP-10 gene expression was measured by qPCR (average + SEM, n=2).

Recent studies provide evidence that the inflammatory response is enhanced in 3D microtissues compared to conventional 2D cell culture (*284*). Microtissues or spheroids are globular aggregates of several thousand cells (mostly tumor cells) that are generated in cell culture and that are used as *in vitro* tumors models. We thus generated MC38 microtissues with a diameter of approximately 300 µm by the hanging drop method using inverted microtest plates (Figure 10A). The LPS- induced inflammatory response was, even in presence of 10% FCS, greatly enhanced in 3D microtissues as indicated by increased IP-10, TNFα and IL6 expression (Figure 10B). Carbonic anhydrase IX (CAIX), a biomarker for induced hypoxia, was only slightly up regulated in 3D cell cultures as compared to 2D cultures, suggesting that the enhanced gene expression was not due to hypoxic areas within the microtissues. Together, these experiments revealed that the LPS-induced inflammatory response in MC38 was strongly enhanced in microtissues compared to 2D culture conditions.

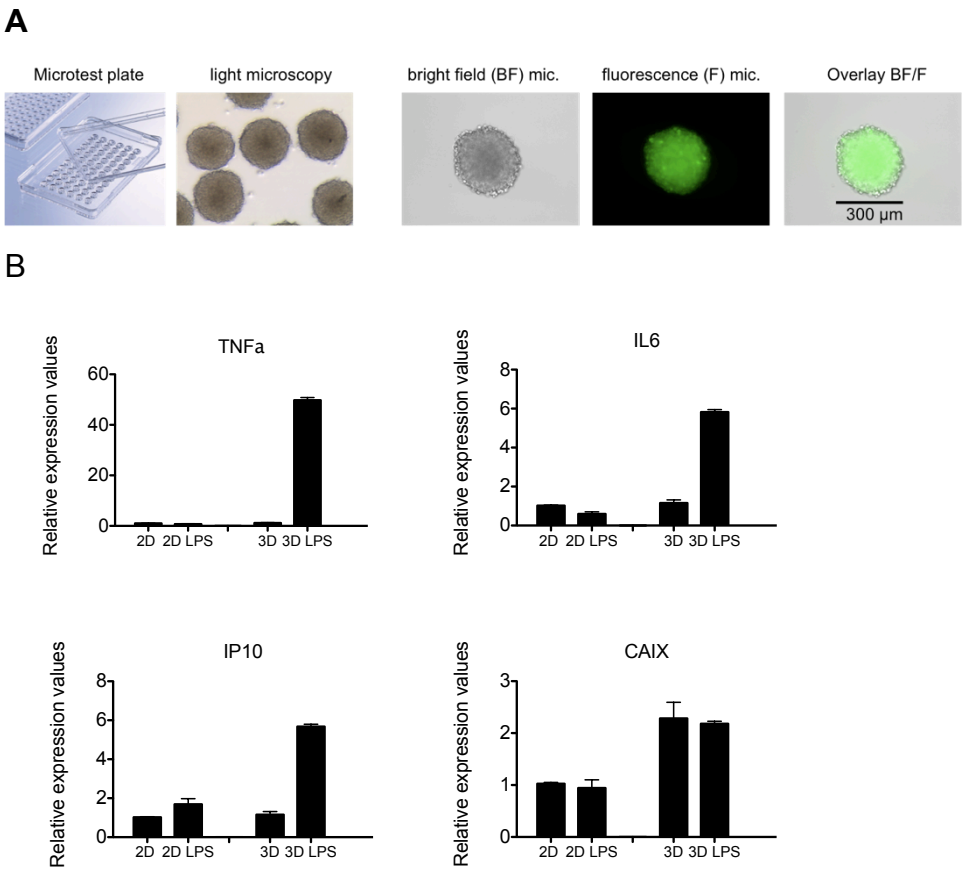

Figure 10: The LPS-induced inflammatory response in MC-38 cells is enhanced in 3D compared to 2D culture conditions. A) Example picture of micro test plates (Greiner bio-one) used for hanging drop method to generate microtissues. In each well 2500 cells per 25 µl drop were seeded. Cells were cultivated in complete medium with 10 % FCS for 2 days. Example pictures of microtissues are shown. After 2 days of growth, microtissues had a diameter of approx. 300 µm. Detection of GFP expression for stable GFP- MC38 was carried out with the fluorescence microscope. B) Gene expression analysis of GFP-MC38 cells grown in 2D (normal cell culture) and 3D cell culture by hanging drop method in complete medium (10 % FCS). Cells were stimulated with LPS (1 h, 1 µg/ml). TNFα, IL6 and IP10 expression levels were measured as markers of the inflammatory response. CAIX was used to control if hypoxia was induced in 2D versus 3D cell culture (average + SEM, n=2).

Impaired inflammatory response after LPS stimulation in shp65 MC38 GFP cells

To investigate the contribution of p65, ARTD1 and ARTD2 to the LPS-induced inflammatory response in MC38 cells, p65/RelA, HIF1α, (established by Wenger group) ARTD1 and ARTD2 were knocked down. sh-targeting sequences for p65, ARTD1 and ARTD2 were cloned into a retroviral vector (pRDI292) and expressed under the regulation of the H1-promoter. After generation of retroviral particles and subsequent transduction of MC38 cells with retroviruses, cells were selected with puromycin (10 µg/ml). Knockdown efficiency was confirmed by qPCR analysis as well as by western blot analysis. Since there is

no reliable mouse ARTD2 antibody available, ARTD2 knockdown was only evaluated by qPCR. The knockdown efficiency was around 80 % for ARTD1 and around 65 % for p65 and ARTD2 (Figure 11A). The influence of shp65, shARTD1 and shARTD2 on defined NF-κB target genes was measured after LPS treatment (1 h or for 4 h with 1 μg/ml LPS) by qPCR comparing two different conditions: 2D cell culture under starving conditions (0% FCS, over night incubation) and 3D cell culture in complete medium (10% FCS) (Figure 11B and 11C). Overall, the gene induction was again greatly enhanced under 3D culture conditions as compared to starved 2D conditions. The expression of TNFα, but not IL6 was impaired in shp65 cells. shARTD1 treatment led to decreased TNFα expression, as compared to shMock cells, although the effect was not statistically significant. shARTD2 treatment rather induced TNFα expression under both conditions, which may hint at different roles of ARTD1 and ARTD2 in NF-κB-dependent gene expression. IL6 expression was reduced in shp65 cells under 2D cell culture conditions, but this effect could not be observed under 3D cell culture conditions. Furthermore, as already shown in our laboratory, IL6 expression was strongly up regulated after LPS treatment in shARTD1 MC38 cells (Fig. 11C and unpublished results).

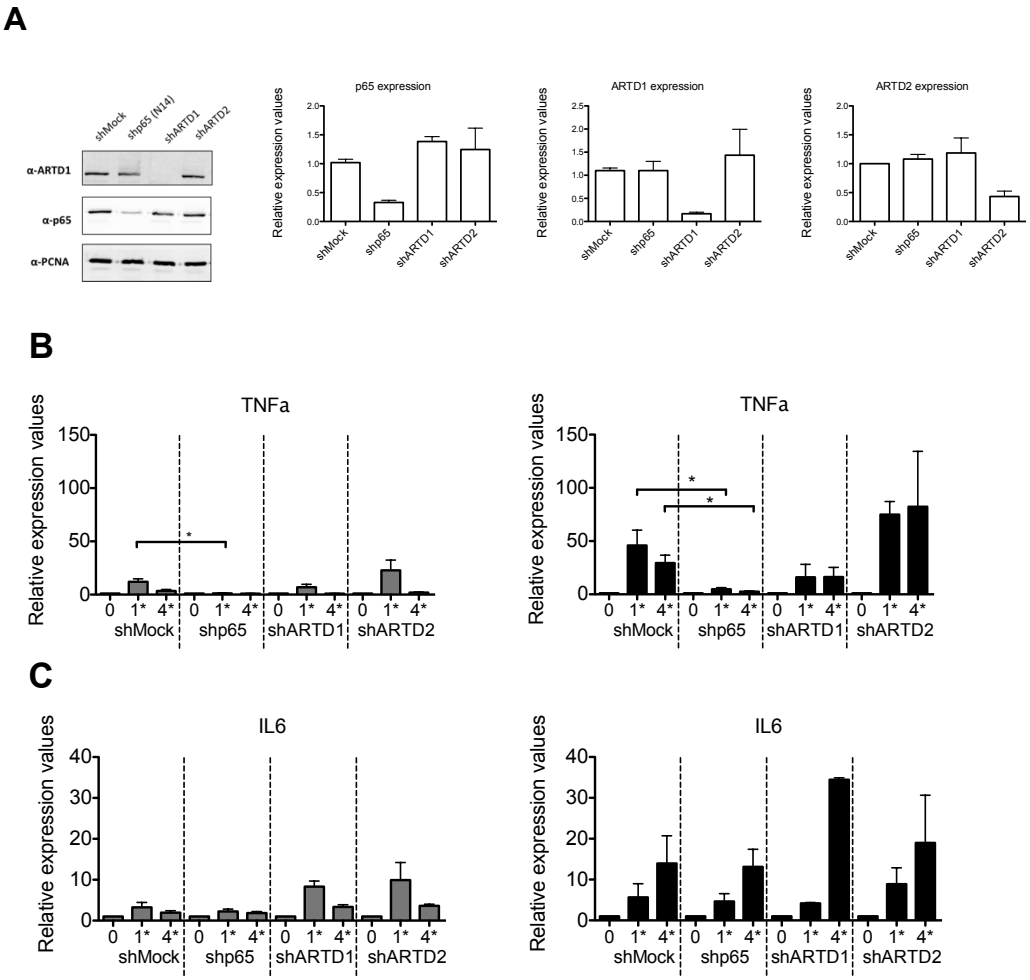

Figure 11: Influence of p65, ARTD1 and ARTD2 on TNFα and IL6 gene expression in GFP-MC38 under 2D and 3D cell culture conditions. A) Western blot analysis of knockdown efficiency of shp65 and shARTD1 treated MC38 cells was performed (left panel). There is no ARTD2 antibody for mouse lysates available**.** qPCR analysis (right panels) of knockdown cells was carried out to measure knockdown efficiency of shp65, shARTD1 and shARTD2 B) and C) Comparison of inflammatory response in 2D cell culture under starving conditions (0% FCS over night, grey bars, right panel) and 3D cell culture (complete medium, 10% FCS, black bars, left panel) in different knockdown conditions after 1h and 4h LPS* stimulation (1 µg/ml) is shown. (average + SEM , n=3, t-test p*<0.05).

Together, TNFα was regulated by p65 and ARTD1 as well as ARTD2, although to different extents. Surprisingly, IL6 expression was not affected in shp65 MC38 cells under 3D cell culture conditions, indicating that other LPS-induced transcription factors than NF-κB are regulating IL6 in MC38. While ARTD1 has a rather stimulatory effect for TNFα, IL6 expression was up regulated in shARTD1 cell, thus ARDT1 has repressory functions on IL6. In contrast, ARTD2 repressed the TNFα expression, while the IL6 expression seemed not to

be strong affected by this protein. To further elucidate these observations, more genes of the inflammatory response have to be analyzed.

RNA deep sequencing analysis revealed strongly reduced p65-dependent expression under hypoxic conditions

Since the 3D culture conditions led to a stronger LPS-dependent gene expression, this condition was used to investigate the p65-dependent genes of MC38 cells under normoxic and hypoxic conditions by using RNA deep sequencing.

For the RNA deep sequencing analysis, three independent experiments with LPS stimulated (1 µg/ml for 1h) or unstimulated MC38 GFP cells under normoxic and hypoxic conditions were performed. To confirm the effective LPS stimulation and hypoxia, TNFα, IL6 and CAIX were quantified by qRT-PCR (Figure 12). IL6 and TNFα expression where induced by LPS under normoxic conditions, while TNFα expression was strongly reduced under hypoxia in comparison to normoxia. p65/RelA-dependence could again be confirmed for *TNFα* in shp65 cells. In contrast to normoxic conditions, IL6 expression was strongly decreased in shp65 cells under hypoxia, indicating that the NF-κB-dependent gene response depended on the oxygen supply. HIF1α knockdown did not affect TNFα or IL6 expression.

These experiments corroborated the previous observation that TNFα expression is dependent on p65, but furthermore also on the oxygen supply, thus a subset of genes might be dependent on p65/RelA only under specific oxygen conditions.

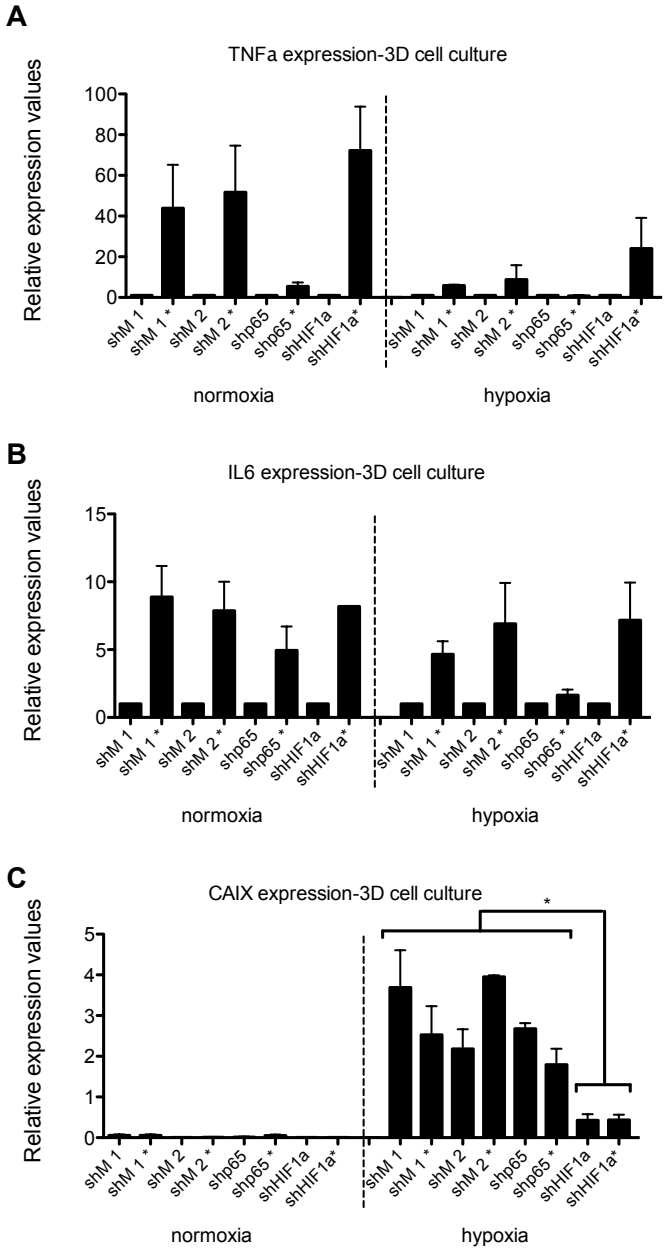

Figure 12: Quality control of samples for RNA deep sequencing. The RNA deep sequencing was performed in collaboration with Wenger group (shMock 1 and shHIF1α established by Wenger group, shMock 2 and shp65 established by Hottiger group). LPS stimulation was performed (* 1 h, 1 µg/ml) under normoxia (21% O_2) and hypoxia (0.2% O_2) and qPCR analysis was carried out for following genes: A) TNFα- expression B) Il6-expression C) CAIX expression (average + SEM, n=3, p*< 0.05,)

Following confirmation of LPS stimulation and hypoxia, RNA deep sequencing was performed and the data was analyzed with the help of the Functional Genomic Center Zürich (FGCZ). After alignment and normalization, 23'300 expressed transcripts were analyzed for the different tested conditions. RNA deep sequencing confirmed a similar induction of TNFα and IL6 expression as observed by qPCR analysis (Figure 13), although RNA deep sequencing was less sensitive (compare scales of the graphs of Figure 13 to Figure 12, 5x up

regulation versus 40x up regulation for TNFα expression), indicating that even small differences in expression levels observed by the RNA deep sequencing are likely relevant.

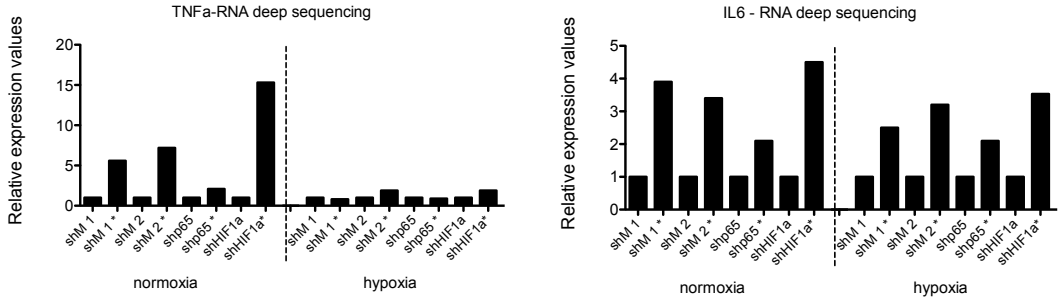

Figure 11: RNA deep sequencing data for TNFα and IL6. Fold induction analyzed from RNA deep sequencing data for the two genes which were used as control before – compare to Figure 12.

The analysis of the RNA deep sequencing run is currently in progress and only a first and initial analysis is presented here. The coverage of a specific transcript measured by RNA deep sequencing was displayed in signal intensities. These values differed from 0 up to 60'000. Since significant changes were also detected for RNA species with low signal intensities, the data were analyzed without a signal threshold. We were especially interested in LPS-induced genes, which were p65/RelA dependent under different oxygen conditions. The thresholds for the fold change of genes after LPS stimulation were defined as 1.5 fold induction and 0.67 fold reduction (over untreated). The induction of gene expression after LPS stimulation was compared for both shMock cell lines and only genes up or down regulated compared to both shMock conditions were considered. Out of 23'300 genes, 359 genes were induced after LPS treatment and 143 genes were reduced after LPS treatment (Figure 14A). Furthermore, out of the 359 induced genes, 213 genes (60 %) were positively regulated by p65 and only 2 (0.5 %) were negatively regulated (Figure 14B). We further analyzed also the HIF1α dependency for the p65 positively regulated genes. 68 genes (32 %) were HIF1α dependent of which only 4 genes (1.8%) were negatively regulated by HIF1α (Figure 14C). The same analysis was carried out for the samples under hypoxic conditions. From the 23'300 identified genes, 202 genes were induced by LPS and 183 genes were reduced (Figure 14D). From the 202 LPS-induced genes, only 76 (37.6 %) were positively regulated by p65 and only 4 (2 %) were negatively regulated by p65 (Figure 14E). From the 76 LPS-induced, p65 positively dependent were genes, 41 genes (54 %) were HIF1α dependent (Figure 14F). Only 109 LPS-induced genes were common for both normoxic and

hypoxic conditions (Figure 14G). The comparison of LPS-induced, p65 positively regulated genes revealed only 18 genes in common under normoxia and hypoxia. Moreover, the LPS, p65 and HIF1α positively regulated genes were even independent between normoxia and hypoxia. Together, the number of induced p65/RelA-dependent inflammatory genes was reduced under hypoxia as compared to normoxic conditions. Moreover, comparison of the induced genes under these two conditions suggests that different genes are induced under normoxia and hypoxia and only a small number of genes are common in both conditions. Furthermore, these LPS-induced and p65-dependent genes were less induced under hypoxic conditions (e.g., Cxcl2: 40x induction under normoxia versus 17x induction under hypoxia, data not shown), suggesting that the induction of the inflammatory response is reduced under hypoxia. Interestingly, certain genes seemed to be regulated by p65 under defined oxygen conditions, whereas other genes are regulated by NF-κB independent of the oxygen conditions. Finally, p65 and HIF1α did not regulate common genes, irrespectively of the tested conditions (Figure 14C). Thus, the possible regulation by p65 and HIF1α is dependent on the oxygen conditions.

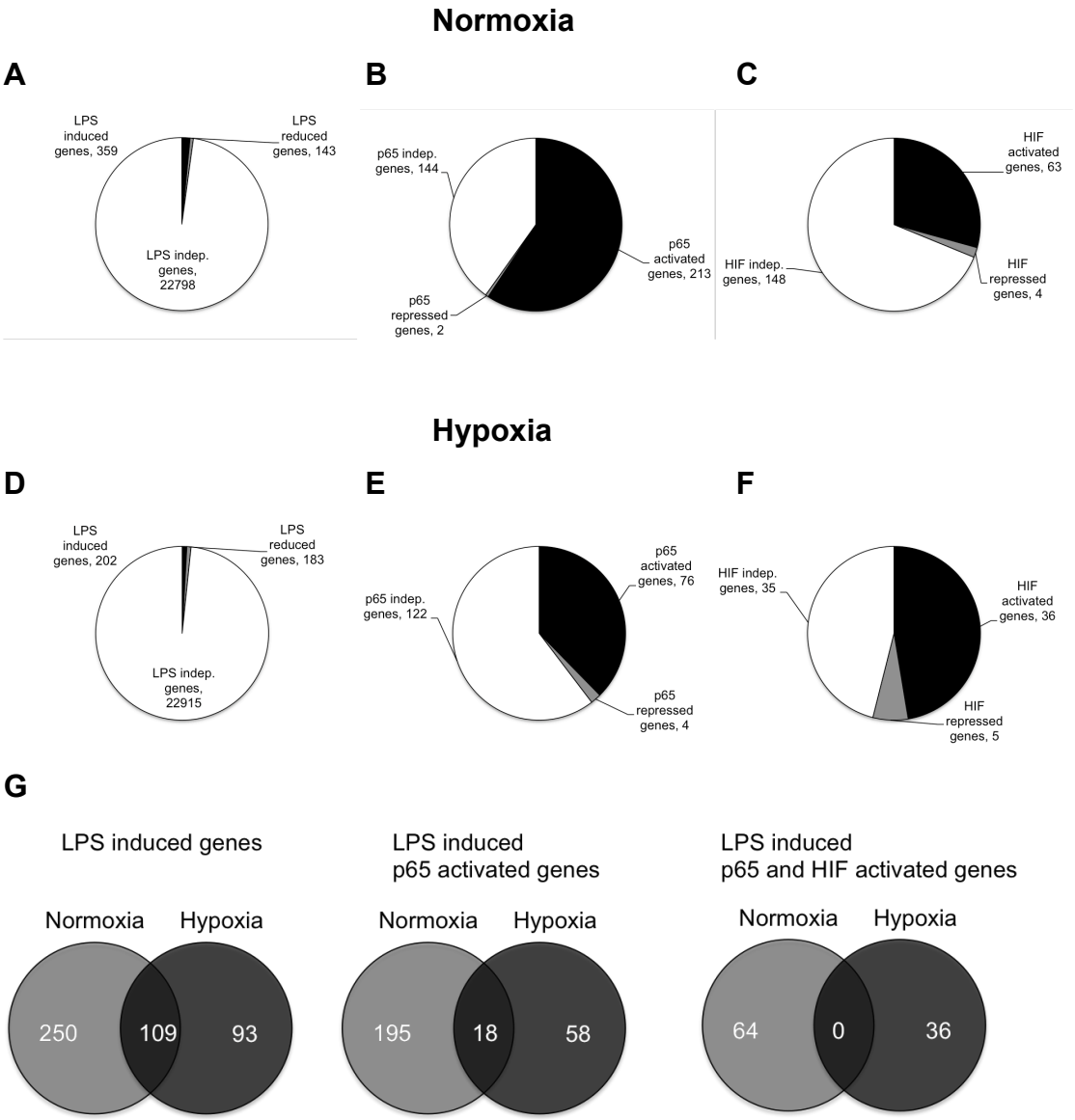

Figure 14: Deep sequencing analysis of LPS-induced genes under normoxic and hypoxic conditions. Threshold for fold induction was set >1.5 or <0.67 over untreated. A) Of 23300 genes, gene expression was induced by LPS stimulation for 359 genes and gene expression was reduced by LPS for 143 genes. B) Of 359 induced LPS genes, 142 genes were independent of p65, 215 genes were positively regulated by p65, 2 were negatively regulated by p65. C) Of 215 LPS-induced and p65 positively regulated genes, expression of 63 genes were positively regulated by HIF1α, 4 genes are negatively regulated by HIF1α D) Of 23300 genes, gene expression was induced by LPS stimulation for 202 genes, gene expression was reduced by LPS for 183 genes E) Of 202 induced LPS genes, 122 genes were independent of p65, 76 genes were positively regulated by p65, 4 were negatively regulated by p65. F) Of 76 LPS-induced and p65 positively regulated gene, expression of 36 genes was activated by HIF1α, 5 genes were negatively regulated by HIF1α G) Comparison of overlapping normoxic and hypoxic induced genes after LPS stimulation

In collaboration with the Borsig and Jurisica laboratory, a functional interaction map was established by using the NAViGaTOR software indicating similar functional pathways for

the LPS-induced, p65-dependent genes under hypoxic and normoxic conditions (Figure 15). NAViGaTOR uses highly optimized layout algorithms to enable interactive visualization of large networks (*285*). The software program predicts possible functional interactions between proteins based on database searches of known (published) interaction partners. The map displays interaction of p65-dependent genes induced under normoxia (rectangle, left side) and under hypoxia (triangles, right side) after LPS stimulation. The diamonds in the middle display the genes, which were found to be regulated significantly under both conditions, whereby the width of the symbols displays the positive up regulation under normoxia and the height displays the fold induction under hypoxia. Interestingly, the genes with the most likely functional interactions were not necessarily those, which were up regulated the most. For example, Cxcl2 was up regulated the most in both conditions, but showed only a small interaction network. This analysis provides only a first insight into the functional relevance of obtained data. Further validation and interaction studies will follow. Interesting targets will moreover be verified by controlling their gene coverage using the genome viewer and by measuring their expression levels by qPCR analysis. In addition, interesting NF-κB target genes will be studied in the shARTD1 and shARTD2 background to evaluate to which extent these two proteins influence the gene expression profile of MC38 cells.

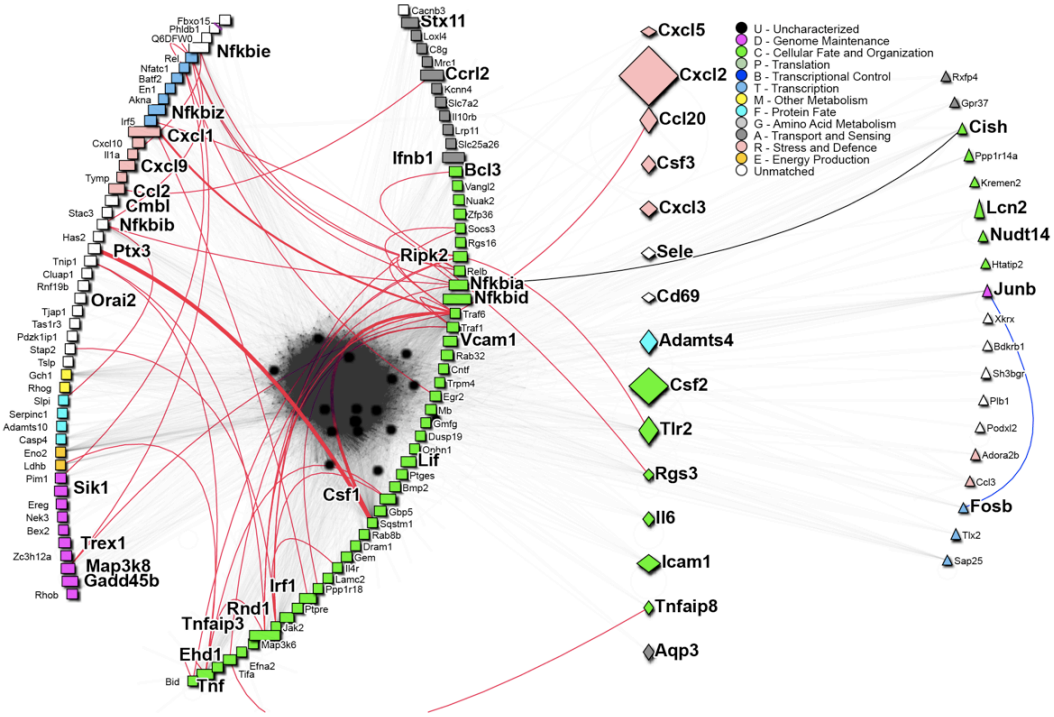

Figure 15: Functional interaction map of p65 dependent target genes. Genes under normoxia (rectangle) are displayed on the left, for hypoxia (triangle symbol) on the right side. Diamond symbols display genes common for both conditions. The width of the rectangle symbols correlate with positive gene expression. The height of the triangle symbols correlate with fold induction of expression. Thus, genes regulated under normoxia and hypoxia (diamond symbols) change in width and height. Red lines display interaction of genes emanating from normoxic conditions. The bigger the letters, the more interaction partners exist. Grey lines display interaction between both conditions and blue line symbols interaction between hypoxic partners. Cxcl2 was the strongest induced gene after LPS stimulation in both conditions; therefore it is biggest displayed in size of its symbol.

3.2.6 Materials and Methods

Cell culture

The T24 urinary bladder cancer cell line was cultivated in McCoy's 5A medium (Gibco, Invitrogen, CA, California, USA) at 37°C. NIH 3T3, HEK 293, H596 as well as U2OS cells were cultivated in Dulbecco's Modified Eagle's Medium (DMEM) (PAA, Pasching, Austria). 231-MD-MBA cells were cultivated in Roswell Park Memorial Institute medium (RPMI) (Gibco, Invitrogen, CA, California). Mouse embryonic fibroblast (MEF) cells were obtained from wildtype (WT) and ARTD1 knockout mice and also cultivated in DMEM. The GFP-transduced MC38 cell line was provided by Dr. Lubor Borsig (Institute of Physiology, University of Zurich, Switzerland) and was cultivated in DMEM supplemented with 1% (v/v) non-essential amino acids and 1% (v/v) sodium-pyruvate. Every 3rd passage, Geneticin (G418; 1 mg/ml) (Gibco, Invitrogen, CA, California) was added to select transduced cells. All media were supplemented with 1% (v/v) Penicillin/Streptavidin and 10% (v/v) fetal calf serum (Gibco, Invitrogen, CA, California, USA).

Antibodies

Following antibodies were used: From Santa Cruz Biotechnology, Inc (Dallas, TX, USA): PARP1/ARTD1 (H-250, rabbit); PCNA (PC10. mouse); p53 (FL-393,rabbit); Rb (IF8, mouse), p65 (C-20, rabbit), cyclin E (HE12, mouse), , mouse). From Active motif (Carlsbad, CA, USA): PARP2 (rabbit). From Sigma Aldrich (St. Louis, MO, USA): tubulin (mouse). From Epitomics Inc. (Burlingame, CA, USA): Rb (rabbit). Homemade: PAR 10H (mouse).

Immunoprecipitation

Cells were harvested with a scraper after adding 400 µl ice-cold lysis buffer (50 mM Tris-Hcl pH 7.5, 120 mM NaCl, 20 mM NaF, 1 mM EDTA, 6 mM EGTA, 15 mM Na-pyrophosphate, 0.5 mM Na-orthovanadate, 1 mM Benzamidine, 0.1 mM PMSF, 1% Nonidet P-40). After lysis (10 min on ice), cells were collected (12,000 rpm, 10 min) and proteins were quantified by the Bradford assay. Immunoprecipitation was carried out with 2 µg of antibody per 500 µg of extract at 4°C for 3h. Sepharose G or A beads were added (20 µl per reaction, incubation for 30min at 4°C). Beads were washed with extraction buffer, 6x Laemmli buffer (4 µl) were added and the reaction was boiled for 5 min at 95°C. SDS-PAGE and western blot analysis were performed as described previously.

Colony survival assay

Cells were seeded in 6-well-plates (500 cells per well), treated as indicated and grown for at least 7 days. The medium was discarded and cells were washed once with PBS and stained with Crystal violet solution (0.5% w/v crystal violet powder, 20% ethanol). Plates were washed twice with water and colonies were counted after drying.

WST-1 assay (Roche, Basel, Switzerland)

$2x10^4$ cells were seeded in a 96-well-plate per well. Treatment was carried out as indicated and 10 µl of the WST-1 substance was added to each well. WST-1 turnover was measured after 60min at a wavelength of 450nm with the microplate reader Infinite® Pro 200 (Tecan, Männedorf, Switzerland).

Cloning of sh-constructs

For stable knockdown in MC38 cells, sh-constructs for ARTD1, ARTD2 and p65 were cloned. Primers were designed for a 19 nucleotide target sequence flanked by specific sequences allowing to build a hairpin structure. Sequences for p65: forward primer: 5' GATCCCCAGGGCAAACTGTAGAGTCATTCAAGAGAT GACTCTACAGTTTGCCCTTTTTTGGAAA, Reverse primer: 5'AGCTTTTCCAAAAAAGGGCAAACTGTAGAGTCATCTCTTGAATGACTCTACAGT TTGCCCTGGG, for ARTD2: Forward primer: 5' GATCCCC CCATGAAAGTAATGAG TTTTTCAAGAGAAAACTCATTACTTTCATGG TTTTTGGAAA Reverse primer: 5' AGCTTTTCCAAAAACCATGAAAGTAATGAGTTTTCTCTTGAAAAACTCATTACTT TCATGG GGG

The oligos were annealed, phosphorylated and ligated into the pSUPER vector. The construct and the H1-RNA promoter for expressing hairpin RNAs were cut out with BamH1 and SalI and ligated into the pRDI292 vector (received from Paul O. Hassa). The final vector was transformed in bacteria, purified and sequenced to control the correct insertion.

Virus production

HEK 293 cells were seeded ($4x10^6$ cells per 10 cm plate) 1 day before calcium phosphate transfection with 10 µg transfer plasmid with the desired sh-sequence, 6 µg of packaging plasmid, and 3.5 µg viral envelope plasmid. Medium was changed 6-8 h post transfection and

after 40h, cells and supernatant were harvested, centrifuged and filtered (0.45 µg cellulose acetate filters). Supernatant containing the virus was frozen at -20°C in 1 ml aliquots.

Viral transduction – Virus infection

Cells were seeded 1 day prior to transduction on a 6-well- plate ($5x10^5$ cells per well). Polybrene was added to a final concentration of 4 µg/ml over night. 1 ml of supernatant containing virus was added per well. The medium was replaced 8 h post infection and to selective-medium after 1 day (Puromycin, 10 µg/ml for MC38 cells, 0.7 µg/ml for T24 cells) (Invivogen, San Diego, CA, USA). Cells were kept under constant selection.

3D cell culture for hypoxic/normoxic LPS stimulation experiment

Viral transduced GFP-MC38 cells were seeded on micro test plates (2500 cells/25 µl drop) (Greiner bio-one, Kremsmünster, Austria) for hanging drop 3-D cultivation. Cells were kept at 37°C for 2 days until a micro tissue was formed and were then transferred to constant hypoxic (0.2 % O_2) or normoxic (21 % O_2) conditions for 7 h. Following, cells were transferred to DMEM medium with or without LPS (1 µg/ml, Sigma Aldrich, St. Louis, MO, USA) in a bacterial plate to avoid attachment of micro tissues to the plate) and incubated at the corresponding O_2 concentration for 1 h. Microtissues were collected, washed once with PBS and lysed in RNA lysis buffer RA1 (Nucleospin RNA II extraction kit, Macherey-Nagel, Düren, Germany)

RNA deep sequencing

RNA deep sequencing analysis was performed at the Functional Genomics Center Zurich (University of Zurich), supervised by Dr. Hubert Rehrauer and by Catharine Aquino. RNA was extracted and pooled from 3 independent, LPS-stimulated 3D-cultures that were grown under hypoxia or normoxia and that were treated with shMock, shp65 or shHIF1α. Ribosomal RNA in the pooled RNA was depleted (Encore® Complete RNA-Seq Library Systems, NuGEN, San Carlos, CA, USA) and RNA deep sequencing was performed with the Illumina HiSeq 2000 sequencer (San Diego, CA, USA).

RNA deep sequencing analysis

Isoform and gene expression levels were computed with RSEM (Version 1.2.0). (http://www.biomedcentral.com/1471-2105/12/323). RSEM was run in stranded-mode with

the additional option to estimate the distribution of the read start positions. The expression levels were normalized for sequencing depth using the geometric mean. The geometric mean was computed using only genes that had an abundance above zero in all samples. For heatmap visualizations at logarithmic scale, zero-valued abundance values were replaced with a small positive value. To attenuate expression ratios for low abundance genes, a fixed value of 5 was added to all expression values before computing the log-ratio.

4 DISCUSSION AND PERSPECTIVES

The aim of this thesis was to investigate if ARTD1 and ARTD2 regulate different cellular processes or use different mechanisms to regulate common processes. To corroborate this hypothesis, we investigated the involvement of ARTD1 and ARTD2 during the diverse biological functions, the genotoxic stress response and the re-entry into cell cycle progression.

4.1 ARTD2 activity is stimulated by RNA

H_2O_2 and MNNG are well known inducers of genotoxic stress. Upon treatment of cells, PAR is formed in the nucleus. In this study we demonstrated that treatment of cells with H_2O_2 or MNNG induced PAR formation mainly in regions of the nucleoli of different cell lines (e.g., T24 and NIH 3T3). The inhibition of RNA polymerase I by Actinomycin D (ActD) in combination with the treatment of H_2O_2 or MNNG stimulated a massively increased and prolonged PAR formation. ARTD1 and ARTD2 were previously described to also localize to the nucleolus, although their localization only partially overlapped, which already hinted at different functions of both enzymes (*153*). Earlier studies also reported that the nucleolar localization of unstimulated ARTD1 and ARTD2 enzymes is disrupted upon ActD treatment (*153, 286*). Our experiments included not only the treatment of cells with ActD, but also a co-treatment with genotoxic stress inducers. These conditions rather lead to an activation of the enzymes than their re-localization (*112, 116*).

Treatment of cells with ActD alone did not induce PAR formation, although it was described to induce DNA double-strand breaks (*287*). The induction of strand breaks could be confirmed but only with a high concentration of ActD (1 µg/ml for 4 hours), which induced γH2AX foci, whereas only few foci were found at low concentration (50 ng/ml, 20h treatment, data not shown). Together, our findings indicate that strong stimulation of PAR formation by ActD in combination with H_2O_2 or MNNG was not due to the induction of DNA double-strand breaks, but rather due to its inhibitory effect on RNA polymerase I. Moreover, treatment with H_2O_2 or Olaparib with ActD did not cause significant changes on mitochondrial gene expression as already observed for ActD alone (chapter 3.2.3), indicating that the general lack of mitochondrial gene expression (e.g., ND1 and CO-1) and the possible reduction of ribosomes is most probably not involved in the induction of nuclear PAR formation. Moreover, the knockdown of ARTD1 by siRNA revealed that the initial PAR formation after H_2O_2 treatment was mainly dependent on this enzyme. However, knockdown

of ARTD2 revealed that ARTD2 is mainly responsible for the delayed and prolonged PAR formation after ActD exposure, indicating that the detected PAR is synthesized by the two different enzymes ARTD1 and ARTD2.

Our experiments furthermore provide evidence that RNA (and also single stranded DNA, data not shown) is able to activate the enzymatic activity of ARTD2. Thus, the massive synthesis of short non-coding RNA transcripts by inhibiting RNA polymerase I (*55*) may thus be detected *in vivo* by ARTD2 and lead to its activation. Moreover, our data provides evidence that the SAP domain of ARTD2 is important for the activation by RNA. Furthermore, the WGR domain seems to be generally essential for ARTD2 activity, since upon deletion of the WGR domain the overall ARTD2 activity was reduced. Using an ARTD1 mutant lacking the DNA binding domain, earlier studies have shown that ARTD1 binds RNA via the WGR domain, which induces PAR formation (*68*), thus the possibility of the ARTD2 WGR domain to bind RNA has to be further analyzed. Moreover, the WGR domain might work as a linker domain allowing ARTD2 to undergo certain conformational changes required for the ARTD2 activation by RNA. Unfortunately, there are currently no crystal structures of ARTD2 available to further elucidate this aspect. In addition to ARTD1 and ARTD2, only ARTD3 contains a WGR domain, but neither a SAP domain nor zinc-fingers (*61*). Interestingly, ARTD3 was also activated by RNA whereas ARTD10, which does not contain a WGR domain, was not stimulated by RNA (data not shown). This provides further evidence that the WGR domain may represent a general activation domain. In contrast to ARTD2, both ARTD1 and ARTD3 were stimulated to a lower extent by RNA, which might be explained by a different domain- and amino acid sequence composition of the CAT domains of these enzymes. The zinc-finger domains of ARTD1, which are distantly located from the catalytic domain, preferentially bind DNA (*116*) and induce a conformational change of the overall structure that may prevent further RNA binding (*288*). The observed activation of ARTD1 by RNA may thus only be relevant under special conditions *in vivo* and most likely not under genotoxic stress response.

Interestingly, the stimulatory effect of ActD *in vivo* was dependent on co-treatment with H_2O_2 or MNNG. It is possible that ARTD2 forms short polymers or oliogmers of poly-ADP-riboses after ActD treatment, which are not detectable due to the PAR length-specificity of the antibody (*77*). The activity of endogenous PARG might be high enough to immediately shorten the newly formed PAR to a length, which is below the detection limit of the antibody. The additional genotoxic stress could induce a post-translational modification of ARTD2,

which hyper-activates ARTD2, subsequently allowing the formation of longer PAR chains. This can be addressed *in vitro* by elucidating a possible modification of ARTD2 by using different kinase-, methyltransferase- and acetyltransferase- modification assays or by knocking down these enzymes by siRNA and reanalyze the functional consequence on ARDT2 dependent activity after H_2O_2 or MNNG treatment. Alternatively, H_2O_2 or MNNG treatment might lead to the temporal inactivation of PARG (e.g., by a post-translational modification), which would also result in an enhanced PAR formation. Another possibility is that ADP-ribosylation is induced upon RNA damage. It was shown that H_2O_2 causes greater oxidation in cellular RNA than in DNA (*289*) and could thus also be a stimulator of ARTDs. Moreover, the RNA molecule is less compacted than the DNA, which makes it more susceptible to oxidative damage. Little is known about RNA repair mechanisms, but it was shown that alkylation damage of RNA is similarly repaired as in DNA *in vivo* (*290*). ARTDs could thus be involved in the recognition of damaged RNA molecules. This could be further analyzed by *in vitro* PAR activity assays using damaging agents on RNA or by RNA immunoprecipitation experiments allowing detecting which RNA molecule are indeed binding to ARDT2 *in vivo*.

The activation of ARTD2 by RNA might additionally hint at new functions of ARTD2 in the cell. ARTD2 might for example recognize nascent RNA transcripts. In the context of the stress-response, this could be an important function. RNA polymerases stall when they approach a bulky DNA lesion (*291*). As a consequence, the transcription-coupled repair (TCR) pathway is activated (*292*). ARTD2 might recognize the nascent transcript of a stalled RNA polymerase and either recruit factors involved for the TCR pathway or inhibit RNA degrading enzymes, thus protecting the RNA. One could therefore investigate whether activated ARTD2 is able to interact with Mfd or other members of the TCR pathway or whether ARTD2 depletion induces defects of the TCR pathway. A general involvement of ARTD2 in RNA polymerase processivity could moreover be foreseen. It is known that transcription elongation factor 5 (Spt5) stimulated the processivity of RNA polymerase II and is later involved in factor recruitment for 3' processing and chromatin modification factors (*291*). ARTD2 could play a similar function in transcription by recognizing the nascent RNA and recruiting mRNA modifying enzymes following its auto-modification. ARTD1 was already described to affect mRNA processing by PARylating the poly(A) polymerase (PAP) upon heat stress, which leads to the eviction of PAP and ARTD1 from the mRNA transcript (*293*). Further investigations are required to determine the minimal length of the RNA, which

can stimulate ARTD2 activity, and to assess whether the induction of PAR formation is dependent on a specific RNA sequence or structure. Since ARTD1 also seems to be activated by RNA, which was already reported by Guetg *et al.* during heterochromatin formation (*131*), we cannot exclude yet that the two enzymes are likely redundant with respect to this function.
In our studies, PAR was found to mainly localize to nucleoli, but some foci were also detected in other regions of low DAPI staining, indicating that other nuclear bodies or chromatin structures could also contain PARylated targets. For example, other euchromatic sites, which are actively transcribed, but also nuclear speckles, which are also known as interchromatin granule clusters, enriched in pre-mRNA splicing factors and thus important for the processing of mRNA (*294*). In close proximity of the nuclear speckle are the recently identified paraspeckles, which are comprised of long, non-coding RNA and a few RNA binding proteins. At least 5 types of speckles are present in the nucleus, which are all rearranged upon transcriptional inhibition (*294*). So far, no clear function of paraspeckles could be identified. Since paraspeckles are built around long non-coding RNA, they are also sensitive to RNase treatment (*294*). RNase A treatment was shown before to change also the nucleolar localization of ARTD1 (*131*). Co-localization studies of PAR, ARTD2 and ARTD1 with proteins of these nuclear speckles and paraspeckles, (e.g., paraspeckle protein 1) with or without RNase treatment would provide further evidence for spatial interaction. Knockdown experiments with siARTD1 and siARTD2 would potentially clarify if they play a role in paraspeckle or nuclear speckle assembly and maintenance.
Finally, we could very recently observe that ARTD2 is not only stimulated by RNA, but also by single-stranded DNA molecules (data now shown). Single-stranded DNA is generated during stalled replication or upon torsional chromatin stress (*77, 295*). ARTD2 might thus be activated also under these conditions, independent of DNA damage. Further experiments along this line should provide more insights for a possible function of ARTD2 during these processes.

4.2 ARTD1 and ARTD2 in cell cycle progression

To investigate the function of ARTD1 and ARTD2 during cell cycle progression, we chose to work with the T24 urinary bladder carcinoma cell line as a model. These cells enter a quiescent state upon reaching confluence and cell cycle progression can be easily followed upon splitting. This allowed avoiding the treatment of cells with chemicals for their synchronization (e.g., Aphidicolin, Nocodazol, Thymidine), which were observed to induced

PAR formation (data not shown, Vetmed Dissertation of Sandra Bäckert, 2009). To address a possible function of ARTD1 or ARTD2, the enzymes were knocked down by siRNA treatment before splitting cells. The results presented here demonstrated that ARTD1 and ARTD2 are both important regulators of cell cycle re-entry or progression. ARTD1 was important for the expression of *Cyclin E,* likely by modulating its promoter site. In contrary, ARTD2 was identified to repress *p27* gene expression, again indicating that ARTD1 and ARTD2 are regulating the same cellular process differentially. A detailed discussion of these aspects follows in the next two paragraphs.

4.2.1 ARTD1 regulates *Cyclin E* promoter activity

In this study we have found that ARTD1 positively influences *Cyclin E* expression during cell cycle re-entry and G_1–S phase progression. We could show that chromatin marks at the *Cyclin E* promoter were changed when ARTD1 was knocked down, thus identifying ARTD1 as a positive regulator of the *Cyclin E* transcription. The observed increased recruitment of ARTD1 to the *Cyclin E* promoter during G_0 to G_1 phase transition provides evidence that rather the initiation than the prolongation of *Cyclin E* transcription is affected. Since the treatment of cells with PARP inhibitors did not induce comparable changes of the *Cyclin E* expression levels, PAR formation seems not be important for the mechanism described here. This is different to published studies, where PARylation of KDM5B, a demethylase, prevented demethylation of H3K4me3 and thus kept promoters in an active state (*142*). Since the levels of H3K4me3 were not changed upon siARTD1 treatment in our studies, the changes at the *Cyclin E* promoter were probably induced by other mechanisms than altered histone modifications. In ARTD1 depleted cells, H1 levels, which mark closed chromatin, were increased and the marker for active transcription sites H2A.Z was decreased. It was shown before that ARTD1 and H1 occupancy have reciprocal binding at diverse promoter sites (*141, 249*). It is possible that ARTD1 itself replaces H1 at the Cyclin E transcription start site, perhaps by the interaction with other chromatin associated modifiers or by remodeling complexes as it has already been observed for the exchange of histone variants (*296*). Moreover, the presence of ARTD1 at transcription start sites could be regulated by posttranslational modifications of ARTD1 (e.g., phosphorylation or mono-ADP-ribosylation), which is not inhibited by commonly used PARP inhibitors (*157*). To test this hypothesis, the recruitment of ARTD1 to the *Cyclin E* promoter could be analyzed by inhibitor studies with

different kinase inhibitors, for example for ERK1/2 (*120*). Another explanation for the transcriptional changes of *Cyclin E* could be due to the transcriptional co-factor function of ARTD1. ARTD1 was reported to interact with p300, an acetyltransferase and co-activator of transcription (*136*). E2F-1 requires the interaction with acetyltransferase p300 in order to be transcriptionally active (*203*). Interestingly, the H4ac mark was slightly reduced upon knockdown of ARTD1. H4 acetylation levels may thus be decreased due to a reduced recruitment of p300 to the *Cyclin E* transcription start site. ARTD1 may therefore be involved in the recruitment of p300 to the *Cyclin E* promoter, similar to the described function of ARTD1 and p300 for NF-κB (*136*). Therefore, it would be important to investigate if E2F-1 binding is changed at the promoter site of *Cyclin E* after ARTD1 depletion. These experiments failed so far due to the lack of an E2F-1 antibody allowing chromatin immunoprecipitation. Furthermore, luciferase activity assays could be carried out for ARTD1 and p300 to confirm a possible cofactor function at the *Cyclin E* promoter.

Our studies revealed that the E2F-1-dependent microRNAs 15 and 16 expression levels are strongly enhanced after siARTD1 treatment. Since these miRNA negatively regulate Cyclin E expression, another layer of regulation involving a feedback loop after cell cycle interruption has to be considered (*244*). However, this is unlikely the chase, since no Cyclin E mRNA could be detected by qPCR. Knocking down the expression of microRNAs 15 and 16 would further exclude that these RNAs contribute differently to the observed cell cycle progression phenotype.

Interestingly, the ARTD1 depleted T24 cells are able to overcome the reduced Cyclin E expression in the course of three days, indicating that chromatin plasticity is able to overcome the lack of ARTD1. This observation was confirmed when ARTD1 was stably knocked down by shRNA (data not shown). Alternatively, other cell cycle regulatory factors such as Cylin D and A, which were up regulated at the transcriptional level in siARTD1 treated T24 cells, could functionally compensate the loss of Cyclin E. This is in agreement with the observation that Cyclin E knockout mice are still viable and healthy (*297*).

4.2.2 ARTD2 positively regulates G_0-G_1 progression

The function of ARTD2 during the cell cycle re-entry and progression, and in particular a possible redundant function with ARTD1, was not studied before and was thus an important aim of this work. siARTD2 treated T24 cells did not progress through the cell cycle, but were

early arrested at the G_0/G_1 transition and subsequently induced apoptosis. The cell cycle arrest was due to a strong induction of p27 levels. While the CIP/KIP family member *p57* was also up regulated on mRNA levels (data not shown), the DNA damage response protein p21 was not altered, indicating that the observed effect was not DNA damage dependent. ChIP analyses of the *p27* promoter revealed a strong enrichment of H3K4me3, which may explain the up regulation of *p27*. ARTD2 was recently described to form a complex with HDACs and G9A methyltransferase and to negatively regulated *MYC* expression (*152*). ARTD2 might thus be responsible for the recruitment of chromatin regulators such as histone methylases. Therefore, further ChIP analyses have to be carried out in order to study the recruitment of such factors in presence or absence of ARTD2. Unfortunately, the current lack of ARTD2 antibodies for ChIP analysis does not allow confirming the recruitment of ARTD2 to the *p27* promoter. ARTD2 was already described to have repressory functions on *SIRT1* expression, which is a deacetylase that modifies histones (*148*). Whether SIRT1 expression is differently regulated in siARTD2 treated T24 cells has to be further elucidated. Interestingly, we did not observe the G_0/G_1 phase arrest in siARTD2 treated asynchronous cells, indicating that ARTD2 is especially important for the exit of cells from G_0 phase. It would be interesting to study if ARTD2 overexpressing T24 cells are still able to enter the G_0 phase or progress through the cell cycle uncontrolled. ARTD2 could thus be a positive regulatory of the early immediate genes

4.2.3 The enzymatic activities of ARTD1 and ARTD2 do not contribute to the function in early cell cycle progression

Interestingly, PARP inhibitors (e.g., Olaparip) did not inhibit progression of cells through the early cell cycle phases, but rather inhibited cell cycle progression at late S phase, indicating that the enzymatic activities of ARTD1 and ARTD2 are not required for the above-described functions during re-entry or early G1 progression. A recent publication by Guetg *et al.* showed that ARTD1 interacts with pRNA and TIP5 during late S phase in an activity-dependent manner and that this interaction was important during the formation of heterochromatin (*131*). PARP inhibitors would lead to a disrupted or unstable heterochromatin formation, which results in sister chromatid exchange formation. Together, our experiments provide further insight in the importance of ARTD1 and ARTD2 independent of their enzymatic activities.

4.3 Role of ARTD1 during immortalization

During the process of immortalization, cells overcome the growth arrest by recombination-dependent mechanisms to retain telomeres and by spontaneous mutations (*254-256*). Our data provide evidence that primary *ARTD1*$^{-/-}$ MEFs reach the transformation state much slower than their wild type counterpart. The process is accompanied by reduced *Cyclin E* mRNA expression in *ARTD1*$^{-/-}$ cells, indicating that ARTD1 plays a direct or indirect regulatory role in *Cyclin E* expression. This observation was comparable to the regulatory effect during cell cycle re-entry and progression after knocking down ARTD1. However, other cell cycle regulatory factors such as pRb and E2F-1 were differentially regulated compared to the T24 analysis. We thus conclude that the overall regulation induced upon transformation is likely different from the regulatory process induced in T24 cells. This might be due to the different nature of the tested cells. While MEFs are primary cells, the T24 cells are transformed tumor cells, which acquired already many mutations. Interestingly, the presence of ARTD1 is beneficial in both processes and confirms that ARTD1 plays an important role during cell growth initiation, although by different mechanisms. Further studies of wild type MEFs grown in presence of PARP inhibitors will reveal, if and how transformation is regulated by ADP-ribosylation.

4.4 PJ-34 as off-target for NQO1 and NQO2

PJ-34 is a potent PARP inhibitor with an IC of 20 nM, but is not specific for an individual ARTD family member (*157, 158, 271*). Recently it was shown that PJ-34 is even able to inhibit Pim kinases (*159*), thus questioning its selectivity. Our own data revealed that the growth inhibitory effect of PJ-34 is ARTD1-independent. A drug-profiling screen (data not shown) with PJ34 identified NQO2 as a potential binding protein for PJ-34. More specific analyses revealed that both, NQO1 and NQO2 might be new off-targets of the PARP inhibitor PJ-34 in T24 cells, NIH 3T3 cells and 231 cells. Thus it is likely that besides ARTD1, PJ-34 also targets NQO1 or NQO2. Interestingly, NQO1 is overexpressed in different cancer types (*277*). The identification of these new PJ34 off targets may thus be highly relevant and can potentially be exploited for cancer treatment. NQO1 inhibition leads to an increase of radical semi-quinones, which in turn cause an increase in ROS formation. ROS formation damages protein, lipids and DNA through oxidation, which eventually results in cell death. In addition, the inhibition of ARTD1 activity leads to an increased DNA

damage. Further experiments are required to strengthen this scenario e.g., by looking at the activation of DNA damage checkpoints or by performing viability assays. Moreover, it would be worthwhile to test the NQO1 activity *in vitro* by measuring NADH recycling in combination with PJ-34 treatment. *In vitro* and *in vivo* binding studies are required to clarify how PJ-34 binds the NQO enzymes in comparison to ARTD1.

The functional correlation of NQO2 with PJ-34 could only be confirmed in human T24 cells, but not with mouse NIH 3T3 cells *in vivo*. NQO2 was shown to have mostly low endogenous activity and shows tissue-specific expression differences (*298*). Since NQO2 uses NHR than NADH, it remains questionable, whether PJ-34 is interacting with the catalytic domain of NQO2 or rather with another domain of the protein. As for NQO1, *in vitro* experiments including enzymatic activity assays should be performed to shed more light onto the exact mechanism. Furthermore, other PARP inhibitors should be tested to clarify, if NQO1 or NQO2 are indeed off-targets of PARP inhibitors.

4.5 Functional role of p65, ARTD1 and ARTD2 during inflammatory signaling in the colon cancer cell line MC-38

Inflammation and hypoxia are prominent characteristics observed in solid tumors. We therefore aimed to compare NF-κB (p65)-dependent gene expression under normoxic (21 % oxygen) and hypoxic (0.2 % oxygen) conditions in MC38 mouse colon cancer cells and to investigate the functional contribution of ARTD1 and ARTD2 for this gene expression.

This project is still in progress and only the first results can be discussed here. RNA transcript levels were analyzed by RNA deep sequencing in collaboration with the Wenger group. LPS-induced (1 h, 1 µg/ml) RNA transcript levels of MC38 cells expressing shMock, shp65 and also shHIF1α grown under normoxic and hypoxic conditions were analyzed. 3D cell cultured microtissues were more sensitive to LPS stimulation than cells cultured under normal 2D conditions. Most likely, the NF-κB response in microtissue is more efficient due to higher expression of LPS-sensitive receptors such as TLR4 on the surface of microtissues and possibly due to the higher interaction of the cells in that three dimensional network.

RNA deep sequencing revealed that more genes are activated by LPS under normoxic conditions as compared to hypoxic conditions. Similar observations were reported by others before, but only for a small number of pro-inflammatory genes (*299, 300*). A possible explanation for this observation is that the HIF1α transcription factor, which is only stabilized

under hypoxic conditions, induces the expression of proteins involved the degradation of certain mRNAs. An indication pointing in this direction is the work of Werno et al., which demonstrates that TNFα mRNA is destabilized by the increased tristetraprolin (TTP) activity under hypoxia (*299*). In addition, the TLR4 receptor, which initiates the LPS-induced inflammatory response, might be down regulated upon hypoxia and thus diminishs the inflammatory response (*300*). However, this explanation is less likely, since we did not see expression changes for TLR4 (based on RNA deep sequencing data, not shown). This could be further investigated by western blot analysis for TLR4.

Furthermore, the reduced expression of NF-κB target genes during hypoxia could be explained by an impaired translocation or chromatin recruitment of NF-κB to the nucleus. Microscopy and ChIP experiments of cells grown under normoxia and hypoxia could address these possibilities.

Comparison of the LPS-dependent genes under hypoxia and normoxia revealed that only up to 50% of all induced genes were common for both conditions and that only 20% of the p65-dependent genes were found under both, normoxia and hypoxia. Thus, hypoxia affected both the intensity of the NF-κB response as well as the type of induced NF-κB-target genes (Figure 12G). Difference in gene expression patterns may be due to the presence of the HIF1α transcription factor under hypoxic conditions. However, the LPS-induced, p65- and HIF1α-dependent genes were completely distinct with no overlapping candidates, suggesting that oxygen levels dramatically affects the inflammatory signaling and subsequent response. Metacore (Pathway) analysis of the deep sequencing data (comparing the LPS and p65-dependent genes) could provide evidence whether there is a shift of signaling pathways that are responsive under the different oxygen supplies. To validate the importance of a distinct pathway under certain conditions, inhibitor and knockdown studies targeting one of the key proteins of a certain pathway and subsequent analysis of the expression profile by qRT-PCR could be carried out.

The interactome analysis performed by the Jurisica/Borsig laboratories with the NAViGaTOR software of the RNA deep sequencing data predicted most likely functional interaction based on known interactions and *in silico* databases. For the analysis of protein-protein interaction networks, it was not important how strong a gene was induced upon stimulation, but in how many interactions the corresponding protein could participate. The interaction analysis confirmed that the LPS-dependent genes induced under normoxia in MC38 are indeed part of an inflammatory network. Furthermore, this software allows

performing an interactome analysis with miRNAs (mirDIP software, (*301*)), which are becoming more and more recognized as regulators of mRNA processing and pathway controls. There are strong evidences that miRNAs are also differently expressed depending on the oxygen levels and it is thus likely that miRNAs play a role in the differences detected in our analysis (*302, 303*). Such *in silico* studies have still to be done and will reveal if and which miRNAs most likely affect the expression of different pro-inflammatory genes and whether they regulate the inflammatory response under different oxygen conditions.

A first analysis revealed potential new p65-dependent target genes. For example, *Rnd1*, *Shroom4* and *Ldhb* were found to be up regulated by LPS under normoxic conditions and positively regulated by p65 and even by HIF1α. Under hypoxic conditions, *Kremen2*, *Schlafen2* and *Sap25* were specific p65- and HIF1α-induced genes (Table 1). To test their relevance for the inflammatory response, validation and knockdown experiments targeting the new genes should be performed and differences in cytokine expression should be detected by qPCR analysis.

Table 1: Potential new identified LPS induced (fold induction over untreated) and p65 and HIF1α regulated genes under normoxic or hypoxic conditions.

Gene	Full name	Function	Fold induction after LPS	
			Normoxia	Hypoxia
Rnd1	Rho family GTPase 1	regulation of actin cytoskeleton upon growth factor	**5.8**	3.7
Shroom4	shroom family member 4	regulator of cyto-skeletal architecture	**1.8**	1.7
Ldhb	lactate dehydrogenase B	catalyzes the reaction from lactate to pyruvate	**1.6**	0.9
Slfn2	schlafen2	regulators of T cell development	3.1	**4.7**
Sap25	Sin3A-associated protein, 25kDa	histone deacetylase complex subunit	1.2	**1.9**
Kremen2	kringle containing transmembrane protein 2	transmembrane receptor	1.0	**1.8**

The newly identified LPS-induced NF-κB target genes in MC38 cells will also be analyzed in regard to a possible regulation by ARTD1 and ARTD2 under LPS stimulation. shARTD1 and ARTD2 treated MC38 cells will be exposed to different oxygen levels and stimulated with LPS. Gene expression analysis will be performed by qRT-PCR for a selected group of genes. ARTD1 is a positive regulator of the inflammatory response (*304, 305*) and regulates NF-κB-dependent gene expression through the direct interaction with p65 (*306*). However, some NF-κB target genes seem to be negatively regulated by ARTD1, as seen in our studies for IL6 in MC38 and by other group members in RAW and 3T3 cells (unpublished data). Since the same gene is positively regulated by ARTD1 in mouse lung fibroblast, the function of ARTD1 seems not only to be gene specific, but also cell type specific. These different regulatory functions of ARTD1 may be due to different roles in the recruitment of chromatin

remodeling and modifying enzymes and have to be examined by ChIP analysis in different cell types.

So far, the role of ARTD2 in inflammatory gene expression has not been studied extensively. There is evidence that ARTD2 impacts T-cell development and improves chronic inflammation disease in an IL-10 deficient background (*307, 308*). It was also shown to reduce TNFα expression similar to the role of ARTD1 (*308*). However, our initial analysis revealed an increased expression of TNFα in shARTD2 cells upon LPS stimulation, which would rather point to a repressory function of ARTD2 during inflammation, whereas the TNFα expression was reduced in ARTD1 depleted cells. It might be that, as shown before, ARTD2 regulates NF-κB-dependent gene expression by recruiting HDACs to promoter sites, which would subsequently lead to a decrease in repressory histone modifications and silencing of target gene expression (*152*). ChIP experiments with ARTD2 and histone acetylation on the specific promoter sites at different time points after LPS treatment will reveal if ARTD2 regulates gene expression by modulating chromatin. Thus, distinct roles of ARTD2 and ARTD1 in the inflammatory response of TNFα seem likely.

4.6 Distinct functions of ARTD1 and ARTD2 in various cellular processes

Among the 18 ARTD family members, ARTD1 and ARTD2 share the highest homology (69% of the catalytic domain) (*69*). The data presented in this thesis document non-redundant functions for these two enzymes during cell cycle re-entry and cell cycle progression (chapter 3.1.2) as well as during the genotoxic stress response (chapter 3.1.1). Furthermore, preliminary experiments analyzing the inflammatory response in MC38 cells indicate different regulatory effects of ARTD1 and ARTD2 (chapter 3.2.5), supporting our hypothesis that ARTD2 is an individual cellular player on its own and mostly acts independently of ARTD1. However, this finding does not exclude redundant function and the formation of heterodimeric complexes of both enzymes (*112*).

ARTD1 is often displayed as the key enzyme of the ARTD family and involved in a variety of processes. Knockdown studies revealed that the siARTD2 effect on the cell cycle was stronger than for siARTD1 treated cells, since cells did not enter the cell cycle and were arrested in early G1 phase. It remains to be investigated how general the function of ARTD2 in tumorigenesis is and whether the cell type contributes to the observed effects. We have

also discovered that ARTD2 is strongly stimulated by RNA, which provides new insights how ARTD2 is regulated and for which cellular processes this might be relevant. Thus, ARTD1 and ARTD2 are stimulated by different substrates and to a different extent. ARTD2 enzymatic activity was more activated by a single-stranded structure (RNA or DNA), whereas ARTD1 recognizes mainly double-stranded DNA.

By investigating different biological functions, we have provided new evidences that ARTD2 is an important and distinct regulator of cellular processes that can act independently of ARTD1.

REFERENCES

1. Redon, C., Pilch, D., Rogakou, E., et al. (2002) Histone H2A variants H2AX and H2AZ, *Current opinion in genetics & development 12*, 162-169.
2. Luger, K., Mader, A. W., Richmond, R. K., et al. (1997) Crystal structure of the nucleosome core particle at 2.8 A resolution, *Nature 389*, 251-260.
3. Raghuram, N., Carrero, G., Th'ng, J., et al. (2009) Molecular dynamics of histone H1, *Biochemistry and cell biology = Biochimie et biologie cellulaire 87*, 189-206.
4. Kepper, N., Foethke, D., Stehr, R., et al. (2008) Nucleosome geometry and internucleosomal interactions control the chromatin fiber conformation, *Biophysical journal 95*, 3692-3705.
5. Waddington, C. H. (1939) Preliminary Notes on the Development of the Wings in Normal and Mutant Strains of Drosophila, *Proceedings of the National Academy of Sciences of the United States of America 25*, 299-307.
6. V.E.A. Russo, R. A. M., A.D. Riggs (1996) *Epigenetic Mechanisms of Gene Regulation*, Vol. 32, Cold Spring Harbor Laboratory Press.
7. Hacques, M. F., Muller, S., De Murcia, G., et al. (1990) Use of an immobilized enzyme and specific antibodies to analyse the accessibility and role of histone tails in chromatin structure, *Biochemical and biophysical research communications 168*, 637-643.
8. Kouzarides, T. (2007) Chromatin modifications and their function, *Cell 128*, 693-705.
9. Berger, S. L. (2007) The complex language of chromatin regulation during transcription, *Nature 447*, 407-412.
10. Messner, S., and Hottiger, M. O. (2011) Histone ADP-ribosylation in DNA repair, replication and transcription, *Trends in cell biology 21*, 534-542.
11. Hottiger, M. O. (2011) ADP-ribosylation of histones by ARTD1: an additional module of the histone code?, *FEBS letters 585*, 1595-1599.
12. Schones, D. E., Cui, K., Cuddapah, S., et al. (2008) Dynamic regulation of nucleosome positioning in the human genome, *Cell 132*, 887-898.
13. Portela, A., and Esteller, M. (2010) Epigenetic modifications and human disease, *Nature biotechnology 28*, 1057-1068.
14. Fukushige, S., and Horii, A. (2013) DNA methylation in cancer: a gene silencing mechanism and the clinical potential of its biomarkers, *The Tohoku journal of experimental medicine 229*, 173-185.
15. How Kit, A., Nielsen, H. M., and Tost, J. (2012) DNA methylation based biomarkers: practical considerations and applications, *Biochimie 94*, 2314-2337.
16. Hentschel, C. C., and Birnstiel, M. L. (1981) The organization and expression of histone gene families, *Cell 25*, 301-313.
17. Marashi, F., Baumbach, L., Rickles, R., et al. (1982) Histone proteins in HeLa S3 cells are synthesized in a cell cycle stage specific manner, *Science 215*, 683-685.
18. Maxson, R., Cohn, R., Kedes, L., et al. (1983) Expression and organization of histone genes, *Annual review of genetics 17*, 239-277.
19. Chow, C. M., Georgiou, A., Szutorisz, H., et al. (2005) Variant histone H3.3 marks promoters of transcriptionally active genes during mammalian cell division, *EMBO reports 6*, 354-360.
20. West, M. H., and Bonner, W. M. (1980) Histone 2A, a heteromorphous family of eight protein species, *Biochemistry 19*, 3238-3245.
21. Nekrasov, M., Amrichova, J., Parker, B. J., et al. (2012) Histone H2A.Z inheritance during the cell cycle and its impact on promoter organization and dynamics, *Nature structural & molecular biology 19*, 1076-1083.
22. Rogakou, E. P., Pilch, D. R., Orr, A. H., et al. (1998) DNA double-stranded breaks induce histone H2AX phosphorylation on serine 139, *The Journal of biological chemistry 273*, 5858-5868.
23. Brown, D. D., and Gurdon, J. B. (1964) Absence of Ribosomal Rna Synthesis in the Anucleolate Mutant of Xenopus Laevis, *Proceedings of the National Academy of Sciences of the United States of America 51*, 139-146.
24. Hadjiolov, A. (1985) *The Nucleolus and Ribosome Biogenesis.* , New York: Springer-Verlag.
25. Melese, T., and Xue, Z. (1995) The nucleolus: an organelle formed by the act of building a ribosome, *Current opinion in cell biology 7*, 319-324.
26. Boisvert, F. M., van Koningsbruggen, S., Navascues, J., et al. (2007) The multifunctional nucleolus, *Nature reviews. Molecular cell biology 8*, 574-585.
27. Smetana, K. (1974) *The Nucleolus and Nucleolar DNA*, Academic press, New York.
28. Savino, T. M., Gebrane-Younes, J., De Mey, J., et al. (2001) Nucleolar assembly of the rRNA processing machinery in living cells, *The Journal of cell biology 153*, 1097-1110.
29. Fatica, A., and Tollervey, D. (2002) Making ribosomes, *Current opinion in cell biology 14*, 313-318.

30. Shaw, P., and McKeown, P. (2011) The Structure of rDNA Chromain, (M, O., Ed.), Springer Science+Business Media, Jackson.
31. Andersen, J. S., Lyon, C. E., Fox, A. H., et al. (2002) Directed proteomic analysis of the human nucleolus, *Current biology : CB 12*, 1-11.
32. Andersen, J. S., Lam, Y. W., Leung, A. K., et al. (2005) Nucleolar proteome dynamics, *Nature 433*, 77-83.
33. Scherl, A., Coute, Y., Deon, C., et al. (2002) Functional proteomic analysis of human nucleolus, *Molecular biology of the cell 13*, 4100-4109.
34. Visintin, R., and Amon, A. (2000) The nucleolus: the magician's hat for cell cycle tricks, *Current opinion in cell biology 12*, 752.
35. Vagnarelli, P., Hudson, D. F., Ribeiro, S. A., et al. (2006) Condensin and Repo-Man-PP1 co-operate in the regulation of chromosome architecture during mitosis, *Nature cell biology 8*, 1133-1142.
36. Olson, M. O. (2004) Sensing cellular stress: another new function for the nucleolus?, *Science's STKE : signal transduction knowledge environment 2004*, pe10.
37. Mayer, C., Bierhoff, H., and Grummt, I. (2005) The nucleolus as a stress sensor: JNK2 inactivates the transcription factor TIF-IA and down-regulates rRNA synthesis, *Genes & development 19*, 933-941.
38. Choesmel, V., Bacqueville, D., Rouquette, J., et al. (2007) Impaired ribosome biogenesis in Diamond-Blackfan anemia, *Blood 109*, 1275-1283.
39. Drygin, D., Rice, W. G., and Grummt, I. (2010) The RNA polymerase I transcription machinery: an emerging target for the treatment of cancer, *Annual review of pharmacology and toxicology 50*, 131-156.
40. Stefanovsky, V., Langlois, F., Gagnon-Kugler, T., et al. (2006) Growth factor signaling regulates elongation of RNA polymerase I transcription in mammals via UBF phosphorylation and r-chromatin remodeling, *Molecular cell 21*, 629-639.
41. Santoro, R. (2011) The Epigenetics of the Nucleolus: Structure and Function of Active and Silent Ribosomal RNA Genes, In *The Nucleolus* (Olson, M. O. J., Ed.), pp 57-82, Springer Science+Business Media, Jackson.
42. Haaf, T., Hayman, D. L., and Schmid, M. (1991) Quantitative determination of rDNA transcription units in vertebrate cells, *Experimental cell research 193*, 78-86.
43. Kuhn, A., and Grummt, I. (1987) A novel promoter in the mouse rDNA spacer is active in vivo and in vitro, *The EMBO journal 6*, 3487-3492.
44. Grimaldi, G., and Di Nocera, P. P. (1988) Multiple repeated units in Drosophila melanogaster ribosomal DNA spacer stimulate rRNA precursor transcription, *Proceedings of the National Academy of Sciences of the United States of America 85*, 5502-5506.
45. Putnam, C. D., and Pikaard, C. S. (1992) Cooperative binding of the Xenopus RNA polymerase I transcription factor xUBF to repetitive ribosomal gene enhancers, *Molecular and cellular biology 12*, 4970-4980.
46. Mayer, C., Schmitz, K. M., Li, J., et al. (2006) Intergenic transcripts regulate the epigenetic state of rRNA genes, *Molecular cell 22*, 351-361.
47. Santoro, R., Li, J., and Grummt, I. (2002) The nucleolar remodeling complex NoRC mediates heterochromatin formation and silencing of ribosomal gene transcription, *Nature genetics 32*, 393-396.
48. Voit, R., Schnapp, A., Kuhn, A., et al. (1992) The nucleolar transcription factor mUBF is phosphorylated by casein kinase II in the C-terminal hyperacidic tail which is essential for transactivation, *The EMBO journal 11*, 2211-2218.
49. O'Mahony, D. J., Xie, W. Q., Smith, S. D., et al. (1992) Differential phosphorylation and localization of the transcription factor UBF in vivo in response to serum deprivation. In vitro dephosphorylation of UBF reduces its transactivation properties, *The Journal of biological chemistry 267*, 35-38.
50. Voit, R., Hoffmann, M., and Grummt, I. (1999) Phosphorylation by G1-specific cdk-cyclin complexes activates the nucleolar transcription factor UBF, *The EMBO journal 18*, 1891-1899.
51. Kirk, J. M. (1960) The mode of action of actinomycin D, *Biochimica et biophysica acta 42*, 167-169.
52. Goldberg, I. H., and Rabinowitz, M. (1962) Actionmycin D inhibition of deoxyribonucleic acid-dependent synthesis of ribonucleic acid, *Science 136*, 315-316.
53. Trask, D. K., and Muller, M. T. (1988) Stabilization of type I topoisomerase-DNA covalent complexes by actinomycin D, *Proceedings of the National Academy of Sciences of the United States of America 85*, 1417-1421.
54. Sentenac, A., Simon, E. J., and Fromageot, P. (1968) Initiation of chains by RNA polymerase and the effects of inhibitors studied by a direct filtration technique, *Biochimica et biophysica acta 161*, 299-308.
55. Hadjiolova, K. V., Hadjiolov, A. A., and Bachellerie, J. P. (1995) Actinomycin D stimulates the transcription of rRNA minigenes transfected into mouse cells. Implications for the in vivo hypersensitivity of rRNA gene transcription, *European journal of biochemistry / FEBS 228*, 605-615.
56. Sobell, H. M. (1985) Actinomycin and DNA transcription, *Proceedings of the National Academy of Sciences of the United States of America 82*, 5328-5331.

57. Perry, R. P., and Kelley, D. E. (1970) Inhibition of RNA synthesis by actinomycin D: characteristic dose-response of different RNA species, *Journal of cellular physiology 76*, 127-139.
58. Bensaude, O. (2011) Inhibiting eukaryotic transcription: Which compound to choose? How to evaluate its activity?, *Transcription 2*, 103-108.
59. Boulon, S., Westman, B. J., Hutten, S., et al. (2010) The nucleolus under stress, *Molecular cell 40*, 216-227.
60. Shav-Tal, Y., Blechman, J., Darzacq, X., et al. (2005) Dynamic sorting of nuclear components into distinct nucleolar caps during transcriptional inhibition, *Molecular biology of the cell 16*, 2395-2413.
61. Hottiger, M. O., Hassa, P. O., Luscher, B., et al. (2010) Toward a unified nomenclature for mammalian ADP-ribosyltransferases, *Trends in biochemical sciences 35*, 208-219.
62. Chambon, P., Weill, J. D., and Mandel, P. (1963) Nicotinamide mononucleotide activation of new DNA-dependent polyadenylic acid synthesizing nuclear enzyme, *Biochemical and biophysical research communications 11*, 39-43.
63. Yamada, M., Miwa, M., and Sugimura, T. (1971) Studies on poly (adenosine diphosphate-ribose). X. Properties of a partially purified poly (adenosine diphosphate-ribose) polymerase, *Archives of biochemistry and biophysics 146*, 579-586.
64. Okayama, H., Edson, C. M., Fukushima, M., et al. (1977) Purification and properties of poly(adenosine diphosphate ribose) synthetase, *The Journal of biological chemistry 252*, 7000-7005.
65. Hassa, P. O., Haenni, S. S., Elser, M., et al. (2006) Nuclear ADP-ribosylation reactions in mammalian cells: where are we today and where are we going?, *Microbiology and molecular biology reviews : MMBR 70*, 789-829.
66. Hassa, P. O., and Hottiger, M. O. (2008) The diverse biological roles of mammalian PARPS, a small but powerful family of poly-ADP-ribose polymerases, *Frontiers in bioscience : a journal and virtual library 13*, 3046-3082.
67. Kraus, W. L. (2008) Transcriptional control by PARP-1: chromatin modulation, enhancer-binding, coregulation, and insulation, *Current opinion in cell biology 20*, 294-302.
68. Huambachano, O., Herrera, F., Rancourt, A., et al. (2011) Double-stranded DNA binding domain of poly(ADP-ribose) polymerase-1 and molecular insight into the regulation of its activity, *The Journal of biological chemistry 286*, 7149-7160.
69. Ame, J. C., Rolli, V., Schreiber, V., et al. (1999) PARP-2, A novel mammalian DNA damage-dependent poly(ADP-ribose) polymerase, *The Journal of biological chemistry 274*, 17860-17868.
70. Haenni, S. S., Altmeyer, M., Hassa, P. O., et al. (2008) Importin alpha binding and nuclear localization of PARP-2 is dependent on lysine 36, which is located within a predicted classical NLS, *BMC cell biology 9*, 39.
71. Altmeyer, M., Messner, S., Hassa, P. O., et al. (2009) Molecular mechanism of poly(ADP-ribosyl)ation by PARP1 and identification of lysine residues as ADP-ribose acceptor sites, *Nucleic acids research 37*, 3723-3738.
72. Haenni, S. S., Hassa, P. O., Altmeyer, M., et al. (2008) Identification of lysines 36 and 37 of PARP-2 as targets for acetylation and auto-ADP-ribosylation, *The international journal of biochemistry & cell biology 40*, 2274-2283.
73. Collier, R. J. (2001) Understanding the mode of action of diphtheria toxin: a perspective on progress during the 20th century, *Toxicon : official journal of the International Society on Toxinology 39*, 1793-1803.
74. Collinge, M. A., and Althaus, F. R. (1994) Expression of human poly(ADP-ribose) polymerase in Saccharomyces cerevisiae, *Molecular & general genetics : MGG 245*, 686-693.
75. Krietsch, J., Rouleau, M., Pic, E., et al. (2012) Reprogramming cellular events by poly(ADP-ribose)-binding proteins, *Molecular aspects of medicine*.
76. Kiehlbauch, C. C., Aboul-Ela, N., Jacobson, E. L., et al. (1993) High resolution fractionation and characterization of ADP-ribose polymers, *Analytical biochemistry 208*, 26-34.
77. Kawamitsu, H., Hoshino, H., Okada, H., et al. (1984) Monoclonal antibodies to poly(adenosine diphosphate ribose) recognize different structures, *Biochemistry 23*, 3771-3777.
78. Wielckens, K., Bredehorst, R., Adamietz, P., et al. (1982) Mono ADP-ribosylation and poly ADP-ribosylation of proteins in normal and malignant tissues, *Advances in enzyme regulation 20*, 23-37.
79. Wielckens, K., Schmidt, A., George, E., et al. (1982) DNA fragmentation and NAD depletion. Their relation to the turnover of endogenous mono(ADP-ribosyl) and poly(ADP-ribosyl) proteins, *The Journal of biological chemistry 257*, 12872-12877.
80. Alvarez-Gonzalez, R., and Althaus, F. R. (1989) Poly(ADP-ribose) catabolism in mammalian cells exposed to DNA-damaging agents, *Mutation research 218*, 67-74.

81. Moss, J., Zolkiewska, A., and Okazaki, I. (1997) ADP-ribosylarginine hydrolases and ADP-ribosyltransferases. Partners in ADP-ribosylation cycles, *Advances in experimental medicine and biology 419*, 25-33.
82. Oka, S., Kato, J., and Moss, J. (2006) Identification and characterization of a mammalian 39-kDa poly(ADP-ribose) glycohydrolase, *The Journal of biological chemistry 281*, 705-713.
83. Brochu, G., Duchaine, C., Thibeault, L., et al. (1994) Mode of action of poly(ADP-ribose) glycohydrolase, *Biochimica et biophysica acta 1219*, 342-350.
84. Brochu, G., Shah, G. M., and Poirier, G. G. (1994) Purification of poly(ADP-ribose) glycohydrolase and detection of its isoforms by a zymogram following one- or two-dimensional electrophoresis, *Analytical biochemistry 218*, 265-272.
85. Koh, D. W., Lawler, A. M., Poitras, M. F., et al. (2004) Failure to degrade poly(ADP-ribose) causes increased sensitivity to cytotoxicity and early embryonic lethality, *Proceedings of the National Academy of Sciences of the United States of America 101*, 17699-17704.
86. Slade, D., Dunstan, M. S., Barkauskaite, E., et al. (2011) The structure and catalytic mechanism of a poly(ADP-ribose) glycohydrolase, *Nature 477*, 616-620.
87. Dunstan, M. S., Barkauskaite, E., Lafite, P., et al. (2012) Structure and mechanism of a canonical poly(ADP-ribose) glycohydrolase, *Nature communications 3*, 878.
88. Rosenthal, F., Feijs, K. L., Frugier, E., et al. (2013) Macrodomain-containing proteins are new mono-ADP-ribosylhydrolases, *Nature structural & molecular biology*.
89. D'Amours, D., Desnoyers, S., D'Silva, I., et al. (1999) Poly(ADP-ribosyl)ation reactions in the regulation of nuclear functions, *The Biochemical journal 342 (Pt 2)*, 249-268.
90. Carbone, M., Rossi, M. N., Cavaldesi, M., et al. (2008) Poly(ADP-ribosyl)ation is implicated in the G0-G1 transition of resting cells, *Oncogene 27*, 6083-6092.
91. Shieh, W. M., Ame, J. C., Wilson, M. V., et al. (1998) Poly(ADP-ribose) polymerase null mouse cells synthesize ADP-ribose polymers, *The Journal of biological chemistry 273*, 30069-30072.
92. Sallmann, F. R., Vodenicharov, M. D., Wang, Z. Q., et al. (2000) Characterization of sPARP-1. An alternative product of PARP-1 gene with poly(ADP-ribose) polymerase activity independent of DNA strand breaks, *The Journal of biological chemistry 275*, 15504-15511.
93. Ferro, A. M., and Olivera, B. M. (1982) Poly(ADP-ribosylation) in vitro. Reaction parameters and enzyme mechanism, *The Journal of biological chemistry 257*, 7808-7813.
94. Zahradka, P., and Ebisuzaki, K. (1982) A shuttle mechanism for DNA-protein interactions. The regulation of poly(ADP-ribose) polymerase, *European journal of biochemistry / FEBS 127*, 579-585.
95. Yung, T. M., Sato, S., and Satoh, M. S. (2004) Poly(ADP-ribosyl)ation as a DNA damage-induced post-translational modification regulating poly(ADP-ribose) polymerase-1-topoisomerase I interaction, *The Journal of biological chemistry 279*, 39686-39696.
96. Thorslund, T., von Kobbe, C., Harrigan, J. A., et al. (2005) Cooperation of the Cockayne syndrome group B protein and poly(ADP-ribose) polymerase 1 in the response to oxidative stress, *Molecular and cellular biology 25*, 7625-7636.
97. Hilz, H., Wielckens, K., Adamietz, P., et al. (1983) Functional aspects of mono- and poly(ADP-ribosyl)ation: subcellular distribution and ADP-ribosyl turnover under conditions of repair and 'starvation', *Princess Takamatsu symposia 13*, 155-163.
98. Williams, G. T., Lau, K. M., Coote, J. M., et al. (1985) NAD metabolism and mitogen stimulation of human lymphocytes, *Experimental cell research 160*, 419-426.
99. Rechsteiner, M., Hillyard, D., and Olivera, B. M. (1976) Turnover at nicotinamide adenine dinucleotide in cultures of human cells, *Journal of cellular physiology 88*, 207-217.
100. Rechsteiner, M., Hillyard, D., and Olivera, B. M. (1976) Magnitude and significance of NAD turnover in human cell line D98/AH2, *Nature 259*, 695-696.
101. Goodwin, P. M., Lewis, P. J., Davies, M. I., et al. (1978) The effect of gamma radiation and neocarzinostatin on NAD and ATP levels in mouse leukaemia cells, *Biochimica et biophysica acta 543*, 576-582.
102. Skidmore, C. J., Davies, M. I., Goodwin, P. M., et al. (1979) The involvement of poly(ADP-ribose) polymerase in the degradation of NAD caused by gamma-radiation and N-methyl-N-nitrosourea, *European journal of biochemistry / FEBS 101*, 135-142.
103. Heeres, J. T., and Hergenrother, P. J. (2007) Poly(ADP-ribose) makes a date with death, *Current opinion in chemical biology 11*, 644-653.
104. Wang, Z. Q., Auer, B., Stingl, L., et al. (1995) Mice lacking ADPRT and poly(ADP-ribosyl)ation develop normally but are susceptible to skin disease, *Genes & development 9*, 509-520.
105. Trucco, C., Oliver, F. J., de Murcia, G., et al. (1998) DNA repair defect in poly(ADP-ribose) polymerase-deficient cell lines, *Nucleic acids research 26*, 2644-2649.

106. Masutani, M., Nozaki, T., Nishiyama, E., et al. (1999) Function of poly(ADP-ribose) polymerase in response to DNA damage: gene-disruption study in mice, *Molecular and cellular biochemistry 193*, 149-152.
107. Yelamos, J., Schreiber, V., and Dantzer, F. (2008) Toward specific functions of poly(ADP-ribose) polymerase-2, *Trends in molecular medicine 14*, 169-178.
108. Menissier de Murcia, J., Ricoul, M., Tartier, L., et al. (2003) Functional interaction between PARP-1 and PARP-2 in chromosome stability and embryonic development in mouse, *The EMBO journal 22*, 2255-2263.
109. Luo, X., and Kraus, W. L. (2012) On PAR with PARP: cellular stress signaling through poly(ADP-ribose) and PARP-1, *Genes & development 26*, 417-432.
110. Helleday, T. (2011) The underlying mechanism for the PARP and BRCA synthetic lethality: clearing up the misunderstandings, *Molecular oncology 5*, 387-393.
111. El-Khamisy, S. F., Masutani, M., Suzuki, H., et al. (2003) A requirement for PARP-1 for the assembly or stability of XRCC1 nuclear foci at sites of oxidative DNA damage, *Nucleic acids research 31*, 5526-5533.
112. Schreiber, V., Ame, J. C., Dolle, P., et al. (2002) Poly(ADP-ribose) polymerase-2 (PARP-2) is required for efficient base excision DNA repair in association with PARP-1 and XRCC1, *The Journal of biological chemistry 277*, 23028-23036.
113. Parsons, J. L., Dianova, II, Allinson, S. L., et al. (2005) Poly(ADP-ribose) polymerase-1 protects excessive DNA strand breaks from deterioration during repair in human cell extracts, *The FEBS journal 272*, 2012-2021.
114. Campalans, A., Kortulewski, T., Amouroux, R., et al. (2013) Distinct spatiotemporal patterns and PARP dependence of XRCC1 recruitment to single-strand break and base excision repair, *Nucleic acids research 41*, 3115-3129.
115. Strom, C. E., Johansson, F., Uhlen, M., et al. (2011) Poly (ADP-ribose) polymerase (PARP) is not involved in base excision repair but PARP inhibition traps a single-strand intermediate, *Nucleic acids research 39*, 3166-3175.
116. D'Silva, I., Pelletier, J. D., Lagueux, J., et al. (1999) Relative affinities of poly(ADP-ribose) polymerase and DNA-dependent protein kinase for DNA strand interruptions, *Biochimica et biophysica acta 1430*, 119-126.
117. Bryant, H. E., Petermann, E., Schultz, N., et al. (2009) PARP is activated at stalled forks to mediate Mre11-dependent replication restart and recombination, *The EMBO journal 28*, 2601-2615.
118. Ray Chaudhuri, A., Hashimoto, Y., Herrador, R., et al. (2012) Topoisomerase I poisoning results in PARP-mediated replication fork reversal, *Nature structural & molecular biology 19*, 417-423.
119. Burkle, A., and Virag, L. (2013) Poly(ADP-ribose): PARadigms and PARadoxes, *Molecular aspects of medicine*.
120. Kauppinen, T. M., Chan, W. Y., Suh, S. W., et al. (2006) Direct phosphorylation and regulation of poly(ADP-ribose) polymerase-1 by extracellular signal-regulated kinases 1/2, *Proceedings of the National Academy of Sciences of the United States of America 103*, 7136-7141.
121. de Murcia, G., Huletsky, A., Lamarre, D., et al. (1986) Modulation of chromatin superstructure induced by poly(ADP-ribose) synthesis and degradation, *The Journal of biological chemistry 261*, 7011-7017.
122. Kim, M. Y., Mauro, S., Gevry, N., et al. (2004) NAD+-dependent modulation of chromatin structure and transcription by nucleosome binding properties of PARP-1, *Cell 119*, 803-814.
123. Boulikas, T. (1989) DNA strand breaks alter histone ADP-ribosylation, *Proceedings of the National Academy of Sciences of the United States of America 86*, 3499-3503.
124. Stone, P. R., Lorimer, W. S., 3rd, and Kidwell, W. R. (1977) Properties of the complex between histone H1 and poly(ADP-ribose synthesised in HeLa cell nuclei, *European journal of biochemistry / FEBS 81*, 9-18.
125. Huletsky, A., de Murcia, G., Muller, S., et al. (1989) The effect of poly(ADP-ribosyl)ation on native and H1-depleted chromatin. A role of poly(ADP-ribosyl)ation on core nucleosome structure, *The Journal of biological chemistry 264*, 8878-8886.
126. Meyer-Ficca, M. L., Lonchar, J. D., Ihara, M., et al. (2011) Poly(ADP-ribose) polymerases PARP1 and PARP2 modulate topoisomerase II beta (TOP2B) function during chromatin condensation in mouse spermiogenesis, *Biology of reproduction 84*, 900-909.
127. Messner, S., Altmeyer, M., Zhao, H., et al. (2010) PARP1 ADP-ribosylates lysine residues of the core histone tails, *Nucleic acids research 38*, 6350-6362.
128. Martinez-Zamudio, R., and Ha, H. C. (2012) Histone ADP-ribosylation facilitates gene transcription by directly remodeling nucleosomes, *Molecular and cellular biology 32*, 2490-2502.
129. Frechette, A., Huletsky, A., Aubin, R. J., et al. (1985) Poly(ADP-ribosyl)ation of chromatin: kinetics of relaxation and its effect on chromatin solubility, *Canadian journal of biochemistry and cell biology = Revue canadienne de biochimie et biologie cellulaire 63*, 764-773.

130. Althaus, F. R. (1992) Poly ADP-ribosylation: a histone shuttle mechanism in DNA excision repair, *Journal of cell science 102 (Pt 4)*, 663-670.
131. Guetg, C., Scheifele, F., Rosenthal, F., et al. (2012) Inheritance of silent rDNA chromatin is mediated by PARP1 via noncoding RNA, *Molecular cell 45*, 790-800.
132. Saxena, A., Wong, L. H., Kalitsis, P., et al. (2002) Poly(ADP-ribose) polymerase 2 localizes to mammalian active centromeres and interacts with PARP-1, Cenpa, Cenpb and Bub3, but not Cenpc, *Human molecular genetics 11*, 2319-2329.
133. Saxena, A., Saffery, R., Wong, L. H., et al. (2002) Centromere proteins Cenpa, Cenpb, and Bub3 interact with poly(ADP-ribose) polymerase-1 protein and are poly(ADP-ribosyl)ated, *The Journal of biological chemistry 277*, 26921-26926.
134. Hassa, P. O., Buerki, C., Lombardi, C., et al. (2003) Transcriptional coactivation of nuclear factor-kappaB-dependent gene expression by p300 is regulated by poly(ADP)-ribose polymerase-1, *The Journal of biological chemistry 278*, 45145-45153.
135. Hassa, P. O., Covic, M., Hasan, S., et al. (2001) The enzymatic and DNA binding activity of PARP-1 are not required for NF-kappa B coactivator function, *The Journal of biological chemistry 276*, 45588-45597.
136. Hassa, P. O., Haenni, S. S., Buerki, C., et al. (2005) Acetylation of poly(ADP-ribose) polymerase-1 by p300/CREB-binding protein regulates coactivation of NF-kappaB-dependent transcription, *The Journal of biological chemistry 280*, 40450-40464.
137. Hassa, P. O., and Hottiger, M. O. (1999) A role of poly (ADP-ribose) polymerase in NF-kappaB transcriptional activation, *Biological chemistry 380*, 953-959.
138. Ju, B. G., Lunyak, V. V., Perissi, V., et al. (2006) A topoisomerase IIbeta-mediated dsDNA break required for regulated transcription, *Science 312*, 1798-1802.
139. Ju, B. G., and Rosenfeld, M. G. (2006) A breaking strategy for topoisomerase IIbeta/PARP-1-dependent regulated transcription, *Cell cycle 5*, 2557-2560.
140. Ju, B. G., Solum, D., Song, E. J., et al. (2004) Activating the PARP-1 sensor component of the groucho/ TLE1 corepressor complex mediates a CaMKinase IIdelta-dependent neurogenic gene activation pathway, *Cell 119*, 815-829.
141. Krishnakumar, R., Gamble, M. J., Frizzell, K. M., et al. (2008) Reciprocal binding of PARP-1 and histone H1 at promoters specifies transcriptional outcomes, *Science 319*, 819-821.
142. Krishnakumar, R., and Kraus, W. L. (2010) PARP-1 regulates chromatin structure and transcription through a KDM5B-dependent pathway, *Molecular cell 39*, 736-749.
143. Krishnakumar, R., and Kraus, W. L. (2010) The PARP side of the nucleus: molecular actions, physiological outcomes, and clinical targets, *Molecular cell 39*, 8-24.
144. Ditsworth, D., Zong, W. X., and Thompson, C. B. (2007) Activation of poly(ADP)-ribose polymerase (PARP-1) induces release of the pro-inflammatory mediator HMGB1 from the nucleus, *The Journal of biological chemistry 282*, 17845-17854.
145. Asher, G., Reinke, H., Altmeyer, M., et al. (2010) Poly(ADP-ribose) polymerase 1 participates in the phase entrainment of circadian clocks to feeding, *Cell 142*, 943-953.
146. Szanto, M., Brunyanszki, A., Kiss, B., et al. (2012) Poly(ADP-ribose) polymerase-2: emerging transcriptional roles of a DNA-repair protein, *Cellular and molecular life sciences : CMLS 69*, 4079-4092.
147. Maeda, Y., Hunter, T. C., Loudy, D. E., et al. (2006) PARP-2 interacts with TTF-1 and regulates expression of surfactant protein-B, *The Journal of biological chemistry 281*, 9600-9606.
148. Bai, P., Canto, C., Brunyanszki, A., et al. (2011) PARP-2 regulates SIRT1 expression and whole-body energy expenditure, *Cell metabolism 13*, 450-460.
149. Malanga, M., and Althaus, F. R. (2004) Poly(ADP-ribose) reactivates stalled DNA topoisomerase I and Induces DNA strand break resealing, *The Journal of biological chemistry 279*, 5244-5248.
150. Meyer-Ficca, M. L., and Meyer, R. G. (2011) Genetic approaches to targeting multiple PARP genes in a mammalian genome, *Methods in molecular biology 780*, 349-376.
151. Quenet, D., Gasser, V., Fouillen, L., et al. (2008) The histone subcode: poly(ADP-ribose) polymerase-1 (Parp-1) and Parp-2 control cell differentiation by regulating the transcriptional intermediary factor TIF1beta and the heterochromatin protein HP1alpha, *FASEB journal : official publication of the Federation of American Societies for Experimental Biology 22*, 3853-3865.
152. Liang, Y. C., Hsu, C. Y., Yao, Y. L., et al. (2013) PARP-2 regulates cell cycle-related genes through histone deacetylation and methylation independently of poly(ADP-ribosyl)ation, *Biochemical and biophysical research communications 431*, 58-64.
153. Meder, V. S., Boeglin, M., de Murcia, G., et al. (2005) PARP-1 and PARP-2 interact with nucleophosmin/B23 and accumulate in transcriptionally active nucleoli, *Journal of cell science 118*, 211-222.
154. Boamah, E. K., Kotova, E., Garabedian, M., et al. (2012) Poly(ADP-Ribose) polymerase 1 (PARP-1) regulates ribosomal biogenesis in Drosophila nucleoli, *PLoS genetics 8*, e1002442.

155. Shall, S., Gaymes, T., Farzaneh, F., et al. (2011) The use of PARP inhibitors in cancer therapy: use as adjuvant with chemotherapy or radiotherapy; use as a single agent in susceptible patients; techniques used to identify susceptible patients, *Methods in molecular biology 780*, 239-266.
156. Basu, B., Sandhu, S. K., and de Bono, J. S. (2012) PARP inhibitors: mechanism of action and their potential role in the prevention and treatment of cancer, *Drugs 72*, 1579-1590.
157. Wahlberg, E., Karlberg, T., Kouznetsova, E., et al. (2012) Family-wide chemical profiling and structural analysis of PARP and tankyrase inhibitors, *Nature biotechnology 30*, 283-288.
158. Kirby, C. A., Cheung, A., Fazal, A., et al. (2012) Structure of human tankyrase 1 in complex with small-molecule inhibitors PJ34 and XAV939, *Acta crystallographica. Section F, Structural biology and crystallization communications 68*, 115-118.
159. Antolin, A. A., Jalencas, X., Yelamos, J., et al. (2012) Identification of pim kinases as novel targets for PJ34 with confounding effects in PARP biology, *ACS chemical biology 7*, 1962-1967.
160. Chevanne, M., Zampieri, M., Caldini, R., et al. (2010) Inhibition of PARP activity by PJ-34 leads to growth impairment and cell death associated with aberrant mitotic pattern and nucleolar actin accumulation in M14 melanoma cell line, *Journal of cellular physiology 222*, 401-410.
161. Peralta-Leal, A., Rodriguez-Vargas, J. M., Aguilar-Quesada, R., et al. (2009) PARP inhibitors: new partners in the therapy of cancer and inflammatory diseases, *Free radical biology & medicine 47*, 13-26.
162. Evers, B., Drost, R., Schut, E., et al. (2008) Selective inhibition of BRCA2-deficient mammary tumor cell growth by AZD2281 and cisplatin, *Clinical cancer research : an official journal of the American Association for Cancer Research 14*, 3916-3925.
163. Donawho, C. K., Luo, Y., Penning, T. D., et al. (2007) ABT-888, an orally active poly(ADP-ribose) polymerase inhibitor that potentiates DNA-damaging agents in preclinical tumor models, *Clinical cancer research : an official journal of the American Association for Cancer Research 13*, 2728-2737.
164. Orlando, L., Schiavone, P., Fedele, P., et al. (2012) Poly (ADP-ribose) polymerase (PARP): rationale, preclinical and clinical evidences of its inhibition as breast cancer treatment, *Expert opinion on therapeutic targets 16 Suppl 2*, S83-89.
165. De Vos, M., Schreiber, V., and Dantzer, F. (2012) The diverse roles and clinical relevance of PARPs in DNA damage repair: current state of the art, *Biochemical pharmacology 84*, 137-146.
166. Martin-Oliva, D., Aguilar-Quesada, R., O'Valle, F., et al. (2006) Inhibition of poly(ADP-ribose) polymerase modulates tumor-related gene expression, including hypoxia-inducible factor-1 activation, during skin carcinogenesis, *Cancer research 66*, 5744-5756.
167. Rajesh, M., Mukhopadhyay, P., Batkai, S., et al. (2006) Pharmacological inhibition of poly(ADP-ribose) polymerase inhibits angiogenesis, *Biochemical and biophysical research communications 350*, 352-357.
168. Pacher, P., and Szabo, C. (2007) Role of poly(ADP-ribose) polymerase 1 (PARP-1) in cardiovascular diseases: the therapeutic potential of PARP inhibitors, *Cardiovascular drug reviews 25*, 235-260.
169. Soriano, F. G., Virag, L., and Szabo, C. (2001) Diabetic endothelial dysfunction: role of reactive oxygen and nitrogen species production and poly(ADP-ribose) polymerase activation, *Journal of molecular medicine 79*, 437-448.
170. Cooper, G. (2000) *The Cell: A Molecular Approach*, 2nd edition ed., Sunderland (MA): Sinauer Associates.
171. Bernard, S., and Herzel, H. (2006) Why do cells cycle with a 24 hour period?, *Genome informatics. International Conference on Genome Informatics 17*, 72-79.
172. Murray, A. H., T (1993) *the Cell cycle*, Oxford University Press, Inc., New York.
173. Dyczkowski, J., and Vingron, M. (2005) Comparative analysis of cell cycle regulated genes in eukaryotes, *Genome informatics. International Conference on Genome Informatics 16*, 125-131.
174. Satyanarayana, A., and Kaldis, P. (2009) Mammalian cell-cycle regulation: several Cdks, numerous cyclins and diverse compensatory mechanisms, *Oncogene 28*, 2925-2939.
175. Sherr, C. J., and Roberts, J. M. (1999) CDK inhibitors: positive and negative regulators of G1-phase progression, *Genes & development 13*, 1501-1512.
176. Malumbres, M., and Barbacid, M. (2005) Mammalian cyclin-dependent kinases, *Trends in biochemical sciences 30*, 630-641.
177. Yam, C. H., Fung, T. K., and Poon, R. Y. (2002) Cyclin A in cell cycle control and cancer, *Cellular and molecular life sciences : CMLS 59*, 1317-1326.
178. Ito, M. (2000) Factors controlling cyclin B expression, *Plant molecular biology 43*, 677-690.
179. Sherr, C. J. (1993) Mammalian G1 cyclins, *Cell 73*, 1059-1065.
180. Ciemerych, M. A., and Sicinski, P. (2005) Cell cycle in mouse development, *Oncogene 24*, 2877-2898.
181. Gudas, J. M., Payton, M., Thukral, S., et al. (1999) Cyclin E2, a novel G1 cyclin that binds Cdk2 and is aberrantly expressed in human cancers, *Molecular and cellular biology 19*, 612-622.
182. Kastan, M. B., and Bartek, J. (2004) Cell-cycle checkpoints and cancer, *Nature 432*, 316-323.

183. Walczak, C. E., and Heald, R. (2008) Mechanisms of mitotic spindle assembly and function, *International review of cytology 265*, 111-158.
184. Maya-Mendoza, A., Tang, C. W., Pombo, A., et al. (2009) Mechanisms regulating S phase progression in mammalian cells, *Frontiers in bioscience : a journal and virtual library 14*, 4199-4213.
185. Litovchick, L., Sadasivam, S., Florens, L., et al. (2007) Evolutionarily conserved multisubunit RBL2/p130 and E2F4 protein complex represses human cell cycle-dependent genes in quiescence, *Molecular cell 26*, 539-551.
186. Humbert, P. O., Rogers, C., Ganiatsas, S., et al. (2000) E2F4 is essential for normal erythrocyte maturation and neonatal viability, *Molecular cell 6*, 281-291.
187. Takahashi, Y., Rayman, J. B., and Dynlacht, B. D. (2000) Analysis of promoter binding by the E2F and pRB families in vivo: distinct E2F proteins mediate activation and repression, *Genes & development 14*, 804-816.
188. Rivard, N., L'Allemain, G., Bartek, J., et al. (1996) Abrogation of p27Kip1 by cDNA antisense suppresses quiescence (G0 state) in fibroblasts, *The Journal of biological chemistry 271*, 18337-18341.
189. Sage, J. (2004) Cyclin C makes an entry into the cell cycle, *Developmental cell 6*, 607-608.
190. Hanahan, D., and Weinberg, R. A. (2000) The hallmarks of cancer, *Cell 100*, 57-70.
191. Wang, Z. M., Yang, H., and Livingston, D. M. (1998) Endogenous E2F-1 promotes timely G0 exit of resting mouse embryo fibroblasts, *Proceedings of the National Academy of Sciences of the United States of America 95*, 15583-15586.
192. Ren, S., and Rollins, B. J. (2004) Cyclin C/cdk3 promotes Rb-dependent G0 exit, *Cell 117*, 239-251.
193. Susaki, E., Nakayama, K., and Nakayama, K. I. (2007) Cyclin D2 translocates p27 out of the nucleus and promotes its degradation at the G0-G1 transition, *Molecular and cellular biology 27*, 4626-4640.
194. Rissland, O. S., Hong, S. J., and Bartel, D. P. (2011) MicroRNA destabilization enables dynamic regulation of the miR-16 family in response to cell-cycle changes, *Molecular cell 43*, 993-1004.
195. Mulligan, G., and Jacks, T. (1998) The retinoblastoma gene family: cousins with overlapping interests, *Trends in genetics : TIG 14*, 223-229.
196. Sherr, C. J. (1996) Cancer cell cycles, *Science 274*, 1672-1677.
197. Weinberg, R. A. (1995) The retinoblastoma protein and cell cycle control, *Cell 81*, 323-330.
198. Friend, S. H., Bernards, R., Rogelj, S., et al. (1986) A human DNA segment with properties of the gene that predisposes to retinoblastoma and osteosarcoma, *Nature 323*, 643-646.
199. Chatterjee, S. J., George, B., Goebell, P. J., et al. (2004) Hyperphosphorylation of pRb: a mechanism for RB tumour suppressor pathway inactivation in bladder cancer, *The Journal of pathology 203*, 762-770.
200. Cobrinik, D. (2005) Pocket proteins and cell cycle control, *Oncogene 24*, 2796-2809.
201. Chen, H. Z., Tsai, S. Y., and Leone, G. (2009) Emerging roles of E2Fs in cancer: an exit from cell cycle control, *Nature reviews. Cancer 9*, 785-797.
202. Dyson, N. (1998) The regulation of E2F by pRB-family proteins, *Genes & development 12*, 2245-2262.
203. Stevens, C., and La Thangue, N. B. (2003) E2F and cell cycle control: a double-edged sword, *Archives of biochemistry and biophysics 412*, 157-169.
204. Morris, L., Allen, K. E., and La Thangue, N. B. (2000) Regulation of E2F transcription by cyclin E-Cdk2 kinase mediated through p300/CBP co-activators, *Nature cell biology 2*, 232-239.
205. Trouche, D., Cook, A., and Kouzarides, T. (1996) The CBP co-activator stimulates E2F1/DP1 activity, *Nucleic acids research 24*, 4139-4145.
206. Chan, H. M., and La Thangue, N. B. (2001) p300/CBP proteins: HATs for transcriptional bridges and scaffolds, *Journal of cell science 114*, 2363-2373.
207. Martinez-Balbas, M. A., Bauer, U. M., Nielsen, S. J., et al. (2000) Regulation of E2F1 activity by acetylation, *The EMBO journal 19*, 662-671.
208. Burke, J. R., Deshong, A. J., Pelton, J. G., et al. (2010) Phosphorylation-induced conformational changes in the retinoblastoma protein inhibit E2F transactivation domain binding, *The Journal of biological chemistry 285*, 16286-16293.
209. Hwang, H. C., and Clurman, B. E. (2005) Cyclin E in normal and neoplastic cell cycles, *Oncogene 24*, 2776-2786.
210. Besson, A., Dowdy, S. F., and Roberts, J. M. (2008) CDK inhibitors: cell cycle regulators and beyond, *Developmental cell 14*, 159-169.
211. Harper, J. W. (1997) Cyclin dependent kinase inhibitors, *Cancer surveys 29*, 91-107.
212. Funk, J. (2005) Cell Cycle Checkpoint Genes and Cancer, *ENCYCLOPEDIA OF LIFE SCIENCES*.
213. Alcorta, D. A., Xiong, Y., Phelps, D., et al. (1996) Involvement of the cyclin-dependent kinase inhibitor p16 (INK4a) in replicative senescence of normal human fibroblasts, *Proceedings of the National Academy of Sciences of the United States of America 93*, 13742-13747.
214. Hara, E., Smith, R., Parry, D., et al. (1996) Regulation of p16CDKN2 expression and its implications for cell immortalization and senescence, *Molecular and cellular biology 16*, 859-867.

215. Chin, L., Pomerantz, J., and DePinho, R. A. (1998) The INK4a/ARF tumor suppressor: one gene--two products--two pathways, *Trends in biochemical sciences 23*, 291-296.
216. Bertwistle, D., Sugimoto, M., and Sherr, C. J. (2004) Physical and functional interactions of the Arf tumor suppressor protein with nucleophosmin/B23, *Molecular and cellular biology 24*, 985-996.
217. Sherr, C. J. (2006) Divorcing ARF and p53: an unsettled case, *Nature reviews. Cancer 6*, 663-673.
218. LaBaer, J., Garrett, M. D., Stevenson, L. F., et al. (1997) New functional activities for the p21 family of CDK inhibitors, *Genes & development 11*, 847-862.
219. Besson, A., Hwang, H. C., Cicero, S., et al. (2007) Discovery of an oncogenic activity in p27Kip1 that causes stem cell expansion and a multiple tumor phenotype, *Genes & development 21*, 1731-1746.
220. Coats, S., Flanagan, W. M., Nourse, J., et al. (1996) Requirement of p27Kip1 for restriction point control of the fibroblast cell cycle, *Science 272*, 877-880.
221. Lee, M. H., Reynisdottir, I., and Massague, J. (1995) Cloning of p57KIP2, a cyclin-dependent kinase inhibitor with unique domain structure and tissue distribution, *Genes & development 9*, 639-649.
222. Matsuoka, S., Edwards, M. C., Bai, C., et al. (1995) p57KIP2, a structurally distinct member of the p21CIP1 Cdk inhibitor family, is a candidate tumor suppressor gene, *Genes & development 9*, 650-662.
223. Malumbres, M., and Barbacid, M. (2001) To cycle or not to cycle: a critical decision in cancer, *Nature reviews. Cancer 1*, 222-231.
224. Bartek, J., and Lukas, J. (2003) Chk1 and Chk2 kinases in checkpoint control and cancer, *Cancer cell 3*, 421-429.
225. Kastan, M. B., and Lim, D. S. (2000) The many substrates and functions of ATM, *Nature reviews. Molecular cell biology 1*, 179-186.
226. Wahl, G. M., and Carr, A. M. (2001) The evolution of diverse biological responses to DNA damage: insights from yeast and p53, *Nature cell biology 3*, E277-286.
227. Maya, R., Balass, M., Kim, S. T., et al. (2001) ATM-dependent phosphorylation of Mdm2 on serine 395: role in p53 activation by DNA damage, *Genes & development 15*, 1067-1077.
228. Donzelli, M., and Draetta, G. F. (2003) Regulating mammalian checkpoints through Cdc25 inactivation, *EMBO reports 4*, 671-677.
229. Bartek, J., Lukas, C., and Lukas, J. (2004) Checking on DNA damage in S phase, *Nature reviews. Molecular cell biology 5*, 792-804.
230. Huang, X., Halicka, H. D., and Darzynkiewicz, Z. (2004) Detection of histone H2AX phosphorylation on Ser-139 as an indicator of DNA damage (DNA double-strand breaks), *Current protocols in cytometry / editorial board, J. Paul Robinson, managing editor ... [et al.] Chapter 7*, Unit 7 27.
231. Lamarche, B. J., Orazio, N. I., and Weitzman, M. D. (2010) The MRN complex in double-strand break repair and telomere maintenance, *FEBS letters 584*, 3682-3695.
232. Xu, B., Kim, S. T., Lim, D. S., et al. (2002) Two molecularly distinct G(2)/M checkpoints are induced by ionizing irradiation, *Molecular and cellular biology 22*, 1049-1059.
233. De Antoni, A., Pearson, C. G., Cimini, D., et al. (2005) The Mad1/Mad2 complex as a template for Mad2 activation in the spindle assembly checkpoint, *Current biology : CB 15*, 214-225.
234. Djuranovic, S., Nahvi, A., and Green, R. (2011) A parsimonious model for gene regulation by miRNAs, *Science 331*, 550-553.
235. Ruegger, S., and Grosshans, H. (2012) MicroRNA turnover: when, how, and why, *Trends in biochemical sciences 37*, 436-446.
236. Esquela-Kerscher, A., and Slack, F. J. (2006) Oncomirs - microRNAs with a role in cancer, *Nature reviews. Cancer 6*, 259-269.
237. Croce, C. M. (2009) Causes and consequences of microRNA dysregulation in cancer, *Nature reviews. Genetics 10*, 704-714.
238. Fabian, M. R., Sonenberg, N., and Filipowicz, W. (2010) Regulation of mRNA translation and stability by microRNAs, *Annual review of biochemistry 79*, 351-379.
239. Friedman, R. C., Farh, K. K., Burge, C. B., et al. (2009) Most mammalian mRNAs are conserved targets of microRNAs, *Genome research 19*, 92-105.
240. Bueno, M. J., and Malumbres, M. (2011) MicroRNAs and the cell cycle, *Biochimica et biophysica acta 1812*, 592-601.
241. Takeshita, F., Patrawala, L., Osaki, M., et al. (2010) Systemic delivery of synthetic microRNA-16 inhibits the growth of metastatic prostate tumors via downregulation of multiple cell-cycle genes, *Molecular therapy : the journal of the American Society of Gene Therapy 18*, 181-187.
242. Liu, Q., Fu, H., Sun, F., et al. (2008) miR-16 family induces cell cycle arrest by regulating multiple cell cycle genes, *Nucleic acids research 36*, 5391-5404.
243. Linsley, P. S., Schelter, J., Burchard, J., et al. (2007) Transcripts targeted by the microRNA-16 family cooperatively regulate cell cycle progression, *Molecular and cellular biology 27*, 2240-2252.

244. Ofir, M., Hacohen, D., and Ginsberg, D. (2011) MiR-15 and miR-16 are direct transcriptional targets of E2F1 that limit E2F-induced proliferation by targeting cyclin E, *Molecular cancer research : MCR 9*, 440-447.
245. Hwang, H. W., Wentzel, E. A., and Mendell, J. T. (2009) Cell-cell contact globally activates microRNA biogenesis, *Proceedings of the National Academy of Sciences of the United States of America 106*, 7016-7021.
246. Kanai, M., Uchida, M., Hanai, S., et al. (2000) Poly(ADP-ribose) polymerase localizes to the centrosomes and chromosomes, *Biochemical and biophysical research communications 278*, 385-389.
247. Augustin, A., Spenlehauer, C., Dumond, H., et al. (2003) PARP-3 localizes preferentially to the daughter centriole and interferes with the G1/S cell cycle progression, *Journal of cell science 116*, 1551-1562.
248. Dynek, J. N., and Smith, S. (2004) Resolution of sister telomere association is required for progression through mitosis, *Science 304*, 97-100.
249. Wright, R. H., Castellano, G., Bonet, J., et al. (2012) CDK2-dependent activation of PARP-1 is required for hormonal gene regulation in breast cancer cells, *Genes & development 26*, 1972-1983.
250. Madison, D. L., and Lundblad, J. R. (2010) C-terminal binding protein and poly(ADP)ribose polymerase 1 contribute to repression of the p21(waf1/cip1) promoter, *Oncogene 29*, 6027-6039.
251. Simbulan-Rosenthal, C. M., Rosenthal, D. S., Luo, R., et al. (1999) Poly(ADP-ribose) polymerase upregulates E2F-1 promoter activity and DNA pol alpha expression during early S phase, *Oncogene 18*, 5015-5023.
252. Simbulan-Rosenthal, C. M., Rosenthal, D. S., Luo, R., et al. (2003) PARP-1 binds E2F-1 independently of its DNA binding and catalytic domains, and acts as a novel coactivator of E2F-1-mediated transcription during re-entry of quiescent cells into S phase, *Oncogene 22*, 8460-8471.
253. Reddel, R. R. (2000) The role of senescence and immortalization in carcinogenesis, *Carcinogenesis 21*, 477-484.
254. Chang, H. Y., Lawless, C., Addinall, S. G., et al. (2011) Genome-wide analysis to identify pathways affecting telomere-initiated senescence in budding yeast, *G3 1*, 197-208.
255. Sedivy, J. M. (1998) Can ends justify the means?: telomeres and the mechanisms of replicative senescence and immortalization in mammalian cells, *Proceedings of the National Academy of Sciences of the United States of America 95*, 9078-9081.
256. Rodier, F., and Campisi, J. (2011) Four faces of cellular senescence, *The Journal of cell biology 192*, 547-556.
257. Pagliarini, D. J., Calvo, S. E., Chang, B., et al. (2008) A mitochondrial protein compendium elucidates complex I disease biology, *Cell 134*, 112-123.
258. Truscott, K. N., Brandner, K., and Pfanner, N. (2003) Mechanisms of protein import into mitochondria, *Current biology : CB 13*, R326-337.
259. Baker, B. M., and Haynes, C. M. (2011) Mitochondrial protein quality control during biogenesis and aging, *Trends in biochemical sciences 36*, 254-261.
260. Haynes, C. M., and Ron, D. (2010) The mitochondrial UPR - protecting organelle protein homeostasis, *Journal of cell science 123*, 3849-3855.
261. Pellegrino, M. W., Nargund, A. M., and Haynes, C. M. (2013) Signaling the mitochondrial unfolded protein response, *Biochimica et biophysica acta 1833*, 410-416.
262. Phillips, R. M., Jaffar, M., Maitland, D. J., et al. (2004) Pharmacological and biological evaluation of a series of substituted 1,4-naphthoquinone bioreductive drugs, *Biochemical pharmacology 68*, 2107-2116.
263. Gaikwad, N. W., Yang, L., Rogan, E. G., et al. (2009) Evidence for NQO2-mediated reduction of the carcinogenic estrogen ortho-quinones, *Free radical biology & medicine 46*, 253-262.
264. Zhu, H., and Li, Y. (2012) NAD(P)H: quinone oxidoreductase 1 and its potential protective role in cardiovascular diseases and related conditions, *Cardiovascular toxicology 12*, 39-45.
265. Nioi, P., and Hayes, J. D. (2004) Contribution of NAD(P)H:quinone oxidoreductase 1 to protection against carcinogenesis, and regulation of its gene by the Nrf2 basic-region leucine zipper and the arylhydrocarbon receptor basic helix-loop-helix transcription factors, *Mutation research 555*, 149-171.
266. Siegel, D., and Ross, D. (2000) Immunodetection of NAD(P)H:quinone oxidoreductase 1 (NQO1) in human tissues, *Free radical biology & medicine 29*, 246-253.
267. Siegel, D., Yan, C., and Ross, D. (2012) NAD(P)H:quinone oxidoreductase 1 (NQO1) in the sensitivity and resistance to antitumor quinones, *Biochemical pharmacology 83*, 1033-1040.
268. Cullen, J. J., Hinkhouse, M. M., Grady, M., et al. (2003) Dicumarol inhibition of NADPH:quinone oxidoreductase induces growth inhibition of pancreatic cancer via a superoxide-mediated mechanism, *Cancer research 63*, 5513-5520.
269. Wu, K., Knox, R., Sun, X. Z., et al. (1997) Catalytic properties of NAD(P)H:quinone oxidoreductase-2 (NQO2), a dihydronicotinamide riboside dependent oxidoreductase, *Archives of biochemistry and biophysics 347*, 221-228.

270. Dunstan, M. S., Barnes, J., Humphries, M., et al. (2011) Novel inhibitors of NRH:quinone oxidoreductase 2 (NQO2): crystal structures, biochemical activity, and intracellular effects of imidazoacridin-6-ones, *Journal of medicinal chemistry 54*, 6597-6611.
271. Madison, D. L., Stauffer, D., and Lundblad, J. R. (2011) The PARP inhibitor PJ34 causes a PARP1-independent, p21 dependent mitotic arrest, *DNA repair 10*, 1003-1013.
272. Bentle, M. S., Reinicke, K. E., Bey, E. A., et al. (2006) Calcium-dependent modulation of poly(ADP-ribose) polymerase-1 alters cellular metabolism and DNA repair, *The Journal of biological chemistry 281*, 33684-33696.
273. Asher, G., Lotem, J., Cohen, B., et al. (2001) Regulation of p53 stability and p53-dependent apoptosis by NADH quinone oxidoreductase 1, *Proceedings of the National Academy of Sciences of the United States of America 98*, 1188-1193.
274. Anwar, A., Dehn, D., Siegel, D., et al. (2003) Interaction of human NAD(P)H:quinone oxidoreductase 1 (NQO1) with the tumor suppressor protein p53 in cells and cell-free systems, *The Journal of biological chemistry 278*, 10368-10373.
275. Tenesa, A., and Dunlop, M. G. (2009) New insights into the aetiology of colorectal cancer from genome-wide association studies, *Nature reviews. Genetics 10*, 353-358.
276. Terzic, J., Grivennikov, S., Karin, E., et al. (2010) Inflammation and colon cancer, *Gastroenterology 138*, 2101-2114 e2105.
277. Naugler, W. E., and Karin, M. (2008) NF-kappaB and cancer-identifying targets and mechanisms, *Current opinion in genetics & development 18*, 19-26.
278. Wang, C. Y., Mayo, M. W., and Baldwin, A. S., Jr. (1996) TNF- and cancer therapy-induced apoptosis: potentiation by inhibition of NF-kappaB, *Science 274*, 784-787.
279. Kim, S., Keku, T. O., Martin, C., et al. (2008) Circulating levels of inflammatory cytokines and risk of colorectal adenomas, *Cancer research 68*, 323-328.
280. Laghi, L., Bianchi, P., Miranda, E., et al. (2009) CD3+ cells at the invasive margin of deeply invading (pT3-T4) colorectal cancer and risk of post-surgical metastasis: a longitudinal study, *The lancet oncology 10*, 877-884.
281. Borsig, L., Wong, R., Hynes, R. O., et al. (2002) Synergistic effects of L- and P-selectin in facilitating tumor metastasis can involve non-mucin ligands and implicate leukocytes as enhancers of metastasis, *Proceedings of the National Academy of Sciences of the United States of America 99*, 2193-2198.
282. Swidsinski, A., Khilkin, M., Kerjaschki, D., et al. (1998) Association between intraepithelial Escherichia coli and colorectal cancer, *Gastroenterology 115*, 281-286.
283. Martin, H. M., Campbell, B. J., Hart, C. A., et al. (2004) Enhanced Escherichia coli adherence and invasion in Crohn's disease and colon cancer, *Gastroenterology 127*, 80-93.
284. Bartosh, T. J., Ylostalo, J. H., Mohammadipoor, A., et al. (2010) Aggregation of human mesenchymal stromal cells (MSCs) into 3D spheroids enhances their antiinflammatory properties, *Proceedings of the National Academy of Sciences of the United States of America 107*, 13724-13729.
285. Brown, K. R., Otasek, D., Ali, M., et al. (2009) NAViGaTOR: Network Analysis, Visualization and Graphing Toronto, *Bioinformatics 25*, 3327-3329.
286. Desnoyers, S., Kaufmann, S. H., and Poirier, G. G. (1996) Alteration of the nucleolar localization of poly(ADP-ribose) polymerase upon treatment with transcription inhibitors, *Experimental cell research 227*, 146-153.
287. Mischo, H. E., Hemmerich, P., Grosse, F., et al. (2005) Actinomycin D induces histone gamma-H2AX foci and complex formation of gamma-H2AX with Ku70 and nuclear DNA helicase II, *The Journal of biological chemistry 280*, 9586-9594.
288. Langelier, M. F., Planck, J. L., Roy, S., et al. (2011) Crystal structures of poly(ADP-ribose) polymerase-1 (PARP-1) zinc fingers bound to DNA: structural and functional insights into DNA-dependent PARP-1 activity, *The Journal of biological chemistry 286*, 10690-10701.
289. Hofer, T., Badouard, C., Bajak, E., et al. (2005) Hydrogen peroxide causes greater oxidation in cellular RNA than in DNA, *Biological chemistry 386*, 333-337.
290. Aas, P. A., Otterlei, M., Falnes, P. O., et al. (2003) Human and bacterial oxidative demethylases repair alkylation damage in both RNA and DNA, *Nature 421*, 859-863.
291. Martinez-Rucobo, F. W., and Cramer, P. (2013) Structural basis of transcription elongation, *Biochimica et biophysica acta 1829*, 9-19.
292. Hanawalt, P. C., and Spivak, G. (2008) Transcription-coupled DNA repair: two decades of progress and surprises, *Nature reviews. Molecular cell biology 9*, 958-970.
293. Di Giammartino, D. C., Shi, Y., and Manley, J. L. (2013) PARP1 represses PAP and inhibits polyadenylation during heat shock, *Molecular cell 49*, 7-17.
294. Nakagawa, S., and Hirose, T. (2012) Paraspeckle nuclear bodies--useful uselessness?, *Cellular and molecular life sciences : CMLS 69*, 3027-3036.

295. Allen, C., Ashley, A. K., Hromas, R., et al. (2011) More forks on the road to replication stress recovery, *Journal of molecular cell biology 3*, 4-12.
296. Mizuguchi, G., Shen, X., Landry, J., et al. (2004) ATP-driven exchange of histone H2AZ variant catalyzed by SWR1 chromatin remodeling complex, *Science 303*, 343-348.
297. Lents, N. H., and Baldassare, J. J. (2004) CDK2 and cyclin E knockout mice: lessons from breast cancer, *Trends in endocrinology and metabolism: TEM 15*, 1-3.
298. Jamieson, D., Wilson, K., Pridgeon, S., et al. (2007) NAD(P)H:quinone oxidoreductase 1 and nrh:quinone oxidoreductase 2 activity and expression in bladder and ovarian cancer and lower NRH:quinone oxidoreductase 2 activity associated with an NQO2 exon 3 single-nucleotide polymorphism, *Clinical cancer research : an official journal of the American Association for Cancer Research 13*, 1584-1590.
299. Werno, C., Schmid, T., Schnitzer, S. E., et al. (2010) A combination of hypoxia and lipopolysaccharide activates tristetraprolin to destabilize proinflammatory mRNAs such as tumor necrosis factor-alpha, *The American journal of pathology 177*, 1104-1112.
300. Ishida, I., Kubo, H., Suzuki, S., et al. (2002) Hypoxia diminishes toll-like receptor 4 expression through reactive oxygen species generated by mitochondria in endothelial cells, *Journal of immunology 169*, 2069-2075.
301. Shirdel, E. A., Xie, W., Mak, T. W., et al. (2011) NAViGaTing the micronome--using multiple microRNA prediction databases to identify signalling pathway-associated microRNAs, *PloS one 6*, e17429.
302. Gorospe, M., Tominaga, K., Wu, X., et al. (2011) Post-Transcriptional Control of the Hypoxic Response by RNA-Binding Proteins and MicroRNAs, *Frontiers in molecular neuroscience 4*, 7.
303. Rahat, M. A., Bitterman, H., and Lahat, N. (2011) Molecular mechanisms regulating macrophage response to hypoxia, *Frontiers in immunology 2*, 45.
304. Altmeyer, M., Barthel, M., Eberhard, M., et al. (2010) Absence of poly(ADP-ribose) polymerase 1 delays the onset of Salmonella enterica serovar Typhimurium-induced gut inflammation, *Infection and immunity 78*, 3420-3431.
305. Ba, X., and Garg, N. J. (2011) Signaling mechanism of poly(ADP-ribose) polymerase-1 (PARP-1) in inflammatory diseases, *The American journal of pathology 178*, 946-955.
306. Liu, L., Ke, Y., Jiang, X., et al. (2012) Lipopolysaccharide activates ERK-PARP-1-RelA pathway and promotes nuclear factor-kappaB transcription in murine macrophages, *Human immunology 73*, 439-447.
307. Popoff, I., Jijon, H., Monia, B., et al. (2002) Antisense oligonucleotides to poly(ADP-ribose) polymerase-2 ameliorate colitis in interleukin-10-deficient mice, *The Journal of pharmacology and experimental therapeutics 303*, 1145-1154.
308. Bai, P., and Virag, L. (2012) Role of poly(ADP-ribose) polymerases in the regulation of inflammatory processes, *FEBS letters 586*, 3771-3777.

CURRICULUM VITAE

Personal information

Name:	LEGER (born MEYER)
Surname:	Karolin
Address:	Greifenseestrasse 17, CH – 8050 Zürich Phone: +41-76-7433550 Email: karolin.meyer@vetbio.uzh.ch
Date of birth:	13th of November 1984
Place of birth:	Magdeburg, Germany
Nationality:	German

Education

May 2009 – present Doctoral Studies in Molecular Biology

- Institute of Veterinary Biochemistry and Molecular Biology, University of Zurich, Switzerland
- Ph.D Program in Cancer Biology/LSZGS
- Degree: Dr. sc. nat.
- Thesis title: Distinct Functions of ARTD1 and ARTD2 in Cell Cycle Entry and the Genotoxic Stress Response

Oct. 2004 – March 2009 Academic Studies

- University of Leipzig
- Field of study: Biochemistry
- Degree: Diplom
- Title of diploma thesis: Development of inverse agonists of the ghrelin receptor as potential therapeutics for obesity

Sep. 2006 – June 2007 Student exchange program „Erasmus“,

- University of Glasgow, Scotland, UK

Aug. 1995 – July 2004 Secondary School

- Humboldt-Gymnasium (before Herder-Gymnasium), Magdeburg
- Degree: Allgemeine Hochschulreife

Grants

July 2011	Forschungskredit der Universität Zürich, Ph.D salary for one year
Oct. 2012	Travel reimbursement of the Cancer Biology Ph.D program for the "EMBO meeting 2012"

List of Publications

Bluwstein A, Kumar N, Léger K, Traenkle J, Oostrum Jv, Rehrauer H, Baudis M, Hottiger MO. (2013). PKC signaling prevents irradiation-induced apoptosis of primary human fibroblasts. *Cell Death Dis,* e498.

Chollet C, Meyer K, Beck-Sickinger AG. (2009). Ghrelin--a novel generation of anti-obesity drug: design, pharmacomodulation and biological activity of ghrelin analogues. *J Pept Sci. 15*, 711-730.

Walther C, Meyer K, Rennert R, Neundorf I. (2008). Quantum dot-carrier peptide conjugates suitable for imaging and delivery applications. *Bioconjug Chem. 19*, 2346-2356.

ACKNOLEWDGEMENT

First of all, I would like to acknowledge my doctoral thesis supervisor Prof. Michael O. Hottiger for his steady support and advices, his investment of time and the positive working atmosphere. I would like to thank him for the chance to work in his laboratory, to learn and grow with my tasks.

Further, I would like to thank my thesis committee members PD Dr. Stefano Ferrari, Prof. Roland Wenger and Prof. Anja Groth for their support, critical remarks, fruitful discussions and materials they provided for experimental setups. Prof. Bernhard Lüscher is kindly acknowledged for reading the thesis as external reviewer.

A special thanks goes to Dr. Florian Freimoser, who helped a lot with the manuscripts and the critical reading of this thesis. Furthermore, I would like to thank our collaborators: Dr. Raffaela Santoro, Prof. Roland Wenger, Dr. Lubor Borsig, Dr. Igor Jurisica, Dr. Hubert Rehrauer, Dr. Peter Richards, Kamila Bartnicka, Carole Oertli, Jesús Glaus, Natasa Savic and Ali Mirsaidi. I would like to thank all the people of the IVBMB and CABMM for creating a nice working atmosphere. There is such a positive and stimulating working environment, which is especially credited to the head of the institute, Prof. Ueli Hübscher. Thank you also for all the nice social excurses.

A big thank you goes to the present and former Hottiger group members. I had a great time with all of you. We all are/were a really good match! Thanks to my lab-bench neighbor Andrej, for all the scientific discussions and the small group meetings spent together.

Especially I would like to thank Moni, for helping me to settle down in the lab and for her constant support during the work life. I'm happy that I got the chance to meet you!

A "no words can tell" thank you goes to the girls – Ingrid, Julia, Mareike, Roby and Rosalba. I'm grateful to call you my friends and hope it will last forever! You have been a great support in regards of science, daily lab work and basically any other problems, especially during the last period.

Most important, I would like to thank my family. Laurent, my great husband, you are my rock in hard times. Thanks for your patience and support for all my decisions during the last years. From the bottom of my heart I thank my parents for their deep love and encouragement to make my way. I would also like to thank my "sister" Babett – we have each other forever! I like to thank my grandmothers and my grandfathers and my whole lovely family. I'm grateful to have such great family bonds.